The role of the extracellular calcium sensing receptor in development and plasticity

Michael J. Newton

A thesis submitted for the award of PhD

September 2013

1. Thesis Summary/Abstract

The extracellular calcium sensing receptor (CaSR) is a G-protein coupled receptor that monitors extracellular, free ionized-calcium levels ($[Ca^{2+}]_o$) in organs that maintain systemic $[Ca^{2+}]_o$ homeostasis. CaSR is also expressed in the nervous system, where this lab recently found that it regulates the axonal growth and branching of sympathetic neurons and the dendritic growth of hippocampal pyramidal neurons during development. Other labs have subsequently shown that CaSR regulates presynaptic physiology in response to activity induced synaptic fluctuations in $[Ca^{2+}]_o$. Although individuals with CaSR mutations may present with seizures from childhood, the developmental significance of synaptic CaSR has not been investigated.

This thesis reports the developmental regulation of *Casr* mRNA expression in multiple brain regions of mice. A previously unreported peak in hippocampal *Casr* mRNA expression at postnatal day 14 led to the testing of the hypothesis that CaSR may play a role in synapse formation. A novel *in vitro* culture method was developed to circumvent perinatal lethality in the available *in vivo* conditional CaSR knockout model. However, this study, using both pharmacological and genetic methods, has been unable to find any evidence to suggest that CaSR regulates synaptogenesis *in vitro.* This thesis also reports an effect of $[Ca^{2+}]_o$ on neurite outgrowth from sympathetic neural cells early in their development. However no deficit in proximal sympathetic axon growth is observed in CaSR knockout embryos *in vivo*. Novel findings suggest that in 2.3 mM $Ca^{2+}{}_o$, elevated wild type CaSR expression is necessary and sufficient for CaSR-promoted axonal growth in late embryonic sympathetic neuron cultures. This effect is not seen in low $[Ca^{2+}]_o$ medium or cells expressing inactivated CaSR mutants, but is shown to require ERK1/2 activation, a portion of the C-terminal domain of CaSR, and is regulated by a PKC phosphorylation site contained therein.

DECLARATION

1.1. This work has not been submitted in substance for any other degree or award at this or any other university or place of learning, nor is being submitted concurrently in candidature for any degree or other award.

Signed  (candidate) Date 28.09.13

STATEMENT 1

This thesis is being submitted in partial fulfillment of the requirements for the degree of PhD

Signed  (candidate) Date 28.09.13

STATEMENT 2

This thesis is the result of my own independent work/investigation, except where otherwise stated.
Other sources are acknowledged by explicit references. The views expressed are my own.

Signed  (candidate) Date 28.09.13

STATEMENT 4: PREVIOUSLY APPROVED BAR ON ACCESS

I hereby give consent for my thesis, if accepted, to be available for photocopying and for inter-library loans **after expiry of a bar on access previously approved by the Academic Standards & Quality Committee.**

Signed  (candidate) Date 28.09.13

2. General Acknowledgements

I would like to thank numerous people without whom this thesis would not have been possible.

Prof. Alun Davies for his expert supervision, guidance, support and inspiration throughout my research in his laboratory.

Dr. Sean Wyatt for being on hand for additional advice during this project, providing technical assistance in the gathering of RT-QPCR data and for proofreading this thesis.

My second supervisor, Dr. Kerrie Thomas, who along with Dr. Riccardo Brambilla, has provided useful critical advice, regular appraisal and helpful suggestions.

Prof. Vincenzo Crunelli for the opportunity to join this PhD program and wise mentoring during the course of my studies.

Prof. Patricia Salinas (UCL) her lab members for their advice and synaptic puncta analysis protocols and Dr. Wenhan Chang (UCSF) for floxed *Casr* mice.

Dr. Tom Vizard for assistance in gathering data, sharing protocols, reagents, experience and his time in tutoring me in methods relating to the study of the peripheral nervous system.

Dr. Pedro Chacón for sharing protocols, reagents, experience and his time in tutoring me in methods relating to the study of the hippocampal neurons.

Dr. Helen Waller Evans for expert assistance in histological methods.

Mr Ronak Ved for enthusiastic assistance gathering some early SCG data.

Other members of the Davies lab, including Matthew White, Catarina Osório, Tom McWilliams, Christopher Laurie, Clara Erice, Lilian Kisiswa and Laura Howard for helping make the PhD experience enjoyable though numerous discussions (of both technically helpful and purely incidental nature) and drinks.

My parents, my sister, my wider family and friends, and especially my wife Angela for their consistent love, support and patience with my science-geekery.

The Wellcome Trust funded this research.

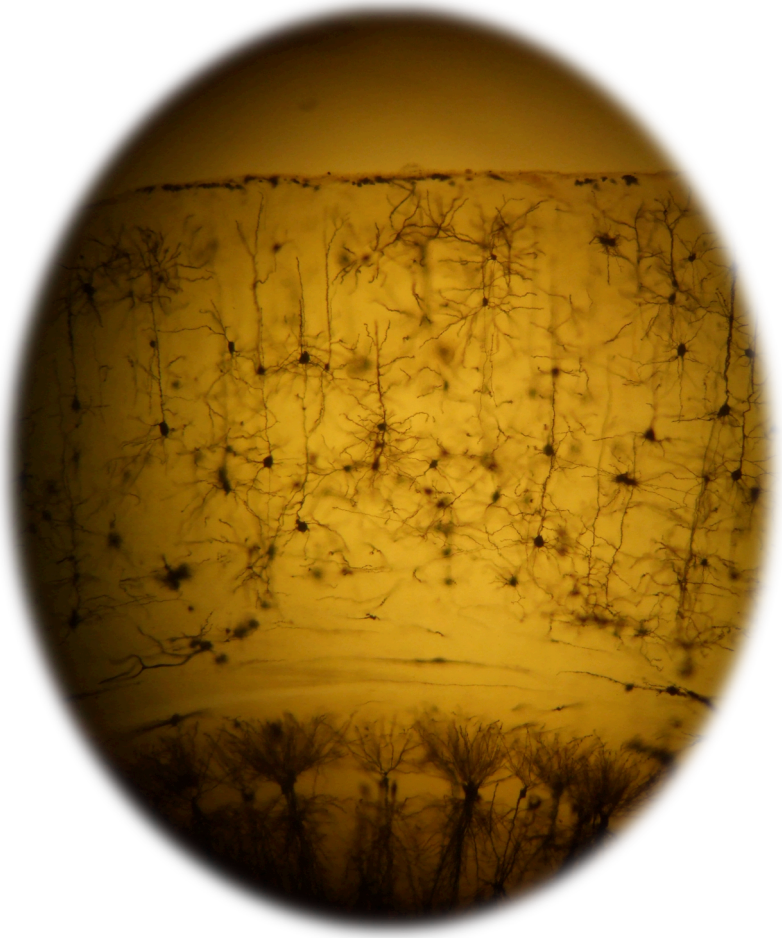

"*Nerve cells and the magical web they weave are things of great beauty and fascination, and the world is full of such things. It is an inexhaustible treasure-trove for those who want to go exploring*"

Professor Alun Davies FRS

On his election as a Fellow of the Royal Society, May 2011

Image: Golgi stained neurons of the murine cortex and hippocampus

Michael J. Newton

With assistance from Helen Waller Evans & Catarina Osório

3. Abbreviations

$[Ca^{2+}]_i$	Intracellular calcium concentration
$[Ca^{2+}]_o$	Extracellular free ionized calcium concentration
$1,25(OH)_2D_3$	1,25-dihydroxyvitamin D
A/P	Anterior-posterior
AA	Arachidonic acid
AC	Adenylyl cyclase
ADH	Autosomal dominant hypocalcemia
ADIS	Agonist-driven insertional signalling
AMPA	2-amino-3-(5-methyl-3-oxo-1,2- oxazol-4-yl)propanoic acid
AMSH	Associated molecule with the SH3 domain of STAM
ANOVA	Analysis of Variance
APP	Amyloid precursor protein
Aβ	Amyloid β
BDNF	Brain Derived Neurotrophic Factor
BSA	Bovine Serum Alubumin
$Ca^{2+}{}_i$	Intracellular calcium
$Ca^{2+}{}_o$	Extracellular free ionized calcium
CAKC	Ca^{2+}-activated K^+ channel
CaMK	Ca^{2+}-calmodulin-dependent protein kinase
cAMP	Cyclic adenosine monophosphate
CaSR	Extracellular Calcium Sensing Receptor
CG	Celiac ganglion
cGMP	Cyclic guanosine monophosphate
CNS	Central Nervous System
$cPLA_2$	Cytosolic PLA_2
CR	Cysteine rich
DAB	3,3'-Diaminobenzidine tetrahydrochloride hydrate
DAG	Diacylglycerol
DDN	Double dominant negative
DG	Dentate Gyrus
DIV	Days in vitro
DN	Dominant negative
DRG	Dorsal root ganglion

E	Embryonic day
E/I	Excitatory/inhibitory
ECD	Extracellular domain
eL-s	Extracellular loops
ERK	Extracellular signal related kinase
FHH	Familial hypocalciuric hypercalcemia
FLIP-L	Long form of FLICE-inhibitory protein
GABA	Gamma-aminobutyric acid
GAP	GTPase Activating Protein
GAPDH	Glyceraldehyde 3-phosphate dehydrogenase
GCL	Granule cell layer
GDNF	Glial cell-derived neurotrophic factor
GEF	Guanine Nucleotide Exchange Factor
GFRα	GDNF-family receptor-α
GITR	Glucocorticoid-induced TNF receptor-related protein
GITRL	GITR ligand
GnRH	Gonadotrophin-releasing hormone
GPCR	G-protein coupled receptor
GSK3	Glycogen synthase kinase 3
GTPases	Guanosine triphosphatases
HBSS	Hank's Balanced Salt Solution
HGF	Hepatocyte Growth Factor
HH	Heptahelical
iL-s	Intracellular loops
IMG	Inferior mesenteric ganglion
IML	Intermediolateral column
IP_3	Inositol-(1,4,5)-trisphosphate
IP_3R	IP_3 receptor
IV	Independent variable
LIV	Leucine-isoleucine-valine
LTD	Long Term Depression
LTP	Long Term Potentiation
M/L	Medial-lateral
MAP	Microtubule associated protein

MAPK	Mitogen-activated protein kinase
MBP	Myelin basic protein
MEF2	Myocyte Enhancer Factor 2
MEK	MAPK/ERK kinases
MEM	Modified Eagle's Medium
mGluR1	Metabotropic glutamate receptor type 1
mGluR3	Metabotropic glutamate receptor type 3
mGluR5	Metabotropic glutamate receptor type 5
mGluR7	Metabotropic glutamate receptor type 5
ML	Molecular layer
MSP	Macrophage stimulating protein
NGF	Nerve Growth Factor
NMDA	N-methyl-D-aspartate
NO	Nitric oxide
NSCC	Non-selective cation channel
NSHPT	Neonatal severe hyperparathyroidism
NT-3	Neurotrophin-3
NT-4	Neurotrophin-4
ORF	Open reading frame
OSE	Ovarian surface epithelial
P	Postnatal day
$p75^{NTR\text{-}ICD}$	Cytoplasmic domain of $p75^{NTR}$
PA	Phosphatidic acid
PC12	Pheochromocytoma 12
PCL	Purkinje cell layer
PCR	Polymerase chain reaction
PF	Parafollicular
PIP_2	Phosphatidyl inositol (4,5) bisphosphate
PKA	Protein kinase A
PKC	Protein kinase C
PLA	Phospholipase A
PLC	Phospholipase C
PLD	Phospholipase D
PNS	Peripheral Nervous System

PP2A	Protein phosphatase 2A
PSD	Post synaptic density
PTH	Parathyroid hormone
PTHrP	Parathyroid hormone-related protein
RAMP	Receptor activity modifying protein
RANK-L	Receptor activator of nuclear factor kappa-B ligand
SC	Sympathetic chain (SC)
SCG	Superior Cervical Ganglion
SDHA	Succinate dehydrogenase complex, subunit A
Sema3A	Semaphorin3A
SFO	Sub-fornical organ
SG	Stellate ganglion
Shh	Sonic hedgehog
SMG	Superior mesenteric ganglion
SRF	Serum Response Factor
TM	Transmembrane
TNF	Tumour necrosis factor
TNFR1	TNF receptor 1
TNFSF	Tumour Necrosis Factor Superfamily
TTF-1	Thyroid transcription factor 1
Ub	Ubiquitin
VACC	Voltage-activated calcium channel
VFT	Venus-flytrap
WT	Wild-type

4. Table of Contents

5. Table of Figures

6. Table of Tables

7. Introduction

The vertebrate nervous system is an object of astonishing complexity and beauty, which must be correctly "wired up" during development in order for normal physiological function of an organism. Understanding the orchestration of such a feat by molecular cues, cellular processes and environmental influences is a major challenge for developmental neurobiology, towards which much progress has been made but many questions remain unanswered.

The experimental chapters of this thesis aim to add to our knowledge of how one particular cue, extracellular calcium (Ca^{2+}_o), contributes to the development of the peripheral and central nervous systems (PNS & CNS) through its modulation of extracellular calcium sensing receptor (CaSR) signalling. Accordingly, this introduction will survey the relevant aspects of what is known about the development of the PNS and CNS, and the structure and functions of the CaSR.

7.1. PNS Development

In this thesis, the roles of CaSR signalling in the developing PNS have been examined in one of the best-studied models of neurodevelopment, the mouse superior cervical ganglion (SCG). The SCG is a population of nerve cells found in the cranial region, at the rostral end of the sympathetic chain, which forms part of the autonomic division of the PNS (Figure 1). Studies focused on the SCG and other PNS ganglia have begun to provide a framework for understanding the principles of neural development (Glebova and Ginty, 2005). The formulation of "The Neurotrophic Hypothesis", its development into "Neurotrophic Theory" and the identification and characterization of neurotrophic factors have been of particular significance for our growing understanding of neural development.

7.1.1. Neurotrophic Theory & Neurotrophic Factors

The neurotrophic hypothesis posits a mechanism to explain the precise matching of the number of neurons innervating a target tissue to the requirements of that target, one of the most striking features of the vertebrate nervous system (Oppenheim, 1991; Davies, 2003). Many more neurons are generated in early development than are required for correct target field innervation in the adult. Following initial target field innervation, superfluous or incorrectly connected

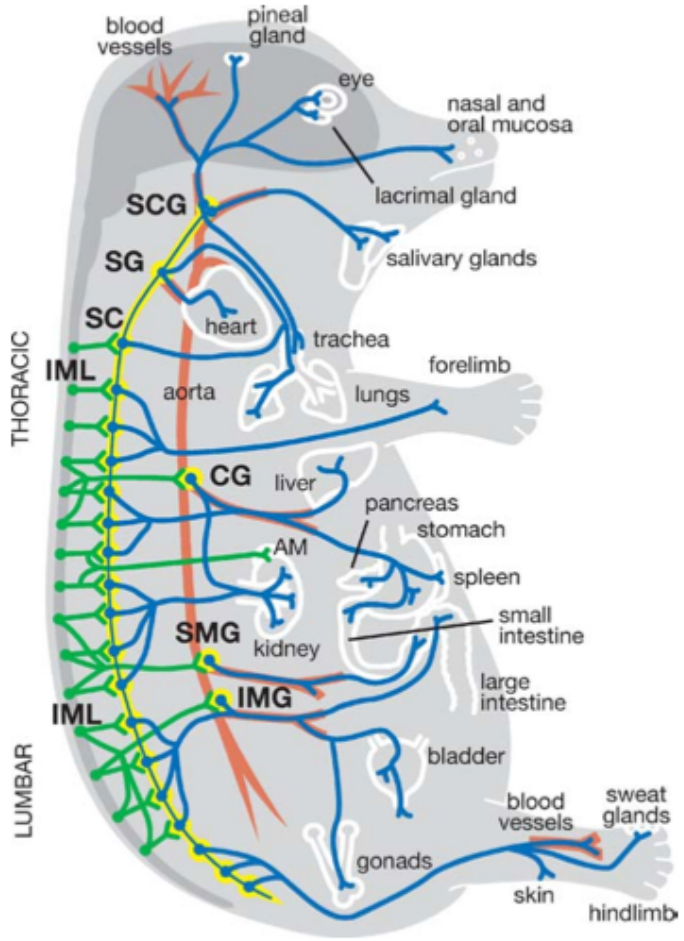

Figure 1: Neuroanatomy of the murine sympathetic nervous system

The SCG is situated in the cranial region, at the rostral end of the sympathetic chain (SC) (yellow) adjacent to a bifurcation of the corotid artery. SCG neurons, and neurons within other sympathetic ganglia such as the SC, stellate ganglion (SG), celiac ganglion (CG), superior mesenteric ganglion (SMG) and inferior mesenteric ganglion (IMG), receive synaptic input from pre-ganglionic neurons whose soma are located in the intermediolateral column (IML) within the spinal cord. The sympathetic nervous system targets a vast array of organs, and the SCG itself has diverse targets including cerebral blood vessels, the pineal gland, the eye, the lacrimal gland, nasal and oral mucosa, salivary glands and the trachea. From Glebova and Ginty (2005).

neurons are eliminated during a period of apoptotic cell death. According to the neurotrophic hypothesis, neurons become dependent on a supply of neurotrophic factors to support their survival shortly after they reach their target fields. Since target fields contain a limiting supply of neurotrophic factors, innervating neurons must compete with one another to achieve adequate trophic support. Those neurons that obtain sufficient amounts of neurotrophic factors will survive, whereas those that do not will die by apoptosis (Davies, 1988; Oppenheim, 1991;

Davies, 2003). Over time, the neurotrophic hypothesis has been modified in the light of data demonstrating that neurotrophic factors promote differentiation, target field innervation, axon terminal arborisation and regulate the functional properties of neurons, in addition to supporting neuronal survival. Moreover, some developing neurons require support from neurotrophic factors to promote their survival before their axons reach their target fields, neurotrophic factors can be produced by neurons themselves and act in an autocrine/paracrine manner to support neuronal survival and some developing neurons require the sequential support of more than one neurotrophic factor to promote their survival (Davies, 1996, 2003).

Several families of neurotrophic factors have been identified and characterised, including the neurotrophins (Nerve Growth Factor (NGF), Brain Derived Neurotrophic Factor (BDNF), Neurotrophin-3 (NT-3) and Neurotrophin-4 (NT-4)) (Davies, 1988; Lewin and Barde, 1996), glial cell-derived neurotrophic factor (GDNF) family ligands (Airaksinen and Saarma, 2002), and the plasminogen-related growth factors hepatocyte growth factor (HGF) and macrophage stimulating protein (MSP) (Davies, 2009).

7.1.1.1. NGF and TrkA

While several neurotrophic factors have key functions at different stages during the development of the SCG, the most extensively characterised neurotrophic factor for SCG neurons is NGF (Davies, 2009). NGF was initially purified from the mouse salivary gland, a target of SCG neurons (Cohen, 1960). Importantly, the injection of antisera raised against this preparation of NGF into SCG targets during the period of target field innervation was shown to dramatically reduce sympathetic neuronal survival (Levi-Montalcini and Booker, 1960). Conversely, injection of endogenous NGF served to rescue neurons that would otherwise have died during development (Levi-Montalcini, 1987). The crucial role that NGF plays in supporting the survival of developing SCG neurons has been confirmed by analysis of transgenic mice with a null-mutation in either NGF (Crowley et al., 1994) or its receptor, TrkA (Smeyne et al., 1994). Neonatal mice lacking either functional NGF or TrkA have dramatically fewer SCG neurons than wild type mice.

NGF is a soluble secretory factor synthesized as a proneurotrophin precursor protein (Lewin and Barde, 1996; Seidah et al., 1996b). Proteolytically cleaved,

mature NGF forms dimers, the crystal structure of which has been solved at 2.3 Å resolution (McDonald et al., 1991). The crystal structure of NGF dimers has indicated that association between NGF monomers is mediated by the conjunction of flat surfaces formed by three anti-parallel β pleated sheets on each monomer (McDonald et al., 1991). The mechanisms by which NGF binds TrkA have been clarified by resolving the crystal structures of ligand/receptor complexes (Wiesmann et al., 1999), isolated TrkA domains (Ultsch et al., 1999; Robertson et al., 2001) and complexes between NGF and mutated TrkA ligand binding domains (Urfer et al., 1998). The data generated from these studies suggests that domain 5 of TrkA (also referred to as the second immunoglobulin domain) plays a key role in NGF binding (Huang and Reichardt, 2003). The binding of a single NGF homodimer to two immunoglobulin domains of TrkA is important for receptor activation. In common with other tyrosine kinase receptors, TrkA is activated by ligand induced receptor dimerization and transphosphorylation of intracellular tyrosine residues (Huang and Reichardt, 2003; Reichardt, 2006). Domain deletion studies have suggested that the immunoglobulin-like domains to which NGF dimers bind inhibit TrkA dimerization and spontaneous receptor activation in the absence of NGF (Arevalo et al., 2000). Taken together, these biochemical studies shed light on the mechanisms by which mature NGF homodimers activate TrkA to induce many of the biological effects of NGF.

One particularly interesting aspect of NGF signalling is understanding how this target-derived factor can have long lasting effects on neuronal growth and survival by engaging signalling mechanisms within the distally located cell soma (Harrington and Ginty, 2013). The earliest clue to answering this question was the detection of radioactivity in the SCG following injection of radiolabelled NGF into SCG target fields (Thoenen and Barde, 1980). It was subsequently found that NGF is specifically transported along sympathetic axons to the SCG in a retrograde manner *in vivo* (Stöckel et al., 1974). The leading hypothesized transport mechanism today is "signalling endosome theory" (Howe et al., 2001), which is now supported by a wealth of data (Harrington and Ginty, 2013). This mechanism entails the internalization of TrkA bound NGF homodimers into signalling endosomes, which may occur by both clathrin dependent and in-dependent mechanisms. Following depolymerisation of a surrounding F-actin barrier by the recruitment of a Rac1-cofilin signalling module (Harrington et al., 2011), these

endosomes become linked to dynein in an interaction promoted by TrkA stimulated, ERK1/2 mediated dynein phosphorylation (Mitchell et al., 2012). The linking of signalling endosomes to dynein enables their retrograde transport to the cell soma along axonal microtubules. The signalling mechanisms that mediate NGF-promoted process growth and survival, both locally in axons and at the cell soma following retrograde transport, are described further in sections 7.1.2.3.3 and 7.1.2.4, respectively.

7.1.1.2. The Neurotrophin family of ligands and their receptors

Since the identification of NGF, three other neurotrophic factors exhibiting notable structural and functional similarities to NGF have been discovered. These are BDNF, NT-3 and NT-4 (Davies, 1988; Lewin and Barde, 1996). Together with the founder member NGF, and on the basis of their similarities, these four factors are grouped into the "Neurotrophin" class of neurotrophic factors.

The sequence similarity observed amongst neurotrophin genes suggests that their evolutionary origins may lie in gene duplication events, followed by diversification (Lewin and Barde, 1996). No NGF gene is found in the ray, whereas NGF, BDNF and NT-3 have all been detected in two teleost fish (salmon and *Xiphophorus*). Furthermore, sequence analysis across species indicates a greater degree of conservation for BDNF than NGF, which can be interpreted as indicating earlier optimization of the BDNF sequence in evolutionary history (Barde, 1994). Interestingly, mutation of only seven residues in human NT-3 is sufficient to generate a neurotrophin that is able to bind to TrkA and TrkB, as well as the cognate NT-3 receptor, TrkC, with high affinity and promote neuronal survival (Urfer et al., 1994). These findings have led to the suggestion that NT-3 may be the original ancestral neurotrophin gene, with BDNF and NGF emerging more recently (Barde, 1994; Lewin and Barde, 1996).

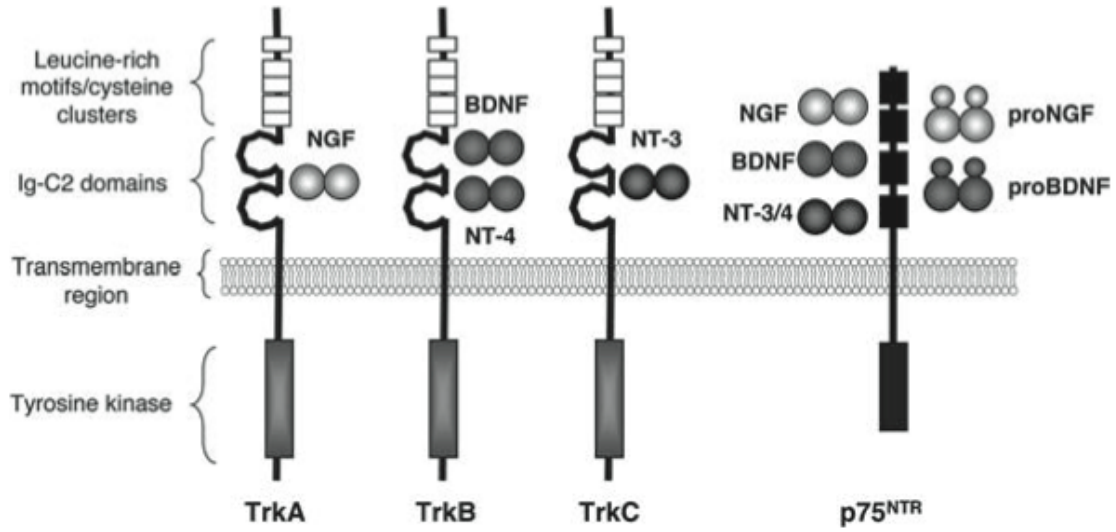

Figure 2: Neurotrophins and their receptors

NGF binds to TrkA, BDNF and NT-4 to TrkB, and NT-3 to TrkC. In addition, each neurotrophin, as well as the pro-forms of BDNF and NGF, can bind with equal affinity to $p75^{NTR}$, which belongs to the tumour necrosis factor superfamily (TNFSF) of receptors. From Arévalo & Wu (2006).

7.1.1.2.1. Neurotrophins and Trk receptors

Neurotrophins are all synthesized as proneurotrophin precursors (Seidah et al., 1996a; Seidah et al., 1996b; Lee et al., 2001), and are cleaved to mature forms that share a common mechanism of action, forming homodimers that each bind preferentially to a member of a family of three receptor tyrosine kinases, the Trk receptors (Figure 2). TrkA is the cognate receptor for NGF, BDNF and NT-4 signal through TrkB and TrkC is the preferred receptor for NT-3, although NT-3 can also signal through TrkA and TrkB in some cellular contexts (Arévalo and Wu, 2006). The central β pleated sheet of the NGF homodimer is also observed in other neurotrophin homodimers, and is thought to be a common interaction site of neurotrophins with Trk receptors. In contrast, N-terminal residues of neurotrophins involved in interactions with the immunoglobulin domain of Trk receptors are less conserved and are thought to confer receptor selectivity (Barde, 1994; Huang and Reichardt, 2003). In each case, binding of neurotrophin homodimers induces Trk receptor dimerization and transphosphorylation, leading to the recruitment of down-stream signalling adaptors which can activate signalling through the Ras/ERK, PI3K/Akt and PLCγ pathways (Figure 3) (Huang and Reichardt, 2003; Arévalo and Wu, 2006).

7.1.1.2.2. Neurotrophins and p75^{NTR}

In addition to the Trk receptors, all of the neurotrophins are able to bind the pan-neurotrophin receptor p75^{NTR}, a member of the tumour necrosis superfamily (Figure 3). The consequences of p75^{NTR} activation can in some instances be complimentary to the actions of neurotrophins through Trk receptors, and in other instances they can be antagonistic (Huang and Reichardt, 2003). Evidence that p75^{NTR} may act in a fashion complimentary to neurotrophin/Trk receptor signalling during PNS development includes the demonstration that p75^{NTR} sensitizes TrkA to activation by NGF (Davies et al., 1993). In accordance with this, it has even been argued that p75^{NTR} is essential for high affinity NGF/TrkA binding (Hempstead et al., 1991). Furthermore, an innervation deficit is observed in selected SCG targets in p75^{NTR} knockout mice (Lee et al., 1994). However, another well characterized consequence of p75^{NTR} activation is the induction of apoptotic neuronal death following neurotrophin binding in the absence of cognate Trk expression (Nykjaer et al., 2005). High-affinity binding of pro-neurotrophins to a p75^{NTR}/sortilin receptor complex also results in apoptosis (Nykjaer et al., 2004). Interestingly, pro-NGF promotes process outgrowth from developing mouse SCG neurons *in vitro* by a p75^{NTR}–dependent signalling mechanism (Howard et al., 2013).

The binding of either neurotrophins or pro-neurotrophins to p75^{NTR} can activate a number of diverse signalling pathways (Reichardt, 2006; Charalampopoulos et al., 2012). For example, the recruitment of TRAF6 to the intracellular domain of ligated p75^{NTR} leads to the activation of the pro-survival NF-κB signalling pathway. In contrast, the recruitment of cdc42 to ligated p75^{NTR} results in the activation of JNK and the subsequent c-JUN mediated transcription of pro-apoptotic genes (Figure 3). Alternatively, neurotrophin stimulated engagement of p75^{NTR} can induce the TACE mediated cleavage of the cytoplasmic domain of p75^{NTR} (p75$^{NTR\text{-}ICD}$). Binding of TRAF6 to soluble p75$^{NTR\text{-}ICD}$ recruits the transcription factor NRIF, which is subsequently ubiquitinated by TRAF6. The TRAF6-p75$^{NTR\text{-}ICD}$-NRIF complex translocates to the nucleus to direct the transcription of pro-apoptotic genes. The binding of neurotrophins to p75^{NTR} can also release p75^{NTR}-bound

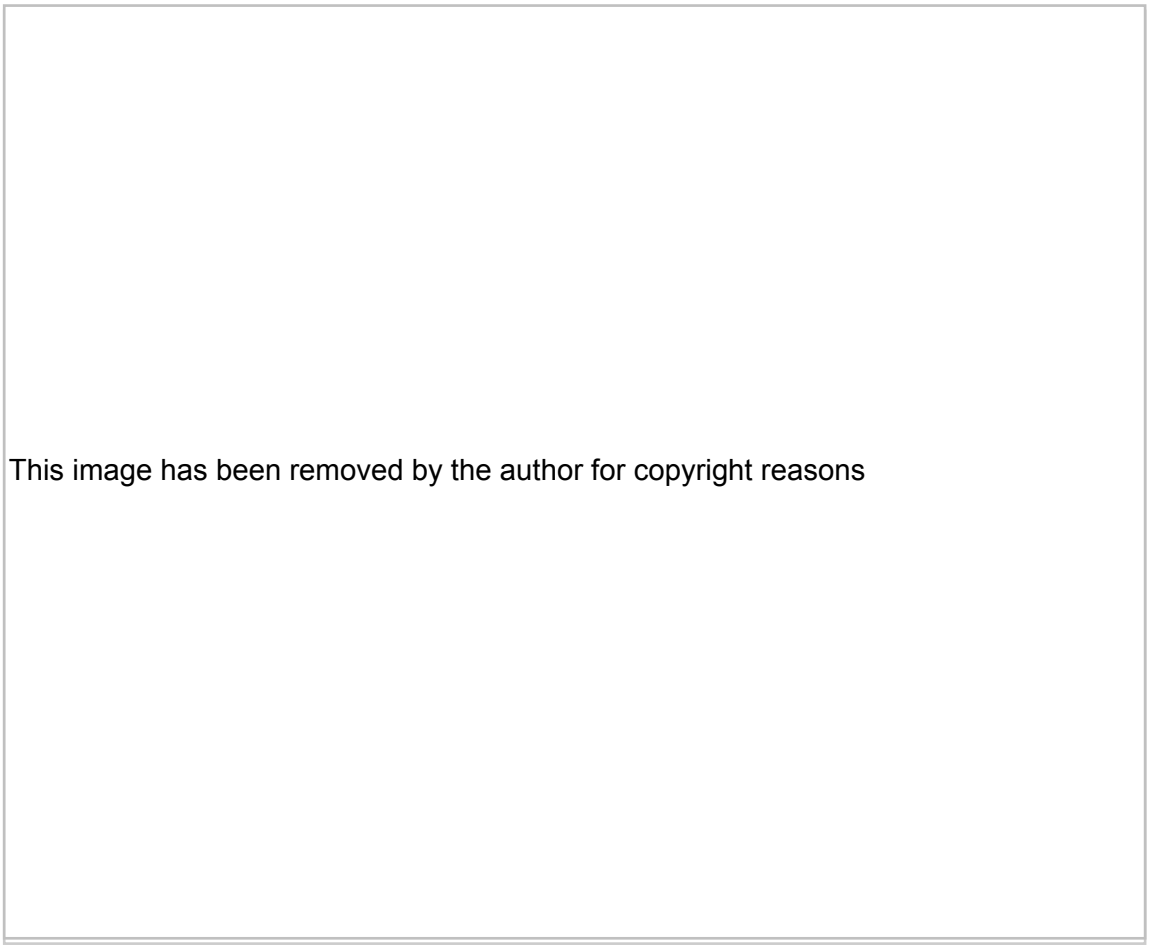

Figure 3: Generalized neurotrophin signalling pathways

Major effector pathways downstream of neurotrophin mediated Trk activation include PLCγ/PKC, PI3K/Akt and Ras/ERK. The docking of adaptor proteins to phosphorylated tyrosine residues in the C-terminal tail of Trk receptors is important for engaging these signalling pathways. In diverse neuronal types, the induction of Trk signalling can lead to a variety of outcomes including enhanced survival, promotion of axonal/dendritic growth, neuronal differentiation and synaptic plasticity. These outcomes are achieved through transcription dependent and independent mechanisms. The binding of neurotrophins to $p75^{NTR}$ can also result in the activation of distinct signalling pathways including, NF-κB, RhoA and JNK dependent pathways. From Reichardt (2006).

RhoGDI, a negative regulator of RhoA activity, into the cytoplasm. Inhibition of RhoA activity by RhoGDI prevents RhoA from inhibiting growth cone motility and enhances neuronal process growth. Finally, neurotrophin bound $p75^{NTR}$ activates membrane sphingomyelinase, thereby increasing the generation of ceramide from the plasma membrane. Ceramide can inhibit the initiation of Trk-dependent PI3K/Akt signalling with the result that neurotrophin/Trk mediated survival is compromised (Reichardt, 2006; Charalampopoulos et al., 2012).

7.1.1.3. GDNF family of ligands and receptors

The GDNF family of ligands comprises GDNF, artemin, neurturin and persephin (Airaksinen and Saarma, 2002). Each of the four ligands in this family bind as a homodimer to their cognate GPI anchored GDNF-family receptor-α (GFRα) receptor, and each GFRα receptor is competent to activate the common RET tyrosine kinase receptor. GDNF preferentially binds to GFRα1, GFRα2 is the preferred receptor for neurturin, artemin binds GFRα3 and persephin binds GFRα4 (Airaksinen and Saarma, 2002). Interestingly, responses to immobilized, membrane bound GDNF, neurturin and artemin are mediated instead by syndecan-3, a heparin sulphate, transmembrane proteoglycan. Syndecan-3 mediated GDNF, neurturin and artemin signalling may be important in some neurodevelopmental contexts (Bespalov et al., 2011).

GDNF was initially described as a trophic factor for embryonic midbrain neurons, although numerous additional roles for this neurotrophic factor have since been characterised (Airaksinen and Saarma, 2002). Whilst the GFRα1 receptor has been implicated as a target derived guidance factor for developing SCG neurons (Ledda et al., 2002), the most relevant member of the GDNF family to this discussion is artemin. The suggested roles of artemin in regulating the proliferation of sympathetic neuroblasts (Andres et al., 2001; Davies, 2009) and promoting proximal axon growth (Glebova and Ginty, 2005; Davies, 2009) are discussed in sections 7.1.2.1 and 7.1.2.2, respectively.

7.1.1.4. HGF and MSP

HGF and MSP are soluble plasminogen-related growth factors which act as ligands for the Met and Ron tyrosine kinase receptors, respectively (Benvenuti and Comoglio, 2007). Both receptors are single membrane pass receptors that form disulphide linked heterodimers, with each subunit derived from a single, proteolytically cleaved polypeptide chain (Benvenuti and Comoglio, 2007). Nonetheless, they appear to have different modes of action in the developing nervous system (Davies, 2009). Both HGF and Met are expressed in the SCG during the early stages of its development and several roles for HGF/Met signalling were initially reported in early SCG cultures (see section 7.1.2.1) (Maina et al., 1998). In contrast, MSP is expressed by target tissues of both sensory and sympathetic neurons, promoting survival of sympathetic neurons *in vitro* during an early

developmental window, while exerting more potent effects on sensory neurons of the trigeminal ganglion later in development (Forgie et al., 2003). As *Ron* mRNA is expressed in the SCG and trigeminal ganglion throughout development, MSP has been proposed to be a target derived neurotrophic factor (Forgie et al., 2003). In support of this, MSP is also expressed in the targets of a subpopulation of NGF-dependent adult sensory neurons from the dorsal root ganglion (DRG), acting to promote their growth and branching *in vitro* (Franklin et al., 2009).

7.1.2. Overview of SCG development

The SCG contains a population of neural crest derived sympathetic neurons. In mice, SCG neurons can be readily isolated and cultured from as early as embryonic day (E) 13, soon after SCG formation, until late stages of post-natal development. The experimental tractability of the developing rodent SCG has resulted in SCG neuron development becoming very well characterized, with the timing of many key developmental events and the molecules that regulate these events known in some detail (Figure 4).

The temporal pattern of CaSR mRNA expression in the developing SCG has led to an investigation into the potential roles of CaSR signalling during two distinct developmental windows. The first window encompasses the very earliest stages of SCG development, a time when sympathetic neuroblasts are proliferating and differentiating and newly born neurons first extend processes towards their peripheral targets. The second developmental window represents a period when SCG neurons are ramifying in their target fields and competing amongst themselves to obtain sufficient amounts of target-derived NGF to avoid apoptosis. The following introduction to SCG development focuses on developmental processes relevant to these two temporal windows. As previously published data has shown that the CaSR promotes NGF-dependent growth and branching of sympathetic axons during the second developmental window (Vizard et al., 2008), the roles that neurotrophic factors play in regulating the development of SCG neurons will also be considered.

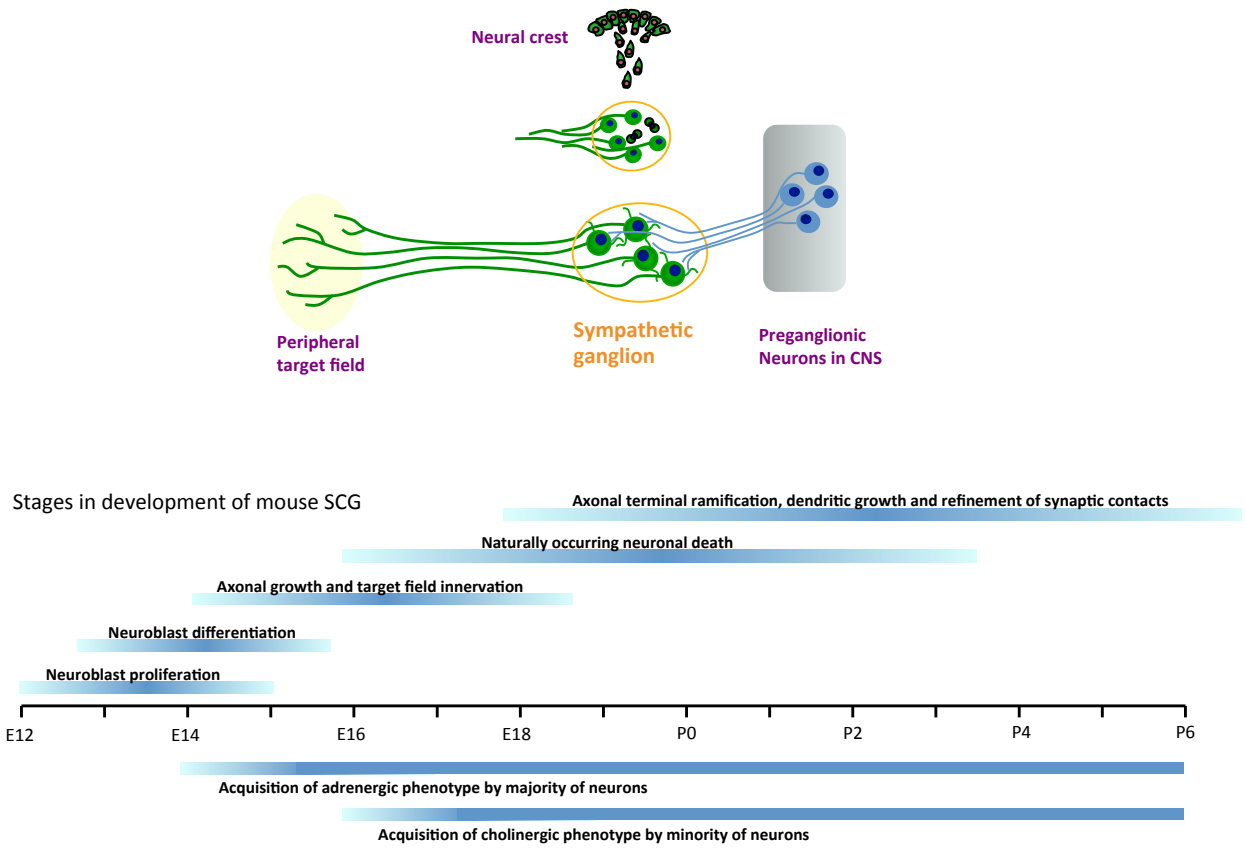

Figure 4: Stages of sympathetic neuron development

The development of rodent SCG neurons has been well characterised due to the experimentally tractable nature of this population of neural crest derived postganglionic sympathetic neurons. Figure modified from Alun Davies (unpublished).

7.1.2.1. SCG formation, neuroblast proliferation and neuronal differentiation

Prior to the formation of the SCG, neural crest cells migrate ventrally from the neural tube, forming a column of sympathetic ganglion primordia that begin to condense around E10.5 (Makita et al., 2008) before migrating rostrally to form the SCG (Glebova and Ginty, 2005). At E13, the early SCG contains a small number of postmitotic neurons and larger number of proliferating neuroblasts. These neuroblasts have acquired many characteristics of mature sympathetic neurons, but have yet to undergo their terminal mitotic division and differentiate into mature sympathetic neurons (Maina et al., 1998). Mouse and chick sympathetic neuroblasts are initially able to survive in culture for several days without added neurotrophic factors when they are plated onto a suitable substratum (Maina et al., 1998). In accordance with this, TrkA is expressed at very low levels in the E13 and E14 mouse SCG, but TrkA expression increases markedly from E14 to E15 as newly born SCG neurons become responsive to NGF (Wyatt and Davies, 1995). Although SCG neuroblasts do not require NGF to promote their survival, multiple lines of evidence suggest that HGF, signalling through the Met receptor, may regulate the survival and differentiation of a proportion of neuroblasts, both *in vitro* and *in vivo,* possibly though an autocrine signalling mechanism (Maina et al., 1998). In addition, artemin, a member of the GDNF family that signals through the Ret/GFRα3 complex, has been shown to promote the proliferation of cultured mouse SCG neuroblasts and exert a transient survival promoting action on newly generated sympathetic neurons (Andres et al., 2001). However the *in vivo* relevance of artemin-promoted proliferation of SCG neuroblast is unclear, as a deficit in neuron number has only been found in the SCG of one out of two GFRα3 knockout strains (Honma et al., 2002; Davies, 2009). Interpreting the effects of a deficiency in artemin/GFRα3 signalling on the survival of postmitotic SCG neurons *in vivo* is complicated by the observation that artemin is required for the correct rostral migration of SCG progenitors (Nishino et al., 1999). Moreover, vasculature derived artemin enhances the earliest stages of SCG target innervation and the loss of artemin/GFRα3 signalling *in vivo* leads to an inadequate innervation of SCG target fields and the apoptotic death of SCG neurons due to their restricted access to target field-derived NGF (Honma et al., 2002; Davies, 2009).

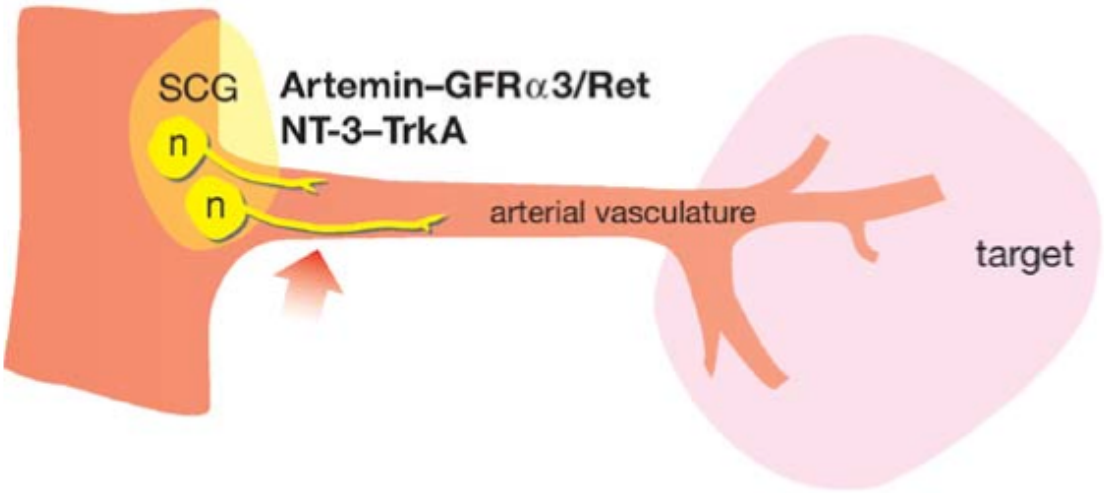

Figure 5: Proximal axon growth from newly generated SCG neurons

Axons begin to course along the arterial vasculature, en route to their distal targets, soon after SCG neurons are born. Trophic factors, including artemin, NT-3 and endothelin-3 (not shown) are expressed along the vasculature and regulate axon growth by binding to and activating neuronal GFRα3/Ret, TrkA and EndrA receptors, respectively. Glebova & Ginty (2005).

7.1.2.2. Proximal axon growth

The first axons emerge from the SCG soon after it forms. Axon growth proceeds rapidly, with axons initially coursing along the vasculature en route to their targets, which may begin to be reached as early as E15 in rats (Rubin, 1985; Glebova and Ginty, 2005). Some of the trophic factors that promote the early stages of proximal axon growth from the developing SCG have been identified (Figure 5). As mentioned above, one such factor is artemin, which is expressed by the vasculature and by cells near to initial sympathetic projections (Honma et al., 2002). Both components of the artemin receptor, Ret (Pachnis et al., 1993) and GFRα3 (Honma et al., 2002) are expressed by neurons within the sympathetic chain from the earliest stages of development (Davies, 2009). Furthermore, artemin has been found to regulate the outgrowth of sympathetic neuron processes from cultured explants (Enomoto et al., 2001; Yan et al., 2003) and exert chemoattractive effects on sympathetic axons *in vitro* and *in vivo* (Enomoto et al., 2001; Honma et al., 2002; Yan et al., 2003). Crucially, axon growth deficits are observed in separate mouse strains deficient for *artemin, GFRα3* (Honma et al., 2002) and *Ret* (Enomoto et al., 2001). Taken together, these findings constitute an extremely strong case for artemin as a regulator of SCG neuron proximal axon growth. However, at least partial target field innervation is achieved in animals

deficient in any one of these components of artemin signalling, indicating that other factors must be involved in promoting the proximal growth of some axons (Glebova and Ginty, 2005).

Two other such factors that promote early axon growth from SCG neurons have been identified. Most recently, one study has implicated Endothelin-3 as a vascular-derived growth and guidance factor that acts early in development on a subset of SCG neurons projecting to the salivary glands along the external carotid artery (Makita et al., 2008). Endothelin-3 does not regulate initial axon growth from SCG neurons that innervate other target tissues, suggesting that newly born sub-populations of SCG neurons are molecularly distinct and different sub-populations of SCG neurons may be guided to their correct target fields by specific molecular cues (Makita et al., 2008). In addition, NT-3 is expressed along blood vessels during the initial period of sympathetic axon growth (Scarisbrick et al., 1993; Francis et al., 1999), and has been found to regulate neurite outgrowth *in vitro* through activation of TrkA (Belliveau et al., 1997). While the decreased survival of SCG neurons in NT-3 $^{-/-}$ mice was initially attributed to an ability of NT-3 to support neuronal survival through TrkA-dependent signalling (Belliveau et al., 1997; Francis et al., 1999), the finding that proximal axon growth is impaired in NT-3 $^{-/-}$ embryos before a reduction in the number of SCG neurons is apparent (Kuruvilla et al., 2004) has led to a reinterpretation of these findings. It is now thought that primary role of NT-3 in the developing sympathetic nervous system is to regulate proximal axon growth along the vasculature, and deficits in SCG neuron number later in development are secondary to the failure of sympathetic neurons to fully innervate their targets and obtain an adequate supply of NGF (Glebova and Ginty, 2005). HGF/Met signalling has also been shown to promote process outgrowth in cultures of embryonic (Maina et al., 1998) and postnatal (Yang et al., 1998) SCG neurons, although further work will be required to determine whether this is physiologically relevant *in vivo* (Glebova and Ginty, 2005; Davies, 2009).

7.1.2.3. Target field innervation

The establishment of adequate connectivity between neuronal populations and their target fields during development constitutes a basic requirement for the function of an adult nervous system and the survival of any organism. SCG neurons innervate a number of distinct targets including the iris where they regulate pupil

dilation; the lacrimal glands; the nasal and oral mucosa; the submandibular salivary glands where they regulate the volume and composition of salivary secretions; cranial blood vessels where they regulate vasoconstriction; the trachea where they regulate bronchodilation and the pineal gland. Although viable, mice lacking a functional sympathetic nervous system only survive in conditions entirely lacking environmental stress and temperature fluctuations (Glebova and Ginty, 2005).

SCG axons first begin to reach their peripheral targets around E15 (in rats) (Rubin, 1985; Glebova and Ginty, 2005) and proceed to grow and ramify in their target fields over a period of development extending into adolescence (Glebova and Ginty, 2005). This period of development has proved informative in understanding the actions of NGF, which succeeds NT-3 and artemin as the key regulator of axonal growth in late embryonic and early postnatal SCG development. Interestingly, a hierarchical cascade of neurotrophin signalling has been proposed to regulate the switch from NT-3 to NGF signalling. By this model, target-derived NGF is encountered by SCG neurons from E15 onwards and this up-regulates $p75^{NTR}$ expression. Increased expression of $p75^{NTR}$ reduces the ability of NT-3 to bind to and signal through TrkA, whilst concomitantly enhancing the efficacy of NGF/TrkA signalling (Kuruvilla et al., 2004). Of further interest, the perinatal period during which functional target field innervation begins to be established also represents the period at which the first role for CaSR signalling in the sympathetic nervous system was uncovered (Vizard et al., 2008). Thus, this process shall be discussed further, with particular emphasis on the critical role played by NGF.

7.1.2.3.1. Requirement for NGF-promoted axonal growth for innervation of distal SCG targets

In addition to its ability to promote the survival of developing SCG neurons (discussed in detail, section 7.1.2.4), NGF also promotes SCG neuron axon growth and branching. These two neurotrophic actions of NGF have been powerfully dissociated using an *NGF*$^{-/-}$/ *Bax*$^{-/-}$ double knock-out approach (Glebova and Ginty, 2004): Since Bax is an essential component of the apoptosis induction cascade in sympathetic neurons, *Bax*$^{-/-}$ animals do not exhibit the naturally occurring postnatal death of sympathetic neurons (Deckwerth et al., 1996). Therefore, the

innervation phenotype of *NGF*$^{-/-}$/*Bax*$^{-/-}$ double knock-out mice is independent of the survival promoting effects of NGF. Proximal axon growth still occurs in these animals, underscoring the importance of trophic factors other than NGF in regulating this process (Glebova and Ginty, 2005), but there is a striking failure to innervate many sympathetic target organs. *NGF*$^{-/-}$/*Bax*$^{-/-}$ mice display a total absence of innervation in some distal SCG targets, including the eye and the submandibular gland. However, the magnitude of innervation deficits varies according to the target, with some sympathetic targets, such as the trachea, exhibiting normal innervation at E16.5, indicating that, in contrast to the requirement for NGF to support the survival of all sympathetic neurons, some sympathetic neurons exhibit a heterogeneous requirement for NGF to achieve correct target innervation (Glebova and Ginty, 2004). This suggests that other factors may promote growth and ramification of axons in targets, such as the trachea, where innervation is not perturbed by NGF deletion (Glebova and Ginty, 2004).

7.1.2.3.2. Modulation of NGF-promoted axonal growth and branching

Whilst the crucial role that NGF plays in promoting sympathetic neuron axon growth and target field innervation has been well established, factors that modulate the efficacy of NGF in regulating axon growth have more recently been identified. Most relevant to this discussion is the discovery that Ca^{2+}_o regulates the NGF-dependent growth and branching of sympathetic axons of the SCG via CaSR-dependent signalling (Vizard et al., 2008). The modulation of NGF-dependent axon growth and branching by Ca^{2+}_o is restricted to a developmental window between E18 and postnatal day 0 (P0), a period during which CaSR expression is high. Although NGF also promotes the survival of SCG neurons during this period, Ca^{2+}_o dependent CaSR signalling does not modulate NGF-promoted survival *in vitro* or *in vivo* (Vizard et al., 2008).

In addition to CaSR, other factors have been identified that modulate NGF-promoted growth and branching of SCG neuron axons. For example, Glucocorticoid-induced tumor necrosis factor receptor-related protein (GITR), a member of the TNFSF, and its ligand (GITRL) have been shown to be expressed in developing SCG neurons during the period of target field innervation, and activation of GITR enhances NGF-promoted process outgrowth and branching

from these neurons (O'Keeffe et al., 2008) through reciprocal regulation of ERK and NF-κB signalling pathways (McKelvey et al., 2012). Furthermore, the long form of FLICE-inhibitory protein (FLIP-L) interacts with TrkA to enhance NGF-promoted growth of SCG neuron axons by facilitating the activation of ERK and NF-κB signalling pathways (Moubarak et al., 2010). Wnt5a, which is expressed at high levels by developing SCG neurons during the period of distal target field innervation, has also been shown to influence NGF-promoted growth *in vitro* and *in vivo* (Bodmer et al., 2009). In this case, *in vitro* data suggests that NGF/TrkA signalling promotes the expression of Wnt5a by SCG neurons and that Wnt5a in turn enhances the rapid branching and longer term elongation of SCG neuron axons through the local activation of PKC. Importantly, mice deficient for Wnt5a reduced innervation of NGF-expressing target tissues (Bodmer et al., 2009). Whilst GITR/GITRL signalling, FLIP-L and Wnt5a all modulate the efficacy of NGF-promoted axon outgrowth and branching from SCG neurons, none of these factors play a role in regulating NGF-promoted SCG neuron survival (O'Keeffe et al., 2008; Bodmer et al., 2009; Moubarak et al., 2010).

7.1.2.3.3. Intracellular effectors of NGF-promoted axonal growth and branching

The fact that Ca^{2+}_{o}, FLIP-L, Wnt5a and GITR/GITRL signalling all modulate NGF-promoted axonal growth and branching independently of NGF-promoted survival suggests that the intracellular signalling pathways that link NGF receptor activation to either axon growth or cell survival are divergent. The binding of NGF to TrkA has been shown to initiate numerous intracellular signalling pathways across a variety of cell types (Huang and Reichardt, 2003; Reichardt, 2006) (see Figure 3). These pathways will be briefly reviewed before focusing on the likely signalling mechanisms underlying NGF-promoted growth of sympathetic axons.

7.1.2.3.4. General aspects of NGF/TrkA signalling pathways

NGF-induced dimerization of TrkA leads to the phosphorylation of tyrosine residues in the cytoplasmic C-terminal domain of the receptor. Of the ten evolutionarily conserved tyrosines present, much research has focused on Y490 and Y785 (numbers refer to human TrkA). Phosphorylation of Y490 permits the docking of adaptor proteins that initiate the Ras/ERK signalling pathways, whereas phosphorylation of Y785 promotes the binding of phospholipase C (PLC)

γ and the activation of the PLCγ / protein kinase C (PKC) signalling pathway (Figure 3) (Huang and Reichardt, 2003; Reichardt, 2006). Both of these pathways are thought to mediate neuronal process outgrowth downstream of activated TrkA in certain cell types, as is the PI3K/Akt signalling pathway (Reichardt, 2006). The generalized signalling mechanisms for each of these three pathways are outlined below. In addition, a less well characterized signalling pathway involving Rho family GTPases, that may also mediate NGF/TrkA-promoted axon growth, is discussed briefly.

Transient activation of the Ras/MEK/ERK pathway can be achieved by binding of the Shc adaptor protein to phospho-Y490 (Reichardt, 2006). Tyrosine phosphorylation of Shc by TrkA promotes recruitment of a further adaptor protein, Grb2 coupled to Ras exchange factor SOS, thereby promoting Ras activity (Reichardt, 2006). In addition to promoting signalling through c-Raf/ERK and p38MAPK pathways (Xing et al., 1998), activated Ras may also crosstalk with the PI3K signalling pathway through the Ras binding domain of class I PI3Ks (Vanhaesebroeck et al., 2001; Vanhaesebroeck et al., 2010). However, in the pathway leading to activation of ERK1/2, Ras activation of Raf leads to the phosphorylation and activation of MAPK/ERK kinases (MEKs), which in turn activate ERK1/2 by phosphorylation on a tyrosine and a threonine residue. (English et al., 1999). These two residues are situated in the activation loop of ERK1/2 and have been identified as Thr202/Tyr204 and Thr185/Tyr187, in human ERK1 and ERK2 respectively (Roskoski, 2012). Ras can also activate ERK5 through the sequential activation of Wnk1, MEKK2 and MEK5 (Reichardt, 2006). Prolonged activation of the Ras/MEK/ERK pathway can be achieved by the binding of Frs2, rather than Shc, to phospho-Y490 (Reichardt, 2006). While Frs2 recruitment, like Shc, can result in the activation of ERK via sequential Grb2/SOS/Ras/c-Raf interaction, Frs2 can also signal through Rap-1 and B-Raf to activate MEK1/2 (Reichardt, 2006). In some instances, different MAPK signalling modules may converge on the same target molecule (Reichardt, 2006). For example, NGF promotes CREB phosphorylation at S133 through both ERK1/2 and p38 MAPK activation (Xing et al., 1998). In other cases MAPK targets may be non-overlapping (Reichardt, 2006). For instance, signalling endosome associated phospho-ERK1/2 extracted from NGF treated rat pheochromocytoma 12 (PC12) cells can activate the transcriptional regulator, Elk (Howe et al., 2001).

Interestingly, MAPK signalling pathways intersect with signalling pathways that are downstream of activated GPCRs at several points, permitting cross-activation in some instances. For example, PKC can activate both B-Raf and c-Raf, while PKA can activate Rap-1 (Sugden and Clerk, 1997; Luttrell, 2003).

The binding of PLCγ-1 to phospho-Y785 of TrkA results in its activation by phosphorylation (Reichardt, 2006). Activated PLCγ cleaves phosphatidyl inositol (4,5) bisphosphate (PIP_2) to inositol-(1,4,5)-trisphosphate (IP_3) and diacylglycerol (DAG). IP_3 binds to receptors in the membrane of the endoplasmic reticulum, resulting in release of Ca^{2+} into the cytoplasm. Together, DAG and elevated intracellular calcium (Ca^{2+}_i) are able to activate almost all isoforms of PKC, in addition to other targets including Ca^{2+}-calmodulin-dependent protein kinases (CaMKs) (Berridge et al., 2003; Reichardt, 2006). Ca^{2+}_i signalling is a complex process, involving many regulatory proteins and downstream effectors which can affect cellular function (Berridge et al., 2003; Petersen et al., 2005). These regulatory proteins and downstream effectors may include members of other signalling pathways downstream of TrkA. Interestingly, PKCδ is required for NGF promoted MEK1 and ERK1/2 activation in PC12 cells and hippocampal neurons (Corbit et al., 1999).

PI3K can be activated downstream of TrkA by both Ras dependent mechanisms, and Ras independent signalling through Shc-GAB1 or Irs1 (Reichardt, 2006). Activated PI3K phosphorylates phosphatidyl inositol substrates generating 3-phosphoinositide species. These phospholipids can have key roles in a wide variety of cellular processes, such as promoting survival by regulating Bax activity via Akt-dependent phosphorylation of BAD and regulating the NF-κB signalling via Akt-dependent phosphorylation of the regulatory IκB subunit (Reichardt, 2006). Bax is known to be a key component of the apoptotic death cascade in neurons deprived of trophic support (Deckwerth et al., 1996), while NF-κB has numerous roles in the regulation of neuronal survival and axonal growth during development (Gutierrez et al., 2005; Gutierrez et al., 2008; Gavalda et al., 2009; Gutierrez and Davies, 2011). Interestingly, PI3K represents a point where signalling pathways downstream of GPCRs may converge with signalling pathways downstream of TrkA. While different isoforms of PI3K were originally thought to be differentially coupled to Trk receptors and GPCRs, the former to class IA PI3Ks (which bind the

regulatory subunit p85) and the latter to class IB PI3Ks (which bind different regulatory subunits), some degree of crossover is now recognized (Vanhaesebroeck et al., 2010). The ability of both Trk receptors and GPCRs to activate Ras, which can in turn activate PI3K, provides one point of possible interaction between GPCR and TrkA-dependent signalling, while the direct activation of members of both PI3K sub-classes by GPCR-associated $G_{\beta\gamma}$ subunits provides another (Vanhaesebroeck et al., 2010).

Neurotrophins are also able to activate the Rho family of GTPases, which control aspects of cytoskeletal dynamics (Huang and Reichardt, 2001, 2003; Reichardt, 2006). RhoA reduces growth cone motility and inhibits axon growth from cultured ciliary ganglion neurons. The addition of NGF to cultures of these neurons inhibits the activity of RhoA and promotes axon elongation (Yamashita et al., 1999). However, whilst ciliary ganglion neurons express $p75^{NTR}$, they do not express TrkA, so the inhibition of RhoA activity by NGF and the concomitant increase in axon growth must be mediated by $p75^{NTR}$. Therefore, the inhibition of RhoA is unlikely to contribute to NGF/TrkA-mediated axon growth from other neuronal types (Huang and Reichardt, 2001). There is some evidence that Rho family GTPases comprise part of the intracellular signalling network that regulates axonal growth and guidance in response to neurotrophins in other neural cell types. For example, Cdc42 and Rac activity mediate Xenopus spinal neuron axon turning in response to a BDNF gradient (Yuan et al., 2003). In addition, RhoG appears to act upstream of Cdc42 and Rac to mediate NGF-promoted process outgrowth from PC12 cells (Katoh et al., 2000). Although the mechanisms by which Trk receptors couple to Rho family GTPases are not yet clearly defined, numerous pathways have been suggested, including the regulation of Rac activity by Ras or SOS and the localized activation of Rho family GTPases at the plasma membrane following PI3K stimulated accumulation of 3-phosphoinositides (Huang and Reichardt, 2003; Reichardt, 2006). Interestingly, CaSR can couple to and activate RhoA downstream of an interaction between filamin and the C-terminal tail of CaSR (Pi et al., 2002).

In conclusion, three major signalling pathways lie downstream of activated TrkA, and experiments in a variety of cell types have led to the suggestion that each could contribute to the intracellular signalling cascade that mediates NGF-promoted axonal growth and branching (Huang and Reichardt, 2001, 2003;

Reichardt, 2006). Importantly, there are contexts in which CaSR signalling can converge with each of these signalling pathways (Hofer and Brown, 2003; Ward, 2004), providing potential opportunities for crosstalk downstream of activated CaSR and TrkA receptors. One major caveat of the data currently in the literature is that much of it has been obtained from experiments with PC12 cells, a common model of NGF-promoted axon growth. In addition to the fact that PC12 cells are a transformed cell line, both differentiation into a neuron-like phenotype and axon extension are stimulated by NGF in these cells (Xing et al., 1998; Corbit et al., 1999; Howe et al., 2001; Sofroniew et al., 2001; Goold and Gordon-Weeks, 2005; Mitchell et al., 2012). Therefore, unambiguous verification of which signalling pathways are actually involved in mediating NGF-promoted axonal growth, as distinct from artefactual effects on differentiation, requires both *in vitro* and *in vivo* data from real neurons.

7.1.2.3.5. NGF-promoted axonal growth signalling in sensory neurons

The most advanced studies into the signalling mechanisms that underlie NGF promoted axonal growth, in isolation from survival and *in vitro* differentiation related artifacts, have been performed in sensory neurons. A recent study has used transgenic mice that allow a conditional deletion of functional MEK1/2 and ERK1/2 specifically in sensory neurons to define the roles of ERK1/2 signalling in NGF-dependent survival of and cutaneous target field innervation by sensory neurons of the DRG (Newbern et al., 2011). ERK1/2 signalling is not required to promote the survival of NGF-dependent DRG neurons, nor is it required for initial axon outgrowth from DRG neurons. However, postnatal mice lacking functional ERK1/2 in DRG neurons display a significant reduction in the density of cutaneous innervation by DRG neurons compared to wild type mice (Newbern et al., 2011). Downstream targets of activated ERK1/2 include the transcription factor, Serum Response Factor (SRF). ERK1/2-dependent activation of SRF is required for NGF-promoted axon outgrowth from embryonic mouse DRG neurons *in vitro* and for correct target field innervation by NGF-responsive DRG neurons *in vivo* (Wickramasinghe et al., 2008). In contrast, SRF does not mediate the NGF-dependent survival of DRG neurons *in vitro* or *in vivo*. (Wickramasinghe et al., 2008; Newbern et al., 2011). Thus, there is good evidence that ERK1/2 and its downstream target, SRF are selectively required for NGF/TrkA-promoted axon growth from sensory neurons.

7.1.2.3.6. NGF-promoted axonal growth signalling in sympathetic neurons

There are numerous indications that local actions of NGF on distal axons of SCG neurons are critical to its growth-promoting effects (Harrington and Ginty, 2013). Early experiments in compartment cultures showed that NGF applied into a distal axonal compartment supports local axon growth, whereas application of NGF to the soma compartment only does not support the extension of axons into a compartment lacking NGF (Campenot, 1977). It was subsequently found that local PKC activity in distal axons supports sympathetic axon growth (Campenot et al., 1994). An important recent study has revealed that calcineurin, a Ser/Thr phosphatase responsive to changes in Ca^{2+}_i, is required for NGF-, but not NT-3-promoted sympathetic axon growth, both *in vitro* and *in vivo* (Bodmer et al., 2011). Calcineurin promotes growth by acting locally in distal axons, downstream of NGF-induced PLCγ activation, to regulate TrkA internalization via dynamin1 dephosphorylation (Bodmer et al., 2011). Interestingly, the modulation of NGF-promoted sympathetic axon growth by Wnt5a is mediated by local axonal PKC activity downstream of Wnt receptor-induced PLCγ activation (Bodmer et al., 2009). It therefore seems likely that local PLCγ activity and signalling through Ca^{2+}_i responsive kinases/phosphatases together constitute a key mediator of NGF-promoted axonal growth in sympathetic neurons.

Interestingly, Y785 of TrkA is substituted for glutamine at the equivalent residue of the single Trk species expressed by Amphioxus (Benito-Gutiérrez et al., 2006) and mammalian neurotrophins are unable activate PLCγ signalling from it (Reichardt, 2006). This raises the possibility that the coupling of Trk receptors to the PLCγ/PKC pathway may be a vertebrate evolutionary advance, paralleling the evolution of the neural crest, thus lending further support to the suggestion that the PLCγ/PKC signalling pathway plays a key role in regulating axon growth from neural crest derived, mammalian sympathetic neurons (Reichardt, 2006).

Whilst short-term NGF-promoted growth (<24 hours) of cultured SCG neuron axons does not require transcription, longer-term axon growth in response to NGF does (Bodmer et al., 2011). This has led to the suggestion that distinct signalling mechanisms may translate TrkA activation into short-term local growth and longer-term sustained growth (Harrington and Ginty, 2013). Since sustained axonal growth in response to NGF requires transcription, one possible signalling

mechanism underlying long term axonal growth could be ERK1/2 mediated activation of SRF that has been shown to be required for NGF-promoted growth of embryonic DRG neuron axons (Wickramasinghe et al., 2008). Indeed, it has been suggested that SRF-dependent transcription may underlie the increase in Wnt5a expression in response to NGF that appears to mediate NGF-promoted axon growth and branching (Bodmer et al., 2009). Alternatively, NFAT family transcription factors, downstream targets of calcineurin, have also been implicated in mediating the NGF-dependent growth of sensory neuron axons *in vivo* (Graef et al., 2003). In addition, NGF promotes significantly less axonal outgrowth from E13.5 DRG and E16.5 SCG explants derived from CREB null-mutant embryos compared to explants from wild type embryos (Lonze et al., 2002). Whilst there are dramatic peripheral innervation defects in CREB null mice *in vivo*, CREB is also required to promote the survival of developing sensory and sympathetic neurons, making it hard to dissociate the roles of CREB in promoting survival and regulating target field innervation. Moreover, the analysis of CREB deficient embryos suggests that CREB is also part of NT-3- and BDNF-induced signalling pathways, not just NGF-induced signalling (Lonze et al., 2002).

ERK1/2 has also been frequently implicated as an intermediary in the signalling cascade that leads to the NGF-promoted growth of sympathetic axons. Unfortunately, although Wnt1-cre-induced conditional deletion of ERK1/2 was reported to effectively extinguish ERK1/2 expression in sympathetic neurons (Newbern et al., 2011), the authors only reported phenotypic data on the effect of ERK1/2 deletion on developing peripheral sensory neurons. However, ERK1/2 signalling has been shown to mediate NGF-promoted process growth from both PC12 cells and sympathetic neurons *in vitro* (Thompson et al., 2004; Goold and Gordon-Weeks, 2005), by modulating glycogen synthase kinase 3 (GSK3) β-dependent phosphorylation of microtubule associated protein (MAP) 1B (Goold and Gordon-Weeks, 2005). Furthermore, proteins that have been shown to selectively modulate NGF-promoted axon growth do so by regulating ERK1/2 signalling. These proteins include, GITR (O'Keeffe et al., 2008; McKelvey et al., 2012), FLIP-L (Moubarak et al., 2010) and reverse signalling by TNFR1 through TNFα (Kisiswa et al., 2013).

7.1.2.4. Death versus survival in the developing SCG

There is now ample evidence to support neurotrophic theory within the PNS (Oppenheim, 1991), and the vital role played by NGF in promoting the survival of developing sympathetic neurons has been demonstrated by their near total loss in neonatal *NGF* $^{-/-}$ and *TrkA* $^{-/-}$ mice (Crowley et al., 1994; Smeyne et al., 1994; Fagan et al., 1996).

Recent data have provided an interesting new insight into the mechanism of neuronal death in the absence of neurotrophin signalling. TrkA and TrkC (but not TrkB) have been reported to act as "dependence receptors", which promote apoptosis in the absence of NGF and NT-3, respectively (Nikoletopoulou et al., 2010). In support of this, the majority of neurons in SCG cultures established from E17 TrkA deficient embryos survive in the absence of NGF, whereas wild type SCG neurons of the same age rapidly die when cultured without NGF. The pro-apoptotic action of non-ligated TrkA appears to be independent of the tyrosine kinase activity of TrkA (Nikoletopoulou et al., 2010). These data may provide an explanation for the neurotrophin-independent survival of early sympathetic neuroblasts and neurons (Ernsberger et al., 1989), since the onset of NGF-dependent survival parallels the developmental up-regulation of TrkA at the earliest stages of target innervation when neurons begin to encounter NGF *in vivo* (Wyatt and Davies, 1995). Although E17 TrkA deficient SCG neurons survive in culture without NGF, the addition of NGF to cultures rapidly induces their apoptotic death. The additional deletion of $p75^{NTR}$ from TrkA deficient E17 SCG neurons protects most neurons from NGF-induced apoptosis indicating that, in the absence of TrkA expression, NGF induces the death of SCG neurons by $p75^{NTR}$-dependent signalling (Nikoletopoulou et al., 2010). These data suggest that a reinterpretation of the mechanism underlying the loss of sympathetic neurons in *TrkA* $^{-/-}$ mice (Smeyne et al., 1994; Fagan et al., 1996) may be warranted. Rather than SCG neuron death in these mice simply being due to the lack of NGF/TrkA survival signalling, death may also be induced by NGF/$p75^{NTR}$ death signalling (Nikoletopoulou et al., 2010).

BDNF, acting via $p75^{NTR}$ at the cell soma can also induce the apoptosis of SCG neurons exhibiting low levels of retrograde NGF/TrkA signalling from distal axonal arbors (Davies, 2008; Deppmann et al., 2008). Interestingly, retrograde NGF/TrkA

signalling induces the synthesis of BDNF, suggesting a potential mechanism whereby a subset of SCG neurons that have high levels of retrograde NGF/TrkA signalling can induce the apoptosis of less competitive neighboring neurons within the SCG (Davies, 2008; Deppmann et al., 2008). Accordingly, apoptosis does not occur during its normal developmental window in $p75^{NTR\,-/-}$ animals (Bamji et al., 1998). Additional evidence has accumulated over the years pointing to a role for $p75^{NTR}$ in the induction of apoptotic neuronal cell death (Glebova and Ginty, 2005).

In the presence of NGF, signalling through TrkA promotes the survival of SCG neurons through mechanisms that are incompletely characterized (Glebova and Ginty, 2005; Harrington and Ginty, 2013). It is likely that this involves the suppression of pro-death signalling, including blocking the translocation of Bax to the outer mitochondrial membrane, thereby inhibiting the release of cytochrome c from the inter-membrane space and preventing apoptosome-mediated caspase activation (Deckwerth et al., 1996; Putcha et al., 1999). In addition, it is likely that pro-survival transcriptional pathways are also engaged by NGF/TrkA-dependent signalling (Harrington and Ginty, 2013). Pro-survival pathways may include the activation of CREB in the soma following retrograde NGF/TrkA signalling from the periphery (Riccio et al., 1997). In support of this, retrograde NGF/TrkA signalling has been shown to activate ERK5, which in turn induces the activation of CREB to promote the survival of embryonic rat DRG neurons (Watson et al., 2001). In addition, CREB deficient mice display a significant reduction in the number of DRG and SCG neurons compared to wild type mice (Lonze et al., 2002). NGF/TrkA retrograde signalling and ERK5 activation can also promote the survival of embryonic rat DRG neurons by increasing the expression of the MEF2D transcription factor, thereby enhancing the expression of bcl-w, an anti-apoptotic member of the bcl2 family (Pazyra-Murphy et al., 2009). Thus, both transcription dependent and independent mechanisms, impinging on pro- and anti-apoptotic pathways, are likely to be involved in the NGF-promoted survival of SCG neurons.

In conclusion, there is now ample evidence to support neurotrophic theory in the PNS (Oppenheim, 1991; Davies, 1996, 2003; Glebova and Ginty, 2005). The ability of NGF, the founding member of the neurotrophins, to promote the survival of developing SCG neurons and to enhance the growth of their axons is well established (Levi-Montalcini, 1987; Huang and Reichardt, 2001; Glebova and Ginty,

2004, 2005; Harrington and Ginty, 2013). These effects can be dissociated (Glebova and Ginty, 2004), and may be regulated by distinct NGF-dependent signalling pathways. Finally, signalling pathways that have been shown to mediate NGF-promoted axonal growth provide numerous opportunities for intersection with signalling pathways downstream of GPCRs, such as CaSR (Sugden and Clerk, 1997; Huang and Reichardt, 2003; Davies, 2009).

7.2. CNS Development

In contrast to the PNS, the whole CNS develops from the embryonic neural tube, the rostral part of which can be subdivided on the basis of three vesicles: The forebrain, the midbrain and the hindbrain. The following section will review the development of two forebrain structures; the hippocampus (where the majority of CNS experimental data contained in this thesis has been obtained) and the cortex, along with the hindbrain structure of the cerebellum. Information on the cortex and cerebellum are provided for comparative purposes and to help interpret CaSR expression data in these brain regions.

7.2.1. Overview of Hippocampal Development

One structure that emerges from the developing forebrain is the telencephalon. In the mouse, the dorsomedial portion of the telencephalon invaginates between E10.5 - 12.5 to give rise to the hippocampal primordia of each cerebral hemisphere (Grove and Tole, 1999; Tole and Grove, 2001). Most of the cell types populating the adult hippocampus derive from the hippocampal primordia, with the exception of interneurons which migrate into the hippocampus from the ventral telencephalon (Danglot et al., 2006). In adulthood, the hippocampus forms part of the medial temporal lobe, and plays important roles in learning and memory including episodic memory, spatial navigation, imagining the future and the familiarity component of recognition memory (Aggleton and Pearce, 2001; Brown and Aggleton, 2001; Aggleton and Brown, 2006; Eichenbaum et al., 2007; Maguire and Mullally, 2013). It has been proposed that hippocampal dependent learning and memory may require structural plasticity, which along with numerous technical advantages, has led to the establishment of the hippocampus as a leading model for studies of synapse formation and function (Bourne and Harris, 2008). The development of the hippocampus, especially hippocampal synaptogenesis, is a key aspect of the experimental data of this thesis and shall thus be reviewed in some detail here.

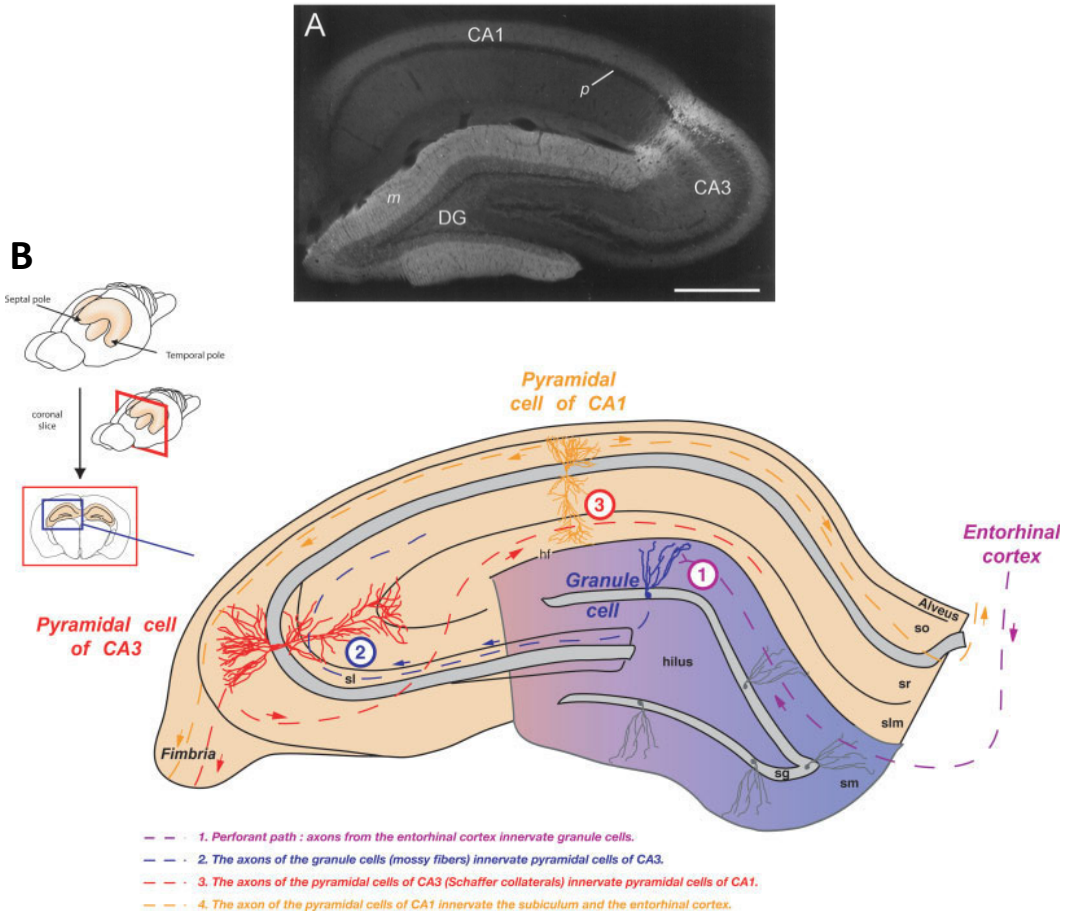

Figure 6 The hippocampal formation

A, A rat hippocampal slice immunostained for the post-synaptic protein α-actinin-2 revealing the various subfields. The small CA2 region is highlighted by the enrichment of α-actinin-2 expression. p = pyramidal layer, m = molecular layer, scale bar = 500µm. From (Wyszynski et al., 1998).
B, Information processing by the hippocampal formation has traditionally been understood in light of the anatomically formed "tri-synaptic loop" between entorhinal cortex, dentate gyrus granule cells, pyramidal neurons of CA3 and pyramidal neurons of CA1. so = stratum oriens, sr = stratum radiatum, slm = stratum lacunosum-moleculare, sm = stratum moleculare. From Danglot *et al,* 2006.

7.2.1.1. Early Specification & Generation of Pyramidal Neurons

The neuroepithelium of the hippocampal primordium contains progenitor cells that will give rise to pyramidal neurons, granule cells and glial cells of the mature hippocampus (Altman and Bayer, 1990). The mature hippocampus is composed of several subfields: The Dentate Gyrus (DG), CA1, CA3 and CA2, the latter of which is a transitional region between CA1 and CA3 (Figure 6). Although the hippocampal subfields only begin to be distinguishable by morphological and gene expression criteria around E15.5 (Grove and Tole, 1999; Tole and Grove, 2001), there is evidence to suggest that subfield-specific progenitors are molecularly specified as early as E12.5 during the formation of the hippocampal primordium (Tole and Grove, 2001). Despite this, there are large differences between the developmental stages at which neurogenesis occurs within different subfields in the maturing hippocampus (Figure 7) (Danglot et al., 2006). In mice, the generation of pyramidal neurons occurs between E14-15 for CA3 and E15-16 for CA1, after which newly born neurons migrate radially towards the hippocampal plate (which later in development becomes the pyramidal layer). Whilst migration takes CA1 neurons four days to complete, CA3 neurons take longer as they must follow a curved trajectory around CA1 (Danglot et al., 2006). As the pyramidal neurons migrate, they maintain a process attached to the ventricular zone, and extend one ahead of their direction of travel to the hippocampal fissure. Thus, by late in embryonic development, hippocampal pyramidal neurons only exhibit a very simple dendritic tree, which will branch further as afferent axons arrive in early postnatal development (Turner et al., 1998). DG granule cell neurogenesis begins much later than pyramidal cell neurogenesis (at E20 in rat) and 85% of the DG cell population is generated postnatally (Danglot et al., 2006).

7.2.1.2. Origin and Migration of Interneurons

It has emerged that both the origin and migration of interneurons are strikingly different from those of pyramidal cells. Hippocampal interneurons are not produced in a local proliferative zone, but in the caudal & medial ganglionic eminences of the ventral telencephalon. Newly generated interneurons are then required to undergo a long distance, tangentially oriented, dorsal migration towards the developing hippocampus (Danglot et al., 2006; Huang et al., 2007c). Whilst this is in marked contrast to the shorter radial migration of pyramidal cells, interneurons may finally adopt a form of radial migration to colonize the

hippocampus or cortex towards the end of their migration (Danglot et al., 2006; Huang et al., 2007c).

Interestingly, gamma-aminobutyric acid (GABA)-ergic neurons initially colonize the *stratum lacunosum moleculare* and *stratum radiatum* (Figure 6B), between postnatal day (P) 0 and P5, where they establish synaptic contacts with hippocampal afferents before the dendrites of pyramidal neurons, the eventual targets of such afferents, have been established (Supèr et al., 1998; Danglot et al., 2006). After P5, there is an approximately 50% reduction of GABAergic neurons in these layers that is thought to result from a combination of apoptosis and the migration of interneurons into other laminae between P5 – P15 (Jiang et al., 2001).

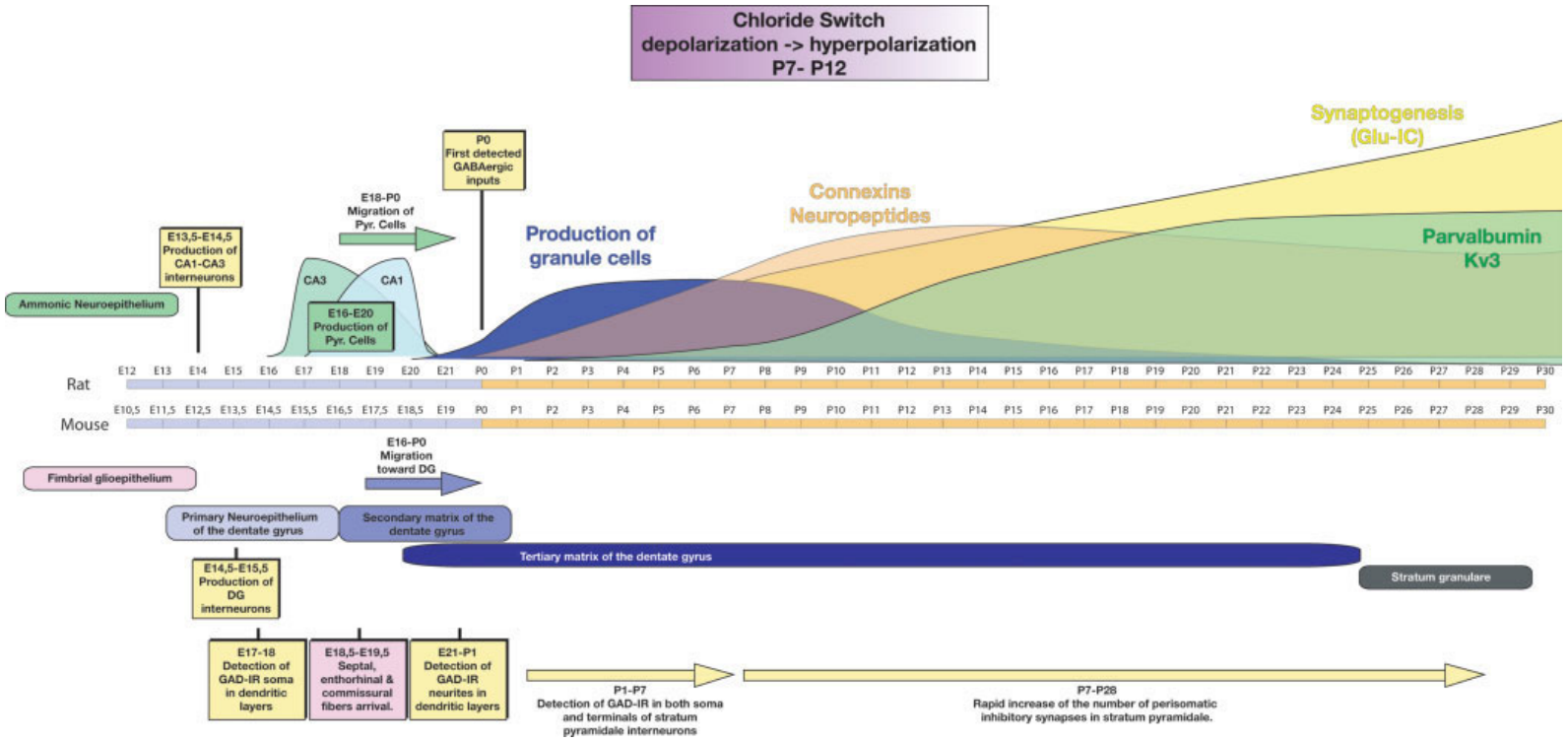

Figure 7: Stages of *in vivo* hippocampal development

Production of interneurons and pyramidal cells, the principle output cells of the hippocampus occurs embryonically. The vast majority of dentate gyrus granule cells are produced postnatally. Synaptogenesis also occurs predominantly in the postnatal period, as afferent fibres innervate the hippocampal formation. From Danglot *et al,* 2006.

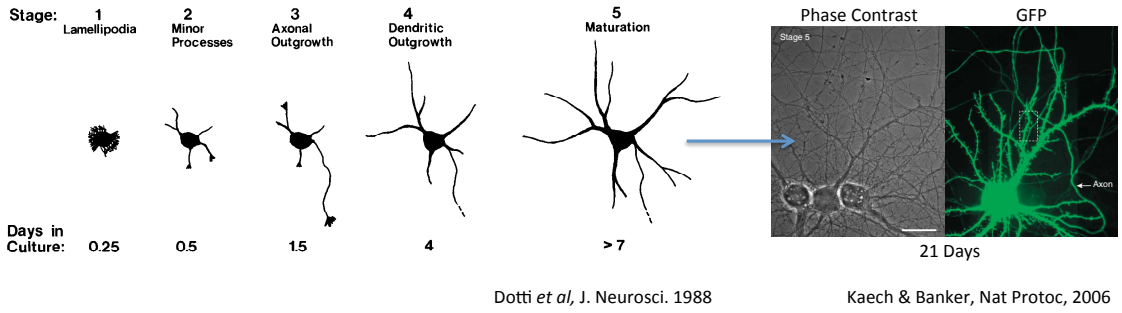

Figure 8: Stages of *in vitro* hippocampal neuron development

Over time in culture, hippocampal neurons dissected from late embryonic rodents follow a well-defined sequence of transitions through maturation into a form that shares many characteristics of their adult form *in vivo*. After initial extension of lamellipodia, neurons initiate several minor processes. At around 1.5 days *in vitro* (DIV), one of these processes is specified as the axon and begins to grow rapidly. Later, the remaining processes, now specified as dendrites, also increase their rate of growth, and from about 7 DIV the neuron acquires an arborized structure and forms many synapses. By 21 DIV neurons will have extended dendritic spines. Since hippocampal neurons require high density cultures to survive, a fraction are frequently visualised by ectopic expression of GFP, which allows careful analysis of their morphology. Adapted from Dotti *et al* (1988) and Kaech & Banker (2006).

7.2.1.3. Overview of development *in vitro*

The relative simplicity of the dendritic tree, comparatively easy dissociation of tissue and lack of granule cells in the late embryonic hippocampus has led many researchers to investigate the developmental maturation of pyramidal neurons in dissociated hippocampal cultures. The *in vitro* developmental maturation of hippocampal pyramidal neurons has been characterized into clearly defined stages by Dotti *et al* (Figure 8) (Dotti et al., 1988) that encompass the initial extension of lamellipodia and neurites; polarization and axonal growth; dendritic growth and arborization, and functional and morphological maturation. Hippocampal neuron cultures provide a particularly attractive model for investigating pyramidal neuron development, as the pyramidal population of the hippocampus is less diverse than the cortex, the majority of neurons in the hippocampus are pyramidal and cultured hippocampal neurons display similar morphological criteria *in vitro* compared to those by which they are recognizable *in vivo* (Kaech and Banker, 2006).

7.2.1.4. Polarization, axonal and dendritic growth

One of the most distinguishable characteristics of pyramidal neurons is their polarization. Pyramidal neurons extend a single axon, which is often long, thin and

highly branched, and multiple dendrites, which are shorter, tapered processes extending radially from the cell soma (Dotti et al., 1988; Kaech and Banker, 2006). In hippocampal cultures, polarization begins by the selective accumulation and/or activation of key cellular components within one of the undifferentiated neurites that is destined to become the axon (Arimura and Kaibuchi, 2007; Shelly et al., 2010). These cellular components include evolutionarily conserved proteins such as small guanosine triphosphatases (GTPases), including Cdc42, RAP1B and R-Ras, and PI3K. PI3K in particular, along with related signalling proteins, is emerging as a key regulator of polarization and axonal elongation by signalling to the cytoskeleton and modulating actin and microtubule dynamics (Shi et al., 2003; Da Silva et al., 2005; Jiang et al., 2005; Arimura and Kaibuchi, 2007; Fivaz et al., 2008; Barnes and Polleux, 2009). The coordination of specifying a single process as an axon and the remaining processes as dendrites has recently been found to occur through reciprocal regulation of cyclic adenosine monophosphate (cAMP) and cyclic guanosine monophosphate (cGMP) signalling. cAMP levels are specifically increased in the process that becomes the axon, thereby decreasing cAMP levels in the other processes that become specified as dendrites. Conversely, cGMP levels are higher in specified dendrites than they are in axons (Shelly et al., 2010). In this manner, the initiation of a single axon is ensured. While the application of modern techniques indicates that polarization may occur as neurons migrate *in vivo,* further work is required to assess the *in vivo* relevance of the factors and signalling pathways involved in polarization *in vitro* (Barnes and Polleux, 2009).

The branching pattern of the dendritic tree has a large effect on the transmission of electrical activity from synapses to the cell soma, and thus has enormous functional importance for information processing in the CNS (Häusser et al., 2000). Many studies have used late embryonic hippocampal cultures to reveal roles for neurotrophic factors, including NGF (Chacón et al., 2010) and BDNF (Ji et al., 2005; Ji et al., 2010), in regulating dendritic growth. In addition, studies using neonatal hippocampal organotypic slices have demonstrated that Nogo-a/Ngr1 and $p75^{NTR}$ signalling regulate dendrite architecture (Zagrebelsky et al., 2005; Zagrebelsky et al., 2010). Most dendritic development *in vivo* takes place postnatally. While still simple at late gestational stages, both apical and basal dendrites of the hippocampal pyramidal neurons begin to branch to a limited degree in the first days of postnatal development. However, it is when the first synapses from

afferent connections begin to form during the first postnatal week that structural remodeling of dendrites begins in earnest. During this period, many smaller side branches are added to both apical and basal dendrites, and dendritic spines form (see section 7.2.1.6). By about P20, the dendritic tree acquires its mature adult shape (Turner et al., 1998). The acquisition of dendritic complexity during the first few postnatal weeks raises the possibility that, whilst intrinsic developmental programs may play an important role in the acquisition of basic dendritic form, the establishment and maintenance of a highly branched dendritic tree may require active synapses and extracellular factors.

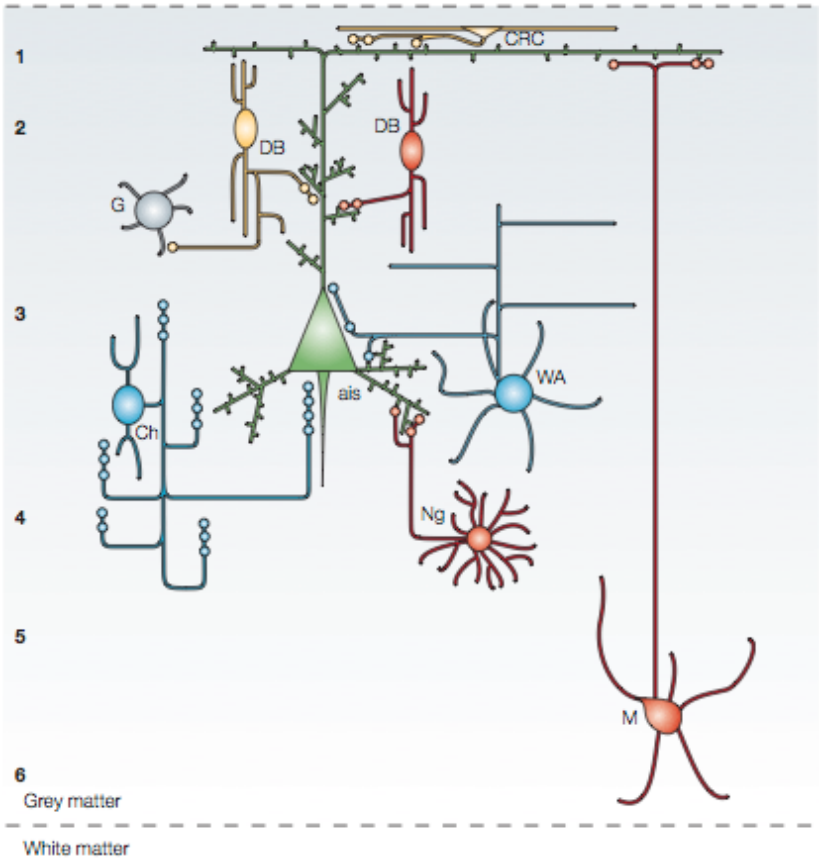

Figure 9: Different interneuron classes target characteristic compartments of post-synaptic pyramidal neurons

Unlike excitatory synapses, which characteristically form onto dendritic spines, inhibitory interneurons target various morphological regions of pyramidal neurons (green). In the cortex for example, Chandelier cells (Ch) contact the axon initial segment and proximal dendrites, wide-arbour basket cells (WA) target the cell soma in addition to proximal dendrites, and Martinotti neurons (M) provide inhibitory input to distal dendrites of pyramidal cells. From Lewis *et al* (2005).

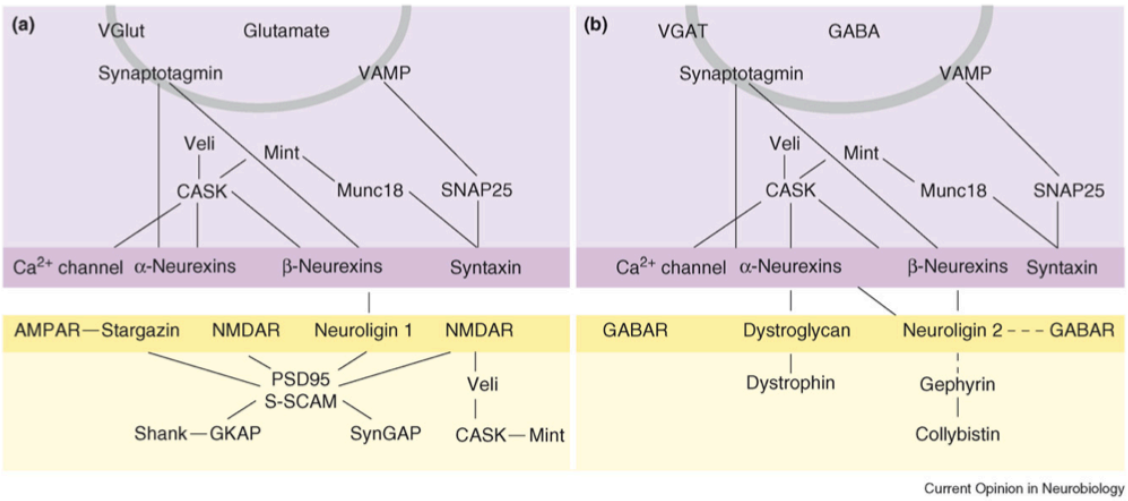

Figure 10: Distinctive molecular architecture of excitatory and inhibitory synapses

Excitatory synapses (left) can be distinguished from inhibitory synapses (right) on the basis of several molecular components, in addition to their cellular localisation and electrophysiological properties. These include the presynaptic expression of the vesicular neurotransmitter transporters, vGlut versus vGAT, respectively, and the post-synaptic scaffolding proteins PSD-95 and Gephyrin that are found at excitatory and inhibitory synapses, respectively. From Craig & Kang (2007).

7.2.1.5. Synaptogenesis

As sites where communication between nerve cells occurs, synapses are critical for the functioning of the nervous system. Accordingly, a vast number of studies have aimed to uncover aspects of the mechanisms by which synapses are formed during development. One major advance in our understanding of synaptic morphology occurred through the work of the pioneer neurobiologist Santiago Ramon y Cajal, who first observed that "the surface of Purkinje cell dendrites appears bristling with thorns or short spines" and proposed that "such spines could be the points where electrical charge or current is received" (Cajal et al., 1888, 1889). It has since become clear that dendritic spines form the postsynaptic component of the majority of excitatory synapses in the mammalian brain, so understanding the mechanisms of spinogenesis has become closely associated with the study of synaptogenesis. In contrast to excitatory synapses, inhibitory synapses do not form onto dendritic spines. Rather, different classes of interneurons directly target characteristic cellular compartments of their post-synaptic neuronal partners (Figure 9) (Craig and Kang, 2007). In addition, while there are several common components of excitatory and inhibitory synapses, several important molecular distinctions can be drawn between these two basic synaptic classes (Figure 10) (Craig and Kang, 2007).

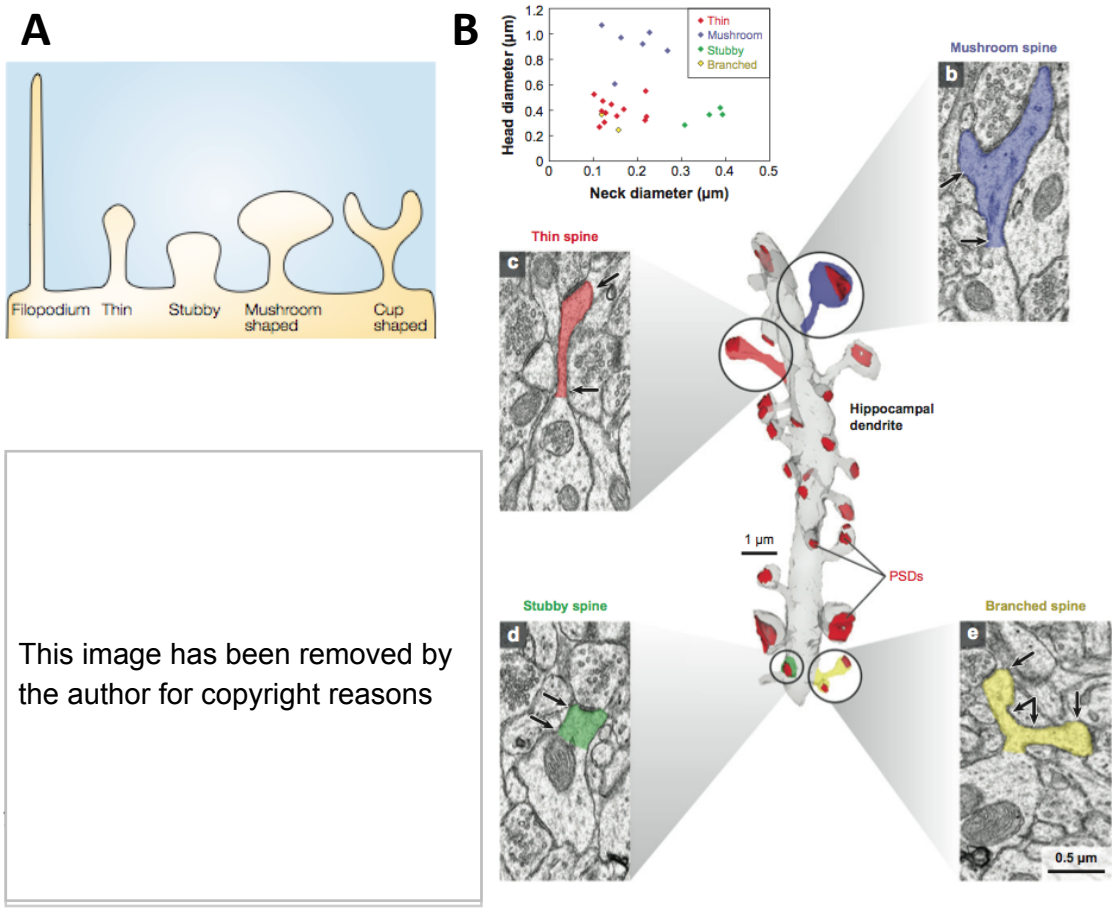

This image has been removed by the author for copyright reasons

Figure 11: Morphological classification and developmental plasticity of dendritic spines

A, Dendritic spines are found in a variety of shapes and sizes, from long, thin filopodia to a variety of headed protrusions that are attached to the dendritic shaft by a thin neck. Modified from Hering & Sheng (2001).
B, The wide variety of spine morphologies can be most accurately imaged by electron microscopy, from which it can be incontrovertibly established that all headed spine types can bear post synaptic densities (PSDs). Modified from Bourne & Harris (2008).
C, Through postnatal development there is a decrease in the number of filopodia and a concomitant increase in the number of headed protrusions, resulting in an overall increase in spine density. In many cases, changes in the size of dendritic spines correlate with functional synaptic changes such as LTP and LTD, being increased and decreased in size, respectively (See text). Modified from Sala *et al* (2008).

7.2.1.5.1. Excitatory synapse formation

Dendritic spines are tiny, actin-rich sub-cellular compartments, usually between 0.2-2 µm in diameter and up to 5 µm long (Ji et al., 2005; Jiang et al., 2005; Calabrese et al., 2006; Bourne and Harris, 2008), which can exhibit a variety of morphologies (Figure 11A, B). Characteristic changes in spine morphology and density occur over postnatal development (Figure 11C) (Sala et al., 2008). As

development proceeds, the number of dendritic filopodia decreases and there is a concomitant increase in the number of mature, headed dendritic spines. A number of studies have sought to investigate whether there could be a causal link between these two developmental trends, and have found evidence that contact between a dendritic filopodia and an axon can lead to the transformation of the filopodia into a dendritic spine in both hippocampal cultures (Ziv and Smith, 1996) and the cortex *in vivo* (Zuo et al., 2005). These findings have contributed to a model in which highly mobile filopodia are considered spine precursors, sampling the extracellular environment and transforming into a mature spine after contact with an axon branch or terminal (Figure 12A, B) (Ethell and Pasquale, 2005; Sala et al., 2008; Yoshihara et al., 2009). In this model, axon/filopodia contact leads to synapse assembly at the point of contact and this is followed by the subsequent maturation of the filopodia into a dendritic spine. Ephrin/EphB receptor forward signalling has been shown to induce dendritic spine formation (Kayser et al., 2008). The loss of functional EphB receptors at early developmental stages reduces filopodial motility, synaptogenesis and spine formation in dissociated cortical neuron cultures. In contrast, the loss of functional EphB receptors at later developmental stages has no effect on spine motility and little effect on synaptogenesis (Kayser et al., 2008). Taken together, these data suggest that the filopodia-mediated mechanism of synaptogenesis and spinogenesis may predominate at early developmental stages, at least in cortical neurons (Yoshihara et al., 2009).

However, other models of spinogenesis have also been proposed that do not involve dendritic filopodia (Figure 12A) (Ethell and Pasquale, 2005). In a second model, axonal filopodia (such as those from growth cones) may initiate a direct contact with a dendritic shaft, inducing spinogenesis and subsequent synaptogenesis. This model has been suggested as a dominant mechanism for axon terminal synapse formation (Shen and Cowan, 2010) A third model proposes that spinogenesis substantially precedes axonal contact and synaptogenesis. In support of this, spines can emerge *de novo* from dendritic shafts, without filopodial intermediates and axonal contact, in developing cortical slices following the uncaging of glutamate by two-photon microscopy (Kwon and Sabatini, 2011).

A

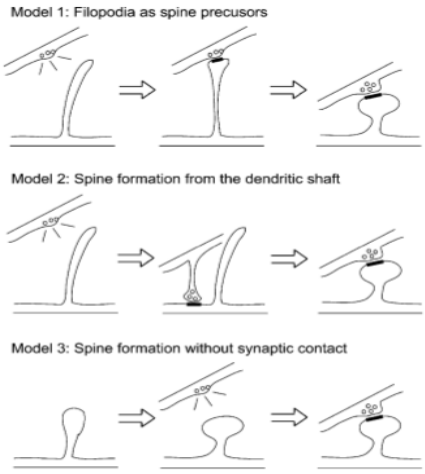

B

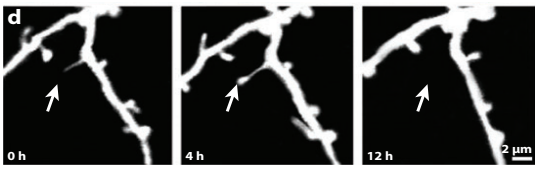

C

Molecules involved in dendritic filopodia formation.

Molecule	Description	Approach	Filopodia formation	Spine formation	Reference
Brakes of spine maturation					
Telencephalin (TLCN; ICAM-5)	Ig superfamily cell adhesion molecule that interacts with ERM proteins	Overexpression Gene knockout	Up Down	Down Up	Matsuno *et al.* [32**]
Ezrin/Radixin/Moesin (ERM)	Actin-binding proteins that interact with TLCN	Constitutive active Gene silencing	Up Down	Not analyzed Up	Furutani *et al.* [33]
SynGAP	Ras GTPase-activating proteins	Gene knockout	Down	Up	Vazquez *et al.* [30]
Ras-PI3K-Akt-mTOR	Small GTPase and its downstream signaling molecules	Constitutive active Dominant negative	Up Down	Down Up	Kumar *et al.* [31]
Polo-like kinase 2 (Plk-2; SNK)	Ser/Thr kinase that phosphorylates and destabilizes spine-associated RapGAP (SPAR)	Overexpression	Up	Down	Pak and Sheng [29]
Accelerators of spine maturation					
CaMKII	Calcium/calmodulin-dependent Ser/Thr kinase	Constitutive active	Up	Up	Jourdain *et al.* [19]
Syndecan-2	Heparan sulfate proteoglycan linked to neurofibromin-PKA-Ena/VASP pathway	Overexpression Gene silencing	Up Down	Up Down	Ethell and Yamaguchi [26] Lin et al. [27]
Paralemmin-1	Lipid-anchoring phosphoprotein	Overexpression Gene silencing	Up Down	Up Not analyzed	Arstikaitis *et al.* [28]

Figure 12: Models of and factors involved in spinogenesis

A, The dominant model for the formation of dendritic spines in development is that they proceed from a filopodial intermediate (Model 1), which exists for only ~10 minutes, but is highly mobile and samples the extracellular environment. Upon contact with an axon, synapse formation between the axon and filopodia is initiated through recruitment of synaptic scaffolding and adhesion proteins, together with neurotransmitter receptors, at their appropriate pre- and postsynaptic locations. Subsequent postsynaptic rearrangements of the actin cytoskeleton lead to a spine of characteristic shape. These spines may be stabilized or lost in an activity dependent manner. In other contexts, axonal filopodia (such as those from growth cones) may initiate a direct contact with a dendritic shaft, inducing spinogenesis and synaptogenesis (Model 2). A third model proposes that spinogenesis can substantially precede synaptogenesis. Adapted from Ethell & Pasquale (2005).
B, *In vivo*, two-photon imaging illustrating spinogenesis proceeding via a filopodial intermediate. In this case, the resulting spine was later eliminated. Modified from Bhatt (2009).
C, A substantial number of molecules have already been identified as regulators of synapse formation, and have been classified as "accelerators" or "brakes" of spine formation. Brakes of spine maturation are characterised by exerting opposite effects on filopodial and spine formation, with a net decrease in mature spine density being observed in each case. In contrast, accelerators of spine maturation tend to have concordant effects on both filopodia and spines, while increasing the rate of spine maturation overall. From Yoshihara (2009) and references therein.

In order for synaptogenesis to occur through filopodia/axon contact, filopodia must be maintained in a dynamic state until they contact an axon (Bourne and Harris, 2008). Much progress has been made in identifying molecules that regulate the formation of spines and filopodia, which have been classified as either "accelerators" or "brakes" of spine maturation (Figure 12C) (Yoshihara et al., 2009). While many more molecules that regulate the formation of filopodia and spines undoubtedly remain to be uncovered, those known so far comprise a diverse array of molecular factors including; adhesion molecules, intracellular kinases, small GTPases and their associated regulatory proteins (Yoshihara et al., 2009). A critical common feature of these molecules seems to be their ability to signal to the actin cytoskeleton, the reorganization of which must ultimately underlie filopodia and spine dynamics (Cingolani and Goda, 2008). In this context, it is interesting to note that PI3K is emerging as an important regulator of filopodia and spine growth, in parallel to its role in modulating axon polarization and elongation earlier in development, and that PI3K can act downstream of neurotrophins such as BDNF (Luikart et al., 2008; Yoshihara et al., 2009; Shen and Cowan, 2010; Cuesto et al., 2011).

7.2.1.5.2. Inhibitory synapse formation

Functional GABAergic synapses are established before glutamatergic synapses in hippocampal development (Danglot et al., 2006). The axosomatic synapses of basket cells made within the pyramidal neuron layer are the best studied to date (See Figure 9). This class of inhibitory synapse is found in an immature form by P5, but undergoes a major increase in number between P7 and P21 (Marty et al., 2002). Although the mechanisms of inhibitory axon guidance and synaptogenesis remain incompletely understood, there is some evidence that the process may involve both molecular cues and neural activity (Danglot et al., 2006; Huang et al., 2007c).

Basket cell terminals form successfully in organotypic slices of the isolated CA3 region from P1 rat, a preparation in which both extra-hippocampal and intra-hippocampal afferents are unable to form, suggesting that molecular cues must play a significant role in this form of inhibitory synaptogenesis (Marty, 2000). Furthermore, a preferential targeting of GABAergic over glutatmatergic synapses to pyramidal cell soma is even observed in dissociated hippocampal cultures

(Benson and Cohen, 1996), suggesting that the cellular localization of molecular recognition tools, rather than guidance cues derived from the tissue architecture, are the primary determinant of targeted inhibitory synaptogenesis (Danglot et al., 2006). Therefore, it seems likely that an array of molecular recognition tools must be available to support the exquisite selectivity over which post-synaptic cellular compartment is targeted by axons from different classes of interneuron (Huang et al., 2007c).

One group of molecules that have been shown to play an important role in inhibitory synapse formation comprises the neurexins and neuroligins. These are transmembrane proteins, trafficked to the pre and postsynaptic cellular compartments, respectively (Craig and Kang, 2007). Neurexins and neuroligins interact with each other in the synaptic cleft to promote synaptic differentiation and receptor clustering (Thomson and Jovanovic, 2010). While this system does not function exclusively at GABAergic synapses, neuroligin 2 is enriched in inhibitory post-synaptic membranes and there is evidence that it acts specifically in their formation (Huang and Scheiffele, 2008). Interestingly, neuroligin 2 interacts with the inhibitory synaptic scaffold protein gephyrin, though an unknown mechanism, which may be important for the role of neuroligin 2 in promoting the post-synaptic clustering of $GABA_A$ receptors (Craig and Kang, 2007; Fritschy et al., 2008).

However, there is evidence that neural activity also plays a role in the formation of inhibitory synapses. For example, blocking neural activity with tetrodotoxin during a critical period can greatly reduce the postnatal increase in basket cell inhibitory synapses, while partial knockdown of the expression of the GABA synthesizing enzyme, GAD67 in individual interneurons results in them forming fewer synapses in slice culture preparations (Huang et al., 2007c). A link between these observations has emerged based on the finding that GAD67 synthesis is promoted by neural activity (Huang, 2009).

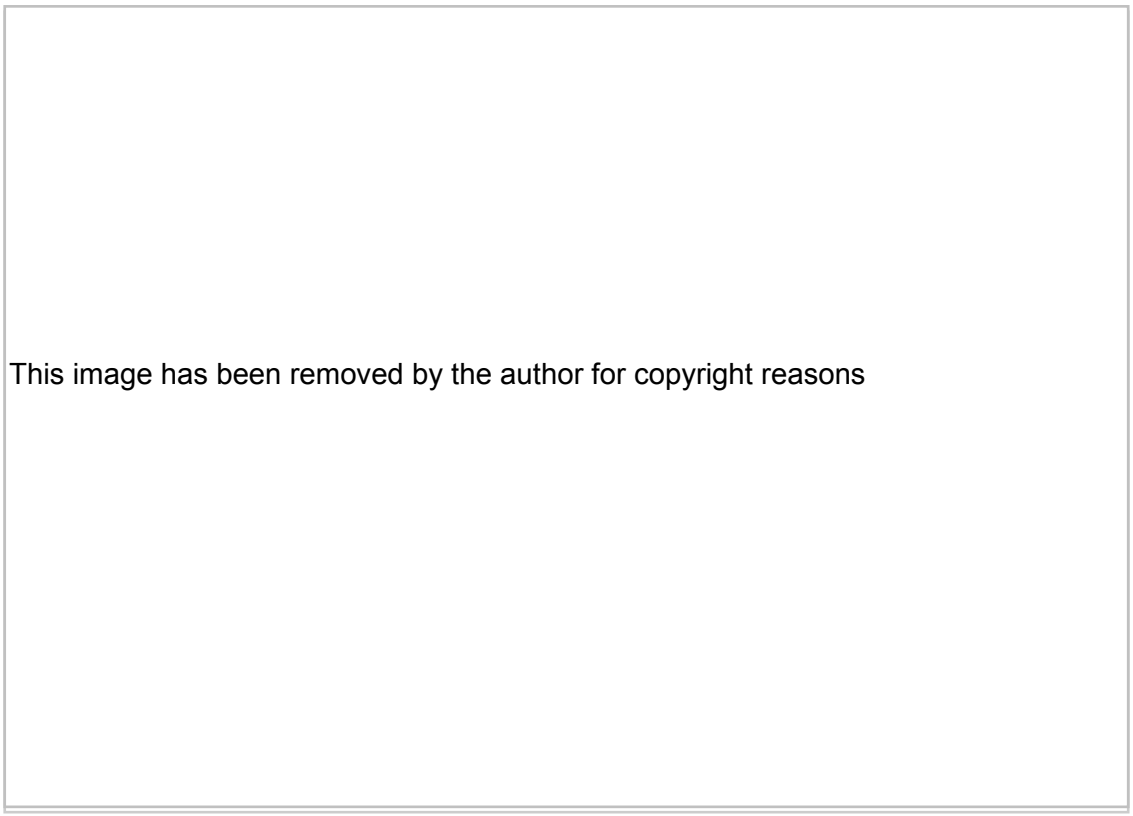

Figure 13: Chloride transporter balance underlies a developmental switch in GABA responsiveness

The Chloride transporter, NKCC1 transports Na^+, K^+, and Cl^- ions into neurons, whilst KCC2 transports K^+ and Cl^- ions out of neurons. During the first postnatal week, the expression of NKCC1 is high, while KCC2 expression is low. This results in high intracellular [Cl^-], with the result that GABA induced gating of $GABA_A$ receptors results in an excitatory Cl^- current, down an outwardly directed electrochemical gradient. At some point during the second postnatal week, the balance between the expression of NKCC1/KCC2 is reversed, resulting in low intracellular [Cl^-], with the result that GABA induced gating of $GABA_A$ receptors causes an inhibitory Cl^- current, down an inwardly directed electrochemical gradient. From Lu *et al* (1999).

7.2.1.5.3. Excitatory/inhibitory balance

A correct balance between excitation and inhibition is critically important for the proper development and function of neural networks. An emerging view indicates that excitation dominates in early, immature networks, and the slower maturation of GABAergic circuitry is largely responsible for the development of mature excitatory/inhibitory (E/I) balance (Supèr et al., 1998). One key reason for the late emergence of mature inhibitory circuitry, despite the earlier establishment of GABAergic synapses (see section 7.2.1.5.2), is that the effects of GABA in early development are excitatory. This reversal is possible because $GABA_A$ receptors are ligand-gated chloride (Cl^-) channels. In early development, the cytoplasmic

concentration of Cl^- ions in inhibitory interneurons is higher than that in surrounding extracellular milieu, producing an outwardly directed Cl^- electrochemical gradient, with the result that GABA induced opening of $GABA_A$ channels leads to a depolarizing Cl^- current. As development proceeds, the Cl^- gradient across the neuronal plasma membrane is reversed, so that opening of $GABA_A$ receptors leads to a hyperpolarizing Cl^- current (Payne et al., 2003). The reversal of the Cl^- gradient across the neuronal plasma membrane as development proceeds is due to developmentally regulated transcription of the electro-neutral Cl^- co-transporters, KCC2 and NKCC1 (Figure 13). NKCC1 transports Na^+, K^+, and Cl^- ions into neurons, whilst KCC2 transports K^+, and Cl^- ions out of neurons. In the early neonatal period, NKCC1 expression levels are high whilst KCC2 is expressed at low levels. During the second postnatal week, the ratio between NKCC1 and KCC2 expression is reversed, so that KCC2 expression predominates (Lu et al., 1999; Rivera et al., 1999; Payne et al., 2003; Stein et al., 2004; Lee et al., 2005).

There are additional steps in the maturation of interneurons that are key to the normal establishment of nervous system function and plasticity. In particular, the late maturation of parvalbumin positive interneurons in the visual cortex is thought to define the critical period for visual plasticity, as the maturation of these cells parallels its onset (Hensch, 2005). In support of this, reducing GABAergic function through GAD65 deletion, or increasing it through benzodiazepine treatment and BDNF overexpression, can shift the critical period for visual plasticity later or earlier, respectively (Hensch, 2005).

7.2.1.6. Dendritic spine plasticity

There is a good evidential basis for the view that dynamic changes in dendritic spines play a key role in learning and memory processes. For example, it has been shown that changes in the size of mature spine heads correlate with long term potentiation (LTP) and long term depression (LTD), thought to be synaptic correlates of learning and memory, with increases in head size accompanying LTP and decreases in head size accompanying LTD (Tada and Sheng, 2006; Sala et al., 2008). The molecular mechanisms that lead to changes in actin dynamics, and hence spine morphology, in LTP and LTD within the developing postnatal rodent brain are summarised in Figure 14. In brief, synapse associated cell adhesion molecules and glutamate induced opening of N-methyl-D-aspartate (NMDA)

receptors induce intracellular signals that modulate actin polymerisation or depolymerisation in the post-synaptic dendritic spine. Key signalling molecules that regulate actin dynamics include Rho family GTPases, such as RhoA and Rac, along with the GAPs that activate them and GEFs that inactivate them (Tada and Sheng, 2006; Sala et al., 2008). In addition to synapse associated cell adhesion molecules and NMDA receptors, activity induced release of the neurotrophin, BDNF can also modulate Rho GTPase activity and act to stabilize LTP induced morphological changes. In addition to morphological changes, LTP and LTD also lead to functional changes at synapses. For example, LTP leads to strengthening of synapses, in part through the insertion of 2-amino-3-(5-methyl-3-oxo-1,2- oxazol-4-yl) propanoic acid (AMPA) receptors into the post-synaptic membrane (Tada and Sheng, 2006). However, while the implied correlation between structural and functional plasticity in LTP and LTD often holds, there are notable exceptions. One example is the cerebellar parallel fibre/purkinje cell synapse, where LTD is not accompanied by changes in spine size and stimuli inducing global retraction of purkinje synapses do not change synaptic currents (Sdrulla and Linden, 2007). It seems, therefore, that changes in spine size do not underlie all forms of plasticity in the postnatal brain, even at glutamatergic synapses (Sdrulla and Linden, 2007; Cingolani and Goda, 2008).

While the adult brain is undoubtedly more static than the postnatal brain, which is undergoing network formation and refinement, it does seem that dendritic spines exhibit a remarkable degree of structural dynamics even into adulthood. Two-photon imaging studies of live mice have recently revealed that the formation and stabilization of dendritic spines is an important mechanism of encoding lifelong memories *in vivo* (Xu et al., 2009; Yang et al., 2009). The causal link between spine growth and memory in the adult has been further strengthened by a recent study taking advantage of the observation that the transcription factor, myocyte enhancer factor 2 (MEF2) inhibits spinogenesis both *in vitro* and *in vivo.* Virally mediated overexpression of MEF2 in the anterior cingulate cortex of adult mice not only blocks spinogenesis, but also prevents the consolidation of contextual fear memory, a process that is dependent on this region of cortex (Vetere et al., 2011). Furthermore, deficits in spine density and morphology have been reported in a number of neurodegenerative diseases and mental health disorders (Lin and Koleske, 2010; Penzes et al., 2011).

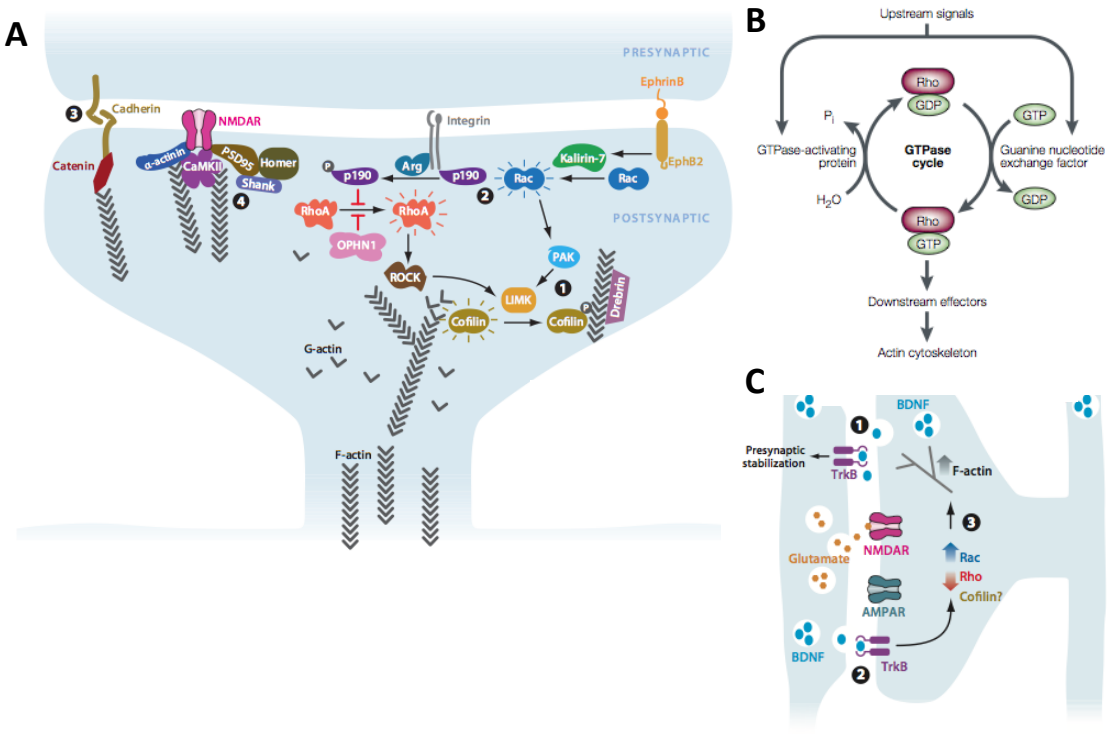

Figure 14: Regulators of mature dendritic spine stability signal to the actin cytoskeleton

A, Signals from cell adhesion proteins and glutamate, mediated by NMDA receptors, can induce actin polymerization or depolymerization through a variety of mechanisms. Rho family GTPases such as RhoA and Rac, along with the GAPs that activate them and GEFs that inactivate them are key regulators of actin dynamics. While Rac and RhoA generally exert opposite effects (stabilising and destabilising spines respectively), they share some common effectors like LIMK. The mechanisms by which differential regulation of common effectors can occur remains to be determined. Adapted from Lin & Koleske (2010).
B, A general model for Rho family GTPase function as molecular switches regulated by GEFs and GAPs. Adapted from Luo (2000).
C, Model for the synapse stabilising effect of BDNF mediated by TrkB. 1. Activity dependent release of BDNF from the postsynaptic compartment stabilises the synaptic bouton by binding presynaptic TrkB. 2-3. BDNF released presynaptically after neural activity also activates postsynaptic TrkB, which may activate Rac, inhibit Rho, and regulate cofilin to stimulate increased F-actin assembly to stabilize synapses. Adapted from Lin & Koleske (2010).

It appears that numerous regulators of developmental spine maturation may also continue to play a role in adult spine plasticity (Lin and Koleske, 2010). One major factor in common between developmental plasticity and activity-dependent morphological plasticity of spines in adulthood is the common target of the actin cytoskeleton. A large number of molecules that regulate actin dynamics have already been identified (Figure14A), many of which are small GTPases and their

associated regulatory partners (Ethell and Pasquale, 2005; Cingolani and Goda, 2008; Lin and Koleske, 2010). Three Rho family GTPases, along with a number of guanine nucleotide exchange factors (GEFs) and GTPase activating proteins (GAPs) that regulate their activity (Figure 14B), deserve to be highlighted. RhoA, Rac1 and Cdc42, have come to be viewed as key signalling hubs underlying the development and plasticity of spines (Ethell and Pasquale, 2005; Tada and Sheng, 2006; Bourne and Harris, 2008; Cingolani and Goda, 2008; Von Bohlen Und Halbach, 2009; Lin and Koleske, 2010). Studies characterizing the functions of these three GTPases in non-neuronal cells preceded much of the recent work confirming their importance in modulating spine morphology (Luo, 2000). In both cellular contexts, RhoA, Rac1 and Cdc42 have been shown to regulate the actin cytoskeleton in different manners (Ethell and Pasquale, 2005). In non-neuronal cells, RhoA increases cell contractility by inducing stress fibre formation (Ridley and Hall, 1992), Cdc42 induces filopodia formation (Nobes and Hall, 1995) and Rac1 promotes lamellopodia formation and membrane ruffling (Ridley et al., 1992). These findings prompted investigations that found analogous roles in spine formation and plasticity; in general Rac1 and Cdc42 promote spine stabilization, while RhoA promotes spine destabilization (Nakayama et al., 2000; Tashiro et al., 2000; Lin and Koleske, 2010) However, a recent study imaging RhoA and Cdc42 activation within individual dendritic spines of CA1 neurons undergoing structural plasticity associated with LTP indicated that while local Cdc42 activation promoted the maintenance of structural plasticity through Pak, RhoA activation promoted initial spine growth through ROCK (Murakoshi et al., 2011). The surprising direction of the effect of RhoA activation has been suggested to imply that some level of actin destabilization is required for growth and restabilization of the actin cytoskeleton in a larger form (Murakoshi and Yasuda, 2012).

BDNF also regulates dendritic morphology at multiple stages of development. As mentioned above, BDNF is released from the presynaptic bouton in an activity-dependent manner at mature synapses. Secreted BDNF activates postsynaptic TrkB receptors leading to increased Rac1 and decreased RhoA activity, enhanced F-actin assembly and an increase in the size and stability of dendritic spines. (Figure14C) (Lin and Koleske, 2010). BDNF also promotes filopodial growth and synapse formation in the developing hippocampus by a PI3K dependent signalling mechanism (Luikart et al., 2008). At earlier developmental stages, BDNF can also

promote dendritic growth from cultured embryonic rodent hippocampal neurons. Whilst BDNF promoted spinogenesis is facilitated by cAMP, BDNF enhances dendrite growth independently of cAMP (Ji et al., 2005).

7.2.2. Overview of cortical development

Like the hippocampus, the cerebral cortex is derived from the telencephalon and contains many similar cell types. However the cortex possesses a greater diversity of cellular sub-types, and a more complex structural organization.

The diverse and complex structure of the cortex befits the important and wide ranging functions that it serves. Anatomical divisions of the cortex have long been recognized (Zilles and Amunts, 2010), providing a diversity of neural networks that enable functional localization. Pathological studies and comparative anatomy suggest that regions of the expanded human neocortex underlie higher cognitive functions, such as language and voluntary movement (Kaas, 2008; Rakic, 2009). A brief overview of aspects of cortical development shall be provided here for comparative purposes, and to aid in the interpretation of CaSR expression data.

7.2.2.1. Cell type generation, cell migration & structural organization

Several cell types cooperate in the ontogenesis of the cerebral cortex. A notable difference to the cell types involved in hippocampal development is the role of radial glia. Radial glia cells are characterized by an apical-basal polarity, extending a short process basally to contact the ventricle and a longer process apically to contact the meninges, basal lamina and blood vessels, while their soma are located in the neuroepithelium or subventricular zone (Kriegstein and Alvarez-Buylla, 2009). Radial glia are of particular importance during cortical development, as they not only act as neural precursors, but also provide a migratory pathway for newly generated cortical neurons (Noctor et al., 2001; Kriegstein and Alvarez-Buylla, 2009). The asymmetric division of radial glia produces neuronal precursors and neurons that migrate along the apical process of the radial glial cell that generated them (Noctor et al., 2001; Kriegstein and Alvarez-Buylla, 2009). A distinctive feature of cortical development is that neurons destined for inner layers of the cortex are generated before those that will reside in the outer cortical layers. Therefore, later born neurons must migrate through inner cortical layers, along the radial glia scaffold, to reach their final destination. Thus, corticogenesis is an "inside-out" process (Figure 15) (Bielas et al., 2004). In this manner, the mature

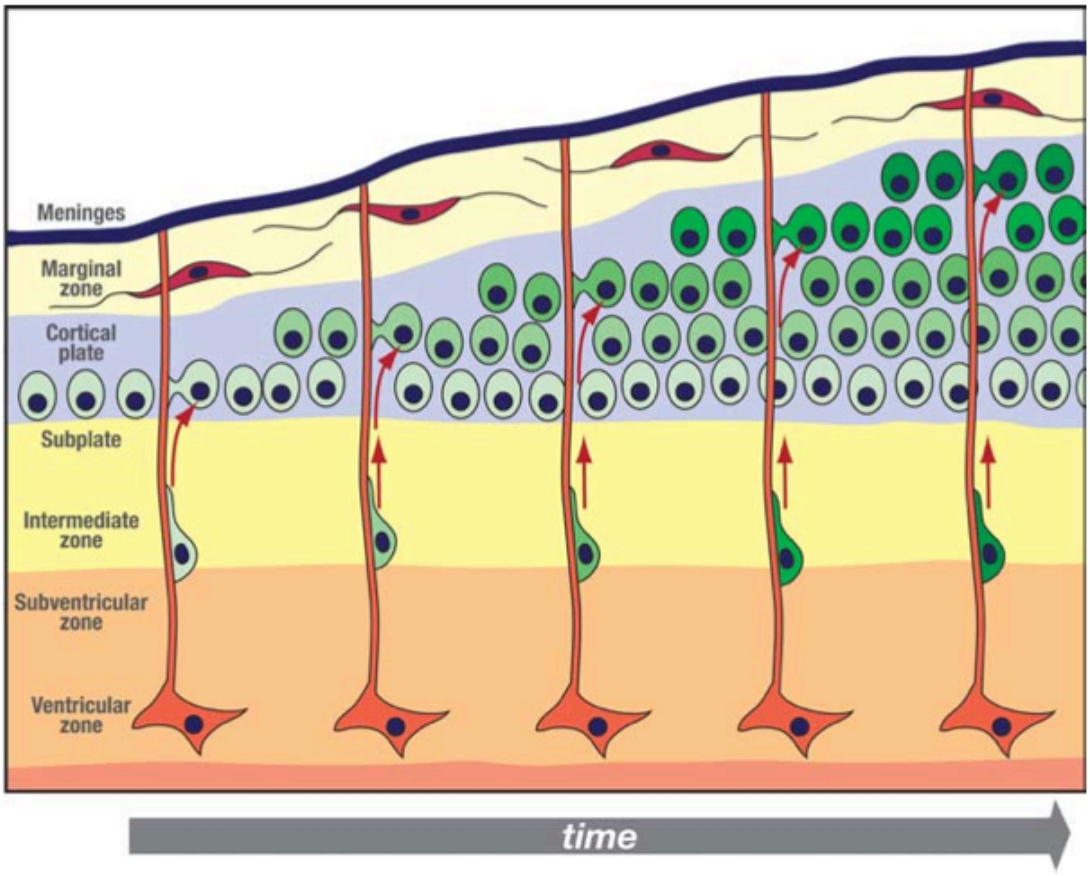

Figure 15: Inside-out corticogenesis

During embryonic corticogenesis, neurons and neuron progenitors (green) migrate radially along the processes of radial glia (orange). Radial glia cell soma are located in the ventricular zone, thus neurons must travel through the subventricular zone, the intermediate zone and the subplate, before reaching the cortical plate. Earlier born neurons (pale green) terminate their migration closer to the subplate than later born neurons (darker green), which must migrate through the layers of early born neurons to form new layers closer to the marginal zone. Cajal-Retzius (red) cells in the marginal zone secrete reelin, a key regulator of inside-out corticogenesis (see text). From Bielas *et al* (2004).

cortex is composed of ontogenetic columns of cells derived from a single radial glial source (Rakic, 1988).

The processes of cortical neuron generation and migration take place during embryonic development. Whilst neural migration by somal translocation, independent of radial glia, can occur during the initial stages of corticogenesis (E10-13 in mice), radial glia guided migration is the dominant process between E14-18 (Bielas et al., 2004). Some progress has been made in understanding the mechanisms controlling embryonic neuronal migration. The secreted glycoprotein,

reelin has long been known to play a critical role in this process (Tissir and Goffinet, 2003), acting through the very-low-density lipoprotein receptor and apolipoprotein E receptor 2 in a manner shown to be dependent on Ephrin Bs (Sentürk et al., 2011). Reelin mutations result in an "outside-in" phenotype of cortical lamination, which first becomes evident at E14.5. Reelin mutations also result in ectopic positioning of neurons belonging to other structures, including the hippocampus and cerebellum (Tissir and Goffinet, 2003). Interestingly, whilst TrkB and TrkC regulate the migration of cortical neurons, in this context TrkB- and TrkC-dependent signalling appears to be initiated by EGF-induced transactivation rather than BDNF and NT-3 binding, respectively (Puehringer et al., 2013).

Radial glial cells are progressively lost during the first postnatal week, mostly by transformation into astrocytes (Mission et al., 1991; Kriegstein and Alvarez-Buylla, 2009). In addition, it is thought that oligodendrocytes may also be derived from radial glia, albeit indirectly via various oligodendrocyte precursors (Kriegstein and Alvarez-Buylla, 2009). The number of glial cells in the developing cortex increases by six- to eight-fold during the first three postnatal weeks. This increase appears to be generated by the local proliferation of differentiated astrocytes, rather than the conversion of remaining radial glia (Ge et al., 2012).

Like the hippocampus, inhibitory interneurons of the cortex have distinct developmental origins from their excitatory counterparts (Bielas et al., 2004; Danglot et al., 2006). Specifically, inhibitory interneurons derive from the caudal and medial ganglionic eminences of the ventral telencephalon. Interneurons initially follow a tangential migratory path from the ganglionic eminences to arrive in the correct cortical area, before turning and taking a radial path and finally halting in a given cortical layer (Bielas et al., 2004). The timing of the cessation of migration determines the eventual location of interneurons, and is regulated by both cell intrinsic and extrinsic processes. Intrinsic mechanisms for migration termination include the upregulation of KCC2 expression (Bortone and Polleux, 2009; Miyoshi and Fishell, 2011). During the early stages of migration, GABA dependent gating of the $GABA_A$ receptor promotes the motility of interneurons. The increase in KCC2 expression during the late stages of migration results in the hyperpolarization of interneurons in response to GABA and a reduction in the frequency of spontaneous Ca^{2+}_i transients initiated by L-type voltage-sensitive

calcium channels. This reduction in Ca^{2+}_i transients reduces the motility of interneurons (Bortone and Polleux, 2009; Miyoshi and Fishell, 2011). Interestingly, interneurons partition in cortical layers with excitatory projection neurons with which they share a birth date, despite their distal origins (Valcanis and Tan, 2003). Genetic and transplant based manipulations of distinct excitatory neuron subtypes disrupt interneuron laminar distribution, suggesting that excitatory projection neurons (subtypes of which are born at different developmental stages and reside selectively in particular cortical layers (Fame et al., 2011)) exert extrinsic regulatory effects on the timing of interneuron migration cessation (Lodato et al., 2011). Thus the transcriptomic and functional differences between different cortical layers may be related to coordinated differences in birth dates, cellular sub-types and targets of the cells that comprise them (Belgard et al., 2011).

7.2.2.2. Development of connectivity

In order to acquire adult functionality, the developing cortex must establish synaptic connectivity following the growth and elaboration of axons and dendrites. Each process shall be briefly reviewed, with an emphasis on developmental timing.

Axon growth from cortical excitatory neurons begins between E11 and E17, during their migration along radial glia (Barnes and Polleux, 2009). This migratory route provides a structural scaffold for polarization *in vivo*. As a new-born neuron begins to migrate radially along a radial glia cell, it extends one process in the direction of travel. This leading process later becomes the apical dendrite. The migrating neuron also extends a second trailing process, backwards towards the origin of migration. The trailing process elongates tangentially within the intermediate zone and later becomes the axon (Barnes and Polleux, 2009). Numerous signalling molecules and pathways, each of which can be modulated by numerous extracellular cues, regulate cortical axon initiation and growth. Signalling pathways that modulate axon initiation and elongation include; PI3K, MAPK, the Ras and Rho families of small GTPases, JNK and GSK3 (Barnes and Polleux, 2009; Hirai et al., 2011).

In addition to the requirement for axon growth, long-range axons of each cell type must be adequately guided to their target fields, a critically important process involving a large number of attractive and repulsive extracellular cues, along with their cognate receptors (O'Donnell et al., 2009). Since no particular type of cortical

neuron is studied in detail in this thesis and axon growth and guidance largely occurs during the embryonic period (in contrast to the postnatal focus of CaSR expression data), these processes shall not be further discussed.

In contrast, the majority of dendritic growth and branching in the cortex occurs in the first three postnatal weeks (Wong and Ghosh, 2002; Barnes and Polleux, 2009). For instance, in corticothalamic projection neurons, branches are added to simple apical dendrites during the two days prior to birth in rats, while basal dendrites first begin to be extended over the same period (Hsu et al., 2011). Neurotrophins have been shown to regulate cortical neuron dendritic growth (Whitford et al., 2002). For example, BDNF regulates primary dendrite formation through PI3K and MAPK signalling pathways in both E18 dissociated and P7 slice cultures of cortex (Dijkhuizen and Ghosh, 2005). The abilities of neurotrophins to enhance dendrite growth and branching can exhibit cortical layer specificity. For instance, NT-3 increases dendrite complexity of layer 4, but not layer 5 cortical neurons (Whitford et al., 2002). Apart from neurotrophins, other secreted proteins also regulate the growth and branching of cortical neuron dendrites. One example is the Semaphorin family member, Semaphorin3A (Sema3A). An analysis of transgenic mice has demonstrated that Sema3A promotes the growth and branching of basal dendrites from layer 5 cortical neurons and that the effects of Sema3A are mediated by a neuropilin1/plexinA_4 receptor complex (Tran et al., 2009). Remarkably, Sema3A also acts as both a chemoattractant for the apical dendrites of cortical neurons, and a chemorepellent for their axons, thus Sema3A contributes to several aspects of cortical pyramidal neuron development (Whitford et al., 2002). It has been argued that activity-induced elevation of $Ca^{2+}{}_i$ plays a central role as an intracellular mediator of dendritic growth and branching during the period of cortical synaptogenesis (Wong and Ghosh, 2002). There is evidence that elevated $Ca^{2+}{}_i$ increases the activity of CaM kinase IV in cortical neurons and CaM kinase IV, in turn, increases the activity of CREB, a transcription factor that is required for activity induced dendrite growth from cortical neurons (Redmond et al., 2002). In addition, the expression of CaM kinase IV within cortical neurons is increased over the second and third postnatal weeks, a period that coincides with the peak period of dendrite growth and branching (Redmond et al., 2002). Since other studies have reported that BDNF expression is regulated by CREB, it has

been suggested that elevated Ca^{2+}_i and BDNF promoted dendritic growth may be connected (Wong and Ghosh, 2002).

Cortical neurons participate in both local and widely dispersed networks. Excitatory projection neurons are responsible for interhemispherical connectivity (callosal projection neurons), ipsilateral circuit connectivity (ipsilateral circuit connection neurons) and connectivity with subcortical areas (corticofugal projection neurons) (Fame et al., 2011). Excitatory synaptogenesis involving cortical projection neurons begins to occur early in cortical development. For example, reciprocal connections between the cortex and the thalamus are established between E13 and E19 (López-Bendito and Molnár, 2003). Furthermore, during the perinatal period (E18 – P0 in rats), corticothalamic projection neurons have been shown to receive increasing numbers of excitatory synapses (Hsu et al., 2011). However, no such increase in inhibitory synapses is observed over the same period (Hsu et al., 2011). Local circuits are also important for cortical function and a notable feature of such circuits is the preferential connectivity of sister excitatory neurons within ontogenetic columns (Yu et al., 2009). This connectivity is established by synaptogenesis during the second postnatal week (Yu et al., 2009), and is promoted by the formation of transient electrical synapses between the same neurons early in the first postnatal week (Yu et al., 2012). Excitatory synaptogenesis within the developing cortex during the first two postnatal weeks is modulated by a number of regulatory molecules. One of these regulatory molecules is BDNF (Yoshii and Constantine-Paton, 2010). In the rodent central visual system, eye opening towards the end of the second postnatal week increases BDNF/TrkB signalling, the formation of mature dendritic spines and visual cortical synaptic plasticity (Yoshii et al., 2011). PSD-95 is a major postsynaptic scaffold protein at excitatory synapse and is essential for synapse maturation and learning. Following eye opening, BDNF/TrkB signalling promotes the translocation of PSD-95 to the synapses of excitatory neurons within the visual cortex (Yoshii et al., 2011).

Functional maturation of inhibitory circuits appears to occur later in cortical development than that of excitatory circuits (Hensch, 2005). For instance, the formation of both electrical and chemical synapses between fast-spiking GABAergic interneurons in layer 5/6 and their targets (other fast-spiking

GABAergic interneurons and excitatory pyramidal neurons) occurs at detectible levels from P5 to P18 (Pangratz-Fuehrer and Hestrin, 2011). The slow maturation of this class of interneuron is thought to have important functional consequences in governing the timing of critical (or sensitive) periods when experience can alter cortical connectivity more extensively than in adulthood (Hensch, 2005). Modulation of the maturation of this inhibitory neuron subtype can alter the timing of the critical period, be it through pharmacological (e.g. Benzodiazepine infusion), environmental (e.g. dark rearing) or genetic (e.g. BDNF overexpression, Gad65 deletion) means (Hensch, 2005). Whilst the most well characterised example of a critical period occurs within the visual cortex (Wiesel and Hubel, 1963), other sensory systems, such as the auditory cortex, have been shown to exhibit a critical period (Barkat et al., 2011). Whether the maturation of fast-spiking GABAergic interneurons also regulates the timing of the critical period in the auditory cortex remains to be determined. However, it is clear that control of the excitatory/inhibitory balance is a crucial mechanism for the regulation of plasticity during the development of the visual cortex (Hensch, 2005; Bavelier et al., 2010).

7.2.3. Overview of cerebellar development

The cerebellum derives from the dorsal rhombencephalon and emerges as a distinct territory at E9 in the mouse (Sillitoe and Joyner, 2007). The cerebellar territory subsequently undergoes a 90° rotation between E9 and E12 to form the cerebellar primordium, such that the anterior-posterior (A/P) axis becomes the new medial-lateral (M/L) axis, which remains into adulthood (Sillitoe and Joyner, 2007). The ML and AP axes act as a dual coordinate system for establishing the complex anatomical and molecular patterning of the cerebellum through development, which becomes important for guiding cerebellar circuit development (Sillitoe and Joyner, 2007). Although there are diverse gene expression profiles amongst different developing cerebellar regions (Sillitoe and Joyner, 2007), the details of this molecular coding are outside the scope of this section, which provides a brief overview of general aspects of cerebellar development. The focus shall be on several cell types that compose the cerebellum, and the timing of key developmental events, particularly those occurring postnatally. This information shall serve a comparative purpose and aid in the interpretation of CaSR expression data.

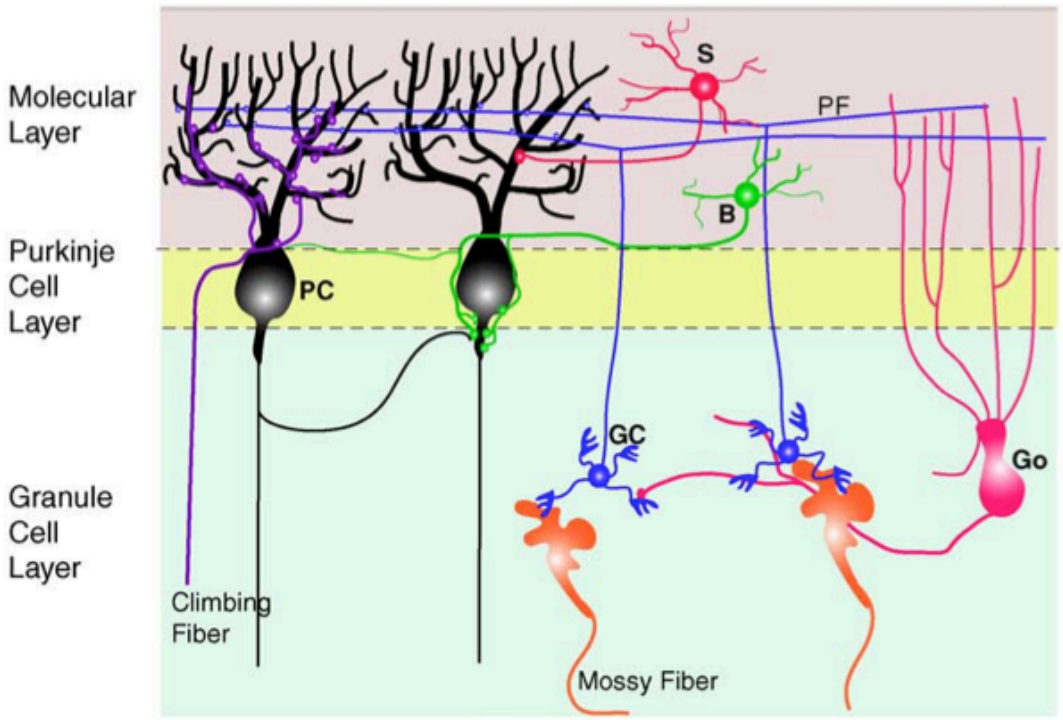

Figure 16: Cell types of the cerebellum

The histology of the cerebellum is more simple than that of the cortex, with only three cell layers present; the granule cell layer (GCL), Purkinje cell layer (PCL) and the molecular layer (ML). The ML contains two major cerebellar interneuron classes; basket (B) cells and stellate (S) cells. The PCL contains the soma of Bergmann glia (not pictured) and the output neurons of the cerebellum, the Purkinje cells (PC). Processes of both cell types extend into the ML, with PC dendritic trees exhibiting a highly branched structure. B and S both target PCs, predominantly within the PCL and the ML, respectively. The GCL contains the glutamatergic granule cells (GC) in addition to other interneurons such as Golgi cells (Go). GCs extend a single axon radially though the PCL, which branches once in the ML (the Parallel fiber, PF) and forms *en passant* synapses with dendritic spines of PCs. The two major excitatory inputs to the cerebellum are the mossy fibers, which target GCs and climbing fibers, which each form multiple synapses with a single PC. From Chédotal (2010).

7.2.3.1. Cell type generation, cell migration & structural organization

In contrast to the complexity of the ML/AP patterning of the cerebellum, its histology is comparatively simple. Throughout the structure, the cerebellum comprises three layers built on top of a central core of white matter. The three layers are the granule cell layer (GCL), Purkinje cell layer (PCL) and the molecular layer (ML) (Sillitoe and Joyner, 2007; Chédotal, 2010). Particular cell types segregate into each of these layers, the soma of granule cells are found in the GCL; Purkinje cells and Bergmann glia are found in the PCL; Basket cells and stellate cells, the major interneurons of the cerebellum, are found in the ML alongside

Purkinje cell dendrites, processes of Bergmann glia and the axons of granule cells (Sillitoe and Joyner, 2007; Chédotal, 2010) (Figure 16).

The cells of the cerebellum derive from two germinal zones (Sillitoe and Joyner, 2007). The ventricular zone gives rise to most cerebellar GABAergic neurons, including Purkinje cells. Purkinje cells become postmitotic between E11 and E13 in mice, after which they migrate along radial glia to form a monolayer in the PCL by late embryonic stages (Sillitoe and Joyner, 2007). In contrast, the rhombic lip gives rise to granule cell precursors (Chédotal, 2010). By E15, granule cell precursors have migrated to form a transient structure, the external granule layer, which lies on top of the ML. Granule cell precursors continue to proliferate for the first two to three postnatal weeks, with peak proliferation occurring at P8 (Sillitoe and Joyner, 2007; Chédotal, 2010). During this time, some granule cell precursors exit the cell cycle and differentiate into granule cells (Chédotal, 2010; de la Torre-Ubieta and Bonni, 2011). Between P1-P8, newly differentiated granule cells develop polarization in an orthogonal plane to the Purkinje cell dendrites, migrate tangentially, extend a process radially into the ML, and migrate into the ML. Following this, immature granule cells migrate through the PCL into the GCL along radial glia, leaving behind a branched process that extends into the ML. This branched process later becomes the granule cell axon, which is also termed a parallel fiber (Wong and Ghosh, 2002; Chédotal, 2010; de la Torre-Ubieta and Bonni, 2011). BDNF/TrkB and Sema6A/PlexinA2 mediated signalling are both thought to regulate the migration of granule cells (Chédotal, 2010).

One of the most striking features of the cerebellum is its foliated structure. This is first evident at E17 in mice, when four fissures divide the cerebellum into five cardinal lobes (Sillitoe and Joyner, 2007). During the first two postnatal weeks, the outgrowth and subdivision of these cardinal lobes results in the formation of multiple lobules within each lobe (Sillitoe and Joyner, 2007). Whilst the mechanisms regulating foliation are poorly understood, it is thought that sonic hedgehog (Shh) mediated control of granule cell proliferation is involved (Sillitoe and Joyner, 2007). Foliation is complete by P14 in mice (Sillitoe and Joyner, 2007).

7.2.3.2. Development of connectivity

Although dramatic changes in cerebellar connectivity are observed in the first two to three postnatal weeks, a rudimentary cerebellar circuitry is already present at

birth (Sillitoe and Joyner, 2007). Between birth and P9, rat Purkinje cell dendrites are short but multipolar and exhibit an immature physiological output (McKay and Turner, 2005). Thereafter, the electrophysiological output and degree of branching of Purkinje cell dendrites mature in parallel. This maturation process proceeds especially rapidly between P12 and P18 and displays only minor refinements from P18 to P90 (McKay and Turner, 2005). Between P8 and P12, granule cells form *en passant* synapses between their parallel fibers and maturing Purkinje cell dendrites, and undergo dendritic growth and pruning themselves (Chédotal, 2010; de la Torre-Ubieta and Bonni, 2011). It has been suggested that parallel fiber input may have a role in regulating Purkinje cell dendritic branching (Wong and Ghosh, 2002).

Purkinje cells are innervated by climbing fibers that arise from the inferior olive in the brainstem (Sillitoe and Joyner, 2007). This projection is largely formed in late embryonic development, with each climbing fiber initially contacting multiple Purkinje cells (Sugihara, 2005). A refinement of surplus projections occurs predominantly between P5 and P7, such that in the mature cerebellum one climbing fiber makes multiple synaptic contacts with a single Purkinje cell (Sugihara, 2005). Based on data from a denervation/reinnervation model, a reduction in the efficacy of BDNF signalling, due to a switch in the ratio between full length TrkB and truncated TrkB expressed in the inferior olive and cerebellum, has been suggested to play a role in this process (Sherrard et al., 2009). In addition, there is *in vivo* evidence for the involvement of postsynaptic P/Q type Ca^{2+} channels in the elimination of surplus climbing fiber contacts (Hashimoto et al., 2011). While climbing fibers initially contact both the soma and the dendrites of Purkinje cells, in the adult they predominantly contact dendrites (Ichikawa et al., 2011). Between P7 and P20 there is a progressive switch in the innervation of Purkinje cell soma. Whilst climbing fiber inputs to perisomatic spines decrease during this period, inputs from GABAergic basket cells increase, and these inhibitory synapses become ensheathed by Bergmann glial cell processes (Ichikawa et al., 2011). Bergmann glial cell ensheathment of excitatory synapses also occurs at dendritic spines of Purkinje cells, a process which when disrupted *in vivo* causes an increase in spine number (Lippman Bell et al., 2010).

Apart from climbing fibers, the other major input to the cerebellum are mossy fibers, which arise from several brain regions to innervate the GCL between E13 and P0, the exact timing being dependent on the mossy fiber region of origin (Sillitoe and Joyner, 2007). Despite the early arrival of mossy fibers into the GCL, it takes into the second postnatal week for synapse formation with granule cells to begin in earnest, since granule cell migration is incomplete when mossy fibers first arrive (Hall et al., 2000). The growth cones of mossy fibers enlarge as they contact granule cells, permitting multiple synaptic contacts to be made with more than one granule cell in structures known as glomerular rosettes (Hall et al., 2000). The expression of Wnt7a by granule cells increases as this process occurs in the second postnatal week (Lucas and Salinas, 1997). Accordingly, Wnt7a has been shown to promote axonal remodeling and synapse formation in rosette development (Hall et al., 2000). By adulthood, mossy fibers contact specialized structures of granule cells known as dendritic claws, which form following dendritic pruning in the second postnatal week (de la Torre-Ubieta and Bonni, 2011).

In conclusion, the first three postnatal weeks see rapid changes in dendritic architecture and synaptic connectivity across the hippocampus, cortex and cerebellum. While numerous factors involved in these developmental processes have already been identified, a greater understanding of these processes and their molecular controls will not only provide fascinating insights into the development of an exceedingly beautiful and complex structure, but may yield knowledge that will prove useful in the treatment of developmental neuropsychiatric disorders (Ehninger et al., 2008; LeBlanc and Fagiolini, 2011; Owen et al., 2011).

7.3. CaSR

CaSR is a GPCR initially cloned from the bovine parathyroid gland (Brown et al., 1993). It has a key role in systemic calcium homeostasis, acting as a sensor for Ca^{2+}_o, stimulating the release of parathyroid hormone following reductions in serum calcium levels in order to maintain $[Ca^{2+}]_o$ within narrow physiological limits (Brown, 1991; Brown and Macleod, 2001). Soon after the initial cloning of CaSR, it became clear that the receptor was expressed widely outside of the parathyroid gland and could be detected in a variety of organs including rat kidney, lung, pituitary, ileum and brain, being localized to nerve terminals in the latter (Ruat et al., 1995). For this reason, it has long been thought that CaSR must have physiological functions beyond its role in systemic calcium homeostasis (Brown et al., 1993). Over the last two decades, experimental studies in other tissues have increasingly illuminated the multifarious functions of CaSR (Riccardi and Kemp, 2012).

Since this thesis aims to increase our knowledge of the roles of CaSR in the development and plasticity of the nervous system, what is presently known about the expression, function, structure and signalling of CaSR shall be systematically reviewed here, with a focus on those aspects most pertinent to the nervous system.

7.3.1. CaSR Expression

The wide expression of CaSR has been suggested ever since the first group to clone the receptor from the bovine parathyroid gland indicated expression in the bovine kidney, thyroid gland, cerebral cortex and cerebellum (Brown et al., 1993). CaSR has subsequently been found to be expressed in a wide variety of tissues including the placenta, gut, embryonic lung and bone, with many sites of CaSR expression have no apparent connection to the initially described function of global Ca^{2+}_o homeostasis (discussed in 7.3.2) (Brown and Macleod, 2001; Hofer and Brown, 2003; Riccardi and Kemp, 2012). Furthermore, CaSR has been shown to be expressed in a wide variety of species, shedding some light on its evolutionary origins (Brown and Macleod, 2001; Hofer and Brown, 2003; Herberger and Loretz, 2013b). These interesting aspects of CaSR expression shall be briefly reviewed here, before focussing on what is known about CaSR expression in the nervous system.

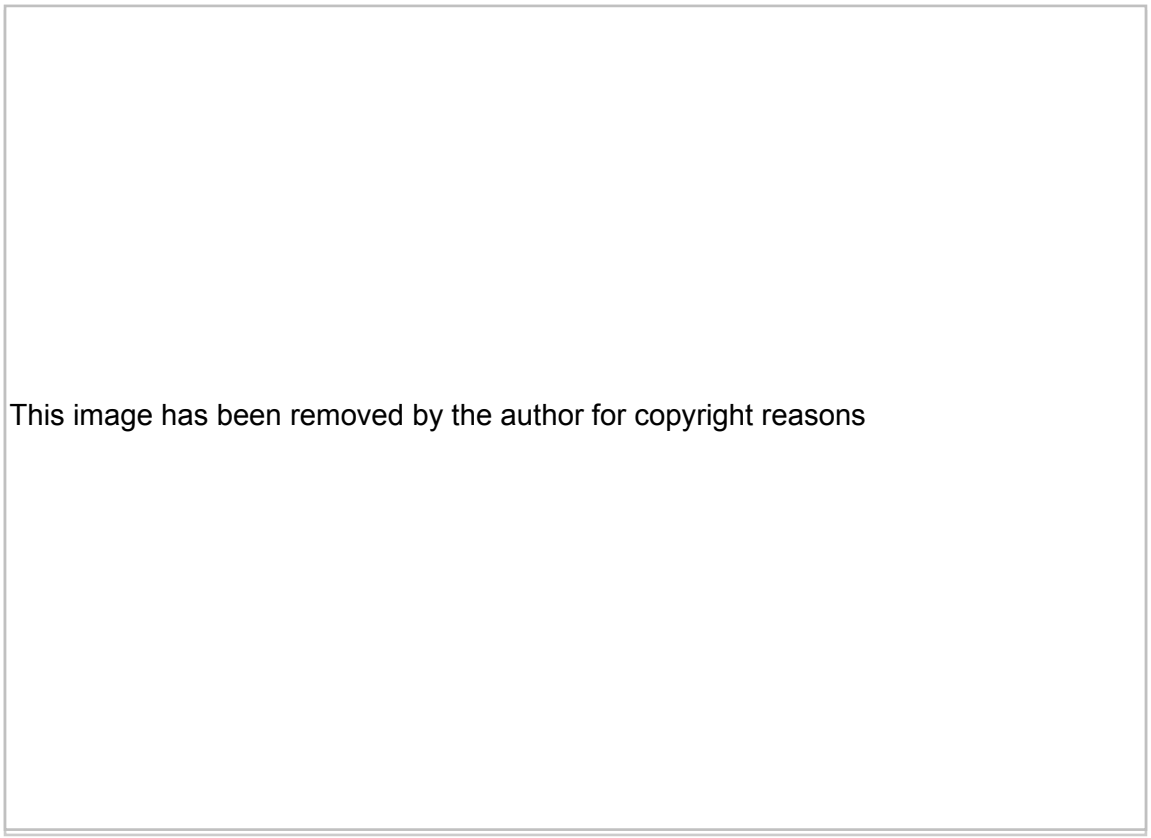

Figure 17: Evolutionary relationships of family C GPCRs

Group I comprises the mGluRs; CaSR falls within group II along with a sub-family of vomeronasal putative pheromone receptors, VRs and GoVNs; Group III includes the leucine-isoleucine-valine (LIV) bacterial nutrient-binding protein and $GABA_B$ receptors. The arrangement in a tree diagram indicates closeness of evolutionary relationships. From E M Brown, R J MacLeod 2001.

7.3.1.1. Sequence comparisons and the evolutionary origins of CaSR

Comparison of the sequences of the *Casr* gene and CaSR protein to other GPCRs, and to *Casr* and *Casr*-like genes in other species, has shed some light on the likely evolutionary origins of this receptor, which in turn aid our understanding of its various functions (Brown and Macleod, 2001; Loretz, 2008; Herberger and Loretz, 2013b).

Sequence comparisons place CaSR within family C of the GPCR superfamily, which are defined on the basis of sharing ≥ 20% amino acid identity within their transmembrane, heptahelical (HH) domain (Brown and Macleod, 2001). Within family C there are three known groups of receptors: Group I comprises the mGluRs; Group II includes both CaSR and a sub-family of vomeronasal putative pheromone receptors, VRs and GoVNs; Group III includes the leucine-isoleucine-

valine (LIV) bacterial nutrient-binding protein and $GABA_B$ receptors (See Figure 17). The homology with LIV-BP has been interpreted as support for the hypothesis that CaSR, as well as other family C GPCRs, owe their evolutionary origin to a fusion event between an existing GPCR and a periplasmic nutrient binding protein, the latter of which contributed the ancestral "venus-flytrap" (VFT) domain that characterizes the extracellular region of this GPCR family (Brown and Macleod, 2001; Loretz, 2008). Interestingly, each of these three groups has a strong connection to the nervous system; the synaptic roles of mGluRs and $GABA_B$ receptors are well known, while VRs are expressed in neurons of the rat vomeronasal organ, and roles for CaSR in the nervous system are emerging (Ryba and Tirindelli, 1997; Brown and Macleod, 2001).

Cross species sequence comparisons have revealed that *Casr* homologues are found widely within the tetrapods, and also the teleost and elasmobranch fishes (Hofer and Brown, 2003; Loretz, 2008). Since such fishes lack a parathyroid gland it is clear that the evolutionary origin of CaSR predates that of the gland in which its function was first described (Brown and Macleod, 2001). Accordingly, the hypothesized evolutionary relationship between fish gills (where CaSR is expressed and can act as a salinity detector involved in osmoregulation) and the parathyroid gland of terrestrial vertebrates, has led to the suggestion that the role for CaSR in systemic $[Ca^{2+}]_o$ homeostasis may have arisen as a consequence of land colonization (Riccardi and Kemp, 2012). Alternatively, the finding that CaSR expression seems to be largely confined to vertebrates and possibly some non-vertebrate chordates, had led to the hypothesis that a more evolutionarily ancient function of CaSR may be the regulation of skeletal development, which has recently been elegantly tested (Chang et al., 2008; Herberger and Loretz, 2013b, a). For more information about the role of CaSR in systemic $Ca^{2+}{}_o$ homeostasis and skeletal development see section 7.3.2.1.

7.3.1.2. CaSR is expressed in the CNS

The first study to investigate CaSR expression in the brain used an immunohistochemical approach in adult rats. It found no evidence of staining in cell bodies of either neurons or glia, but dispersed staining localized to nerve terminals (Ruat et al., 1995). This staining was most evident in the hippocampus, cortex and cerebellum. Since this study, a number of others have sought to define

the spatio-temporal expression of CaSR in the brain more precisely. Within the next two years, two more studies had been published. One study examined the postnatal developmental profile of CaSR expression in the rat hippocampus by *in situ* hybridisation combined with Western and Northern blotting (Chattopadhyay et al., 1997b). This analysis found a significant increase in hippocampal CaSR expression across all CA subfields and the DG between P5 and P10, which remained high for several weeks before dropping down to adult levels by P45. Because this period of elevated CaSR expression coincides with a period of rapid structural remodelling in the hippocampus (Turner et al., 1998; Danglot et al., 2006), and the earliest developmental age at which LTP can be induced, it was interpreted as supporting a possible role for CaSR in regulating learning and memory (Chattopadhyay et al., 1997b; Yano et al., 2004). The second study assessed CaSR expression more broadly in adult rat brain by *in situ* hybridisation and confirmed expression of CaSR mRNA in the adult hippocampus, with CA3 reported as the highest expressing subfield (Rogers et al., 1997). In the cortex, only scattered CaSR expressing cells were detected, while, in contrast to a previous report (Ruat et al., 1995), high expression in cerebellar Purkinje neurons was observed. The highest levels of CaSR expression were reported in the sub-fornical organ (SFO) (Rogers et al., 1997).

A further CaSR expression analysis used *in situ* hybridisation to assess mRNA levels across a wide a variety of brain regions and over several postnatal developmental ages, and found CaSR expression in both neurons and oligodendrocytes (Ferry et al., 2000). This study confirmed adult expression of CaSR in the SFO, but revealed that CaSR expression actually peaked during an early phase of postnatal development in many brain regions. Furthermore, this study failed to detect CaSR expression in cerebellar Purkinje cells or in the CA1 field of the hippocampus (Ferry et al., 2000), as found previously (Chattopadhyay et al., 1997b; Rogers et al., 1997). Interestingly, high levels of expression were found in the CA2 subfield of the hippocampus, peaking around P7-9 and declining into adulthood. Thus, the findings of this study are both spatially and temporally different from the earlier analyses of CaSR expression in hippocampal development (Chattopadhyay et al., 1997b). Until recently, it was thought that LTP could not be induced in CA2, so the data produced by Ferry et al., (2000) would have seemed to contradict the earlier suggestion that CaSR could be involved in

learning and memory related processes. However, a more recent investigation has found that LTP can indeed be induced in CA2 (Chevaleyre and Siegelbaum, 2010). Another more recent expression study has also reported high CaSR mRNA expression in the CA2 field of the adult rat hippocampus (Mudò et al., 2009). Thus, while there are some significant discrepancies in the literature related to the sites of CaSR expression within the CNS, both studies that examined a developmental time course suggest hippocampal CaSR expression changes dynamically in the first few postnatal weeks (Chattopadhyay et al., 1997b; Ferry et al., 2000). However, it should be noted that all of these investigations used non-quantitative techniques and lacked a high degree of temporal resolution. Taken together, data on CaSR expression within the developing CNS raise the possibility that CaSR may play a role in the critical developmental processes that occur over the first few postnatal weeks, such as dendritic arborisation and synaptogenesis (Turner et al., 1998). If this is the case, CaSR may contribute to processes such as hippocampal dependent learning and memory, either indirectly through facilitating the development of the neural networks on which it depends (Vizard et al., 2008), or directly, for example, through the regulation of synaptic function (Phillips et al., 2008; Chen et al., 2010; Vyleta and Smith, 2011).

CaSR expression has also been described in the select population of gonadotrophin-releasing hormone (GnRH) neurons within the developing hypothalamus (Chattopadhyay et al., 2007) and in several types of glial cells (Bandyopadhyay et al., 2010) The potential significance of these observations will be explored in sections 7.3.2.2.3 and 7.3.2.2.5, respectively.

7.3.1.3. CaSR is expressed in the PNS

The expression of CaSR in the PNS has also been investigated, although to a lesser extent than the CNS. CaSR mRNA expression has been reported in the late embryonic and postnatal mouse SCG, with a sharp peak in expression being observed at E18 (Vizard et al., 2008). Unpublished data indicate that CaSR is also expressed at high levels during the early stages of SCG development (Figure 33A, Results Chapter 1, Tom Vizard, personal communication), with a dip in expression at E16 dividing these two developmental windows of gene expression (Vizard et al., 2008). In addition, other studies have shown that CaSR mRNA is expressed in adult rat dorsal root ganglia (Ferry et al., 2000; Mudò et al., 2009), and CaSR mRNA

and protein are expressed within adult rat trigeminal ganglia and their sensory axons (Heyeraas et al., 2008).

7.3.1.4. Splice variants

Since the initial cloning of *Casr,* it has been found to be alternatively spliced (Oda et al., 1998; Brown and Macleod, 2001). A naturally occurring splice variant, lacking exon 5, which encodes 77 amino acids of the extracellular domain, was initially identified in human keratinocytes (Oda et al., 1998). The co-expression of this splice variant with the full-length receptor in HEK293 cells reduces the levels of IP_3 produced in response to changes in extracellular calcium concentration compared to HEK293 cells only expressing full length CaSR (Oda et al., 1998). In addition, keratinocytes from neonatal mice lacking exon 5 of *Casr* display impaired $[Ca^{2+}]_o$ -dependent differentiation of keratinocytes compared to wild type mice (Oda et al., 2000). Furthermore, expression of the splice variant lacking exon 5 has also been reported in growth plate, and kidney (Chang et al., 2008). Mice containing a targeted deletion of *Casr* exon 5 die in the first two postnatal weeks, due to a deficit in systemic calcium homeostasis, and display bone abnormalities and retarded growth (Ho et al., 1995; Kos et al., 2003). A conditional knockout approach (see Figure 18) has demonstrated that the deletion of exon 7 of *Casr* has a more severe phenotype than the loss of exon 5, which still leaves a partially functional CaSR protein being expressed (Chang et al., 2008). The early conditional deletion of floxed *Casr* exon 7 in chondrocytes, using a cre-recombinase driven by the type II collagen-α1 subunit promoter, produces an embryonic lethal phenotype prior to E13. A tamoxifen-inducible deletion of exon 7 from chondrocytes at E15-E16 generates viable mice with chondrocyte growth plate abnormalities and shortened limbs. (Chang et al., 2008). Therefore, it appears as if the exon 5-less splice variant of *Casr* may be sufficient to provide a functional rescue following the early deletion of exon 5 in chondrocytes, although whether this is a partial or full rescue remains to be determined (Chang et al., 2008). Notably, however, the exon 5-less splice variant is not expressed in E18 SCG (Vizard et al., 2008).

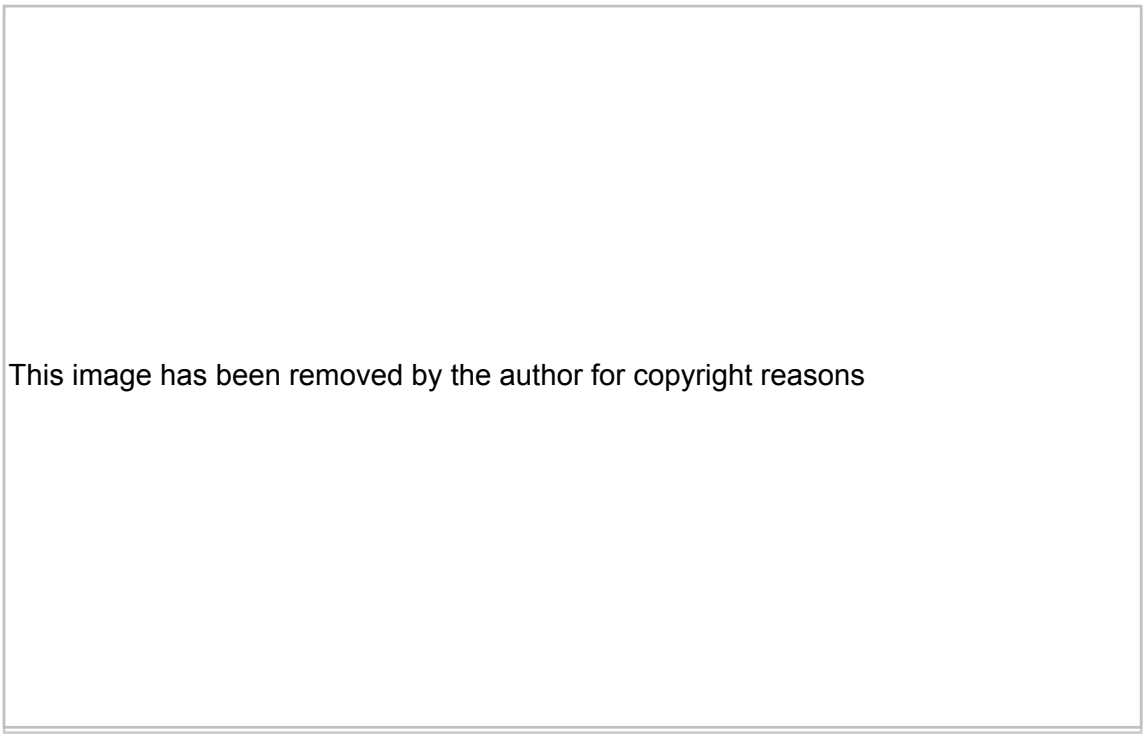

Figure 18: Generation and genotyping of floxed *Casr* mice

***A*,** The targeting construct used in the generation of floxed *Casr* mice contained three loxP sites, two of which flanked the cytidine deaminase (CD)–neomycin (NEO) gene cassette, while the other was 3' of *Casr* exon 7. This targeting construct was introduced into 129/SvJae ES cells by transfection, where homologous recombination resulted in the insertion of the recombinant sequence into the endogenous *Casr* locus. These ES cells were injected into C57/BL6 blastocysts, resulting in chimeric mice that were bred to give heterozygous (*Casr* $^{fl/+}$) and homozygous (*Casr* $^{fl/fl}$) mice.
Cre recombinase exposure results in the excision of Exon 7 of *Casr.*
B*,** Genotyping of ES cells containing a floxed *Casr* allele and of tail DNA from wild-type, *Casr* $^{fl/+}$ and *Casr* $^{fl/fl}$ mice, using primers positioned as detailed in ***A.
***C*,** Polymerase chain reaction (PCR) analysis of DNAs detailed in B exposed to Cre recombinase *in vitro*. Where a floxed *Casr* allele is present, exon 7 is excised and P4/P3L amplify a smaller fragment of 284 bp.
Figure and data from Chang *et al* 2008.

7.3.1.5. Regulation of CaSR expression

Considering the large number of reports assessing CaSR expression in various tissues across various species, comparatively little is understood about the mechanisms governing the regulation of CaSR expression. However, in addition to the reported alterations in CaSR expression levels that occur during development (Chattopadhyay et al., 1997b; Ferry et al., 2000; Brown and Macleod, 2001; Vizard et al., 2008; Riccardi and Kemp, 2012), numerous other physiological or disease

states appear to be associated with altered CaSR expression (Brown and Macleod, 2001; Cavanaugh et al., 2012).

CaSR expression has been reported to be up-regulated in the rat SFO in response to dehydration (Hindmarch et al., 2008) and in the brain following lesions induced via kainate administration or needle penetration (Mudò et al., 2009). Interestingly, the expression of CaSR was found to correlate with that of Wnt2 in a spatio-temporal analysis of mRNA expression from post-mortem human brains taken during development, adulthood and aging (Kang et al., 2011). Cell culture experiments have also revealed scenarios where CaSR expression may be regulated. For example, when placed in culture, bovine parathyroid cells undergo a rapid (1-2 hours) down-regulation of CaSR mRNA, with CaSR protein expression dropping around 80% over 1-2 days (Brown and Macleod, 2001). In contrast, CaSR mRNA increases from 3 DIV to higher levels at 5 and 7 DIV in rat osteoblast cultures (Chattopadhyay et al., 2004).

The CaSR targeted pharmaceuticals NPS R-568 and NPS 2143, positive (a "calcimimetic") and negative (a "calcilytic") allosteric modulators, respectively are also capable of modulating CaSR expression. Following a 12 hour treatment of cultured HEK293 cells, NPS R-568 increases CaSR expression at the protein level while NPS 2143 decreases CaSR protein expression (Huang and Breitwieser, 2007). Interestingly, high $[Ca^{2+}]_o$ has been reported to promote CaSR expression in its own right in the AtT-20 cell line and has also been shown to promote the expression of the vitamin D receptor in the rat parathyroid gland. These observations could underlie the synergistic effects of $Ca^{2+}{}_o$ and the vitamin D metabolite, 1,25-dihydroxyvitamin D ($1,25(OH)_2D_3$) on promoting the differentiation of Caco-2 cells and the expression of calbindin D_{28K} in the kidney (Brown and Macleod, 2001). Furthermore, the thyroid transcription factor 1 (TTF-1) has been found to coordinate transcriptional responses to altered $[Ca^{2+}]_o$ in neural crest-derived parafolicular C-cells, including the regulation of CaSR, calmodulin and calcitonin transcription (Suzuki et al., 1998). Interestingly, TTF-1 is also expressed in the parathyroid glands, embryonic lung and developing diencephalon (Lazzaro et al., 1991), and has thus been proposed as a major mediator of $[Ca^{2+}]_o$-dependent gene expression, which may include the regulation of CaSR mRNA expression (Suzuki et al., 1998). In conclusion, the available data

raise the possibility that CaSR activation and a variety of other stimuli could regulate CaSR expression. The signalling mechanisms by which this may occur may involve TTF-1, but largely remain to be determined, as does the biological significance of the correlation between CaSR and Wnt2 expression in human brain.

7.3.2. Physiological roles of CaSR

The widespread expression of CaSR underscores an involvement in numerous physiological processes (Brown and Macleod, 2001; Hofer and Brown, 2003; Riccardi and Kemp, 2012). For the purposes of this introduction, the roles of CaSR in tissues contributing to systemic Ca^{2+} homeostasis shall be briefly reviewed, before focusing on putative and demonstrated functions in the nervous system.

7.3.2.1. CaSR in systemic Ca^{2+} homeostasis

There are two distinct fashions in which CaSR can contribute to systemic Ca^{2+} homeostasis: The direct regulation of parathyroid hormone (PTH) secretion from the parathyroid gland, or the regulation of other organs involved in systemic Ca^{2+} homeostasis, namely kidney and bone, via PTH-dependent or independent mechanisms (Riccardi and Kemp, 2012).

7.3.2.1.1. Parathyroid

The parathyroid gland acts as a key regulator of systemic Ca^{2+} through the secretion of PTH, which is stored in secretory granules within parathyroid chief cells (Riccardi and Kemp, 2012). The presence of CaSR on chief cell plasma membranes permits serum calcium control through a negative feedback loop, where reduced serum $[Ca^{2+}]_o$ is coupled to PTH release by CaSR signalling through $G\alpha_q/PLC/Ca^{2+}{}_i$ (Brown, 1991). Unusually, elevated $[Ca^{2+}]_i$ reduces PTH-containing vesicle fusion with chief cell plasma membranes and leads to reduced PTH secretion. Decreased serum $[Ca^{2+}]_o$ leads to increased PTH secretion as a result of decreased CaSR activity and a concomitant reduction in $[Ca^{2+}]_i$ (Brown, 1991). Since PTH secretion is approximately 50% maximal at physiological serum $[Ca^{2+}]_o$, enhanced CaSR activity can also reduce PTH secretion in response to increased serum $[Ca^{2+}]_o$ (Brown, 1991; Riccardi and Kemp, 2012).

7.3.2.1.2. Kidney

Since approximately 8 g of Ca^{2+} is filtered from the blood in the glomeruli of the kidney per day, but less than 2% of this is excreted in urine, the kidney also

extensively reabsorbs Ca^{2+} (Hoenderop et al., 2005). Classically, the manner in which kidney is involved in systemic Ca^{2+} homeostasis is the selective reuptake of Ca^{2+} from pro-urine in response to the PTH-induced synthesis of $1,25(OH)_2D_3$ in the proximal tubule of the kidney (Hofer and Brown, 2003). However, CaSR is also widely expressed in the kidney itself where it participates more directly in PTH independent regulation of Ca^{2+} homeostasis, along with further roles including water and NaCl reabsorption, renin secretion and acidification of urine (Riccardi and Kemp, 2012). Interestingly, renal CaSR expression is polarized, such that in some regions of the kidney the receptor is localised to the apical membrane (in contact with the urinary space), while in others it is localized to the basolateral membrane (in contact with the interstitial plasma) (Riccardi and Brown, 2010). For instance, CaSR is expressed apically in the proximal tubule, where upon activation it antagonises the negative regulation of inorganic phosphate reabsorption exerted by PTH. Activation of apical CaSR in the distal convoluted tubule promotes Ca^{2+} reabsorption through TRPV5 channels (Riccardi and Kemp, 2012). In contrast, CaSR is expressed basolaterally in the thick ascending limb of the loop of Henle, where CaSR activation reduces the activity of apical ion transporters such as NKCC2 (Riccardi and Kemp, 2012).

7.3.2.1.3. Bone

The classical contribution of bone to systemic Ca^{2+} homeostasis is the net release of Ca^{2+} by bone under the influence of sustained elevated PTH, which contributes to returning low serum $[Ca^{2+}]_o$ to normal levels (Hofer and Brown, 2003). However, numerous PTH independent effects of CaSR in bone have also come to light. CaSR is expressed by osteoblasts (cells that form bone), osteocytes (mechanosensory bone cells) and osteoclasts (cells that resorb bone) (Dvorak et al., 2004; Riccardi and Kemp, 2012). CaSR appears to regulate several aspects of osteoblast function *in vitro*, including survival, proliferation and mineralization (Dvorak et al., 2004). An *in vivo* study has revealed that PTH independent, constitutive CaSR activation promotes osteoclast generation, enhanced bone resorption and expression of Receptor activator of nuclear factor kappa-B ligand (RANK-L), a well-known modulator of osteoclast differentiation, activation and survival (Dvorak et al., 2007). CaSR activation has also been shown to promote osteoclast differentiation and mature osteoclast apoptosis *in vitro* (Mentaverri et al., 2006). Interestingly, activation of CaSR by elevated $[Ca^{2+}]_o$ induces the

apoptosis of mature osteoclasts by a signalling mechanism involving PLC-dependent nuclear translocation of NF-κB, the same signalling mechanism engaged by RANK-L to induce osteoclast apoptosis (Mentaverri et al., 2006).

A landmark *in vivo* study into the role of CaSR in skeletal development has used a conditional transgenic approach to demonstrate that the loss of functional CaSR in either osteoblasts or the parathyroid gland impairs skeletal growth, supporting the conclusion that regulation of bone growth by CaSR can occur by either PTH-dependent or independent mechanisms (Chang et al., 2008). As mentioned above, the loss of functional CaSR in late embryonic chondrocytes impairs cartilage formation *in vivo* (Chang et al., 2008). Interestingly, the loss of $GABA_B$ receptors, which interact with CaSR in cultured chondrocytes, impairs the capacity of CaSR to signal via ERK1/2 and PLC and reduces chondrocyte proliferation and survival (Chang et al., 2007). Strikingly, CaSR knockdown in zebrafish embryos also impairs skeletal development, raising the possibility that the regulation of skeletal growth by CaSR may represent an evolutionarily conserved mechanism (Herberger and Loretz, 2013a).

7.3.2.2. CaSR functions in the Nervous System

The numerous reports of CaSR expression in the developing and adult brain (Ruat et al., 1995; Chattopadhyay et al., 1997b; Ferry et al., 2000; Mudò et al., 2009) have lead to a growing interest in the potential functions of CaSR in the nervous system. The roles reported to date shall be discussed in some detail, beginning with a recently reported role for CaSR in the developing PNS (Vizard et al., 2008).

7.3.2.2.1. CaSR and SCG axon growth & branching

An unexpected novel role for CaSR has recently been discovered in the developing SCG. During the second developmental peak of CaSR mRNA expression at E18, CaSR activation by constitutively raised $[Ca^{2+}]_o$ increases NGF-promoted growth and branching of sympathetic axons *in vitro,* without affecting neuronal survival. Moreover, the relevance of these effects to *in vivo* development has been confirmed with the finding that the innervation density of the iris (a target of the SCG) is reduced in P1 $CaSR^{-/-}$ mice compared to littermate wild type controls, while the number of neurons in the SCG of remains unchanged. The role of CaSR in transducing the effect of increases in $[Ca^{2+}]_o$ into enhanced SCG neuron axon growth and branching has been confirmed *in vitro* by the use of; the calcimimetic

NPS-R467, the calcilytic NPS- 89636, over-expression of a mutant construct exerting a dominant-negative effect on CaSR activity and cultures established from *Casr* $^{-/-}$ mice (Vizard et al., 2008). The efficacy of CaSR signalling in regulating SCG neuron axon growth and branching appears to be regulated by the level of CaSR expression, as no effect of altered $[Ca^{2+}]_o$ on axonal growth and branching is observed in cultures of neurons established from embryos and neonates at ages either side of the developmental peak in CaSR expression at E18. Moreover, elevated $[Ca^{2+}]_o$ can promote axonal growth and branching from cultured P1 SCG neurons over-expressing wild type CaSR, while over-expression of the wild-type receptor does not enhance the ability of elevated $[Ca^{2+}]_o$ to promote axonal growth and branching at E18 (Vizard et al., 2008). The studies that comprise part of this thesis aim both to further characterise the CaSR-mediated promotion of SCG neuron axonal growth and branching at E18 and to investigate potential roles for CaSR during its earlier developmental peak of expression in the SCG between E13 and E15 (Figure 33A, Results Chapter 1), a time period when proximal axon growth, proliferation and differentiation of sympathetic neurons are occurring *in vivo* (Glebova and Ginty, 2005).

7.3.2.2.2. CaSR in synaptic physiology, excitability and dendritic growth

Theoretical work preceded experimental data in predicting a role for CaSR in modulating synaptic physiology. Modelling studies predict that fluctuations in $[Ca^{2+}]_o$ should occur in the confined volume of the synaptic cleft as a result of neural activity (Egelman and Montague, 1998, 1999), as Ca^{2+} influx into pre- and post-synaptic termini are important events for vesicular neurotransmitter release and plasticity related changes, respectively (Figure 19). A simplified modelling study has suggested that fluctuations in $[Ca^{2+}]_o$ within the synaptic cleft are likely to be dependent upon the frequency of neuronal stimulation (Vassilev et al., 1997a). This simplified model predicts that at 3 Hz (low frequency) each pulse may cause a drop in synaptic cleft $[Ca^{2+}]_o$ from 1.5 mM to 1.39 mM, with full recovery of $[Ca^{2+}]_o$ to 1.5mM occurring in the 333 ms between pulses through lateral diffusion and efflux across the postsynaptic membrane via Ca^{2+} pumps and exchangers. In contrast, $[Ca^{2+}]_o$ in the synaptic cleft may be depleted to just 0.8 mM at 100 Hz (high frequency) (Vassilev et al., 1997a). Since CaSR in the parathyroid gland can detect changes in serum $[Ca^{2+}]_o$ of just 2-3% (Brown, 1991), such activity

induced changes in synaptic cleft $[Ca^{2+}]_o$ are certainly of a magnitude theoretically detectable by pre- or postsynaptic CaSR (Vassilev et al., 1997a).

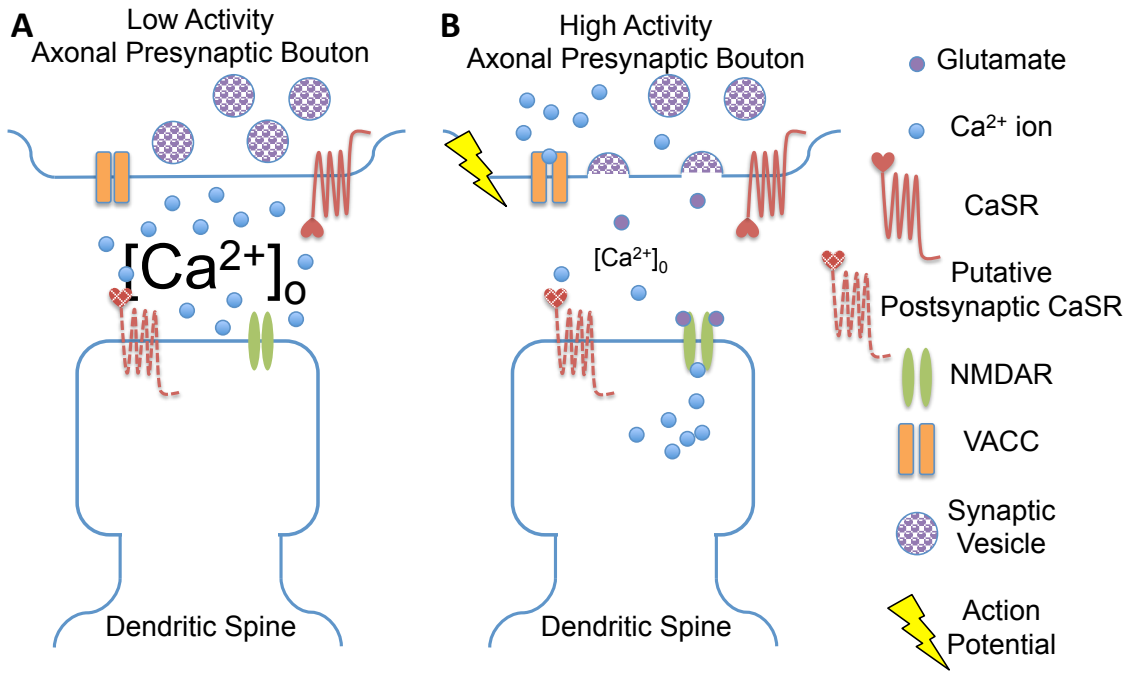

Figure 19: Schematic illustrating synaptic cleft $[Ca^{2+}]_o$ depletion during synaptic activity

***A*,** At resting state, $[Ca^{2+}]_o$ remains around normal physiological levels
***B*,** During periods of high frequency synaptic activity, $[Ca^{2+}]_o$ drops. Ca^{2+} influx into the presynaptic bouton though VACC is required for activity-dependent docking of synaptic vesicles. Neurotransmitters such as glutamate can diffuse across the synaptic cleft to activate receptors including NMDARs, which when activated permit Ca^{2+} entry into the postsynaptic dendritic spine. Since both calcium conductances draw on $Ca^{2+}{}_o$ and the synaptic cleft is limited in volume, reductions in cleft $[Ca^{2+}]_o$ that are detectable by CaSR can occur during high-frequency stimulation, as the time between stimulation is insufficient for $[Ca^{2+}]_o$ to be returned to resting levels by Ca^{2+} extrusion mechanisms and lateral diffusion.

In accordance with this body of theoretical work, activity dependent depletions of $[Ca^{2+}]_o$ have since been demonstrated in hippocampal slices by the use of a dynamic fluorescent probe that is sensitive to changes in $[Ca^{2+}]_o$ (Rusakov and Fine, 2003). Activation of presynaptic CaSR has been shown to depress synaptic transmission between cultured cortical neurons (Phillips et al., 2008) by inhibiting the gating of a presynaptic, non-selective cation channel (NSCC), thereby reducing NSCC currents and reducing the probability of neurotransmitter release (Phillips et al., 2008; Chen et al., 2010). By this means, CaSR can transduce fluctuations in synaptic $[Ca^{2+}]_o$ into physiologically meaningful effects. The CaSR-mediated

attenuation of synaptic transmission at normal synaptic cleft $[Ca^{2+}]_o$ means that reduced inhibitory CaSR tone acts to compensate for the fall in neurotransmitter release probability accompanying activity induced reductions in $[Ca^{2+}]_o$ within the synaptic cleft (Figure 20) (Phillips et al., 2008; Chen et al., 2010).

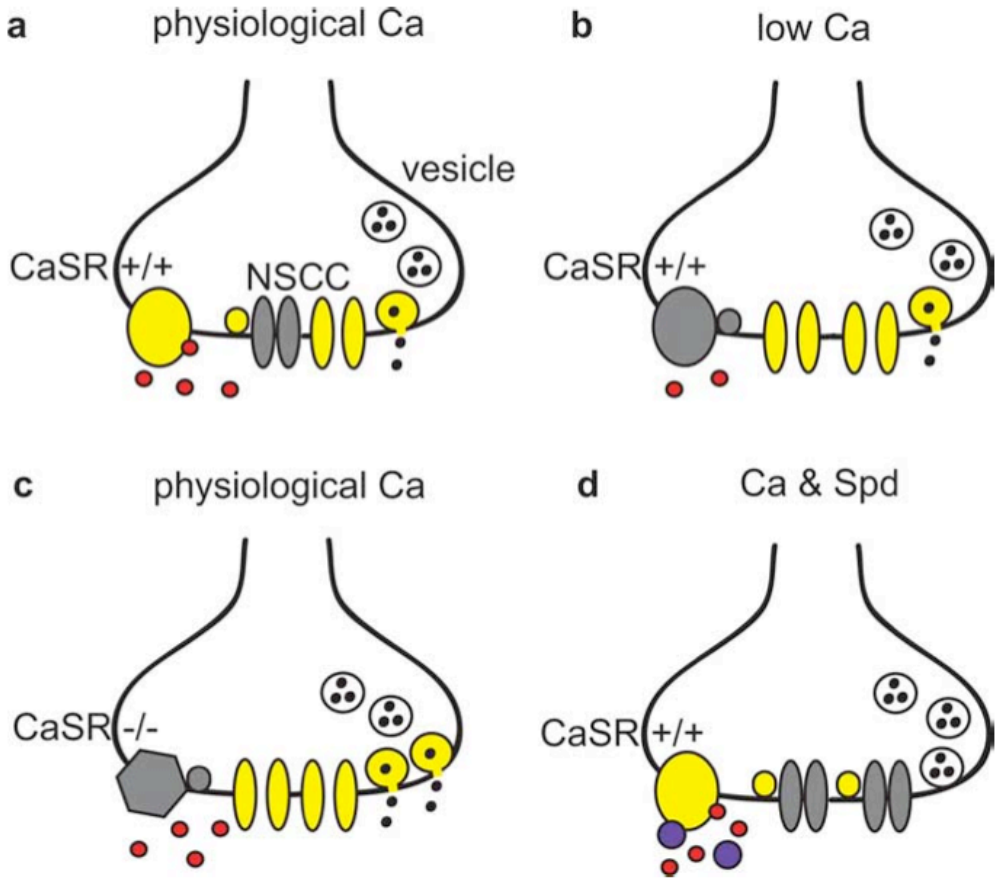

Figure 20: Model for CaSR modulation of neurotransmitter release

A, Model depicts nerve terminal membrane containing CaSR (yellow oval) which is activated by Ca^{2+}_o (red). A proportion of the NSCCs are closed (gray) by an unknown CaSR-mediated signal (yellow circle). At physiological $[Ca^{2+}]_o$, CaSR is not fully activated and some active NSCC (yellow) facilitate vesicle fusion and transmitter release.

B, At reduced $[Ca^{2+}]_o$, such as during high frequency stimulation, CaSR is no longer activated (gray) and in the absence of this signal NSCC may be activated (yellow) by depolarization. Because reduced $[Ca^{2+}]_o$ will also decrease Ca^{2+} entry through VACC and the probability of exocytosis, the increase in NSCC activity may partially compensate by facilitating vesicle fusion.

C, At physiological $[Ca^{2+}]_o$ reduced affinity (exon 5-deficient) $CaSR^{-/-}$ (gray hexagon) is less likely to be activated than $CaSR^{+/+}$.Consequently, there is reduced signalling to NSCC, which remains active, increasing the average probability of neurotransmitter release.

D, Application of spermidine (Spd; purple circles) or Ca^{2+} to wild-type neurons fully activates CaSR reducing NSCC activity and transmitter release. Unlike Ca^{2+}, Spd does not enter the terminal and trigger exocytosis directly. Active molecules are colored yellow and inactive molecules are colored gray. Figure from Phillips *et al* (2008).

A role for CaSR activity in attenuating neural activity and synaptic transmission through the regulation of ion channel opening when $[Ca^{2+}]_o$ is in the normal physiological range appears to be an emerging theme (Riccardi and Kemp, 2012). In addition to the aforementioned modulation of NSCC gating (Phillips et al., 2008; Chen et al., 2010), there is also evidence that presynaptic CaSR activation regulates the opening of a Ca^{2+}-activated K^+ channel (CAKC) in cultured wild type, but not *Casr* $^{-/-}$, postnatal hippocampal neurons (Vassilev et al., 1997b). Normal levels of $[Ca^{2+}]_o$ leads to CaSR mediated opening of CAKC channels. The authors hypothesised that opening of CAKCs results in hyperpolarization of presynaptic terminals, the subsequent inhibition of voltage-activated calcium channel (VACC) opening and reduced neurotransmitter release. Alterations in $[Ca^{2+}]_o$ have also been shown to regulate the gating of the voltage–insensitive, non-selective sodium channel, NALCN in cultured postnatal hippocampal neurons (Lu et al., 2010). NALCN is responsible for an inward sodium leak current that acts to depolarise neurons. Normal physiological $[Ca^{2+}]_o$ inhibits the opening of NALCN, thereby inducing hyperpolarisation. Reductions in $[Ca^{2+}]_o$ increase the opening of the channel, via a CaSR-dependent mechanism, thereby increasing neuronal excitability. CaSR appears to regulate the gating of NALCN by a signalling mechanism that includes both G-proteins and a physical interaction between CaSR, NALCN and two other proteins, UNC79 and UNC80 (Vyleta and Smith, 2011; Riccardi and Kemp, 2012).

In an interesting contrast to CaSR mediated inhibition of synaptic transmission described above, presynaptic CaSR activation can enhance spontaneous glutamate release (Vyleta and Smith, 2011). In contrast to action potential evoked glutamate release, this process does not seem to require VACCs or increases in $[Ca^{2+}]_i$, since it is not blocked by cadmium mediated blockade of VACC or by infusion of the Ca^{2+} chelator, BAPTA into the presynaptic terminal (Vyleta and Smith, 2011). Therefore, whilst the mechanism linking CaSR activation to vesicle exocytosis remains unclear, it differs from the other mechanism of synaptic modulation involving CaSR (Phillips et al., 2008), and the mechanism of PTH secretion in the parathyroid gland (Hofer and Brown, 2003), by a seeming lack of dependency on $Ca^{2+}{}_i$, (Vyleta and Smith, 2011).

CaSR also plays a role in regulating the gross dendritic architecture of hippocampal neurons from the CA2 and CA3 subfields in short-term organotypic slice cultures, established from early postnatal mice (Vizard et al., 2008). Given the growing evidence that CaSR has functional roles in synaptic physiology and since a number of molecules including BDNF (Ji et al., 2005; Ji et al., 2010), $p75^{NTR}$ (Zagrebelsky et al., 2005), Nogo-A (Zagrebelsky et al., 2010) and Cux1/2 transcription factors (Cubelos et al., 2010) regulate both the overall branching of dendrites and the morphology of dendritic spines, it will be interesting to assess whether CaSR also regulates spine morphology or excitatory synapse formation.

7.3.2.2.3. CaSR in neuronal migration

Another emerging role for CaSR in the CNS is the regulation of the migration of GnRH neurons. GnRH neurons form a key component of the hypothalamic-pituitary-gonadal axis and migrate from the anterior nasal compartment of the olfactory placode to the basal forebrain and hypothalamus (Wierman et al., 2004). In mouse, this migration is underway when GnRH neurons are first detectable at E10-11, the cribriform plate is crossed from E12-17 and migration is complete around birth (see Figure 21) (Wierman et al., 2004). It has been shown that migration of GnRH neurons from E11.5 nasal explants is dependent on Ca^{2+}_o, and that it is partially mediated by N-type VACCs (Toba et al., 2005). CaSR expression has subsequently been detected in GnRH cells *in vivo*, and in two cell lines commonly used for *in vitro* modelling studies, GT1-7 and GN11 cells. GT1-7 cells are derived from the hypothalamus and considered a model for GnRH cells undergoing the closing stages of migration, whereas GN11 cells are derived from the olfactory placode and are considered a model for early migratory stages (Figure 21) (Chattopadhyay et al., 2007). Furthermore, the expression of a dominant-negative CaSR construct impairs the Ca^{2+}_o promoted migration of both cell types and approximately 25% fewer GnRH neurons are observed in the hypothalamus of 4-5 week old *Casr* $^{-/-}$; *PTH* $^{-/-}$ mice compared to age matched *Casr* $^{+/+}$; *PTH* $^{-/-}$ controls (Chattopadhyay et al., 2007). Whether Ca^{2+}_o-promoted migration of GnRH neurons involves an interaction between CaSR and VACCs remains to be determined, as does whether CaSR can regulate the migration of other discreet populations of neuronal cells.

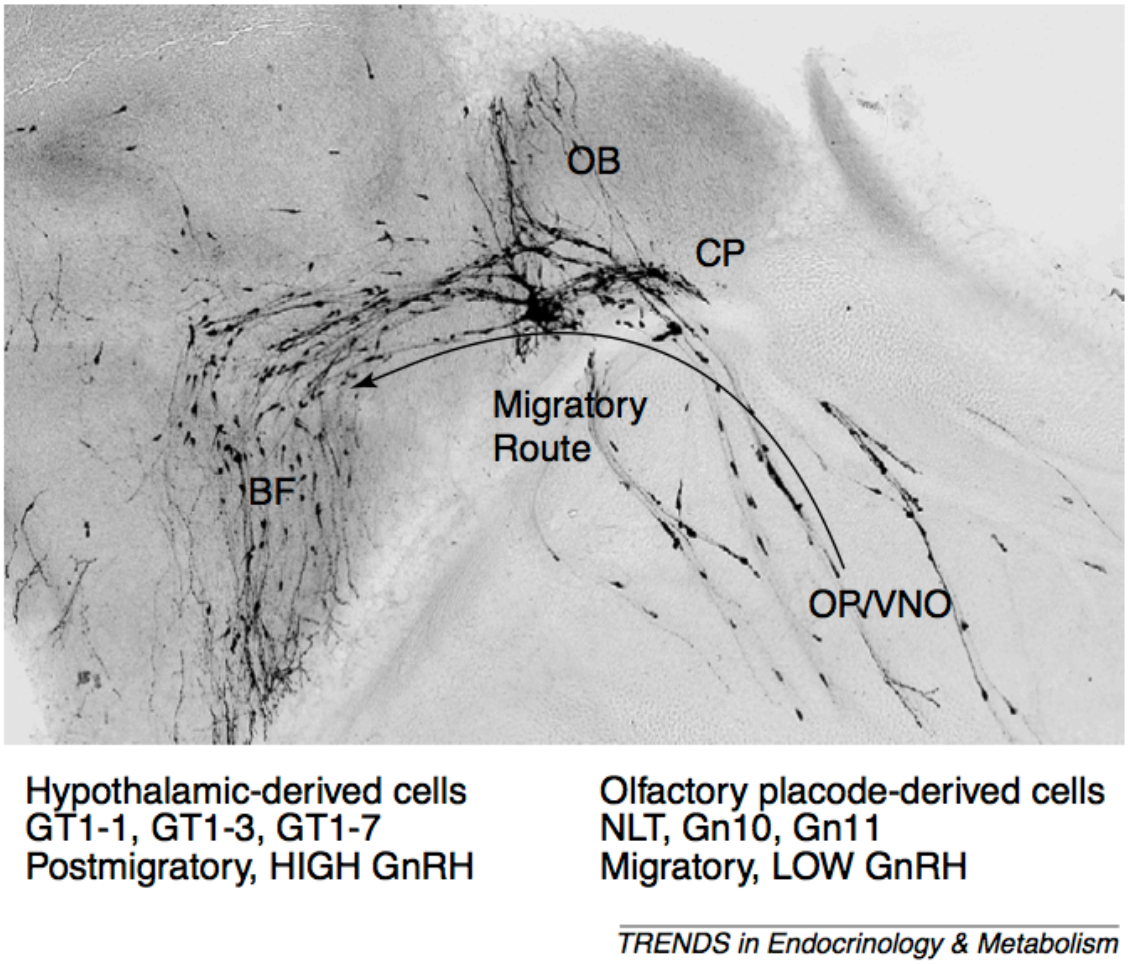

Figure 21: GnRH neuron migratory route & derivation of GnRH cell lines

The photomicrograph is from E15 mouse brain stained for GnRH and peripherin, and shows the normal migratory route of GnRH neurons from the olfactory placode region across the cribriform plate to the forebrain.
Immortalized NLT and Gn GnRH neuronal cells were derived from a tumor in between the olfactory region and cribriform plate, whereas the GT GnRH neuronal cells were derived from a tumor in the forebrain.
Abbreviations: BF, basal forebrain; CP, cribriform plate; OB, olfactory bulb; OP/VNO, olfactory placode/vomeronasal organ.
Figure from Wierman *et al* (2004).

7.3.2.2.4. CaSR and Alzheimer's disease

Some limited evidence has emerged to link CaSR with the aetiology of Alzheimer's disease (Yano et al., 2004; Conley et al., 2009; Bandyopadhyay et al., 2010). Firstly, it appears that the N-terminal fragment of amyloid precursor protein (APP), amyloid β (Aβ) can activate CaSR *in vitro* (Ye et al., 1997). In cultured postnatal hippocampal neurons from *Casr* $^{+/+}$, but not *Casr* $^{-/-}$ mice, application of $A\beta_{1\text{-}40}$ activates a calcium permeable NSCC. Furthermore, NSCC activation is also observed following Aβ exposure in CaSR expressing HEK293 cells, but not in non-

transfected cells (Ye et al., 1997). However, the consequences of NSCC activation for cellular or synaptic function are yet to be explored, as is whether such an effect could operate *in vivo*. Nonetheless, a separate study has provided further evidence of an activation of CaSR by Aβ (Conley et al., 2009). Cos-1 cells transfected with a CaSR expression construct exhibit a greater increase in PKC-responsive promoter driven Luciferase activity compared to control transfected neurons when exposed to $A\beta_{1-42}$ (Conley et al., 2009). Furthermore, $A\beta_{1-42}$ has been shown to promote astrocytic CaSR activation (discussed more fully in section 7.3.2.2.5) (Chiarini et al., 2009). In addition, a dinucleotide repeat polymorphism within intron 4 of the CASR gene has been found to significantly correlate with Alzheimer's disease status in a case/control study (cases n = 692; controls n = 435) (Conley et al., 2009). However, the impact of this intronic polymorphism on CaSR function has yet to be determined.

7.3.2.2.5. CaSR and glia

Several lines of evidence point to potential physiological roles for CaSR signalling in oligodendrocytes, astrocytes, astrocytoma cells and microglia (Yano et al., 2004; Bandyopadhyay et al., 2010).

The most convincingly supported glial function for CaSR involves oligodendrocytes (Bandyopadhyay et al., 2010). CaSR expression in these cells has been observed both *in vivo* (Ferry et al., 2000) and *in vitro* (Chattopadhyay et al., 1998). Indeed, CaSR mRNA is expressed at higher levels in cultured cortical oligodendrocytes than cultured cortical neurons or astrocytes (Chattopadhyay et al., 2008). Furthermore, the stimulation of CaSR *in vitro* has been shown to activate PLC (Ferry et al., 2000) and a CAKCs (Chattopadhyay et al., 1998) in this cell type (Yano et al., 2004; Bandyopadhyay et al., 2010). This may have functional significance, as there is evidence that CaSR activation promotes the proliferation of oligodendrocyte precursor cells and increases the mRNA levels of myelin basic protein (MBP). Importantly, MBP protein levels are decreased in the P12 cerebellum from *Casr* $^{-/-}$ mice compared to *Casr* $^{+/+}$ littermates (Chattopadhyay et al., 2008).

CaSR expression has also been detected in primary embryonic human astrocytes (Chattopadhyay et al., 2000), primary human astrocytomas (Chattopadhyay et al., 2000) and two astrocytoma cell lines (Chattopadhyay et al., 1999b; Chattopadhyay

et al., 1999a). In primary astrocytes and astrocytomas, elevated $[Ca^{2+}]_o$ promotes the synthesis and secretion of parathyroid hormone-related protein (PTHrP) in a CaSR-dependent manner (Chattopadhyay et al., 2000). Whilst PTHrP has been shown to inhibit astrocytic proliferation (Yano et al., 2004), mixed data have been reported regarding potential roles for CaSR in regulating the proliferation of astrocytoma cell lines. For example, CaSR agonists promote the proliferation of the U373 cell line and the opening of NSCCs (Chattopadhyay et al., 1999b). In contrast elevated $[Ca^{2+}]_o$ does not promote the proliferation of U87 cells, although CaSR activation induces the opening of a midi-type outward rectifying K^+ channel (Chattopadhyay et al., 1999a). Notably, the regulation of ion channels by CaSR is again a commonly reported theme (Riccardi and Kemp, 2012). Intriguingly, it has been reported that activation of astrocytic CaSR by $A\beta_{1\text{-}42}$ stimulates MAPK signalling pathways, resulting in the production of nitric oxide (NO) and its subsequent decay to highly reactive peroxynitrate. Since peroxynitrate can cause neuronal damage, it may play a role in Alzheimer's disease pathogenesis (Chiarini et al., 2009).

Finally, CaSR expression has been reported in microglia, the resident immune cells of the brain, where its stimulation promotes the opening of an outward rectifying K^+ channel (Chattopadhyay et al., 1999c). Since CaSR agonists appear to stimulate DNA synthesis and chemotaxis in the J774 monocyte/macrophage cell line, and increases in $[Ca^{2+}]_o$ also elicit a chemotactic response via CaSR in mature mouse monocytes/macrophages, it has been proposed that CaSR could serve a similar function in microglia (Yano et al., 2004). However, no unified, well-evidenced hypothesis of a role for CaSR in this cell type has yet been proposed (Bandyopadhyay et al., 2010).

7.3.3. Diseases linked to CaSR mutations

The importance of CaSR function in normal physiology is underscored by the number of diseases linked to CaSR mutations (Riccardi and Kemp, 2012). Inactivating mutations of CaSR are responsible for two human diseases, familial hypocalciuric hypercalcemia (FHH) and neonatal severe hyperparathyroidism (NSHPT). FHH arises in individuals who have a single copy of the *Casr* gene containing an inactivating point mutation, while NSHPT occurs in individuals with both *Casr* alleles containing an inactivating mutation (Hofer and Brown, 2003).

While FHH may be asymptomatic in some cases, possibly due to the ability of one wild-type *Casr* allele to compensate for the defective allele, individuals who have one copy of the *Casr* gene containing a point mutation that generates a dominant-negative CaSR, including an Arg185Gln substitution (R185Q), can present with a more severe phenotype (Hofer and Brown, 2003). NSHPT can be fatal, unless treated by parathyroidectomy, with surviving individuals exhibiting elevated serum $[Ca^{2+}]_o$, elevated serum [PTH], decreased urinary $[Ca^{2+}]_o$, along with other symptoms including severe skeletal abnormalities, developmental delay and spastic quadriparesis (a severe form of cerebral palsy) (Cole et al., 1990a; Hofer and Brown, 2003). Conversely, a form of autosomal dominant hypocalcemia (ADH) can be caused by activating mutations of CaSR (Pollak et al., 1994; Hofer and Brown, 2003). The first reported mutation of this kind was a Glu128Ala substitution (E128A), which was inherited in an autosomal dominant fashion, with affected individuals presenting with sub-normal serum $[Ca^{2+}]_o$, but normal serum [PTH] (Pollak et al., 1994). Since cells heterologously expressing the E128A mutant exhibit elevated IP_3 responses to high $[Ca^{2+}]_o$, it was concluded that a single copy of E128A is sufficient to increase CaSR activation levels in low serum $[Ca^{2+}]_o$, preventing compensation by increased PTH secretion (Pollak et al., 1994).

The key role of CaSR defects in producing FHH, and NSHPT has been further supported by mouse models (Hofer and Brown, 2003). The original *Casr* $^{-/-}$ mouse model, produced by deletion of exon 5, results in phenotypes highly reminiscent of FHH and NSHPT; *Casr* $^{+/-}$ mice exhibit slightly raised serum $[Ca^{2+}]_o$ and [PTH] with hypocalciuria, while *Casr* $^{-/-}$ mice exhibit more severely raised serum $[Ca^{2+}]_o$ and [PTH], along with bone defects, developmental delay and premature death (Ho et al., 1995). However, in accordance with recent findings indicating the original *Casr* $^{-/-}$ mice express a functional, exon 5-less splice variant (See section 7.3.1.4), conditional deletion of exon 7 in the parathyroid gland produces a more severe phenotype than exon-5 deleted *Casr* $^{-/-}$ mice, indicating that the exon 5-less splice variant has partial function in the parathyroid gland (Chang et al., 2008; Ward and Riccardi, 2012). The increase in serum [PTH] in *Casr* exon 5 deficient mice raises the question of what the contribution of raised PTH is to the other phenotypic abnormalities of these mice. This question has been addressed by the analysis of double-transgenic mice with homozygous deletions of both *Casr* exon 5 and *Pth* exon 3 (Kos et al., 2003). The loss of functional PTH rescues *Casr* $^{-/-}$ mice from

neonatal death and prevents the gross developmental abnormalities associated with the loss of *Casr* exon 5. However, serum and urine Ca^{2+} levels appear to be less tightly regulated than in wild type mice, supporting the physiological importance of PTH-independent roles for CaSR in systemic Ca^{2+} homeostasis.

In addition to the aforementioned spastic quadriparesis in some patients with NSHPT (Cole et al., 1990b), neurological phenotypes have been reported in other individuals with CaSR mutations. A genetic linkage analysis of a south Indian family affected by idiopathic generalised epilepsy revealed that an arginine-898 to glutamine (R898Q) substitution in CaSR was responsible (Kapoor et al., 2008). In addition, individuals with an activating mutation of CaSR (alanine-844 to proline substitution) exhibit hypocalcemia and can also present with seizures from childhood (Nakajima et al., 2009). Such findings raise the question of whether these neurological abnormalities are entirely secondary to defects in systemic Ca^{2+} homeostasis, or whether local roles of CaSR in the nervous system could also contribute (Vizard et al., 2008).

In conclusion, the medical conditions caused by CaSR mutations, and the similarities in phenotypes observed in mouse models of CaSR deletion, confirm the important physiological roles that this receptor plays (Ho et al., 1995; Kos et al., 2003; Ward and Riccardi, 2012). Particular CaSR mutations, and how they impinge on structure/function relationships of CaSR, will be discussed in more detail in section 7.3.4.

7.3.4. CaSR structure, pharmacology & signalling

As outlined above, CaSR activation can be linked to the regulation of a very diverse set of cellular processes that include; secretion, apoptosis, proliferation, differentiation, ion-channel gating and chemotaxis. The regulation of each process is mediated by members of a complex network of intracellular signalling molecules (Figure 22B) (Hofer and Brown, 2003). The remainder of this introduction shall discuss the major structural domains of CaSR and review the signalling pathways downstream of activated CaSR.

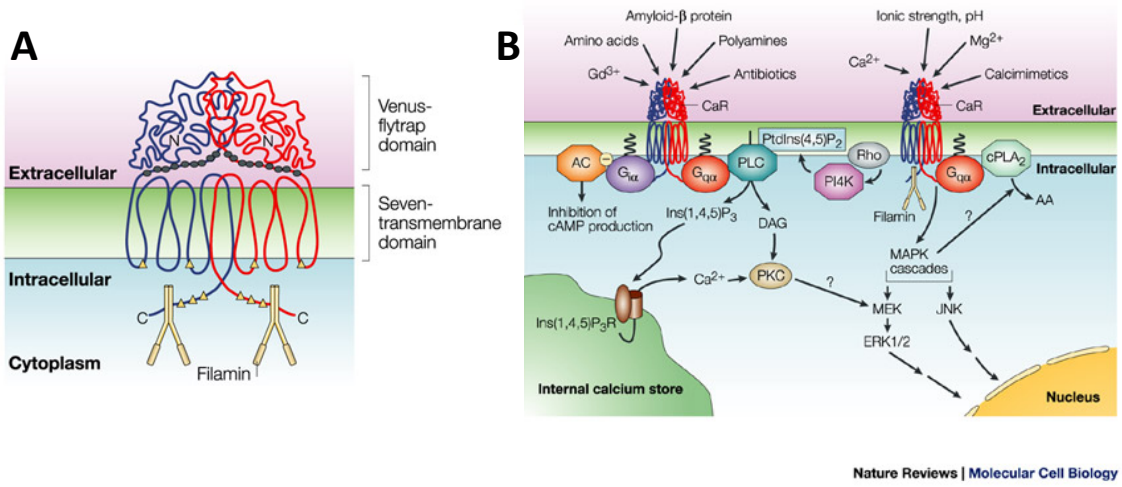

Figure 22: CaSR structure & function

A, CaSR is a GPCR constitutively found in a homodimeric form. In common with other family C GPCRs, it contains a large N-terminal extracellular domain (ECD), which forms a VFT domain and is the site for ligand binding. Individual cysteine residues comprising a cysteine rich domain important for transmitting signal across the trans-membrane helices are marked as grey ovals. Intracellular PKC phosphorylation sites are indicated by yellow triangles.
B, Schematic of CaSR ligands and intracellular signalling. CaSR is a promiscuous receptor, who's function is modified by a large number of extracellular factors. A complex network of intracellular signalling pathways are engaged by ligand binding. Signalling pathways not shown include PI3K/Akt. Figure modified from Hofer & Brown (2003).

7.3.4.1. Major CaSR structural domains

As described in section 7.3.1.1, CaSR belongs to class C of the GPCR superfamily. While family C GPCRs are defined on the basis of sharing ≥ 20% amino acid identity within their HH domain (Brown and Macleod, 2001), they also share a common domain architecture (Figure 22A). Family C GPCRs have in common a large 400–500 amino acid, bi-lobed VFT domain in their N-terminal extracellular region, which contains the Ca^{2+} binding sites of CaSR (Khan and Conigrave, 2010) together with 11 putative glycosylation sites (Ray et al., 1998). With the exception of $GABA_BR1$ (Hu et al., 2000), they also share a 60–70 amino acid cysteine rich (CR) domain. This domain contains nine highly conserved cysteine residues and is important for signal transmission to the membrane spanning HH domain, the domain housing G-protein interaction sites on its intracellular surface (Khan and Conigrave, 2010). Family C GPCRs also possess extensive intracellular C-terminal domains, which are involved in downstream signalling related interactions and

house numerous regulatory sites (Huang and Miller, 2007; Khan and Conigrave, 2010). Each of these CaSR structural domains shall be described in turn, including any relevant pharmacology and mutations.

7.3.4.1.1. VFT domain

Our understanding of the structure-function relationships of CaSR has been greatly facilitated by its homology to another family C GPCR, the metabotropic glutamate receptor type 1 (mGluR1). The crystal structure of dimerized mGluR1 ECD has been solved (Kunishima et al., 2000), as have those of mGluR3 and mGluR7 (Muto et al., 2007), shedding light on the likely structure of CaSR. CaSR is predicted to share the VFT domain conformation of the mGluR1 ECD and bacterial periplasmic binding proteins (O'Hara et al., 1993; Conklin and Bourne, 1994).

The CaSR ligand binding site is found in the VFT domain and exhibits highly cooperative binding, with a Hill coefficient of ~ 3 (Brown, 1991; Brown and Macleod, 2001). This property, and possibly also the homodimeric nature of functional CaSR, contribute to the high sensitivity of CaSR to small variations in $[Ca^{2+}]_o$ over a range likely to occur *in vivo* (Brown and Macleod, 2001). CaSR is half-maximally activated at about 3.5 mM $[Ca^{2+}]_o$, but is sensitive over a range between 0.5-10 mM, and responses to fluctuations in extracellular calcium concentrations as small as 200 μM have been reported. As physiological $[Ca^{2+}]_o$ is maintained at approximately 1.3 mM in most circumstances, such fluctuations can be biologically meaningful (Brown and Macleod, 2001). It has been predicted on the basis of the high Hill coefficient that each CaSR monomer binds at least three Ca^{2+} ions (Bai, 2004). Five potential Ca^{2+} binding sites have been identified in the VFT domain. Two continuous putative binding sites were first to be mapped (designated sites 3 and 5) (Huang et al., 2007b), followed by a further three discontinuous sites (Huang et al., 2009). These five putative Ca^{2+} binding sites are spread across both lobes of the VFT domain (Figure 23) (Huang et al., 2009; Khan and Conigrave, 2010). Furthermore, cooperativity between Ca^{2+} binding sites has been observed, which may result from Ca^{2+} induced conformational changes in the VFT domain, and could help explain the high Hill coefficient of the receptor (Huang et al., 2009). It appears that site 1, situated in the hinge region (Figure 23), has the highest binding affinity for Ca^{2+} and may be the last site occupied in low $[Ca^{2+}]_o$, an idea supported by the findings that it is important for IP_3 responses in transfected

HEK293 cells (Silve et al., 2005) and that its disruption in the Glutamine-297 isoleucine substitution (E297I) mutant results in a shift of the $[Ca^{2+}]_o$ dose-response curve to the right and a reduction in the Hill coefficient (Huang et al., 2009).

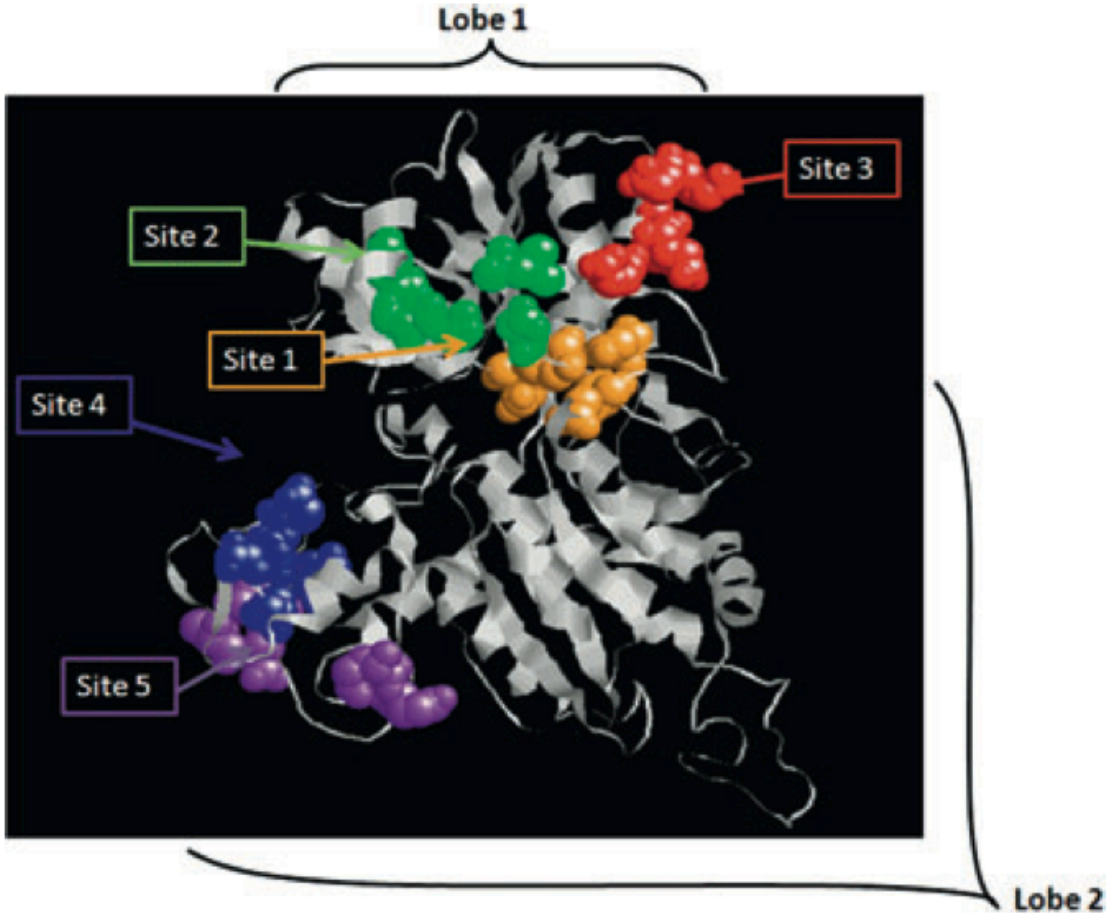

Figure 23: CaSR VFT domain

Molecular model of a CaSR VFT domain. A model of a single subunit based on the mGluR1 crystal structure (Kunishima *et al.,* 2000). Putative Ca^{2+}_o binding sites (1–5) were identified by aromatized terbium luminescence analysis of globular sub-domains (Huang *et al.,* 2009). Site 1, considered to be the primary Ca^{2+}_o binding site, is situated in the cleft between lobe 1 and lobe 2 and also corresponds to the conserved L-amino acid-binding site of class C GPCRs, raising the possibility that Ca^{2+} and L- amino acids may interact to activate CaSR. Figure from Khan and Conigrave, 2010.

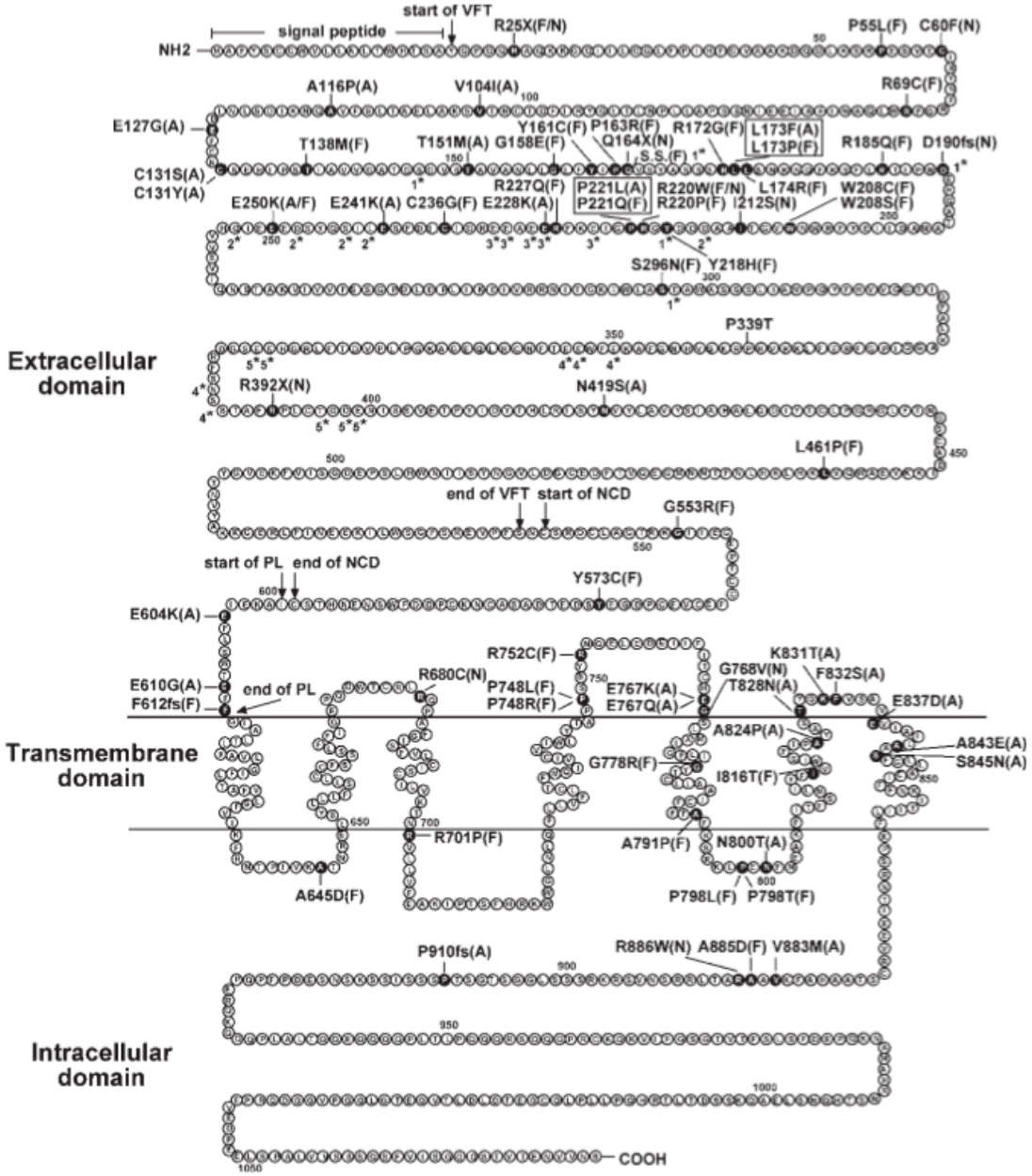

Figure 24: A map of disease causing CaSR point mutations

Schematic representation of the location of 71 disease causing CaSR variants. The CaSR comprises an ECD, which is formed by residues 1–612; an HH domain formed by residues 613–862 and a C-terminal domain formed by residues 863–1078. Every 50th amino acid is indicated. The 612-amino acid ECD consists of the following: an N-terminal signal peptide (amino acids 1–19); a VFT domain (amino acids 20–540); a CR domain (amino acids 542–598) and a peptide linker (PL) (amino acids 599–612) that connects the ECD to the transmembrane domain. The residues involved in forming the five VFT domain Ca^{2+} binding sites are indicated by asterisks. The number preceding the asterisk indicates the respective Ca^{2+} binding site. The 71 CaSR variants reported in Hannan *et al* 2012 are shown in black. The amino acid change is detailed above the mutated residue. The bracketed letter following the amino acid change indicates whether this variant was identified in a patient with FHH (F), NSHPT (N) or ADH (A) or in a patient with both FHH and ADH (A/F). Boxes indicate the mutations associated with either a loss or a gain of function at residues 173 and 221. Figure from Hannan *et al* 2012.

An important recent study provided evidence that clinically identified mutations in the ECD of CaSR tend to cluster around these five Ca^{2+} binding sites (Figure 24) (Hannan et al., 2012). Of 34 missense mutations in the VFT domain, 18 map to positions within 10 Å of one of the predicted Ca^{2+} binding sites, of which 12 are situated in or around the cleft between the two VFT lobes that houses Ca^{2+} binding site 1 (Hannan et al., 2012). The importance of Ca^{2+} binding sites is further underscored by the observation that over 50% of all mutations linked to NSHPT, FHH and ADH map to the ECD of CaSR. Furthermore, mutations of residues 173 and 221, which are situated at the entrance to the cleft housing Ca^{2+} binding site 1, can cause both FHH (inactivating substitution mutations; leucine-173 to proline and proline-221 to glutamic acid) and ADH (activating substitution mutations; leucine-173 to phenylalanine and proline-221 to leucine), supporting the hypothesis that Ca^{2+} access to this site is pivotal for CaSR activation (Huang et al., 2009; Hannan et al., 2012).

However, Ca^{2+} is not the only ligand for CaSR, several other classes of modulators exist (Figure 22B). These include other polyvalent cations such as Mg^{2+} and Gd^{3+} (Brown et al., 1991), Aβ (Ye et al., 1997), antibiotics such as neomycin (Brown and Macleod, 2001), and polyamines such as putrecine, spermine and spermidine (Quinn et al., 1997). Interestingly, CaSR can be allosterically activated by L-amino acids (Conigrave et al., 2000) and a class of pharmacological agents known as "calcimimetics". Inhibitory "calcilytics" have also been created, and both classes of pharmacological agents are designed to be used in therapeutic settings (Brown and Macleod, 2001). How CaSR integrates signals from such a diverse group of ligands is as yet not understood.

Whilst it is not yet known how CaSR integrates signals from such a diverse group of ligands, the binding sites for some, but not all, of these ligands have been mapped to discreet regions of the ECD. Significantly, the binding site for L-amino acids is found in the VFT domain of the ECD of CaSR, as demonstrated by analysis of chimeric receptors (Mun et al., 2004) and mutation analysis (Zhang et al., 2002; Mun et al., 2005). This region represents a conserved binding site for L-amino acids found in several class C GPCRs and is closely associated with Ca^{2+} binding site 1 of CaSR, raising the possibility that these two ligands may interact in activating CaSR (Khan and Conigrave, 2010). Indeed, mixed L-amino acids have been shown

to enhance $[Ca^{2+}]_o$ induced changes in $[Ca^{2+}]_i$ within human parathyroid cells (Conigrave et al., 2000), suggesting that L-amino acids can potentiate CaSR activation (Conigrave and Hampson, 2006).

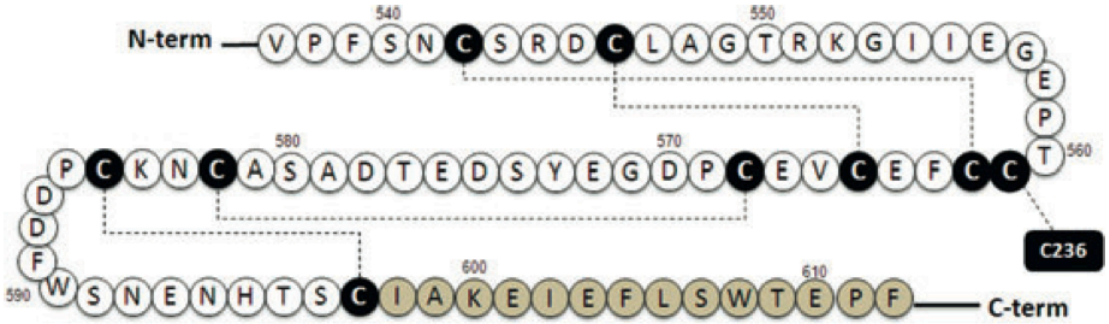

Figure 25: Human CaSR CR domain

The CR domain has nine conserved cysteine residues (black circles), all of which are predicted to participate in di-sulfide bonds (dashed lines). In total there are four predicted intra-domain di-sulfide bonds and one disulfide bond between CaSR residues 561 in the CR domain and 236 in lobe 2 of the VFT domain. A 14 amino acid linker (grey circles) supports signal transmission from the VFT domain to the HH domain. Figure from Khan and Conigrave, 2010.

7.3.4.1.2. CR domain

The VFT domain of CaSR is attached to the HH domain by a 62 amino acid cysteine rich domain and a 14 amino acid linker (Figure 25) (Hu et al., 2000). It appears that the CR domain is necessary for signal transmission to the HH domain upon ligand binding to the VFT domain, since deletion of the entire CR domain abolishes $[Ca^{2+}]_o$ induced PI hydrolysis in HEK-293 cells (Hu et al., 2000). Furthermore, mutation analysis of each of the nine cysteine residues within the domain has shown that all nine are important for normal CaSR function (Fan et al., 1998; Ray et al., 1999; Hu et al., 2000). Several of these cysteine residues are also important for receptor homodimerization, a process that will be discussed in further detail in section 7.3.4.2.1 (Ray et al., 1999). It is thought that the requirement of CR domain residues for dimerization is not the sole reason for the essential role it plays in signal transmission, since structural predictions based on the analogous mGluR3 structure (Muto et al., 2007) suggest that the intra-domain disulphide bonds stabilize a rigid, rod-like structure, thereby conferring a means for the VFT domain to physically control the HH domain (Khan and Conigrave, 2010).

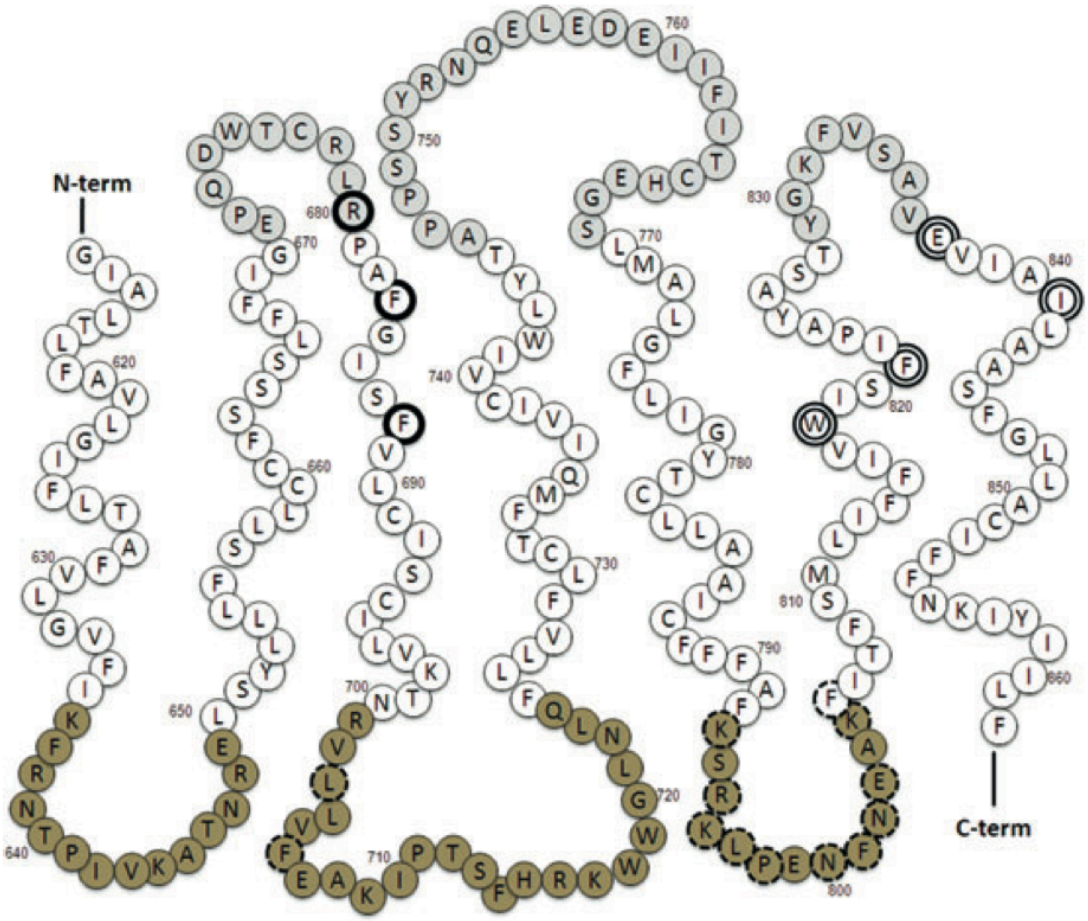

Figure 26: Human CaSR HH Domain

The seven TM α-helices are shown together with the alternating intracellular loops (iL-s) (residues in dark grey) and extracellular loops (residues in light grey). Residues that interact with both calcimimetics and calcilytics are enclosed in double-lined circles. Residues that interact with calcilytics alone are enclosed in single, bold circles. Residues in iL-2 and iL-3 that support $G_{q/11}$-dependent activation of PI-PLC are highlighted with dashed-lines. Figure from Khan and Conigrave, 2010.

7.3.4.1.3. Membrane spanning HH domain

As the membrane-spanning region, the HH domain of GPCRs plays a critical role in signal transduction (Rosenbaum et al., 2009). In all classes of GPCRs, the N-terminal region of the HH domain, extracellular to the first transmembrane (TM) α-helix, connects to the ECD, while a long C-terminal domain connects to the C-terminal region of the HH domain, cytoplasmic to the seventh TM α-helix (Figure 26) (Rosenbaum et al., 2009). Separating the seven TM α-helices of the HH domain are 3 intracellular loops (iL-s) and 3 extracellular loops (eL-s). While no crystal structures of the CaSR HH domain exist, mapping of the CaSR sequence onto the

solved structures of distantly related class A GPCRs has proved informative (Miedlich et al., 2004). Nonetheless, little is known of the stoichiometry of CaSR / G-protein binding or the mechanisms by which HH interfaces between CaSR monomers interact in CaSR homodimers (Khan and Conigrave, 2010).

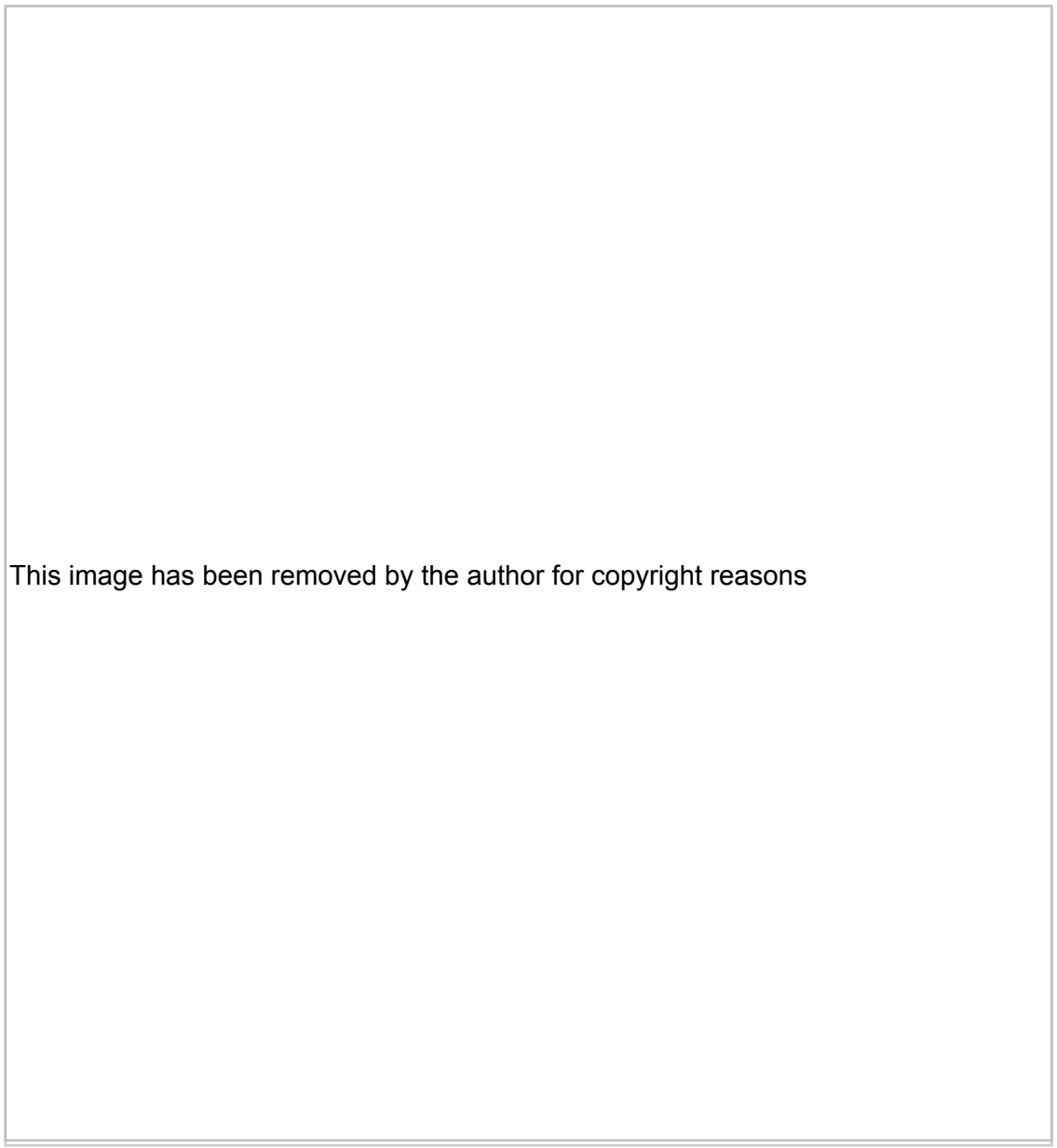

Figure 27: Calcilytics, Calcimimetics and their binding to CaSR

A, Model of NPS 2143 (space fill) binding to human CaSR HH domain (ribbons), based on bovine rhodopsin. From Miedlich *et al* 2004.
B, Close-up of model A, showing residues thought to interact with NPS 2143, including E837. From Miedlich *et al* 2004.
C, Close-up of model indicating site of NPS R-568 binding, including E837 and R680. From Miedlich *et al* 2004.
D, The structures of NPS 2143 and R-568, the calcilytic and a calcimimetic, respectively used in binding studies. Adapted from Petrel *et al* 2004.

While further work is required to elucidate the mechanism of activation for CaSR, some progress has been made in the identification of which residues of the iL-s are required for G-protein docking, at least in the case of $G\alpha_{q/11}$-mediated PLC activation (Chang et al., 2000; Khan and Conigrave, 2010). Alanine-scanning mutagenesis has revealed that regions within iL-2 (amino acids 700–727 of the bovine receptor) and iL-3 (amino acids 786–807 of the bovine receptor) of the CaSR are key to PLC activation in HEK-293 cells (Chang et al., 2000). Interestingly, a dominant-negative arginine-795 to tryptophan substitution (R795W) mutation in human CaSR (corresponding to arginine 786 in the bovine receptor) that leads to FHH lies within the iL-3 residues required for $G\alpha_{q/11}$-mediated PLC activation (Figure 26), leading to the hypothesis that this mutation causes FHH by disrupting G-protein docking or activation (Bai et al., 1996; Hu and Spiegel, 2007; Khan and Conigrave, 2010).

It is thought that the HH domain contains the binding sites of both calcimimetics and calcilytics, along with a supplementary binding site for Ca^{2+} (Khan and Conigrave, 2010). While the consensus is that the VFT domain in the ECD of CaSR is the primary site of Ca^{2+} binding (see section 7.3.4.1.1), mutant receptors entirely lacking an ECD are still able to promote PI hydrolysis in HEK-293 cells, leading to the suggestion that the HH domain also hosts a Ca^{2+} binding site (Ray and Northup, 2002). Calcimimetics and calcilytics stand in marked contrast to Ca^{2+} and L-amino acids by primarily binding to the HH domain of CaSR, as their modulation of intracellular calcium signalling is independent of the presence of the ECD (Miedlich et al., 2004). The first calcimimetic/calcilytic compounds synthesised were phenylalkyamines and include R-568 and NPS 2143 (see Figure 27), which both appear to modulate a broader array of signalling pathways downstream of CaSR than L-amino acids (Khan and Conigrave, 2010). Docking studies using simulated CaSR protein structures, and analysis of the effects of mutant receptors on pharmacological manipulation of Ca^{2+}_o induced Ca^{2+}_i signals, suggest that calcilytics and calcimimetics occupy overlapping but non-identical binding pockets in the HH domain (Figure 27A-C) (Miedlich et al., 2004; Petrel et al., 2004). Residues including E837 (at the extracellular border of transmembrane α-helix 7) have been shown in two studies to contribute to binding of both calcilytics and calcimimetics, while others, including R680 (at the extracellular border of transmembrane α-helix 3) have been reliably shown to contribute only to the

binding of calcilytics (Miedlich et al., 2004; Petrel et al., 2004). In conclusion the HH domain appears to have a pivotal role in signal transduction, G-protein binding and modulation by calcilytics and calcimimetics (Khan and Conigrave, 2010; Ward and Riccardi, 2012).

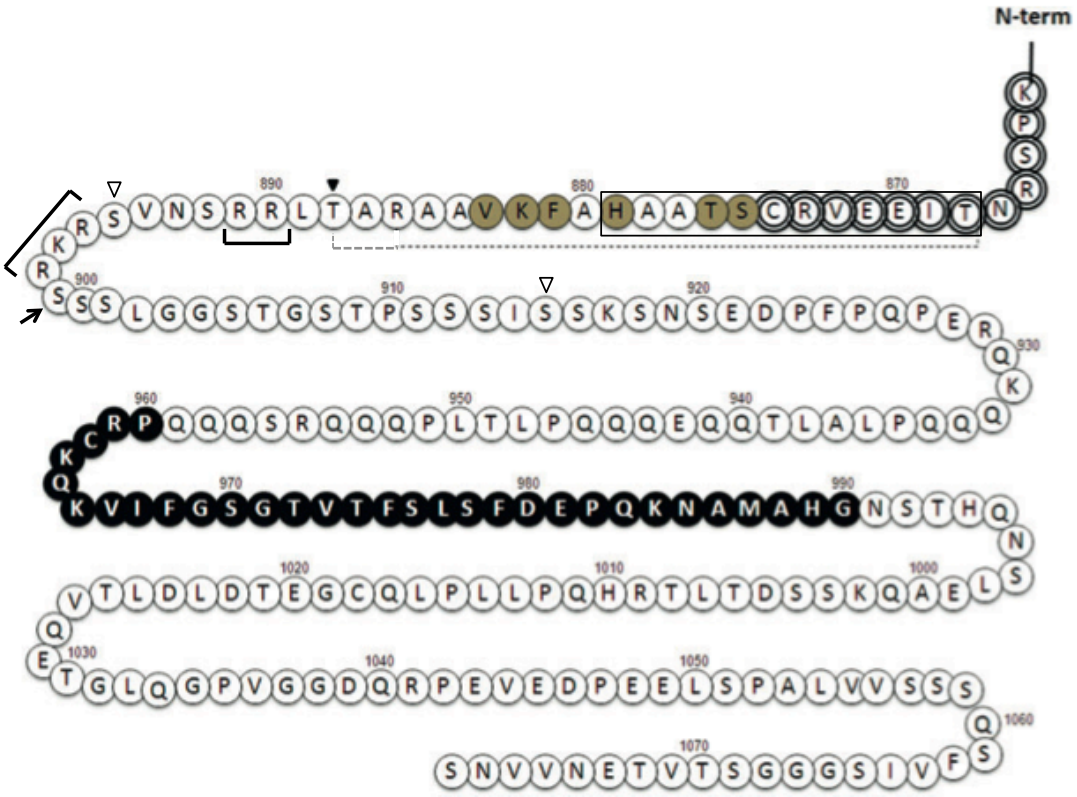

Figure 28: Human CaSR C-terminal Domain

The C-terminal domain supports receptor expression and activation of PI-PLC (residues 863–874; double circles), activation of PI-PLC alone (highlighted in grey), as well as cooperativity, resistance to desensitization and ER retention (residues 868–888 indicated by broken line). Residues 960–990 (labelled in black) provide a high-affinity binding site for filamin-A, while residues 868-879 (in black box) provide a low-affinity binding site for filamin-A. The major PKC phosphorylation site at T888 is labelled by a black arrowhead, while the other PKC phosphorylation sites at S895 and S915 are labelled with white arrowheads. A protein kinase A (PKA) phosphorylation site at S899 is indicated by a black arrow. Arginine rich retention motifs are indicated by black brackets. Interaction sites for dorfin E3 Ub ligase and 14-3-3θ proteins are not indicated (see text).
Figure from Khan and Conigrave, 2010.

7.3.4.1.4. C-terminal domain

Residues 863-1078 of the human CaSR comprise an intracellular C-terminal domain, which has diverse roles in the regulation of receptor expression, trafficking, cooperativity, desensitization and signalling (Khan and Conigrave,

2010). Many of these roles have been shown to be intimately tied to certain regions of the C-terminal domain and relate to sites of interaction with other proteins or modulation by phosphorylation (Figure 28) (Huang and Miller, 2007; Khan and Conigrave, 2010; Ward and Riccardi, 2012). A membrane proximal region from residues 868-886 is thought to be important for receptor cooperativity and desensitization (Gama and Breitwieser, 1998). Evidence for this conclusion came from a study of the capacity of C-terminal truncation mutants expressed in HEK-293 cells to elicit Ca^{2+}_o induced changes in intracellular calcium concentrations, as measured by fura-2 fluorescence. Truncation at T868 (T868X) results in an apparent reduction of affinity for Ca^{2+}_o, a reduced Hill coefficient and enhanced desensitization, whereas other truncation mutants (R886X, S908X and D1024X) are not significantly different from wild-type CaSR with respect to these parameters (Gama and Breitwieser, 1998). Strikingly, these data also imply that residues 886-1078 are dispensable for CaSR coupling to the PI-PLC signalling pathway (Gama and Breitwieser, 1998). These results are in agreement with a prior study of CaSR truncation mutant expression in HEK-293 cells, which indicated that the region between residues 863 and 874 is important for PI-PLC signalling and also promotes cell surface expression of CaSR (Ray et al., 1997). This study also demonstrated that residues between 874 and 888 are needed for PI-PLC signalling, but not CaSR cell surface expression (Ray et al., 1997). Again, residues beyond A887 appear to be dispensable for PI-PLC signalling, although these data do not rule out their contribution to other signalling pathways downstream of CaSR (Ray et al., 1997; Khan and Conigrave, 2010).

It has long been noted that PKC activity can reduce Ca^{2+}_o induced changes in $[Ca^{2+}]_i$ in parathyroid cells, raising the possibility of a PKC-mediated negative feedback mechanism following CaSR stimulation (Brown and Macleod, 2001). Indeed, CaSR contains five potential PKC phosphorylation sites; T646 is in iL-1, S794 is in iL-3 and T888, S895 and S915 are in the C-terminal domain (Bai et al., 1998b). Furthermore, mutational analysis suggests that PKC phosphorylation at one or more of these sites, in particular T888, reduces the ability of CaSR agonists to increase the levels of Ca^{2+}_i (Bai et al., 1998b). This feedback inhibition of CaSR signalling via the C-terminal domain has recently been shown to play an important role in the regulation of downstream signalling (see section 7.3.4.2.8) (Ward and Riccardi, 2012). The *in vivo* importance of T888 has been confirmed by the recent

description of a threonine-888 to methionine substitution (T888M) mutation, which results in ADH (Lazarus et al., 2011).

In addition to PKC, numerous other proteins interact with the C-terminal domain of CaSR to modulate receptor function (see Table 1) (Huang and Miller, 2007). Of these, many are involved in CaSR trafficking and shall be discussed further in section 7.3.4.2.2. In contrast to proteins regulating CaSR trafficking, the interactions of other proteins with the C-terminal domain of CaSR are less well characterised. Caveolin-1 interacts with an unknown region of the C-terminal domain (Kifor et al., 1998; Kifor et al., 2003). In bovine parathyroid cells, caveolin-1 co-localises with CaSR within membrane micro-domains that are rich in cholesterol and glycosphingolipids, known as caveolae, in which G-protein signalling components may be concentrated (Huang and Miller, 2007). Therefore, it has been suggested that the CaSR/caveolin-1 interaction may serve a scaffolding function in promoting receptor cell surface expression, endocytosis and sorting (Huang and Miller, 2007).

Other CaSR C-terminal domain interactors are thought to regulate CaSR ubiquitination status. Dorfin is an E3 Ubiquitin (Ub) ligase that interacts with CaSR at residues 880-900 and covalently links Ub to lysine residues (Huang et al., 2006b). There are nine lysine residues in the C-terminal domain of CaSR and seven are found amongst the three iL-s. Mutagenesis studies have shown that Dorfin-promoted ubiquitination occurs at more than one of these residues and promotes CaSR degradation (Huang et al., 2006b). Interestingly, associated molecule with the SH3 domain of STAM (AMSH), a protein with Ub isopeptidase activity that can limit protein degradation through the removal of Ub (McCullough et al., 2004), actually promotes the degradation of endocytosed CaSR following interaction with the C-terminal domain (Herrera-Vigenor et al., 2006; Reyes-Ibarra et al., 2007).

The K^+ channel Kir4.2 has been shown to interact with CaSR C-terminal domain residues between 907-991, resulting in the inhibition of Kir4.2 channel function, a process that may be involved in regulating Na^+ reabsorption in the kidney (Huang et al., 2007a; Riccardi and Kemp, 2012). Interestingly, the non-functional CaSR mutant, R796W does not interact with Kir4.2 (Huang et al., 2007a). Furthermore, the C-terminal domain of CaSR interacts with filamin through both high affinity (residues 960-990) and low affinity (residues 868-879) binding sites.

Filamin/CaSR interactions are important for MAPK (Awata et al., 2001; Hjälm et al., 2001; Huang et al., 2006a) and Rho signalling (Pi et al., 2002; Huang and Miller, 2007), CaSR scaffolding (Rey et al., 2005) and the regulation of CaSR degradation (Zhang and Breitwieser, 2005).

In conclusion, clinical mutations, pharmacology and molecular biology have revealed the generalized roles of the four structural domains of CaSR. The VFT domain has a major role in sensing $[Ca^{2+}]_o$; the CR domain is key to signal transmission to the HH domain; the HH domain is critical for G-protein binding and provides sites for allosteric modulation of the efficacy of CaSR signalling; the C-terminal domain subserves the dynamic regulation of CaSR signalling and expression (Khan and Conigrave, 2010).

Interacting Protein	Function	Interaction	CaSR Domain	Colocalisation	Reference
14-3-3θ	Signalling	Y2H, GST, Co-IP	C-term: 922-965	Het	(Arulpragasam et al., 2012)
14-3-3ζ	Trafficking/signalling	Y2H, Co-IP	C-term: 922-965		(Arulpragasam et al., 2012)
AMSH	Trafficking/degradation	Y2H, GST	C-term		(Herrera-Vigenor et al., 2006)
β-Arrestin	Trafficking/signalling	M2H, Co-IP, functional	C-term: 877–1079		(Pi et al., 2005; Lorenz et al., 2007)
Caveolin-1	Structural/scaffolding	Co-IP	?	Native, Het	(Kifor et al., 1998; Kifor et al., 2003)
E3 Ub ligase	Trafficking/ubiquitination	Y2H, Co-IP, functional	C-term: 880 –900	Het	(Huang et al., 2006b)
Filamin	Scaffolding/structural/ trafficking	Y2H, Co-IP, GST, functional	C-term: 868-879 & 960-990	Native, Het	(Awata et al., 2001; Hjälm et al., 2001; Pi et al., 2002)
$G\alpha_{q/11}$	Signalling	Co-IP, functional	iL-1, iL-3		(Chang et al., 2000; Lorenz et al., 2007)
$GABA_{B1}$	Trafficking/signalling	Co-IP	ECD	Native, Het	(Chang et al., 2007; Cheng et al., 2007)
$GABA_{B2}$	Trafficking/signalling	Co-IP	ECD	Native	(Chang et al., 2007; Cheng et al., 2007)
Kir4.1	K^+ channel	Y2H, Co-IP, functional	?	Native, Het	(Huang et al., 2007a)
Kir4.2	K^+ channel	Y2H, Co-IP, functional	C-term: 907-991	Het	(Huang et al., 2007a)

Interacting Protein	Function	Interaction	CaSR Domain	Colocalisation	Reference
mGluR1α	Trafficking	Co-IP	?	Native	(Gama et al., 2001)
p24A	Trafficking	Y2H, Co-IP	C-term: 868-1078		(Stepanchick and Breitwieser, 2010)
PI4K	Signalling	Co-IP	?		(Huang et al., 2002)
PKC	Signalling	Functional	C-term, iL-1, iL-3		(Lorenz et al., 2007)
RAMP1 & RAMP3	Structural/trafficking	Co-IP, Functional	?ECD & HH	Het	(Bouschet et al., 2005)
Rho	Signalling	Co-IP	?		(Huang et al., 2002)

Table 1- Known CaSR interacting proteins

Proteins that interact with CaSR are shown in alphabetical order. The table lists the known functions for protein interactions, the techniques used to identify protein interactions with CaSR (Interaction column), the region of CaSR that the interacting proteins bind to (if known; CaSR domain column), whether their colocalisation with CaSR has been shown in heterologous cells (Het) or native tissue/cells (Native) and key references.

Table and legend adapted from (Huang and Miller, 2007).

7.3.4.2. CaSR downstream signalling

CaSR can couple to PLC via G_{q_α} or G_{11_α}, stimulating the release of IP_3 and DAG, which mobilize intracellular calcium stores. The resultant changes in $[Ca^{2+}]_i$ and the downstream activation of PKC and MAPK, are important for the secretion of parathyroid hormone from the parathyroid gland (Ward, 2004). In addition to $G\alpha_q$ and $G\alpha_{11}$, signalling downstream of CaSR can also be mediated by $G\alpha_i$, thereby inhibiting the production of cAMP by adenylyl cyclase (AC) (Chen et al., 1989; Ward, 2004).

The effects of CaSR activation on cellular physiology appear to vary substantially depending on cell type and experimental approach. One possible explanation of the variable outcomes from different *in vitro* studies may be due to the use of CaSR agonists to activate CaSR, rather than Ca^{2+} itself, in some investigations. The effects of CaSR agonists on cultured cells will be modulated by the culture media used, since different culture media contain different amounts of Ca^{2+}. CaSR activation has been reported to exert opposite effects on the proliferation of different cell types, with CaSR inhibiting the proliferation of human colonic epithelial cells (Rey et al., 2010) whilst promoting the proliferation of ovarian surface epithelial cells (Bilderback et al., 2002) and H-500 cancer cells (Tfelt-Hansen et al., 2004). The promotion of ovarian surface epithelial cell proliferation is mediated by PI3K activation, whereas PI3K and p38 MAPK are both required for CaSR-dependent proliferation of H-500 cells. CaSR must employ many signalling mechanisms and numerous intracellular signalling pathways to be able to induce such varied cellular and physiological responses within different cell types (Hofer and Brown, 2003; Ward and Riccardi, 2012). This final introductory section will describe both the signalling pathways to which CaSR is known to couple, and the dynamic cellular mechanisms that may control its function.

7.3.4.2.1. Homo- & Heterodimerization

An interesting feature shared between CaSR and other family C GPCRs, such as mGluR1, mGluR5 and $GABA_B$ receptors, is the capacity to form homodimers (Figure 22A) (Brown and Macleod, 2001). CaSR has been found to be present in HEK-293 cells as homodimers (Bai et al., 1998a), an interaction mediated by both covalent (Ray et al., 1999) and non-covalent linkages (Zhang et al., 2001) that is critical for the receptor's function (Bai et al., 1999). Disulphide bridges between

monomers appear to be mediated by cysteine residues including C129 and C131 (Ray et al., 1999; Zhang et al., 2001), the importance of C131 being attested by the association of two separate point mutations that alter the identity of this residue with ADH (Hannan et al., 2012). Furthermore, CaSR has been shown to heterodimerize with both mGluRs and $GABA_B$ receptors, interactions that can be functionally important for cell-surface expression (Chang et al., 2007; Bouschet et al., 2008) and signal transduction (Chang et al., 2007; Cheng et al., 2007). In particular, co-expression of $GABA_{B2}$ and CaSR in HEK-293 cells results in increased CaSR surface expression and increased coupling of CaSR to PLC activation. In contrast, co-expression of $GABA_{B1}$ and CaSR in the same cell line reduces CaSR expression and impairs PLC activation in response to high $[Ca^{2+}]_o$ (Chang et al., 2007). Accordingly, $GABA_{B1}$ and CaSR co-expression in cultured murine growth plate chondrocytes reduces CaSR surface expression and high $[Ca^{2+}]_o$-induced PLC and ERK1/2 activity (Cheng et al., 2007).

The C-terminal domain of CaSR contains an arginine-rich ER retention motif, regulated by PKA mediated phosphorylation of S899 (Figure 28) (Stepanchick et al., 2010). Importantly, three clinically relevant mutations disrupt this motif: The arginine-886 to aspartic acid substitution (R886D), that results in FHH; the arginine-896 to histidine substitution (R896H) that causes chronic pancreatitis and the arginine-898 to glutamine substitution (R898Q) that results in idiopathic epilepsy (Kapoor et al., 2008; Stepanchick et al., 2010). All of these mutations result in increased plasma membrane targeting of CaSR due to the reduced retention of CaSR within the ER. R896H and R898Q also result in increased $[Ca^{2+}]_o$ stimulated ERK1/2 phosphorylation (Stepanchick et al., 2010). $GABA_{B1}$ contains a similar ER retention motif in its own C-terminal domain, but this motif is shielded by heterodimerization with $GABA_{B2}$, thereby permitting only $GABA_{B1}$/$GABA_{B2}$ heterodimers to be efficiently expressed at the cell surface (Pagano et al., 2001). The shielding of the $GABA_{B1}$ ER retention motif by $GABA_{B2}$ has been proposed to be due to masking by an interaction with an α-helical segment of the $GABA_{B2}$ C-terminal domain (Pagano et al., 2001). Since CaSR also contains a similar putative α-helical segment in its own C-terminal domain, the disruption of which impairs CaSR surface expression (Chang et al., 2001), it has been suggested that CaSR homodimers may share a similar retention masking mechanism to $GABA_{B1}$ /$GABA_{B2}$ heterodimers (Chang et al., 2007). Furthermore, it has been hypothesised

that masking of this arginine-rich ER retention motif in the CaSR C-terminal domain by heterodimerization with $GABA_{B2}$ may explain the increased surface expression observed when these two GPCRs are co-expressed in HEK-293 cells (Chang et al., 2007).

It is interesting to speculate on the functional significance of GPCR heterodimerization for the development and function of the nervous system. For example, the activity of mGluR1 has been shown to be modulated by $[Ca^{2+}]_o$, leading to the speculation that the heterodimerization of mGluR1 with CaSR may contribute to the mGluR1-mediated reduction in postsynaptic efficacy that results from the activity-dependent reduction of $[Ca^{2+}]_o$ in the synaptic cleft (Hardingham et al., 2006). Interestingly, co-expression of CaSR with mGluR1α in HEK-293 cells results in altered trafficking of CaSR compared to CaSR homodimers. Since glutamate induces the internalization of CaSR/mGluR1α heterodimers and Homer1c promotes their trafficking to the cell surface, it appears as if CaSR/mGluR1α heterodimers exhibit trafficking properties similar to mGluR1α (Gama et al., 2001), which has been proposed as a possible explanation for the apparent synaptic localisation of CaSR (Bouschet et al., 2008). Further work is required in order to better understand the functional role and the *in vivo* significance of CaSR heterodimerization with mGluRs or $GABA_B$ receptors in the nervous system.

7.3.4.2.2. Trafficking and cell surface expression

Control of cell surface expression is increasingly being recognised as an important regulator of CaSR function (Bouschet et al., 2008; Grant et al., 2011). As previously stated, it has been shown that mGluR5, $GABA_{B1}$ and $GABA_{B2}$ can all modify the cell surface expression of CaSR, apparently with functional consequences (Bouschet et al., 2008). In addition, dorfin and AMSH regulate the trafficking and degradation of CaSR (see section 7.3.4.1.4) (Huang and Miller, 2007). Other CaSR interacting proteins have also been implicated in the regulation of CaSR trafficking (Table 1) (Huang and Miller, 2007). These include receptor activity modifying protein 1 (RAMP1) and RAMP3, single pass transmembrane proteins originally thought to interact specifically with class B GPCRs. RAMP1 and RAMP3 are necessary for cell surface expression of CaSR, at least in COS-7 cells (Figure 29) (Bouschet and Henley, 2005; Bouschet et al., 2008). In addition, the cargo receptor, p24A appears

to interact with the C-terminal domain of CaSR, stabilising its localization to the early secretory pathway and promoting its maturation into the fully glycosylated form (Stepanchick and Breitwieser, 2010). Furthermore, agonist dependent phosphorylation of CaSR induces the binding of β-Arrestin-1 to the C-terminal domain of CaSR, which promotes receptor desensitisation by reducing the coupling of CaSR to PI-PLC (Lorenz et al., 2007). Deficient PTH secretion in β-Arrestin-2 null mutant mice suggests that a similar effect may operate *in vivo* (Pi et al., 2005). While there is little understanding of the specific mechanism by which β-Arrestins may promote CaSR desensitisation, they typically desensitise other GPCRs by mediating their internalization into endosomes (Rosenbaum et al., 2009). The regulatory proteins, 14-3-3θ and 14-3-3ζ were recently found to bind to the membrane-proximal region of the C-terminal domain of CaSR (Arulpragasam et al., 2012). This binding is independent of PKC phosphorylation and does not require the normal RKR 14-3-3 protein binding motif. Interestingly, while 14-3-3ζ reduces cell surface expression of CaSR by an unknown mechanism, 14-3-3θ has no effect despite the fact that these two proteins share about 80% amino acid identity (Arulpragasam et al., 2012).

It is thought that pharmacological agents can also modulate CaSR trafficking during biosynthesis. For example, NPS R-568 appears to stabilise CaSR and promote its trafficking, increasing the total and plasma membrane levels of the receptor, while NPS 2143 has the opposite effect (Huang and Breitwieser, 2007; Cavanaugh et al., 2012). CaSR mutants exhibit altered sensitivity to the proteasome inhibitor MG132, with the expression of loss of function mutants and wild type CaSR being increased by MG132 and the expression of gain of function mutants being unaffected by MG132 (Huang and Breitwieser, 2007). This has lead to the suggestion that agonist sensitivity exerts a key control at a hypothetical conformational checkpoint during CaSR biosynthesis (Huang and Breitwieser, 2007; Cavanaugh et al., 2012). Since the ER contains Ca^{2+}, it is possible for the proposed checkpoint to follow screening of binding affinity for CaSR agonists and result in the ER retention of receptors with low binding affinity (Cavanaugh et al., 2012). Further support for this idea comes from [^{35}S] Cysteine pulse-chase experiments, which indicate a slow and incomplete maturation to the fully glycosylated form of CaSR during biosynthesis, while truncation experiments and substitution of the C-terminal domain with that of mGluR1 indicate that a region

between amino acids 868 and 888 actively promotes ER retention (Cavanaugh et al., 2010).

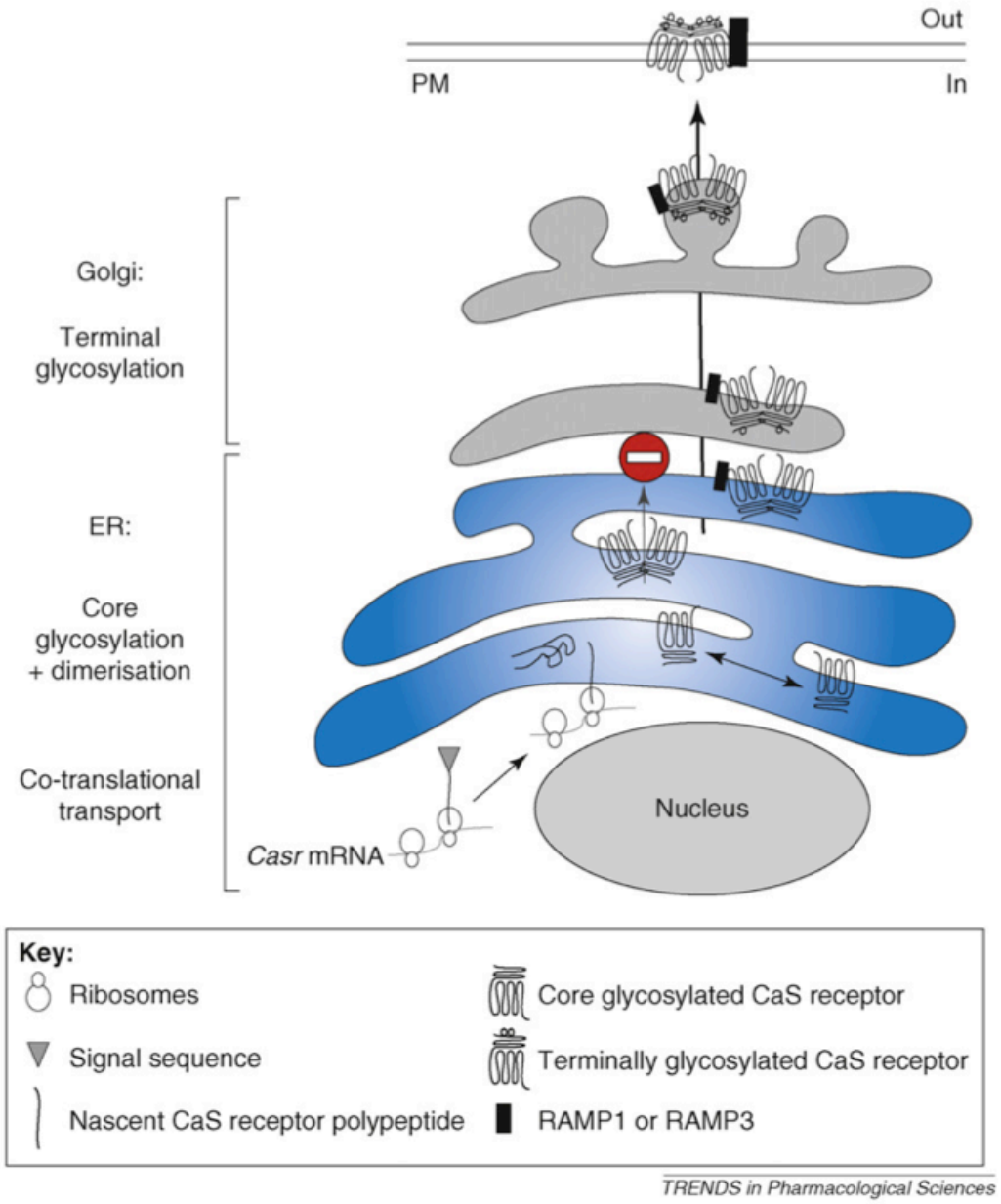

Figure 29: Model of CaSR trafficking.

During synthesis the nascent CaSR polypeptide, together with the ribosome, is targeted to the rough ER due to the presence of the signal sequence (co-translational transport). Upon completion of synthesis, CaSR becomes anchored in the ER membrane in an orientation maintained throughout the secretory pathway. In the ER, CaSR monomers assemble as homodimers, which are retained (stop sign) and undergo core glycosylation. CaSR dimers in association with RAMP1 or RAMP3 bypass the ER retention and reach the Golgi apparatus where they are terminally glycosylated before being delivered to the plasma membrane (PM). For clarity, additional proteins modulating CaSR traffic such as $GABA_{B1}$ and $GABA_{B2}$ are not indicated. The stoichiometry between RAMP and the CaSR is not known but, for simplicity, one RAMP per CaSR homodimer is shown. Figure from Bouschet *et al* 2008.

Some of these strands of evidence have been brought together by a recent study using total internal reflection fluorescent microscopy to study the control of CaSR insertion into the plasma membrane. The authors propose that CaSR undergoes "agonist-driven insertional signalling" (ADIS), since $[Ca^{2+}]_o$ controls the proportion of CaSR found in the cell membrane, which also undergoes constitutive endocytosis (Grant et al., 2011). ADIS appears to be 14-3-3 dependent, since it is impaired when the S899 PKA phosphorylation site that regulates the function of a C-terminal R-rich motif undergoes a phosphomimetic mutation (S899D) that impairs 14-3-3 binding and is promoted by a non-phosphorylatable mutation (S899A), which promotes 14-3-3 binding (Grant et al., 2011). Furthermore, the blockade of glycosylation by tunicamycin only gradually impairs ADIS, which has been interpreted as supporting a model where only fully glycosylated CaSR is inserted into the cell membrane (Grant et al., 2011). This model may provide an interesting rationale for the recognized importance of CaSR trafficking and go some way to explaining how CaSR avoids substantial desensitization under continual exposure to its ligand (Grant et al., 2011).

7.3.4.2.3. Pleiotropic G-protein coupling

While most GPCRs couple predominantly to a single G-protein, CaSR is unusually pleiotropic as it can couple to $G_{i/o}$ and $G_{12/13}$, in addition to $G_{q/11}$ (Hofer and Brown, 2003). The molecular basis of this pleiotropism is not understood and, in most cases, neither are all of the physiological effects of binding to one particular G-protein or another (Khan and Conigrave, 2010). However, it has been noted that the preference of CaSR for $G_{i/o}$ in normal mammary epithelial cells is switched to G_s in two breast cancer cell lines, thus reversing the direction of control that CaSR activation exerts on cAMP synthesis (Mamillapalli et al., 2008). Furthermore, deletion of the genes encoding G_q and G_{11} in the parathyroid gland results in a phenocopy of *Casr* deletion, apart from a notable absence of hypocalciurea (Wettschureck et al., 2007), supporting the conclusion that signalling through $G_{q/11}$ results in the Ca^{2+}_i signals required for PTH secretion (Ward and Riccardi, 2012). Thus, it is possible that the pleiotropism of CaSR G-protein coupling results from molecular, cellular and context specific mechanisms that largely remain to be elucidated (Ward and Riccardi, 2012).

7.3.4.2.4. Phospholipase activation mediated signalling

In bovine parathyroid cells and HEK-293 cells expressing CaSR, Ca^{2+}_o can promote the activity of three phospholipases: PLC, which cleaves PIP_2 to IP_3 and DAG; phospholipase A $(PLA)_2$, which generates arachidonic acid (AA); and phospholipase D (PLD), which cleaves the polar head group of several phospholipids to liberate phosphatidic acid (PA) (Figure 22B) (Kifor et al., 1997; Ward, 2004). The key role of PLC in CaSR signalling has already been mentioned (section 7.3.4.2) and shall be discussed further in the context of the Ca^{2+}_i oscillations it can control section 7.3.4.2.8. Therefore, a brief description of CaSR signalling to PLA_2 and PLD follows.

The CaSR dependency of the Ca^{2+}_o promoted stimulation of PLA_2 reported in transfected HEK-293 cells is supported by an absence of Ca^{2+}_o induced PLA_2 activity in non-transfected cells. Induced PLA_2 activity appears to be sensitive to general PLA_2 inhibitors, but not to bromoenol lactone, which more specifically inhibits Ca^{2+}_i-insensitive PLA_2 isoforms, suggesting that cytosolic PLA_2 ($cPLA_2$) is most likely coupled to CaSR, at least in HEK-293 cells (Handlogten et al., 2001). Furthermore, the co-expression of human $cPLA_2$ with CaSR further increases AA release (Handlogten et al., 2001). While AA release does not seem to require PTX sensitive G-proteins or ERK1/2, there is some evidence that it may be G_q mediated, since AA release is sensitive to the PLCβ inhibitor, U73122 and inhibition of PKC by chronic phorbol ester exposure (Handlogten et al., 2001). It is thought that CaSR stimulated PLA_2 activity and AA production may be physiologically significant in the regulation of K^+ homeostasis in the kidney, since AA processing by P450 results in a metabolite that inhibits the opening of an apical K^+ channel in the epithelial cells of the renal cortex thick ascending limb (Brown and Macleod, 2001).

PLD activity in response to high $[Ca^{2+}]_o$ has been detected in CaSR transfected HEK-293 cells (Kifor et al., 1997). The activation of PLD requires PKC, since PKC inhibition by chronic phorbol ester treatment prevents PLD activation and PKC stimulation by acute phorbol ester treatment promotes PLD activity (Kifor et al., 1997). Furthermore, in CaSR expressing MDCK cells, Ca^{2+}_o promoted stimulation of PLD is PTX insensitive and appears to be $G_{12/13}$/Rho dependent, since over-expression of p115RhoGEF inhibits the response (Huang et al., 2004). However,

little is known of the physiological significance of CaSR promoted PA production via PLD (Brown and Macleod, 2001).

7.3.4.2.5. PI4K & Rho signalling

PI4K, along with PI5K serves to regenerate the cellular PIP_2 pool by the phosphorylation of PI (Ward, 2004). CaSR activates PI4K in CaSR transfected HEK-293 cells through a mechanism that is independent of G_q and G_i, but does require Rho activity, since it is blocked by the C3 toxin (Huang et al., 2002). As CaSR activates both PI4K and PLC in parallel, it is thought that this additional coupling to PI4K may facilitate continued signalling by preventing depletion of the PLC substrate, PIP_2 (Huang et al., 2002; Ward, 2004).

Several roles have been reported for the Rho family of small molecular weight GTPases in CaSR signalling (Ward, 2004), including the aforementioned stimulation of PI4K in CaSR expressing HEK-293 cells (Huang et al., 2002) and stimulation of PLD in MDCK cells (Huang et al., 2004). Rho also appears to required for the production of transient $Ca^{2+}{}_i$ spikes that are observed following amino acid-mediated stimulation of CaSR in epithelial cells (Rey et al., 2010) and for $Ca^{2+}{}_i$ – mediated regulation of the cytoskeleton of HEK-293 cells stimulated by amino acids (Rey et al., 2005). Both Rho kinase inhibition and the expression of a dominant negative RhoA block CaSR-induced actin stress fiber assembly and process retraction in HEK-293 cells (Davies et al., 2006). Interestingly, CaSR-mediated stress fiber assembly and process retraction are not associated with alterations in $[Ca^{2+}]_i$ or the activation of ERK1/2 signalling (Davies et al., 2006). Furthermore, CaSR stimulated activation of SRE appears to be dependent on a filamin-mediated increase in Rho activity (Pi et al., 2002), while CaSR coupling to Rho may require 14-3-3 proteins (Arulpragasam et al., 2012).

7.3.4.2.6. PI3K signalling

CaSR signalling through PI3K has been reported to exert a variety of cellular effects, including proliferation (Hobson et al., 2003; Tfelt-Hansen et al., 2004; Li et al., 2011), secretion (Liu et al., 2003) and migration (Boudot et al., 2010). In some cases CaSR stimulated PI3K signalling appears to interact with MAPK signalling pathways (Ward, 2004). For instance, there is some pharmacological evidence that both PI3K and MAPK signalling are involved in the CaSR-mediated proliferative response of rat pulmonary artery smooth muscle cells to hypoxia (Li et al., 2011).

Furthermore, PI3K inhibition reduces Ca^{2+}_o induced ERK phosphorylation and DNA synthesis in CaSR expressing HEK-293 cells (Hobson et al., 2003). Moreover, both phospho-Akt and phospho-ERK1/2 activation in response to high $[Ca^{2+}]_o$ are abolished by PI3K inhibition in ovarian surface epithelial (OSE) cells (Bilderback et al., 2002). Since PD98059 mediated inhibition of ERK activation has no effect on Akt phosphorylation in response to high $[Ca^{2+}]_o$, PI3K appears to lie upstream of ERK in OSE cells. However, since ERK inhibition was reported to reduce the proliferative response of OSE cells to high $[Ca^{2+}]_o$ by approximately 50%, whereas PI3K inhibition reduces proliferation by 90%, PI3K must also act to promote proliferation through ERK1/2-independent pathways (Bilderback et al., 2002).

Indeed, other cellular responses to CaSR activation that are mediated by PI3K are thought to be independent of MAPKs. For example, CaSR promoted proliferation of H-500 rat Leydig cancer cells involves PI3K and, while p38 MAPK is also required, the effect is not dependent on MEK1/ERK activation (Tfelt-Hansen et al., 2004). Furthermore, pharmacological and Western blot studies suggest that the CaSR-mediated migration of osteoclast precursor RAW 264.7 cells involves PI3K/Akt and PLCβ, but not MAPK, signalling (Boudot et al., 2010). A final example of MAPK independent PI3K signalling downstream of activated CaSR is provided by studies of 5-HT secretion from neural crest-derived neuroendocrine parafollicular (PF) cells (Liu et al., 2003). Kinase assays and measurement of 5-HT secretion from cultured sheep PF cells suggest that CaSR-mediated activation of PI3K signalling (Liu et al., 2003). Furthermore, CaSR stimulated PI3K activation appears to be mediated by $G_{\beta\gamma}$ subunits and promotes secretion through the downstream effectors, PDK1 and PKCζ (Liu et al., 2003). Thus, CaSR may couple to PI3K in a variety of cell systems, to elicit numerous cellular effects, in MAPK-dependent and independent manners (Ward, 2004).

7.3.4.2.7. MAPK signalling

CaSR has been shown to act via all three major MAPK signalling pathways: ERKs, p38 MAPK and JNK (Figure 30) (Tfelt-Hansen et al., 2003). CaSR promoted release of PTHrP from H-500 cells appears to involve all three MAPK signalling pathways (Tfelt-Hansen et al., 2003). The over-expression of CaSR in HEK-293 cells induces a $G_{i/o}$ –mediated accumulation of intracellular ceramide that promotes JNK activity, subsequent c-JUN phosphorylation and caspase-dependent apoptosis (Wu et al.,

2005). JNK activity is also stimulated by CaSR agonists in MDCK cells (Arthur et al., 2000), and JNK mediates the CaSR-induced proliferation of rat osteoblasts (Chattopadhyay et al., 2004). Surprisingly, CaSR-promoted proliferation of the mouse MC3t3-E1 osteoblast cell line is mediated by both p38 MAPK and ERK1/2 signalling, but not JNK activity (Yamaguchi et al., 2000). p38 MAPK has also been reported to mediate CaSR promoted stimulation of a CAKC in the U87 astrocytoma cell line (Ye et al., 2004).

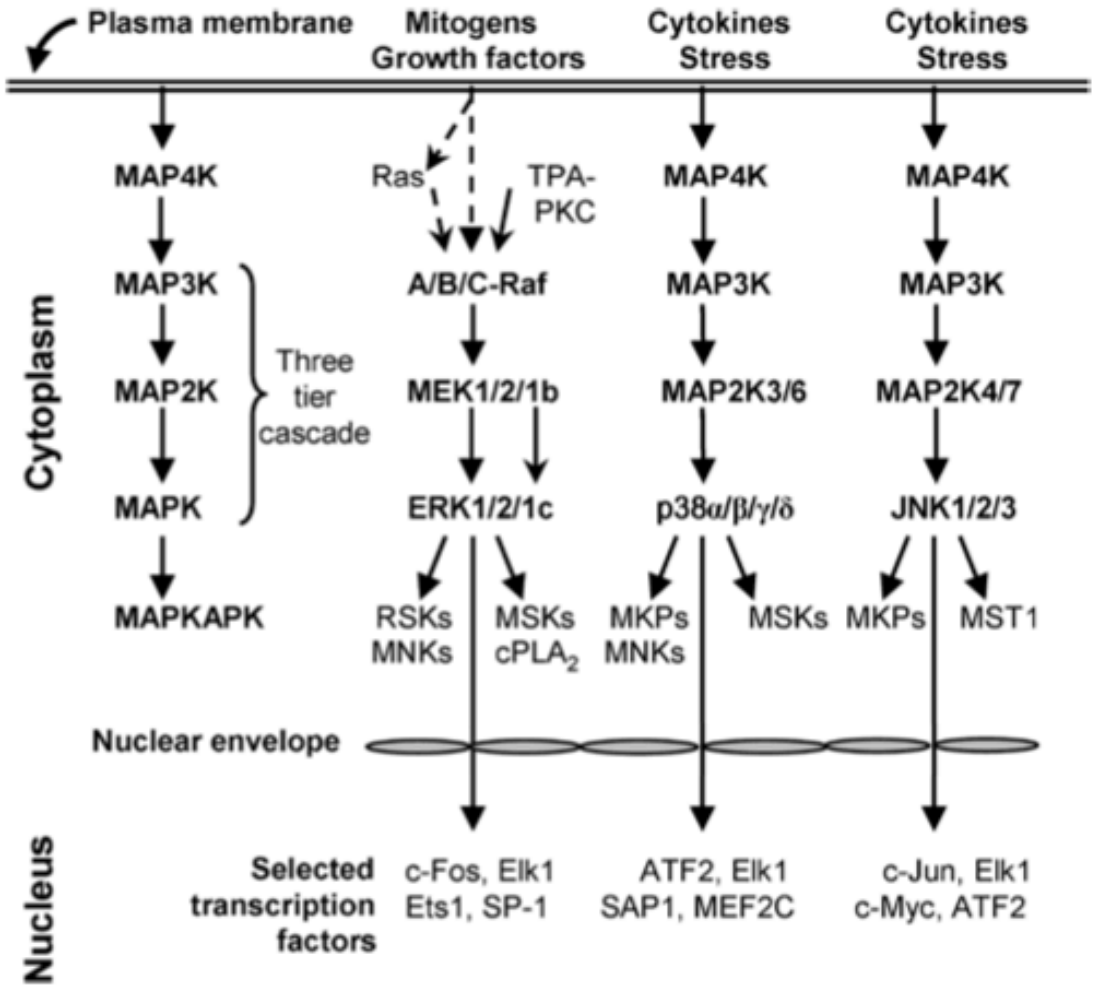

Figure 30: MAPK signalling cascades

CaSR activity has been linked to each of the ERK, p38, and JNK MAP kinase cascades, represented in this schematic. The MAP kinases, which occur in the cytoplasm and can be translocated into the nucleus, catalyze the phosphorylation of dozens of cytosolic proteins and numerous nuclear transcription factors. The core of each parallel pathway involves a three-tier activation cascade. Figure from Roskoski (2012).

Experiments comparing ERK1/2 phosphorylation between native HEK-293 cells, and HEK-293 cells over-expressing either wild type CaSR or R795W mutant CaSR have revealed that, in this cell system at least, the expression of a functional CaSR is necessary and sufficient to induce ERK1/2 phosphorylation and activation (Hobson et al., 2003). Furthermore, a dose-dependent phosphorylation of ERK1/2 is observed in response to increases in $[Ca^{2+}]_o$, and the calcimimetic, NPS R-467 (Kifor et al., 2001). Because ERK1/2 phosphorylation is partially blocked by several compounds, including PTX, phosphotyrosine kinase inhibitors, the PLC inhibitor U73122 and the PKC inhibitor GF109203X, whilst being enhanced by acute PMA-induced stimulation of PKC, it has been suggested that CaSR-dependent ERK1/2 phosphorylation involves both G_q and G_i signalling (Kifor et al., 2001). Since β-arrestin-mediated internalisation of the β2 adrenergic receptor results in G-protein independent ERK1/2 activation (Rosenbaum et al., 2009), it would be interesting to explore whether the interaction between CaSR and β-arrestin (Pi et al., 2005; Lorenz et al., 2007) has any significance for ERK1/2 activation.

Several lines of evidence clearly indicate that a G-protein-independent interaction between CaSR and filamin is important for CaSR mediated ERK1/2 activation (Ward, 2004). The direct association of filamin with CaSR has been reported in both HEK-293 (Awata et al., 2001) and bovine parathyroid cells (Hjälm et al., 2001). Furthermore, blocking the interaction of filamin with the C-terminal domain of CaSR substantially impairs elevated $[Ca^{2+}]_o$ stimulated, but not ADP stimulated, ERK1/2 phosphorylation (Hjälm et al., 2001). In addition, truncation studies have indicated that amino acids between residues 907 to 997 of the CaSR C-terminal domain represent a high affinity filamin-A binding site, which is involved in CaSR promoted ERK1/2 activation (Awata et al., 2001). However, further truncation studies have found that deletion of this binding site does not entirely prevent CaSR coupling to ERK1/2, suggesting the existence of a second filamin binding site at a putative α-helix between residues 868–879 of the juxtamembrane portion of the C-terminal domain (Zhang and Breitwieser, 2005). Accordingly, an siRNA based filamin-A gene silencing approach in HEK-293 cells, has confirmed the requirement for filamin-A in coupling CaSR to the ERK1/2 signalling cascade (Huang et al., 2006a). In conclusion, multiple signalling mechanisms involving filamin, G_q and G_i seem capable of coupling CaSR activity to ERK1/2 activation (Ward, 2004).

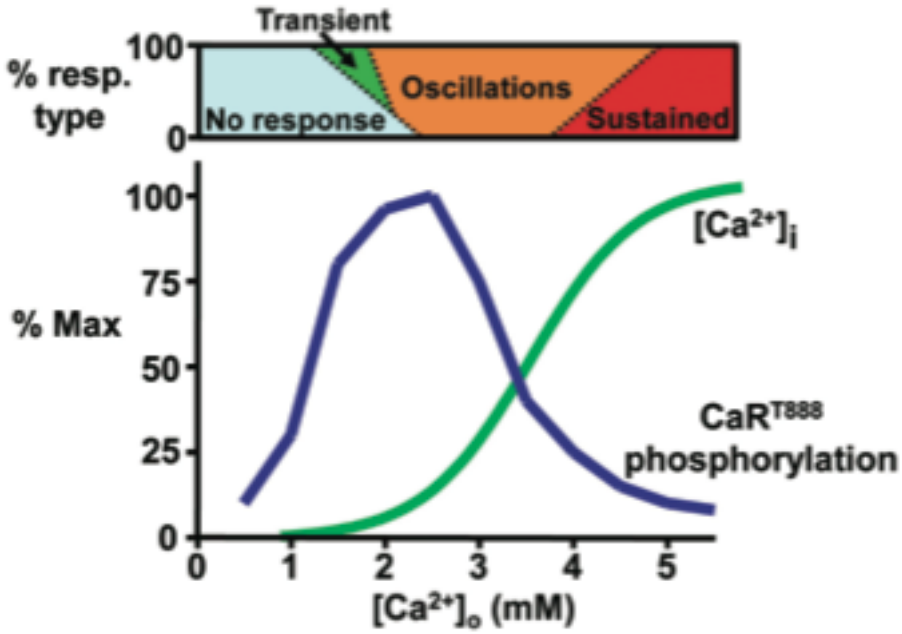

Figure 31: The $[Ca^{2+}]_o$ dependence of T888 phosphorylation, $[Ca^{2+}]_i$ and cellular $Ca^{2+}{}_i$ response type.

The classic sigmoidal concentration dependence of CaSR-induced $Ca^{2+}{}_i$ mobilization is not matched by the relationship between $[Ca^{2+}]_o$ and T888 phosphorylation ,which shows a biphasic (bell-shaped) relationship to $[Ca^{2+}]_o$. Therefore, at higher $[Ca^{2+}]_o$, T888 phosphorylation is low or absent (at least after a brief initial rise), thus permitting the sustained responses seen for $Ca^{2+}{}_i$ mobilization. The top bar shows the relative $[Ca^{2+}]_o$ concentration dependence of the transient (green), oscillatory (orange) and sustained (red) $Ca^{2+}{}_i$ responses normally observed based on data from Davies *et al.* (2007) and McCormick *et al.* (2010). The bar is intended to indicate the heterogeneity of the cellular responses at each concentration (see also Nash *et al.,* 2002). Figure from Ward & Riccardi 2012.

7.3.4.2.8. T888 phosphorylation and $Ca^{2+}{}_i$ oscillations

There have been numerous reports indicating that CaSR can couple variations in $[Ca^{2+}]_o$ to increases in $[Ca^{2+}]_i$. However, some studies have also indicated that when individual cells are considered, CaSR-induced $[Ca^{2+}]_i$ fluctuations often take the form of oscillations (Breitwieser and Gama, 2001; Ward and Riccardi, 2012). Such oscillations involve release of Ca^{2+} from intracellular stores (Ridefelt et al., 1995) and vary in frequency according to an established relationship with $[Ca^{2+}]_o$. Activating $[Ca^{2+}]_o$ (approximately 2 mM, although precise values vary between systems) elicit predominantly transient or low frequency oscillations in $[Ca^{2+}]_i$, increasing $[Ca^{2+}]_o$ to around 3 mM increases the oscillation frequency and $[Ca^{2+}]_o$ of approximately 5 mM result in sustained $[Ca^{2+}]_i$ increases (Figure 31) (Ridefelt et al., 1995; Ward and Riccardi, 2012). It has since been noted that PKC activation is

required for the generation of Ca^{2+}_i oscillations and that HEK-293 cells expressing a mutant receptor where the primary PKC phosphorylation site at T888 is rendered non-phosphorylatable (T888A), do not exhibit oscillations (Young et al., 2002). Interestingly, however, the phosphorylation of T888 by PKC actually inhibits CaSR promoted release of Ca^{2+} from intracellular stores (Bai et al., 1998b). Moreover, phosphomimetic mutations such as T888D and T888E (and curiously, the truncation mutation T888X) also impair $[Ca^{2+}]_o$ induced $[Ca^{2+}]_i$ release in a manner resembling PKC activity (Jiang et al., 2002). Furthermore, the use of an antibody specific for the phosphorylated T888 site indicates that PKC does indeed phosphorylate this residue in response to CaSR activation (Davies et al., 2007). The best explanation for these data is that PKC provides a negative feedback regulation of CaSR coupling to $[Ca^{2+}]_i$ release, via T888 phosphorylation, which is presumed to impair signalling via $G_{q/11}$, thus terminating the Ca^{2+}_i transient (Figure 32Ai-ii)(Bai et al., 1998b; Jiang et al., 2002; Young et al., 2002; Davies et al., 2007; Ward and Riccardi, 2012).

However, in order to generate a Ca^{2+}_i oscillation by such a mechanism, the feedback inhibition would need to decay, thus allowing $[Ca^{2+}]_i$ to rise again (Ward and Riccardi, 2012). An additional difficulty is raised by the observation that a greater proportion of cells respond with high frequency oscillations or sustained elevations in $[Ca^{2+}]_i$ when exposed to higher, compared to moderate $[Ca^{2+}]_o$ (Davies et al., 2007). The explanation is that, although T888 phosphorylation increases with $[Ca^{2+}]_o$ at moderate levels, T888 phosphorylation begins to decline when $[Ca^{2+}]_o$ is further increased until it becomes virtually absent at the very high levels of Ca^{2+}_o that induce sustained increases in $[Ca^{2+}]_i$ (Figure 31) (McCormick et al., 2010). Since 1 μM of the calcimimetic NPS R467 elicits a rapid, but short-lived increase in T888 phosphorylation, resulting in sustained elevated $[Ca^{2+}]_i$, there is evidence that T888 dephosphorylation at very high extracellular calcium concentrations is mediated by CaSR activation (McCormick et al., 2010). Thus, the mechanism for T888 dephosphorylation has aroused recent interest (Ward and Riccardi, 2012). It has been observed that the protein phosphatase 1/2A inhibitor, calyculin prevents T888 dephosphorylation and Ca^{2+}_i oscillations (Davies et al., 2007). Furthermore, the catalytic subunit of protein phosphatase 2A (PP2A) appears to partially colocalise with phospho-T888 in HEK-293 cells (Davies et al., 2007) and exhibits elevated activity when $[Ca^{2+}]_o$ is high (McCormick et al., 2010).

It thus seems plausible that PP2A mediates the decreased T888 phosphorylation that re-engages CaSR mediated $[Ca^{2+}]_i$ release, underlying the resulting oscillatory activity (Figure 32C). It has also been noted that this model, requiring cycles of T888 phosphorylation and dephosphorylation for $[Ca^{2+}]_i$ oscillations, explains why PKC stimulation prevents oscillatory activity and PKC inhibition promotes sustained elevated $[Ca^{2+}]_i$ responses, by preventing the removal and the application of negative feedback within the system, respectively (Figure 32B&D) (Davies et al., 2007; Ward and Riccardi, 2012).

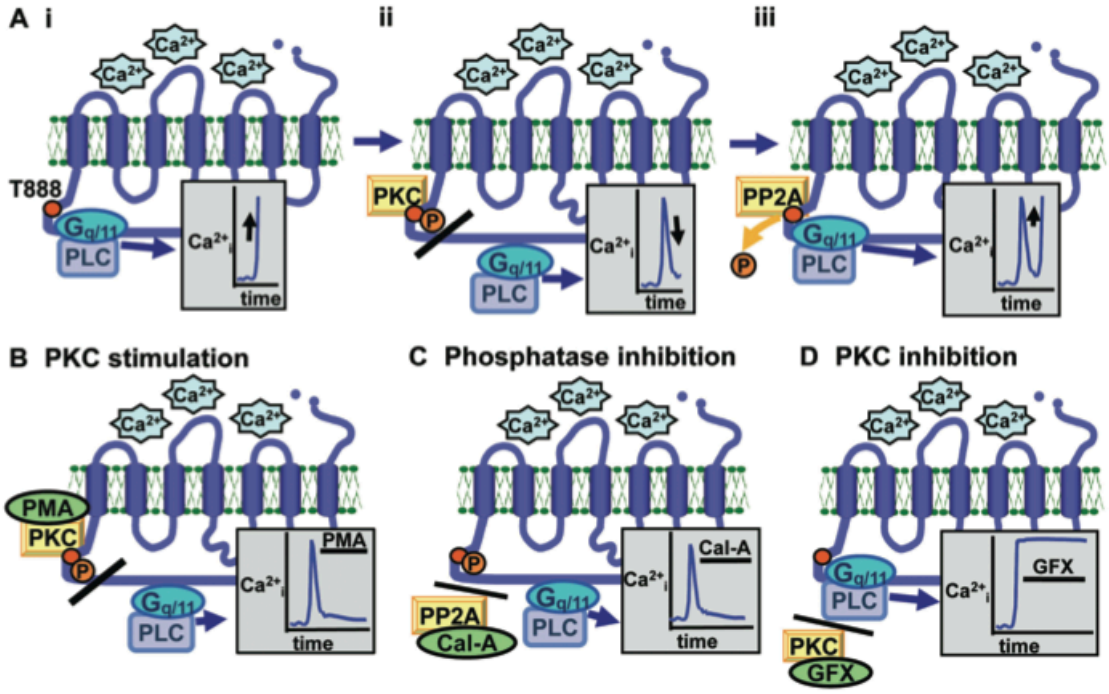

Figure 32: Hypothetical mechanism for the generation of $[Ca^{2+}]_i$ oscillations

A, There are three components of each oscillatory cycle including (i) CaSR activation eliciting Ca^{2+}_i mobilization, (ii) T888 phosphorylation uncoupling the pathway components and (iii) T888 dephosphorylation leading to further Ca^{2+}_i mobilization. This model therefore explains the suppressive effects of PKC stimulation by phorbol ester (PMA, Panel ***B***) and phosphatase inhibition by calyculin-A (Cal-A, Panel ***C***) and the stimulatory effect of the PKC inhibitor GF109203X (GFX, Panel ***D***) on CaSR-induced Ca^{2+}_i mobilization. Figure from Ward & Riccardi 2012.

Interestingly, a similar mechanism for the control of GPCR signalling by dynamic feedback phosphorylation has previously been observed in another class C GPCR, mGluR5 (Nash et al., 2001; Nash et al., 2002). Dynamic feedback phosphorylation of mGluR5 is also mediated by PKC, regulates Ca^{2+}_i oscillations and can be influenced by both agonist concentration and receptor density (Nash et al., 2002).

Furthermore, dynamic feedback phosphorylation of mGluR5 is also controlled by the phosphorylation of a single specific residue in the C-terminal domain, S839 (Kim et al., 2005; Ward and Riccardi, 2012).

7.3.4.2.9. Effects of L-amino acids, calcilytics and calcimimetics on downstream signalling

As has been described, L-amino acids can activate the CaSR by binding to the VFT domain (Zhang et al., 2002; Mun et al., 2004). At submaximal $[Ca^{2+}]_o$, L-amino acids selectively promote low frequency cellular oscillations in $[Ca^{2+}]_i$ (Young et al., 2002), via a signalling pathway involving filamin-A (Rey et al., 2005). However, despite the link between filamin-A and ERK1/2 signalling described above, L-amino acids only mildly enhance ERK1/2 signalling (Lee et al., 2007; Khan and Conigrave, 2010). In contrast, phenylalkyamine calcilytics and calcimimetics, such as NPS 2143 and NPS R-568, which bind the HH domain of CaSR, exert a comparatively uniform modulatory effect on downstream signalling pathways (Khan and Conigrave, 2010). Furthermore, the potency of phenylalkyamines can be greater than L-amino acids, which can result in differential effects on downstream signalling in some cases (Ward and Riccardi, 2012). For example, as a comparatively weak positive allosteric modulator L-Phenylalanine induces a slow increase in phospho-T888 immunoreactivity and slow $[Ca^{2+}]_i$ oscillations, while NPS R-467 induces a rapid but transient increase in phospho-T888 immunoreactivity and sustained increases in $[Ca^{2+}]_i$ (McCormick et al., 2010).

In conclusion, CaSR is a remarkably multifaceted GPCR, expressed in numerous different tissues and regulating a wide array of cellular responses though several signalling pathways (Hofer and Brown, 2003). It also has the capacity to be regulated by various interacting proteins, a capacity that seems likely to contribute to its broad utility (Huang and Miller, 2007). Furthermore, good progress is being made in the mapping of function onto the structural domains of CaSR (Khan and Conigrave, 2010). The knowledge surveyed in this introduction should therefore provide a helpful foundation on which to further probe the functions of CaSR in the development and plasticity of the nervous system.

8. Results Chapters

8.1. Results Chapter 1: CaSR in the early embryonic SCG

8.1.1. Introduction

The sympathetic neurons of the SCG represent an extremely well characterized model for the study of neural development in the PNS (Davies, 2009). Studies focused on the late embryonic and early postnatal SCG have contributed to the development of neurotrophic theory through increases in our knowledge of the regulation of axon growth, target field innervation and the acquisition of NGF dependence for survival (Levi-Montalcini, 1987; Oppenheim, 1991; Glebova and Ginty, 2005). However, the SCG can also be isolated from the very earliest stages of its development (Davies, 2009). The early SCG at E13 contains both postmitotic neurons and proliferating neuroblasts, the latter of which have acquired many characteristics of mature sympathetic neurons, but have yet to undergo their terminal mitotic division or differentiate into mature sympathetic neurons (Maina et al., 1998). Sympathetic neuroblasts are initially able to survive in culture for several days without added neurotrophic factors, when plated on a suitable substrate (Ernsberger et al., 1989). It is thought that, in contrast to later stages of development, their survival is supported by factors, including HGF, acting in an autrocrine or paracrine fashion (Maina et al., 1998; Davies, 2009). Furthermore, the early SCG provides a useful experimental system for the examination of proximal neurite outgrowth, which is also regulated by factors other than NGF (Glebova and Ginty, 2005), such as endothelins (Makita et al., 2008), artemin (Andres et al., 2001; Enomoto et al., 2001; Honma et al., 2002) and NT-3 (Belliveau et al., 1997; Kuruvilla et al., 2004).

CaSR is a GPCR originally cloned from the parathyroid gland (Brown et al., 1993), where one of its best known roles in systemic calcium homeostasis was defined (Brown and Macleod, 2001). However, it has subsequently been found to be broadly expressed in numerous tissues not connected to its originally described function, where it regulates a variety of cellular processes (Hofer and Brown, 2003; Riccardi and Kemp, 2012), including proliferation (Mailland et al., 1997; Chattopadhyay et al., 1998; Chattopadhyay et al., 1999b; Bilderback et al., 2002; Chattopadhyay et al., 2004; Dvorak et al., 2004; Tfelt-Hansen et al., 2004; Rey et al.,

2010; Li et al., 2011), differentiation (Oda et al., 2000; Komuves et al., 2002; Mentaverri et al., 2006; Aguirre et al., 2010) and apoptosis (Lin et al., 1998; Wu et al., 2005; Mentaverri et al., 2006). Furthermore, an unexpected novel role for CaSR was recently described in regulating the NGF-promoted axonal growth of sympathetic neurons of the E18 SCG (Vizard et al., 2008). Importantly, the *in vivo* relevance of this effect is supported by the observation of a deficit in target innervation in the iris of P1 *CaSR* $^{-/-}$ mice (Vizard et al., 2008). This chapter reports the expression of CaSR within the early SCG, which appears to be localized to both neuroblasts and postmitotic neurons, raising the possibility that CaSR may contribute to some aspects of early SCG neuron development. Consistent with this possibility, the data in this chapter reveals that $Ca^{2+}{}_o$ regulates neurite outgrowth in E13 SCG cultures, without exerting any statistically significant effect on cell survival. However, an assessment of proximal neurite outgrowth in conditional CaSR knockout embryos fails to provide evidence that CaSR is required for proximal outgrowth *in vivo*.

8.1.2. Methods

8.1.2.1. Early SCG cultures

Dissociated cultures of early SCG neurons were set up from CD1 mice. Cultures were established on polyornithine/laminin coated 35 mm culture dishes (Greiner), in defined medium (Davies et al., 1993). $[Ca^{2+}]_o$ was manipulated with EGTA or $CaCl_2$, as previously described (Vizard et al., 2008). Where stated, cultures were supplemented with 10 ng/ml NGF (R&D Systems).

8.1.2.2. Early SCG culture neural cell survival quantification

E13 SCG cultures contain a mixture of neuroblasts and postmitotic neurons, but virtually no non-neuronal cells (Maina et al., 1998). Both neuroblasts and neurons (together termed "neural cells") were included in the survival study. The initial neural cell number was ascertained by counting the number of neural cells within a 12x12 mm grid in the centre of each culture dish, for three random dishes, two hours after plating. Neural cell counts were repeated for every dish at 24 and 48 hours after plating using the same grid. Neural cell survival after 24 and 48 hours is expressed as a percentage of the average initial count within each experiment. In all cases, the investigator was blind to experimental conditions. The number of experimental repeats varies, and is stated in the text. Statistical significance was

assessed by 2-way, repeated measures (mixed-model) ANOVA, and was performed using GraphPad Prism 5.

8.1.2.3. Early SCG culture immunostaining and neurite outgrowth quantification

Cultured E13 SCG neural cells were incubated for 24 hrs before being fixed, blocked and stained in accordance with a previously published protocol (Vizard et al., 2008). Briefly, cells were fixed in ice cold methanol for 10 minutes, before washing twice in PBS and blocking with 5% BSA and 0.02% Triton X-100 in PBS for 1 hour at room temperature. The cells were incubated with primary antibody in 1% BSA at 4°C overnight, washed three times in PBS and incubated with secondary antibodies in 1% BSA for 1 hour at room temperature. To determine whether CaSR protein was expressed in proliferating neuroblasts of the SCG, a polyclonal antibody raised against the human CaSR N-terminus (Imgenex, 1/200) was used as a primary antibody (previously published by (Vizard et al., 2008)) together with a mouse monoclonal anti-PCNA antibody (Chemicon, 1/200). Secondary antibodies used were Alexa-488 conjugated anti-rabbit IgG and Alexa-594 conjugated anti-mouse, respectively (both Molecular Probes, 1/500). For neurite outgrowth quantification, cells were stained with a mouse monoclonal antibody to β-III tubulin (Promega, 1/1000) and a rabbit polyclonal antibody to the proliferation marker Ki67 (Abcam, 1/800). Images were acquired using a Zeiss LSM 510 laser-scanning microscope. Neurites were traced in ImageJ (NIH). Statistical pairwise comparisons were by Students t-test (two-tailed).

8.1.2.4. Breeding & use of *Nestin Cre / Casr lox P* mice

In order to knock out *Casr* expression in the nervous system, mice in which Exon 7 of *Casr* is flanked by *loxP* sites (*Casr* $^{loxP/loxP}$, floxed *Casr* mice), previously described by (Chang et al., 2008) and a kind gift from Wenhan Chang (UCSF), were crossed with mice expressing Cre recombinase under the control of the rat *Nestin* promoter and enhancer (*Nestin*-Cre^{+ve} mice) (Tronche et al., 1999; Hanada et al., 2009). *Nestin*-Cre^{+ve} mice were of a C57BL/6 genetic background, while floxed *Casr* mice were of a mixed 129/SvJae & C57BL/6 genetic background, thus the resulting mice were also of a mixed 129/SvJae & C57BL/6 background. Experimental embryo litters were obtained by crossing two mice that each contained at least one copy of the *Nestin*-Cre allele together with a single copy of the floxed *Casr* allele

(*Nestin*-Cre^{+ve} / *Casr*$^{loxP/+}$ mice). Genotypes of adults and embryos were determined as described (Chang et al., 2008), following extraction of genomic DNA from tissue samples using a Maxwell 16 machine (Promega). Tissues from embryos with the genotypes *Nestin-Cre*$^{+ve}$ / *Casr*$^{loxP/loxP}$ and *Nestin-Cre*$^{+ve}$ / *Casr*$^{+/+}$ were used for analysis as described below.

8.1.2.5. Wholemount immunohistochemistry

8.1.2.5.1. Tissue collection

Embryos derived from crosses of *Nestin*-Cre^{+ve} / *Casr*$^{loxP/+}$ mice were closely staged using Theiler criteria (Gkogkas et al., 2012). The portion of tissue containing the SCG and its proximal projections was dissected from E13 embryos that had been bisected along the midline, allowing optimal antibody penetration and separate analysis of each SCG. These tissue portions, along with the body of the embryo, were processed for wholemount immunohistochemistry by a method adapted from Dent *et al* (1989) (Dent et al., 1989), detailed below.

8.1.2.5.2. Histology

Tissue was fixed in ice cold Dent's fixative (1 part DMSO, 4 parts Methanol) before being quenched, overnight at room temperature, in a solution comprising one part 30% H_2O_2, two parts Dent's fixative. Next, embryos underwent five one-hour washes in TBS (10mM Tris-HCl, pH 8.0, 150mM NaCl) at room temperature, before incubation with primary antibodies for three days at room temperature. Tissue portions containing SCG were stained with rabbit anti-TH (1/500, Millipore), while the remaining body was stained with mouse anti-NF160 (1/300, Sigma). Following primary antibody staining, tissues underwent five one-hour washes in TBS before being incubated overnight, at 4°C, either with a peroxidase conjugated goat anti-rabbit antibody (1/100, Vector Laboratories) for TH staining, or a peroxidase conjugated anti-mouse antibody (1/300, Sigma) for NF160 staining. All antibodies were diluted in blocking serum (9 parts goat serum, 1 part DMSO). Following five one-hour washes in TBS, tissue was pre-incubated for 20 minutes, at RT, in 3,3'-Diaminobenzidine tetrahydrochloride hydrate (DAB) that had been diluted to 0.5mg/ml in PBS. After pre-incubation, staining was developed in DAB solution containing 0.006% H_2O_2 and the tissue was washed several times in TBS before being dehydrated in methanol and cleared in BABB (1 part benzyl alcohol, 2 parts benzyl benzoate).

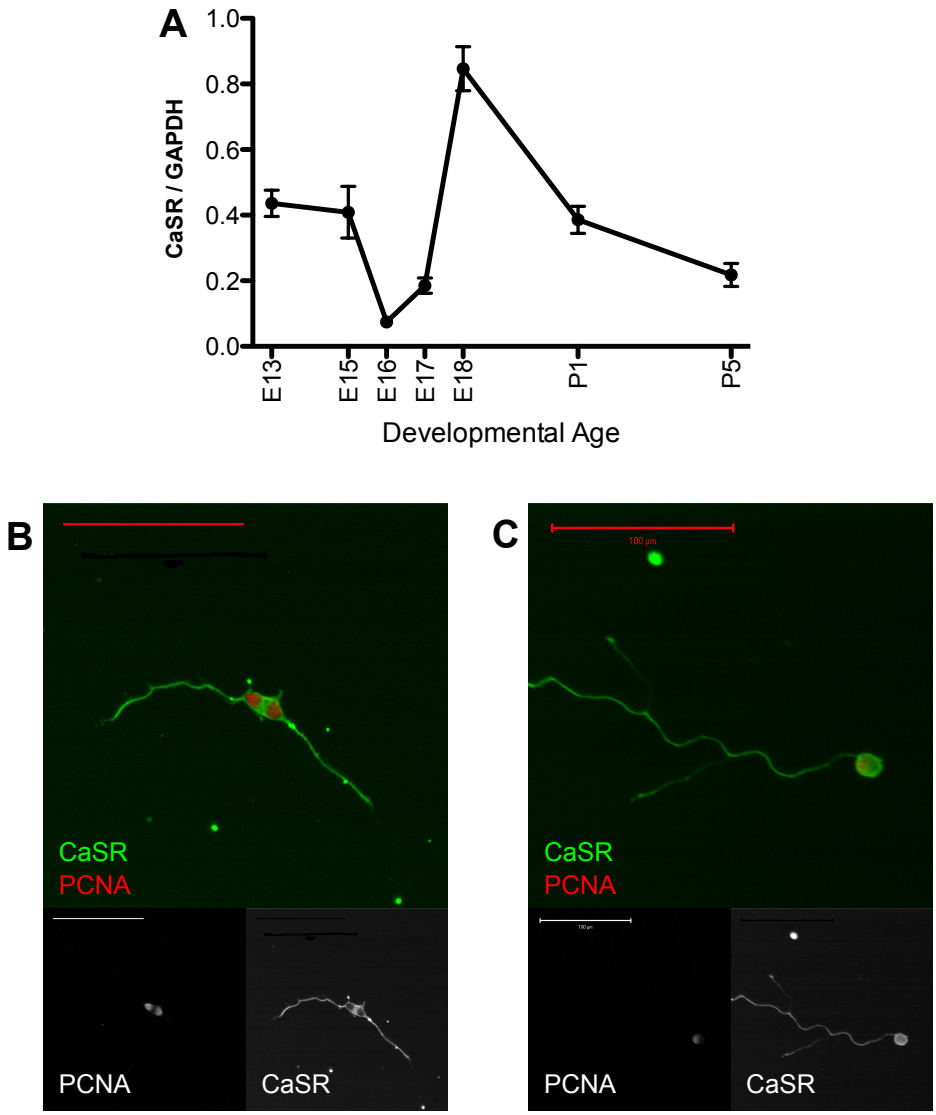

Figure 33: CaSR is expressed in the SCG during early embryonic ages

***A*,** The developmental profile of CaSR mRNA expression levels in the SCG, relative to the housekeeping gene GAPDH, indicates that CaSR mRNA expression is high during an early developmental widow from E13 to E15 before falling dramatically between E15 and E16. The second peak of CaSR mRNA expression at E18 peak has previously been shown to correspond to a period when CaSR can regulate neurite outgrowth from SCG neurons without effecting their survival. Data courtesy of Tom Vizard (Cardiff University, now Oxford University).
***B*,** CaSR immunostaining is detectable in E13 cells possessing a typical neuroblast morphology and with high levels of nuclear PCNA immunostaining.
***C*,** CaSR immunostaining is also detectable in E13 cells possessing a typical post-mitotic neuronal morphology and with low levels of nuclear PCNA immunostaining. Cells were cultured for 24 hours at 1.4 mM $[Ca^{2+}]_o$ without NGF and fixed in MeOH for 10 mins. 100 µm scale bars.

8.1.2.5.3. Imaging & analysis

Images were acquired, whilst moving through the focal planes crossed by SCG projections, using a digital SLR camera (Canon) coupled with an Axiovert 200 inverted microscope (Zeiss). Axons were traced in ImageJ (NIH) from a single image, acquired with a 4x objective, where they were judged to be most clearly resolved, aided by more detailed images acquired with a 20x objective. In all cases, axons were traced from the rostral pole of the SCG and the investigator was blind to embryo genotypes throughout imaging and analysis. The average total length of all rostrally-oriented projections was averaged between the two SCG of each animal. Statistical comparisons were performed by two-tailed t-tests using GraphPad Prism 5.

8.1.3. Results

8.1.3.1. CaSR is expressed in the SCG at early embryonic ages

Previously published work has revealed a peak in CaSR mRNA expression at E18 in the late embryonic SCG (Vizard et al., 2008). Unpublished expression data, courtesy of Tom Vizard (previously at Cardiff University, now at Oxford University), indicates that CaSR mRNA is also expressed in the SCG at early stages of embryonic development (Figure 33A). This novel, early window of CaSR transcript expression extends from E13 to E15, before abruptly decreasing to the previously reported low levels of expression at E16. The early window of elevated CaSR mRNA expression coincides with a period of development in which neuroblasts proliferate and differentiate into postmitotic sympathetic neurons (Maina et al., 1998; Andres et al., 2001), whilst extending axons towards intermediate targets (Glebova and Ginty, 2005) (Figure 4 and 5, Introduction).

As it would be advantageous to use dissociated cell culture to assess the function of CaSR in early embryonic SCG development, it was important to confirm that the expression observed at the mRNA level *in vivo* is also observed at the protein level *in vitro*. CaSR protein expression was investigated by immunocytochemistry, as it afforded the opportunity of addressing whether CaSR is expressed by proliferating neuroblasts, postmitotic neurons, or both. CaSR immunoreactivity was detected in both the soma and processes of cultured E13 neuroblasts and postmitotic neurons (Figure 33B&C). Discrimination between the two cell types was performed on the basis of their distinctive morphologies (Maina et al., 1998) and the knowledge that

PCNA is most highly expressed in proliferating cells (Kurki et al., 1986; Kurki et al., 1988).

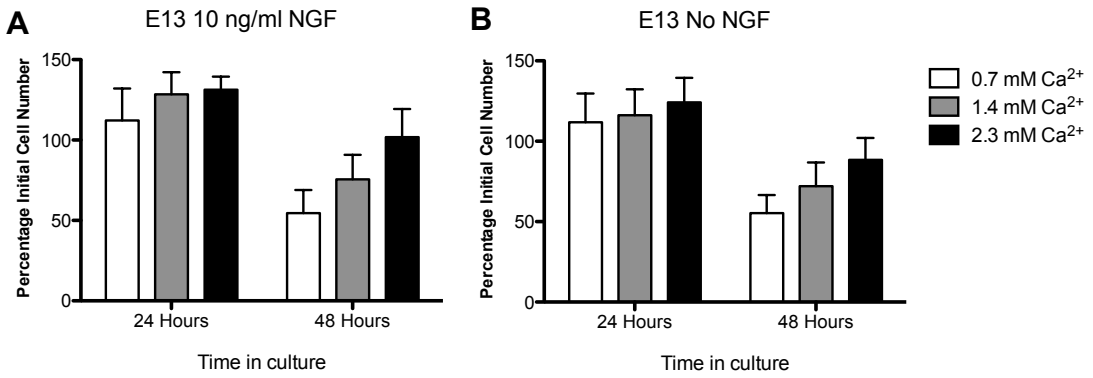

Figure 34 $[Ca^{2+}]_o$ does not regulate the overall number of cells in E13 SCG cultures

Both with (***A***) and without (***B***) 10 ng/ml NGF, no statistically significant differences in the percentage initial cell number of E13 SCG cultures are revealed by performing cell counts at 24 and 48 hours *in vitro*. Cell counts for early SCG cultures represent not only survival, but also proliferation and differentiation. Not surprisingly, time in culture had a significant main effect on cell number, both with ($P < 0.0001$) and without ($P < 0.0001$) NGF. This relates to the decrease in cell number between 24 and 48 hours, following a net increase during the first 24 hours that is indicative of neuroblast proliferation. However $[Ca^{2+}]_o$ had no significant main effect on cell survival, either in the presence ($P = 0.284$) or absence ($P = 0.548$) of NGF. Furthermore, there was no significant interaction between time in culture and $[Ca^{2+}]_o$ ($P = 0.214$), indicating that the decline in cell number over time in culture is not significantly different between different $[Ca^{2+}]_o$. Statistical comparisons by two-way ANOVA. Data represent mean + SEM from 6 independent experiments, each composed of 3 independent cultures.

8.1.3.2. $[Ca^{2+}]_o$ does not regulate the overall number of cells in E13 SCG cultures

During the early developmental window of CaSR expression, neuroblasts proliferate, differentiate into postmitotic neurons and undergo the early stages of neurite outgrowth (Figure 4, Introduction). The detection of CaSR immunoreactivity in both neuroblasts and postmitotic neurons in E13 SCG cultures raises the possibility that CaSR could either regulate the proliferation, differentiation or survival of neuroblasts and/or the survival of postmitotic neurons. For this reason, the broadest hypothesis was tested first, namely that $[Ca^{2+}]_o$ may regulate the overall number of cells surviving in culture, a variable influenced by all four of these cellular processes. E13 SCG neural cells were

cultured in media containing a range of calcium concentrations that have previously been shown to modulate the extent of neurite outgrowth from E18 SCG neurons (Vizard et al., 2008), either with or without 10 ng/ml NGF. The total number of cells surviving in culture was ascertained by performing cell counts at 2 hours, 24 hours and 48 hours after plating. Analysis by two-way analysis of variance (ANOVA) indicates that $[Ca^{2+}]_o$ has no significant effect on cell survival, either with (main effect $[Ca^{2+}]_o$; P = 0.284) or without (main effect $[Ca^{2+}]_o$; P = 0.548) NGF (Figure 34). Furthermore, the lack of a statistically significant interaction (P = 0.214) indicates that there is no change in the effect of $[Ca^{2+}]_o$ on neural cell survival with different times in culture.

8.1.3.3. $[Ca^{2+}]_o$ regulates neurite outgrowth in E13 SCG cultures

A novel and unexpected role for CaSR in regulating NGF-promoted neurite outgrowth and branching has recently been described, acting during a later phase of SCG development (Vizard et al., 2008). Crucially, this effect is restricted to a developmental window of E18 – P0 by the level of CaSR expression. This raises the possibility that CaSR may play a similar role in regulating the early stages of neurite outgrowth in response to Ca^{2+}_o during the first developmental peak in CaSR expression between E13 – E15. To investigate this possibility, E13 SCG neural cells were cultured for 24 hours in medium containing 2.3 mM or 0.7 mM Ca^{2+}_o, either in the presence of absence of 10 ng/ml NGF. This time point was chosen because the number of cells surviving in culture is clearly unaffected by manipulations of $[Ca^{2+}]_o$ at 24 hours (Figure 34). After 24 hours, cells were fixed and stained for β-III tubulin, to identify neural cells, and Ki-67 to distinguish between proliferating neuroblasts and postmitotic neurons (Ki-67 is selectively expressed by proliferating cells (Gerdes et al., 1991)). Following imaging with a laser-scanning microscope, neurite lengths were determined using ImageJ software. The data in figure 35 reveal that the extent of neurite outgrowth from both neuroblasts and postmitotic neurons is significantly greater in medium containing 2.3 mM Ca^{2+}_o compared to medium containing 0.7 mM Ca^{2+}_o, both in the presence and absence of 10 ng/ml NGF (P = 0.024 for neuroblasts in the presence of NGF; $P = 2.6\times10^{-5}$ for postmitotic neurons in the presence of NGF; $P = 5.3\times10^{-8}$ for neuroblasts in the absence of NGF; $P = 5.7\times10^{-13}$ for postmitotic neurons in the absence of NGF; unpaired t-tests). If all neural cells are included in the statistical analysis, the significance of the differences in neurite length between neural cells

cultured in medium containing 0.7 mM or 2.3 mM Ca^{2+}_o is even higher ($P = 1.1x10^{-8}$ in the presence of NGF; $P = 1.29x10^{-15}$ in the absence of NGF; unpaired t-tests).

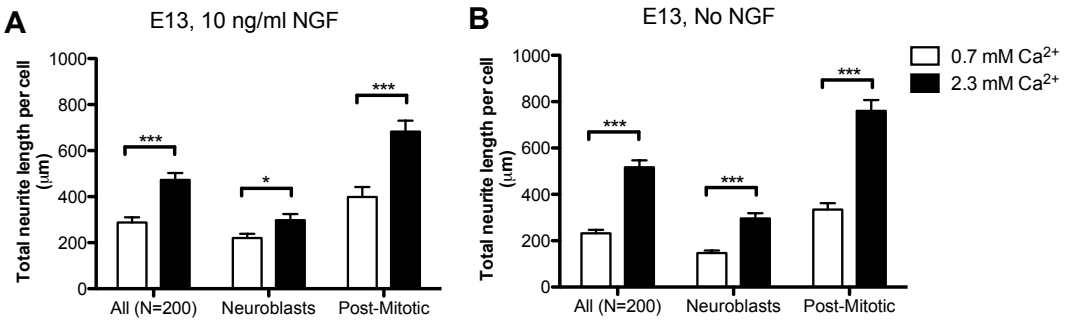

Figure 35: $[Ca^{2+}]_o$ regulates neurite outgrowth in E13 SCG cultures

***A*,** In 10 ng/ml NGF, E13 SCG neurite length is significantly increased in the presence of elevated $[Ca^{2+}]_o$. The results are statistically significant across all cells are analysed, and when neuroblasts and post-mitotic cells are analysed separately. Only cells with nuclei exhibiting staining positive for the proliferation marker Ki67 were assigned to the "neuroblast" bin. *All cells* N = 200 cells (for both 0.7 mM and 2.3 mM $[Ca^{2+}]_o$, $P = 1.1x10^{-8}$). *Neuroblasts* N = 124 for 0.7 mM, N = 109 for 2.3 mM $[Ca^{2+}]_o$ ($P = 0.024$). *Postmitotic neurons* N = 76 for 0.7 mM, N = 91 for 2.3mM $[Ca^{2+}]_o$ ($P = 2.6x10^{-5}$).
***B*,** A significant effect of $[Ca^{2+}]_o$ on the extent of neurite outgrowth is also observed in the absence of NGF. *All cells* N = 200 ($P = 1.29x10^{-15}$). *Neuroblasts* N = 112 for 0.7 mM, N = 105 for 2.3 mM ($P = 5.3x10^{-8}$). *Postmitotic neurons* N = 88 for 0.7 mM, N = 95 for 2.3 mM ($P = 5.7x10^{-13}$).
Comparisons between 0.7 mM and 2.3 mM $[Ca^{2+}]_o$ by unpaired t-tests. Data represents mean + SEM from 5 independent experiments. * = $P < 0.05$, *** = $P < 0.001$

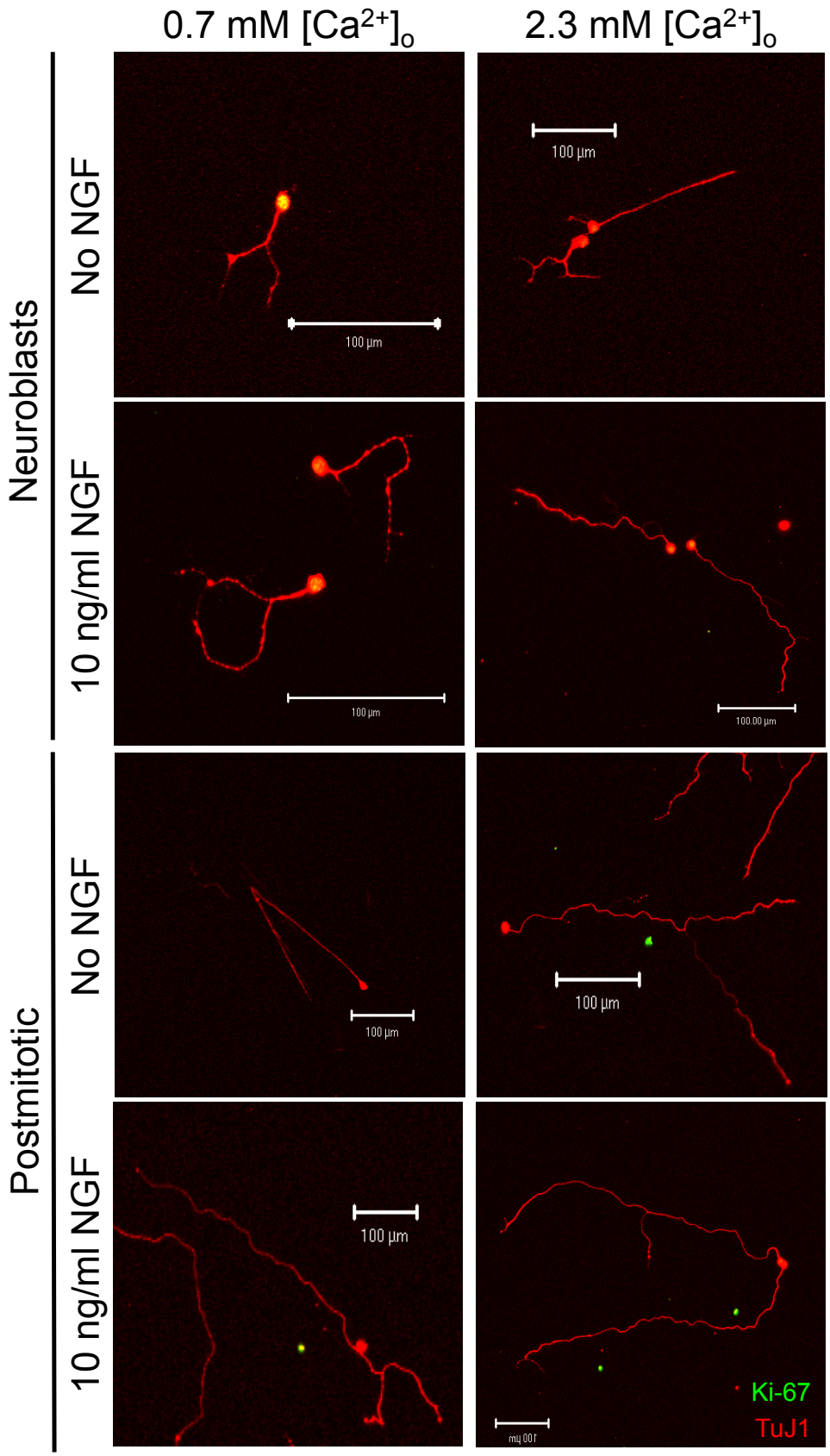

Figure 36: Representative Images for Figure 35

Neurite outgrowth from neural cells in E13 SCG cultures at 24 hours, imaged by confocal microscopy. Scale bars 100 µm.

8.1.3.4. No evidence to suggest CaSR regulates proximal neurite outgrowth *in vivo*

The preceding data raise two critical questions. Firstly, is the effect of Ca^{2+}_o on neurite outgrowth mediated by CaSR; and secondly, does this effect operate *in vivo,* as well as *in vitro*. These questions were investigated simultaneously using wholemount immunohistochemistry in *Nestin Cre / Casr lox P* mice. Deletion of Exon 7 of the *Casr* gene was verified in neural tissue of all experimental embryos using a PCR based approach, where primers binding either side of Exon 7 amplify a smaller, 284 bp fragment following deletion of Exon 7 than they do for WT *Casr*, which yields a 2.0 kb fragment (Figure 18, Introduction) (Chang et al., 2008) (Figure 37A&D). The total length of rostrally oriented fibres in Nestin CaSR-KO (*Nestin*-Cre^{+ve} / $Casr^{loxP/loxP}$) embryos was found to be indistinguishable from that of Cre-expressing control (*Nestin*-Cre^{+ve} / $Casr^{+/+}$) embryos (n = 3 litters; P = 0.6087; Figure 37B). Equivalent levels of proximal neurite outgrowth in Nestin CaSR-KO and control embryos are illustrated in Figure 37C. These data indicate that if CaSR does mediate the effect of $[Ca^{2+}]_o$ *in vitro*, lack of CaSR *in vivo* does not lead to a phenotype that is readily quantifiable by this method of analysis.

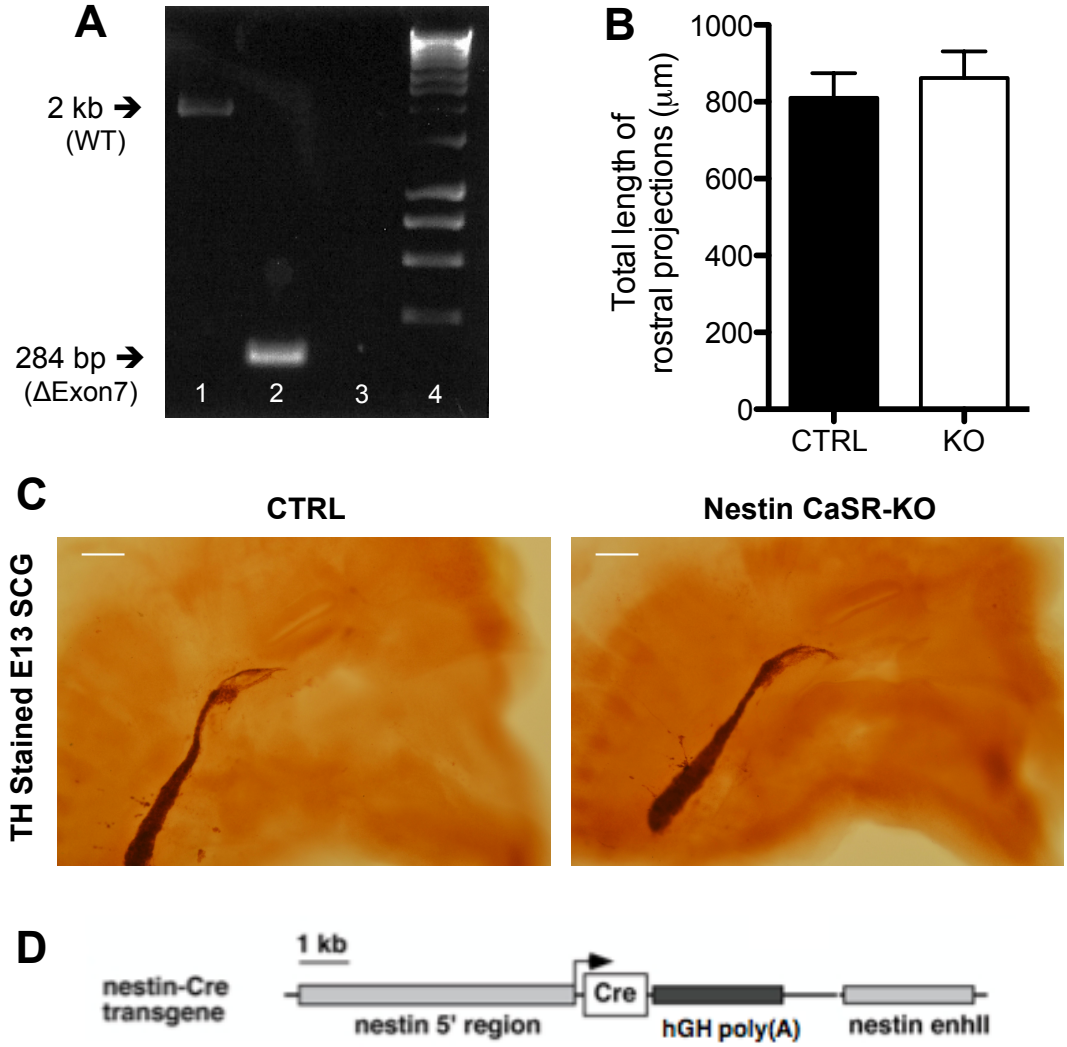

Figure 37: CaSR does not regulate proximal neurite outgrowth *in vivo*

***A*,** PCR analysis of genomic DNA extracted from neural tissue of E13 embryos validates the deletion of CaSR Exon 7 in *Nestin-Cre*$^{+ve}$ / *Casr*$^{loxP/loxP}$ embryos and the lack of deletion in *Nestin-Cre*$^{+ve}$ / *Casr*$^{+/+}$ embryos. Neural tissue samples were taken from hindbrain of embryos that were used for wholemount analysis. Lane 1: *Nestin-Cre*$^{+ve}$ / *Casr*$^{+/+}$ (control animals). Lane 2: *Nestin-Cre*$^{+ve}$ / *Casr*$^{loxP/loxP}$ (Nestin CaSR-KO animals). Lane 3: No DNA (negative control). Lane 4: Hyperladder I.
***B*,** Average total length of all rostral projections from the SCG. n = 3 litters. Each experimental repeat consists of mean values across all embryos of a given genotype within each litter (1-2 KO and 3-4 CTRL embryos analysed per litter). P = 0.6087; t-test.
***C*,** Representative images illustrate the similar levels of proximal neurite outgrowth between genotypes. 200 μm scale bars.
***D*,** Structure of the *Nestin-Cre* transgene. Cre recombinase was expressed under the control of the rat *nestin* promoter and the nervous system-specific enhancer present in the second intron. hGH poly(A), human growth hormone polyadenylation signal. Figure adapted from Tronche *et al* (1999).

8.1.4. Discussion

This study has provided evidence that Ca^{2+}_o regulates neurite outgrowth from E13 sympathetic neurons. This developmental time point corresponds to an early window of enhanced CaSR expression *in vivo*, when CaSR immunoreactivity appears to be localized to both sympathetic neuroblasts and postmitotic neurons *in vitro*. Accordingly, Ca^{2+}_o regulates neurite outgrowth from both cell populations. The regulation of neurite outgrowth from cultured E13 sympathetic neuroblasts and neurons by Ca^{2+}_o is reminiscent of a previous report demonstrating that Ca^{2+}_o modulates the extent of axon outgrowth from E18 sympathetic neurons (Vizard et al., 2008). However, while the regulation of axon outgrowth by Ca^{2+}_o at E18 occurs at a developmental stage when NGF promotes the growth and ramification of sympathetic axons in many of their target fields (Glebova and Ginty, 2005; Davies, 2009), TrkA and $p75^{NTR}$ expression are very low in the E13 SCG and cells within the SCG are not responsive to NGF (Wyatt and Davies, 1995). Accordingly, the regulation of neurite outgrowth by Ca^{2+}_o is not dependent on NGF at E13, while the modulation of axon outgrowth from E18 SCG neurons by Ca^{2+}_o does require NGF (see Results Chapter 2). Therefore, if CaSR does mediate the ability of Ca^{2+}_o to regulate neurite outgrowth *in vitro*, it is possible that there may be differences in the downstream signalling pathways engaged by CaSR at E13 and E18. However, one important caveat is that, whilst the data suggest that CaSR may regulate neurite growth from E13 SCG neural cells *in vitro*, they do not demonstrate it unambiguously. Fluctuations in the concentration of Ca^{2+}_i are crucial for signalling a variety of biological responses, and can occur due to the direct entry of Ca^{2+} from the extracellular space via numerous ion channels (Berridge et al., 2003). Therefore, manipulations of $[Ca^{2+}]_o$ could conceivably affect cell physiology indirectly though processes not dependent on CaSR activation. Establishing that CaSR mediates the ability of increased $[Ca^{2+}]_o$ to promote neurite growth will require other approaches, such as pharmacological manipulation with calcimimetics and calcilytic compounds, or culturing E13 SCG neural cells from embryos genetically deficient in CaSR expression.

This study does not provide evidence to support the hypothesis that Ca^{2+}_o regulates the proliferation, differentiation or survival of cells in E13 SCG cultures. Much like studies of E18 sympathetic neurons, no effect of Ca^{2+}_o was observed on the number of cells surviving in culture at 24 hours, and the trend towards

increased cell counts in higher $[Ca^{2+}]_o$ at 48 hours did not reach significance. Furthermore, the lack of a significant interaction by two-way ANOVA indicates that no $[Ca^{2+}]_o$ tested had a significantly different effect on survival over time in culture compared to than any other $[Ca^{2+}]_o$. However, there is a great deal of evidence that CaSR activation can regulate proliferation (Mailland et al., 1997; Chattopadhyay et al., 1998; Chattopadhyay et al., 1999b; Bilderback et al., 2002; Chattopadhyay et al., 2004; Dvorak et al., 2004; Tfelt-Hansen et al., 2004; Rey et al., 2010; Li et al., 2011), differentiation (Oda et al., 2000; Komuves et al., 2002; Mentaverri et al., 2006; Aguirre et al., 2010) and apoptosis (Lin et al., 1998; Lorget et al., 2000; Wu et al., 2005; Mentaverri et al., 2006) in various cell types. Since the current study only employed a gross measure of the overall number of cells surviving in culture, it cannot exclude the possibility that a subtle effect on one or more of these processes may yet operate below the threshold likely to be detected by the approach used. This possibility could be best examined by tracking the fate of defined cells over time in culture, an approach that has uncovered an effect of HGF on neuroblast differentiation (Maina et al., 1998) and artemin on neuroblast proliferation *in vitro* (Andres et al., 2001).

The regulation of neurite outgrowth from cultured E13 SCG neural cells by Ca^{2+}_o reported here raised the possibility that a reduction in CaSR-mediated axon growth during the early developmental window of enhanced CaSR gene expression could contribute to the previously described target innervation deficit in the iris of P1 *CaSR* $^{-/-}$ mice (Vizard et al., 2008). This possibility was tested using TH stained wholemounts of E13 wild type embryos and embryos with a conditional deletion of *Casr* exon 7, selectively targeted to the nervous system. Tracing of proximal axon outgrowth from the SCGs of these embryos revealed that the there was no deficit in proximal axon growth in the absence of functional CaSR. However, two caveats must be considered. Firstly, the measurements of proximal axon outgrowth will be most heavily influenced by the axons that have extended the farthest from the SCG. Therefore, the possibility that CaSR selectively regulates the growth of shorter axons along a path already defined by what may be considered "pioneer" axons cannot be ruled out. This possibility would seem more likely if Ca^{2+}_o enhances neurite outgrowth from cultured sympathetic neuroblasts more effectively than it does from cultured postmitotic neurons, as neuroblasts have shorter neurites on average than postmitotic neurons (Maina et al., 1998).

However, increased $[Ca^{2+}]_o$ does not appear to preferentially increase the length of neuroblast neurites compared to the neurites of postmitotic neurons. Secondly, in order to maximize the number of SCGs included in the wholemount analysis, whilst minimizing the number of animals culled, the deletion of *Casr* exon 7 was verified in all embryos designated "Nestin CaSR-KO" by PCR analysis of DNA from the hindbrain, rather than DNA from the SCG. Although *nestin* driven Cre-recombinase activity is widespread in the nervous system by E10.5 (see authors' characterization on the Jackson Laboratory website, http://cre.jax.org/Nes/Nes-CreNano.html), and has been found to be effective at deleting loxP flanked DNA in the SCG as early as E16.5 (Bodmer et al., 2011), only verification of *Casr* exon 7 deletion in E13 SCG can explicitly rule out the possibility of inadequate *Casr* deletion in the SCGs of the animals analysed. However, a pilot wholemount experiment (n = 1 litter, data not shown) using E13 embryos from the exon 5-deleted *Casr* $^{-/-}$ mouse strain that was used in the previous study of CaSR function in the SCG (Vizard et al., 2008) did not reveal a deficit in proximal axon growth in the absence of functional CaSR, thereby providing additional support for the conclusion that CaSR appears not to regulate proximal neurite outgrowth from E13 SCG *in vivo*.

8.1.5. Chapter specific acknowledgements

I would like to thank Dr. Tom Vizard (Oxford University) for providing unpublished RT-QPCR data, Mr Ronak Ved (Cardiff University, School of Medicine) for assistance in gathering *in vitro* data and Dr. Helen Waller-Evans (Cardiff University, School of Biosciences) for assistance optimizing histological methods.

8.2. Results Chapter 2: CaSR signalling in late embryonic SCG neurons

8.2.1. Introduction

During the development of the PNS, a variety of extracellular signals act upon axons to regulate their growth, guidance to their target fields and arborization within those target fields (Glebova and Ginty, 2005; Davies, 2009). In the perinatal period, the target derived neurotrophic factor NGF exerts critically important effects on the survival of sympathetic neurons in the SCG (Levi-Montalcini and Booker, 1960; Levi-Montalcini, 1987; Crowley et al., 1994), but also has dissociable effects on the growth and branching of sympathetic axons within many of their targets (Glebova and Ginty, 2004). NGF is able to engage a variety of signalling pathways downstream of its receptors, TrkA and $p75^{NTR}$. These include the Rho family GTPases, PLCγ, PI3K and ERK pathways downstream of TrkA, and the JNK and NF-κB pathways downstream of $p75^{NTR}$ (Huang and Reichardt, 2003; Reichardt, 2006). Furthermore, local actions of NGF on distal axons and growth cones, involving PLCγ activity, Ca^{2+}_i signals, calcineurin and PKC, are thought to be critical for NGF promoted sympathetic axon growth and branching (Campenot, 1977; Campenot et al., 1994; Bodmer et al., 2009; Bodmer et al., 2011; Harrington and Ginty, 2013).

Despite the well characterized role for Ca^{2+}_i in NGF-promoted growth, and numerous recognized roles for Ca^{2+}_i signals in regulating growth cone motility (Henley and Poo, 2004; Chilton, 2006), a role of Ca^{2+}_o in the development of the sympathetic nervous system, both *in vitro* and *in vivo* was only recently uncovered, (Vizard et al., 2008). Ca^{2+}_o regulates the NGF-dependent growth and branching of late embryonic SCG neurons, but does not promote neuronal survival. Ca^{2+}_o promoted axonal growth and branching is mediated by the CaSR and is confined to a perinatal developmental window when CaSR expression is high (Vizard et al., 2008). However, the requirement for NGF in CaSR-promoted axon growth (Vizard et al., 2008) has complicated the analysis of downstream signalling pathways underlying CaSR-promoted axon growth. This chapter aimed to further confirm the key role of CaSR in promoting axon growth and branching from perinatal SCG neurons and to examine the signalling pathways that transduce CaSR activation

into enhanced axon growth and branching. In contrast to NGF supplemented cultures, high $[Ca^{2+}]_o$ fails to increase CaSR expression in the absence of NGF. Whilst the ability of Ca^{2+}_o to promote axon outgrowth is NGF-dependent, the over-expression of wild-type (WT) CaSR in E18 SCG neurons promotes axon growth in the absence of NGF, thereby allowing an investigation into CaSR signalling in the absence of NGF-dependent signalling. These investigations revealed a key role for a portion of the C-terminal domain of CaSR, ERK1/2 activation and a strong modulatory function for the PKC phosphorylation site T888, which has been shown to regulate Ca^{2+}_o induced Ca^{2+}_i signals downstream of CaSR in other cell systems (Jiang et al., 2002; Young et al., 2002; Davies et al., 2007; McCormick et al., 2010).

8.2.2. Methods

8.2.2.1. Culture & Transfection of E18 SCG neurons

Dissociated cultures of E18 SCG neurons were set up from CD1 mice and were grown on polyornithine/laminin coated 4-well 35 mm culture dishes (Greiner), in defined medium (Davies et al., 1993). 50 μM Boc-D-FMK (Merck Millipore) was used to support neuronal survival in all experiments. $[Ca^{2+}]_o$ was adjusted to the required levels with EGTA or $CaCl_2$, these having been measured with a radiometer 125 as previously described (Vizard et al., 2008).

Ganglia were digested by 20 minutes incubation with 0.05% trypsin in Ca^{2+}/Mg^{2+} free Hank's Balanced Salt Solution (HBSS; Invitrogen), at 37°C. The reaction was stopped by washing ganglia twice in F12 medium supplemented with 10% horse serum (Invitrogen). Two further washes in PBS were performed before transfection. Transfection was performed using the Neon Transfection system (Invitrogen) and the MP-100 Microporator (Digital Bio) (Kim et al., 2008), according to the manufacturer's instructions. Briefly, two ganglia were dissociated in 12-15 μl of Resuspension Buffer per transfection by gentle trituration with a P200 pipette tip. 0.5 μg of pCopGFP per transfection was added to the triturated cells, before the cell suspension was split into 12 μl aliquots. Each 12 μl aliquot had 2 μg of function modifying expression plasmid added to it. Each aliquot was transfected separately, with two 30 millisecond pulses at 900 V, before being added immediately to pre-prepared media and then being plated on polyornithine/laminin coated 4-well dishes.

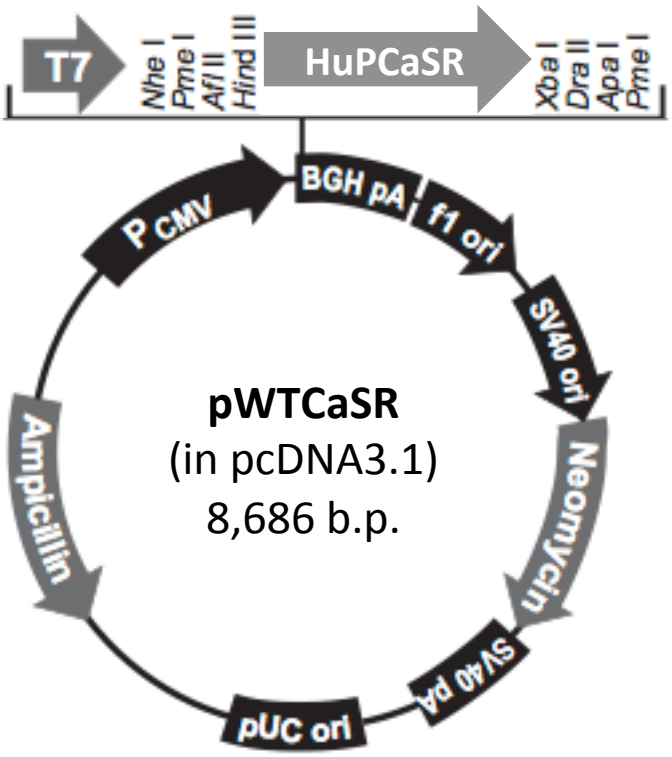

Figure 38: pWTCaSR plasmid map

The ORF of HuPCaSR (including start and stop codons) was cloned into the pcDNA3.1(+) backbone using the *Asp718 I* (lost in the process) and *Xba I* (conserved in the process) restriction sites. Map modified from that of pcDNA3.1(+), Invitrogen, www.invitrogen.com

8.2.2.2. Plasmid preparation, mutagenesis & sequencing

Plasmid stocks were amplified by transformation into JM109 Competent Cells (Promega) according to the manufacturer's protocol. After selection of transformed cells using the appropriate antibiotic, colonies were expanded in LB media. Cells were lysed and plasmids were purified using the PureLink HiPure Plasmid Midiprep Kit (Invitrogen), according to the manufacturer's instructions, and resuspended at the desired concentration in TE buffer.

pWTCaSR represents the open reading frame (ORF) of the human parathyroid CaSR sequence (HuPCaSR, GenBank: U20759.1), cloned into the pcDNA3.1(+) backbone (Invitrogen) (See Figure 38). Restriction digests, excising the CaSR ORF using *Hin*dIII and *Xba* I, and sequencing (MWG Eurofins sequencing service) confirmed both the identity of human CaSR and a lack of mutations in its coding region (data not shown).

Site directed mutagenesis (SDM) was used to produce variants of pWTCaSR. These were either performed in-house by Dr. Tom Vizard or by using MWG Eurofins Site Directed Mutagenesis service (See Table 2). In both cases, the success of SDM was verified by MWG Eurofins sequencing service.

Plasmid	WT Codon	SDM Codon	Produced by
pR185Q-CaSR	CGA	CAA	T. Vizard (Vizard et al., 2008)
pR795W-CaSR	CGG	TGG	T. Vizard
pDDN-CaSR	CGA & CGG	CAA & TGG	T. Vizard
pG907X-CaSR	GGA	TGA	T. Vizard
pA877X-CaSR	GCA	TAG	MWG Eurofins SDM
pT888A-CaSR	ACG	GCG	T. Vizard
pT888D-CaSR	ACG	GAT	MWG Eurofins SDM
pT888X-CaSR	ACG	TAG	T. Vizard

Table 2 - Variants of pWTCaSR produced by SDM

8.2.2.3. Immunocytochemistry

E18 SCG cultures were fixed at 24 hours in 4% PFA, for 20 minutes at room temperature. Fixed neurons were permeabilised with 0.02% TritonX-100 in PBS before being blocked, for one hour at room temperature, in PBS containing 5% bovine serum albumin (BSA). Fixed cultures were incubated overnight, at 4°C, with primary antibodies and washed three times in PBS. Following washing, the cultures were incubated with secondary antibodies for one hour at room temperature. Primary antibodies were diluted in PBS containing 1% BSA. See Table 3 for primary antibodies used and their dilutions. Secondary antibodies were raised in donkey or goat, conjugated to either Alexa-488, or -546 dyes (Invitrogen), and diluted 1/600 in PBS containing 1% BSA. After washing, cells were counterstained with DAPI, washed again and imaged immediately in PBS.

Target	Host	Dilution	Manufacturer
βIII Tubulin	Mouse	1/1000	R&D
CaSR	Rabbit	1/1000	Imgenex
CaSR (phospho-T888)	Rabbit	1/1000	Abcam
copGFP	Mouse	1/500	Origene
Phospho-p44/42 MAPK (P-ERK1/2) (Thr202/Tyr204)	Rabbit	1/100	Cell Signaling Technology
RFP	Mouse	1/250	Abcam
p44/42 MAPK (Total ERK1/2)	Rabbit	1/100	Cell Signaling Technology

Table 3 - Antibodies used for immunocytochemistry.

8.2.2.4. ERK and CaSR staining intensity measurements

All images were acquired using a Zeiss LSM510 confocal microscope. The selection of cells for imaging was performed using only βIII Tubulin staining, to avoid selection bias. Imaging settings for the channel to be quantified were set within the dynamic range of the detector at the start of imaging using the "Range Finder" tool (Zeiss), and were kept constant thereafter. Individual images representing cellular cross sections just above the plane of the primary neurites were acquired using a 40x, 0.80 NA Achroplan immersion objective (Zeiss). Quantification of Phospho-ERK1/2, Total-ERK1/2 and CaSR staining intensities was achieved using standard pixel intensity and region of interest tools within Volocity software (Perkin Elmer).

Briefly, cell soma were identified using the "Find 2D nuclei" tool, applied either to the red channel (for TuJ1 stained and RFP expressing cells) or the green channel (for GFP expressing cells). Detection of the entire soma was facilitated by the supplementary application of the "Dilate" tool (three iterations) and the "Close"

tool (one iteration), followed by the "Fill holes in objects" tool. Average pixel intensity of the desired channel within the identified cell soma was then recorded.

Statistical tests were chosen on the following basis: For simple two condition comparisons (e.g. CaSR expression comparison between pcDNA3.1 and pWTCaSR transfections) normality was confirmed, but equal variance could not be assumed, so the comparison was performed by t-test with Welch's correction for unequal variance. For experiments with one independent variable (IV) of greater than two levels, one-way ANOVAs with Bonferroni's multiple comparison post-hoc tests were performed (e.g. ERK1/2 staining following transfections with pcDNA3.1, pWTCaSR, pA877StopCaSR or pDDNCaSR). For experiments with two IVs, each of two levels (e.g. NGF concentration (present at 10 ng/ml or absent) and $[Ca^{2+}]_o$ (0.7 mM or 2.3 mM) two-way (2x2) ANOVAs were performed, followed by Bonferroni's multiple comparison post-hoc tests. All statistical analyses were performed using Graphpad Prism 5.

8.2.2.5. Imaging & analysis of axon growth

Neuritic arbours were visualized by CopGFP expression (Shagin et al., 2004) allowing imaging to be performed after 24 hours in culture using an Axiovert 200 inverted microscope (Zeiss). Images were acquired using both 20x and 10x objectives using 6.5 second exposure times. Length and branching of neurites were quantified by analysis of digital images using a modified Fast-Sholl (Gutierrez and Davies, 2007) program, which counts the number of intersections made by neurites with a series of concentric rings drawn at 15 μm intervals from the cell soma. In all cases the experimenter was blind to experimental conditions.

Choice of statistical test was defined as follows. In all outgrowth experiments excepting those using pharmacology (see 8.2.2.6) there was only one IV, either $[Ca^{2+}]_o$ or genotype (i.e. the function modifying plasmid used), depending on the experiment. Furthermore, the data were not normally distributed, and could not be reliably normalized by transformation. For these reasons, Mann-Whitney tests were used to compare medians in experiments where the IV had only two levels (e.g. 0.7 mM vs. 2.3 mM $Ca^{2+}{}_o$), while Kruskal-Wallis tests with Dunn's multiple comparison tests were used to compare medians in experiments where the IV had greater than two levels (e.g. pcDNA3.1 vs. pWTCaSR vs. pG907Stop). All statistical analyses were performed using Graphpad Prism 5.

8.2.2.6. Pharmacology

Pharmacological agents used in this study are detailed in Table 4. Compounds were made up to their final concentration in culture medium prior to the addition of transfected cell suspension, and were thus included throughout the course of each experiment in which they were used.

Since all pharmacological experiments aimed to assess whether modification of a particular signalling pathway through the addition of a given compound antagonized CaSR promoted growth, each experiment was designed with two IVs of two levels each. Specifically, these were CaSR genotype (pcDNA3.1 or pWTCaSR transfection) and pharmacological status (including an effective compound or a control). As appropriate for this experimental design, two-way (2x2) ANOVAs were performed, followed by Bonferroni's multiple comparison post-hoc tests. Rejection of the null hypothesis, that CaSR promoted growth is unchanged regardless of pharmacological status, requires a significant interaction term, a test that has been described for synergistic biological relationships (Slinker, 1998) and also for antagonistic biological relationships (Planas et al., 2003). All statistical analyses were performed using Graphpad Prism 5.

Name	Target	Manufacturer	[Final]
2-APB	IP_3R / TrpC	Tocris	50 μM
U0124	Inactive analogue of U0126	Tocris	10 μM
U0126	MEK1/2 inhibitor	Tocris	10 μM

Table 4 - Pharmacological agents used.

8.2.2.7. Survival counts of transfected neurons

Survival of transfected neurons was quantified by counting the total number of neurons per well at 24 hours and again at 48 hours in culture, then expressing the 48 hour count as a percentage of the 24 hour count. Counts were performed using an Axiovert 200 inverted microscope (Zeiss). In all cases the experimenter was blind to experimental conditions. Statistical analyses were performed by unpaired t-tests for experiments with one IV of two levels, one-way ANOVAs with

Bonferroni's multiple comparison post-hoc tests for experiments with one IV of greater than two levels, and two-way ANOVAs with Bonferroni's multiple comparison post-hoc tests for experiments with two IVs. All stats were performed in GraphPad Prism 5.

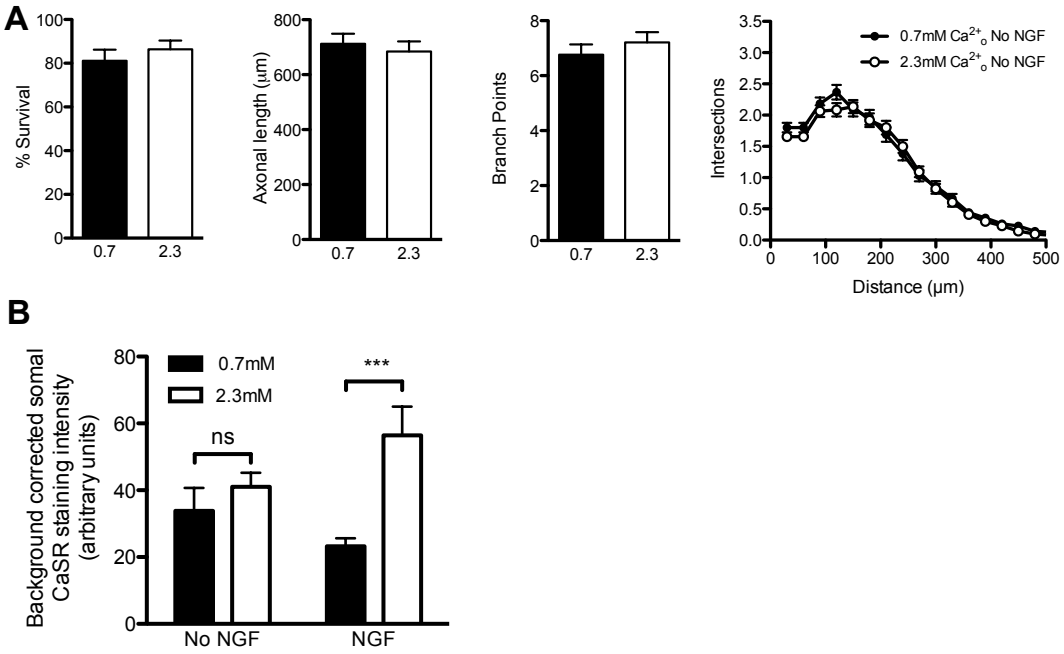

Figure 39: Both CaSR promoted growth and $[Ca^{2+}]_o$ dependent up-regulation of CaSR expression are NGF dependent in E18 SCG cultures

***A*,** The previously reported $[Ca^{2+}]_o$-dependent increase in axon outgrowth from E18 sympathetic neurons is not observed in the absence of NGF. No significant effects were observed on survival ($P = 0.4426$, t-test), axon length ($P = 0.7232$, Mann Whitney test) or branching ($P = 0.3532$, Mann Whitney test). Data in graphs represent Mean ± s.e.m.; n = 4 independent experiments; 231 - 235 cells per condition.

***B*,** CaSR protein expression is up-regulated by elevated Ca^{2+}_o, but only in the presence of NGF. Quantification of somal CaSR immunoreactivity using a previously published polyclonal antibody against the N-terminal extracellular domain of CaSR. A significant interaction ($P = 0.033$) is observed by two-way ANOVA, indicating that the increase in CaSR protein expression in high $[Ca^{2+}]_o$ varies significantly in the presence or absence of NGF. Accordingly, Bonferroni post-hoc tests show a significant difference in CaSR expression between 0.7 and 2.3 mM $[Ca^{2+}]_o$ in the presence of NGF ($P < 0.001$), whereas no significant difference is observed in the absence of NGF. Data in graph represents mean + s.e.m.; n = 24 cells from four independent experiments per condition (6 per experiment). *** = $P < 0.001$, ANOVA with Bonferroni's post-hoc tests.

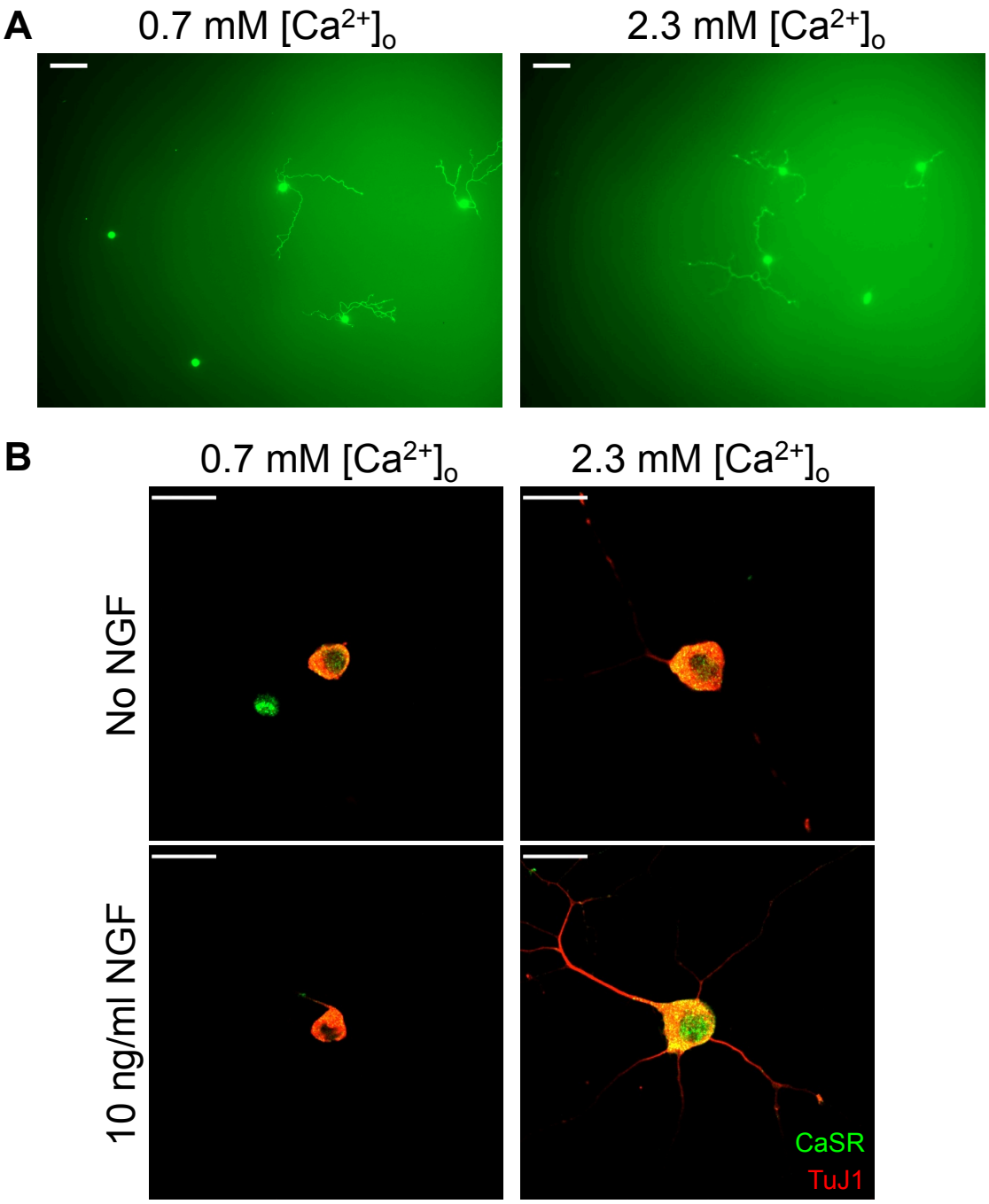

Figure 40: Representative images for Figure 39

A, Neurite outgrowth from E18 SCG neurons grown in 2.3 mM and 0.7 mM $[Ca^{2+}]_o$ in the absence of 10 ng/ml NGF. Scale bars 100 µm.
B, Somal CaSR staining imaging in E18 SCG neurons cultured in 2.3 mM and 0.7 mM $[Ca^{2+}]_o$, with and without 10 ng/ml NGF. Single image planes acquired through the cell soma, just above the plain of the neurites. Scale bars 20 µm.

8.2.3. Results

8.2.3.1. Both CaSR-promoted growth and $[Ca^{2+}]_o$-dependent up-regulation of CaSR expression are NGF-dependent in E18 SCG cultures

Previously published work has revealed a role for CaSR in regulating NGF-promoted axonal growth during a developmental window in which sympathetic axons are ramifying in their target fields under the control of NGF (Vizard et al., 2008). As a first step in examining the signalling pathways downstream of CaSR that lead to enhanced axonal growth, the NGF-dependency of this effect was investigated in cultures of E18 SCG neurons. In the presence of caspase inhibitors, to sustain survival in the absence of NGF, alterations in $[Ca^{2+}]_o$ do not significantly change the extent of axonal outgrowth and branching from E18 SCG neurons cultured without NGF (P = 0.7232 and 0.3532, respectively; comparison between 0.7 mM and 2.3 mM Ca^{2+}; Mann Whitney test), nor do they significantly regulate neuronal survival (P = 0.4426 comparison between 0.7 mM and 2.3 mM Ca^{2+}, t-test) (Figure 39A).

These data raised the question of why the CaSR-mediated regulation of axon growth by Ca^{2+}_o should be dependent on NGF. Since CaSR promoted growth appears to be controlled by the level of CaSR expression (Vizard et al., 2008), and the up-regulation of *Casr* mRNA expression in the SCG between E16 and E18 occurs at a developmental period when sympathetic neurons are most highly responsive to NGF and the expression of TrkA and $p75^{NTR}$ is increasing rapidly (Wyatt and Davies, 1995), it was hypothesized that NGF could regulate the expression of CaSR. This hypothesis was tested *in vitro* by quantifying the levels of somal CaSR immunoreactivity, using a previously published polyclonal antibody directed to the N-terminal extracellular domain of CaSR, when E18 SCG neurons were cultured for 24 hours in medium containing either 0.7 mM or 2.3 mM Ca^{2+}, in the presence or absence of 10 ng/ml NGF (Vizard et al., 2008). Interestingly, CaSR protein expression is significantly up-regulated by elevated Ca^{2+}_o, but only in the presence of 10 ng/ml NGF (two-way ANOVA; Ca^{2+}_o x NGF interaction P = 0.033; P < 0.001 for comparison between 0.7mM and 2.3 mM Ca^{2+} in the presence of NGF; Bonferroni's post-hoc test; Figure 39B). These data raise the possibility that increased CaSR expression in 2.3 mM Ca^{2+}_o may be a component of the mechanism by which CaSR promotes neurite outgrowth in the presence of NGF. Moreover, these data may provide an explanation for the absence of an effect of Ca^{2+}_o in the

absence of NGF (Figure 39A), since they raise the possibility that increased CaSR expression may be necessary and sufficient to promote axon growth at elevated $[Ca^{2+}]_o$.

8.2.3.2. Overexpression of functional CaSR in activating levels of Ca^{2+}_o rescues CaSR promoted growth in the absence of NGF

To test this possibility, WT CaSR was over-expressed in E18 SCG neurons by electroporation of an expression construct expressing the full length human CaSR (pWTCaSR). Electroporation with pWTCaSR leads to a robust and statistically significant increase in CaSR protein expression within the soma of transfected neurons, compared to control transfected neurons (pcDNA3.1), after 24 hours in culture ($P < 0.0001$; unpaired t-test with Welch's correction for unequal variances; Figure 41).

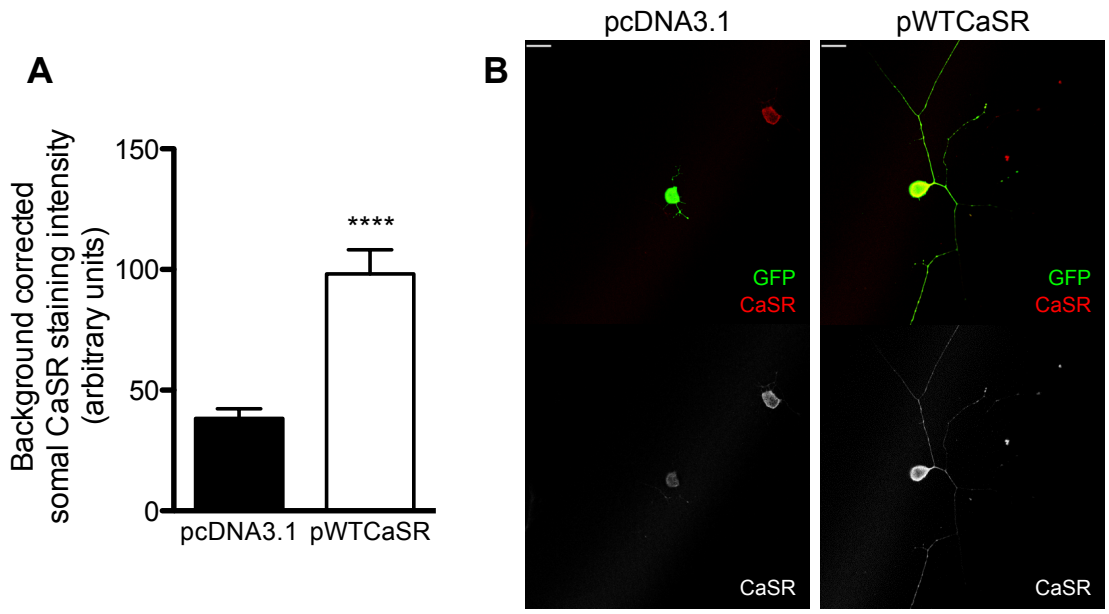

Figure 41: Increased CaSR protein expression is detectable by immunocytochemistry following transfection with pWTCaSR in the absence of NGF

***A*,** Quantification of somal CaSR immunoreactivity using a previously published polyclonal antibody against the N-terminal extracellular domain of CaSR. As expected, transfection with the pWTCaSR construct results in an increase in CaSR protein expression, relative to cells transfected with the control plasmid pcDNA3.1. Data in graph represents mean + s.e.m. n= 24 cells per condition (6 per transfection), from two independent experiments, two separate transfections per experiment. **** = $P < 0.0001$, unpaired t-test with Welch's correction for unequal variances.
***B*,** Representative images illustrating the increase in CaSR immunoreactivity of pWTCaSR transfected cells compared to control transfected cells. 20 µm scale bar.

Having established that transfection with pWTCaSR significantly increases the level of CaSR protein expressed by E18 SCG neurons *in vitro*, the effect of enhanced CaSR expression on the extent of axonal outgrowth in medium containing either 0.7 mM or 2.3 mM Ca^{2+}, but lacking NGF, was determined. Over-expression of WT CaSR significantly increases axon growth and branching compared to control transfected neurons after 24 hours in culture without NGF when the extracellular calcium concentration is 2.3 mM ($P < 0.001$ and $P < 0.01$, respectively; Dunn's post-hoc test comparison with pcDNA3.1 transfection; Figure 42A and B). To further confirm that over-expression of CaSR is sufficient to promote axon growth and branching from E18 SCG neurons cultured without NGF in medium containing activating levels of Ca^{2+}_o, neurons were transfected with CaSR expression constructs containing inactivating mutations that have been shown to lead to FHH in humans (Bai et al., 1996). These mutations were R185Q and R795W. In addition, neurons were also transfected with a CaSR construct containing both inactivating mutations (R185Q / R795W; "DDN"). In contrast to WT CaSR, none of the functionally impaired CaSR mutants promote axon growth or branching from SCG neurons cultured in 2.3 mM Ca^{2+}_o in the absence of NGF (Figure 42A and B). Importantly, the over-expression of either WT or mutated CaSR does not alter the survival of cultured SCG neurons compared to control transfected neurons (Figure 42A, B and C).

CaSR is known to be a highly promiscuous GPCR (Brown and Macleod, 2001), raising the possibility that increased NGF-independent axon growth following CaSR over-expression may reflect heterodimerization of CaSR with another GPCR and not enhanced Ca^{2+}_o sensing. If this were the case, the growth promoting effects of CaSR over-expression would be expected to be substantially independent of the Ca^{2+}_o in the culture medium. The finding that over-expression of WT CaSR does not enhance axon growth and branching in the absence of NGF when the culture medium contains 0.7 mM Ca^{2+} ($P = 0.817$ and 0.533, respectively; comparison to pcDNA3.1 transfection; Dunn's post-hoc test; Figure 42C), supports the notion that CaSR activation by Ca^{2+}_o underlies the growth promoting effects of CaSR over-expression in the absence of NGF. Taken together with the observation that NGF is required to promote the expression of CaSR by elevated $[Ca^{2+}]_o$, these data suggest

that in 2.3 mM Ca^{2+}_o, elevated CaSR expression is necessary and sufficient for CaSR promoted axonal growth in late embryonic SCG cultures.

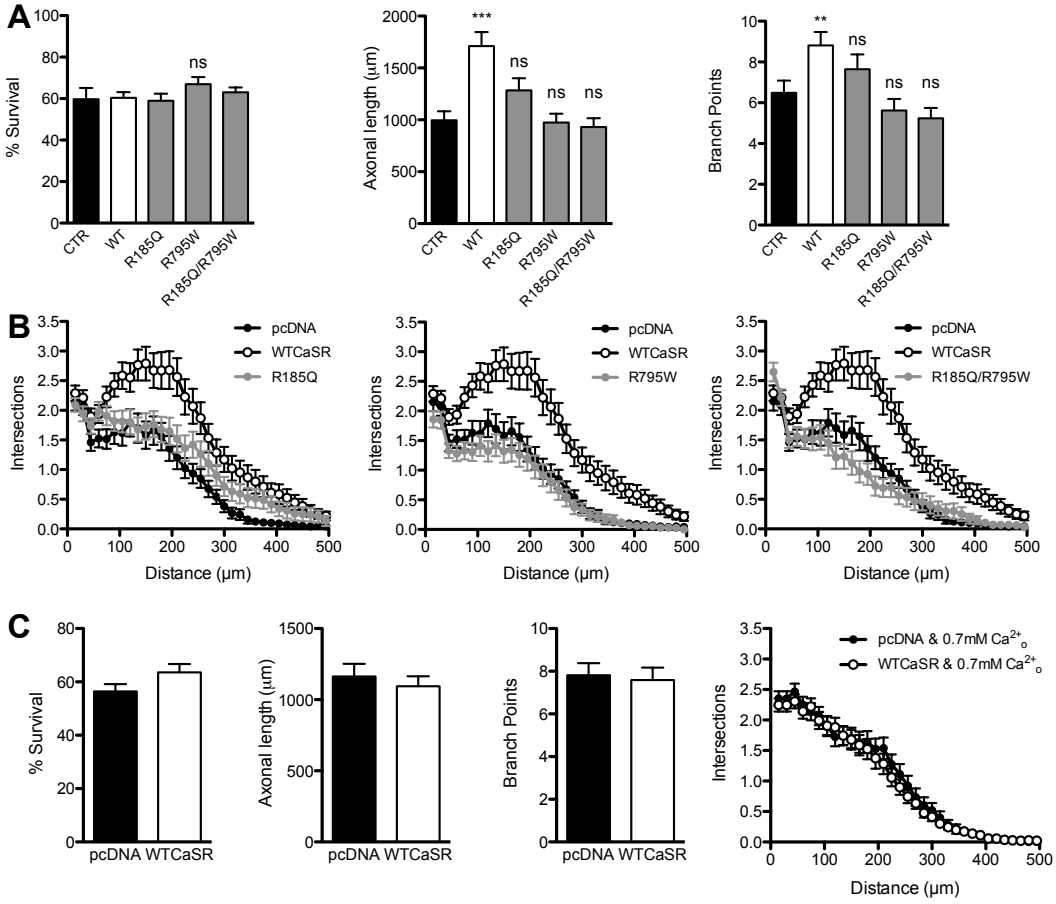

Figure 42: Overexpression of functional CaSR in activating levels of Ca^{2+}_o rescues CaSR promoted growth in the absence of NGF

***A*,** Overexpression of functional CaSR (WT) reconstitutes the effect of CaSR promoted growth in high calcium media (2.3 mM Ca^{2+}_o) in the absence of NGF. Transfection with two distinct dominant-negative CaSR mutant constructs fail to promote growth, as does a construct containing both mutations. No difference in survival is observed between any of the conditions (P = 0.545; one-way ANOVA). Only over-expression of WT CaSR results in a significant increase in axonal length and branching compared to control (CTR) transfected cultures (pcDNA3.1) (P < 0.001 and P = 0.0002, respectively, Kruskal-Wallis test with Dunn's post-hoc tests comparing each column to CTR). The data shown represents means + s.e.m. n = 3 independent experiments, between 59 and 66 cells per experiment per condition.
***B*,** Sholl plots for the data in A. Means ± s.e.m.
C, Overexpression of WT CaSR does not promote growth in low calcium medium (0.7 mM Ca^{2+}_o). No significant differences were observed in survival (P = 0.163; t-test), axon length (P = 0.817; Mann Whitney test) or branching (P = 0.533; Mann Whitney test) between control transfected neurons and neurons transected with WT CaSR. Data in graphs represents means ± s.e.m. 231 – 235 cells per condition.
** = P < 0.01; *** = P < 0.001, Kruskal-Wallis test with Dunn's post-hoc tests.

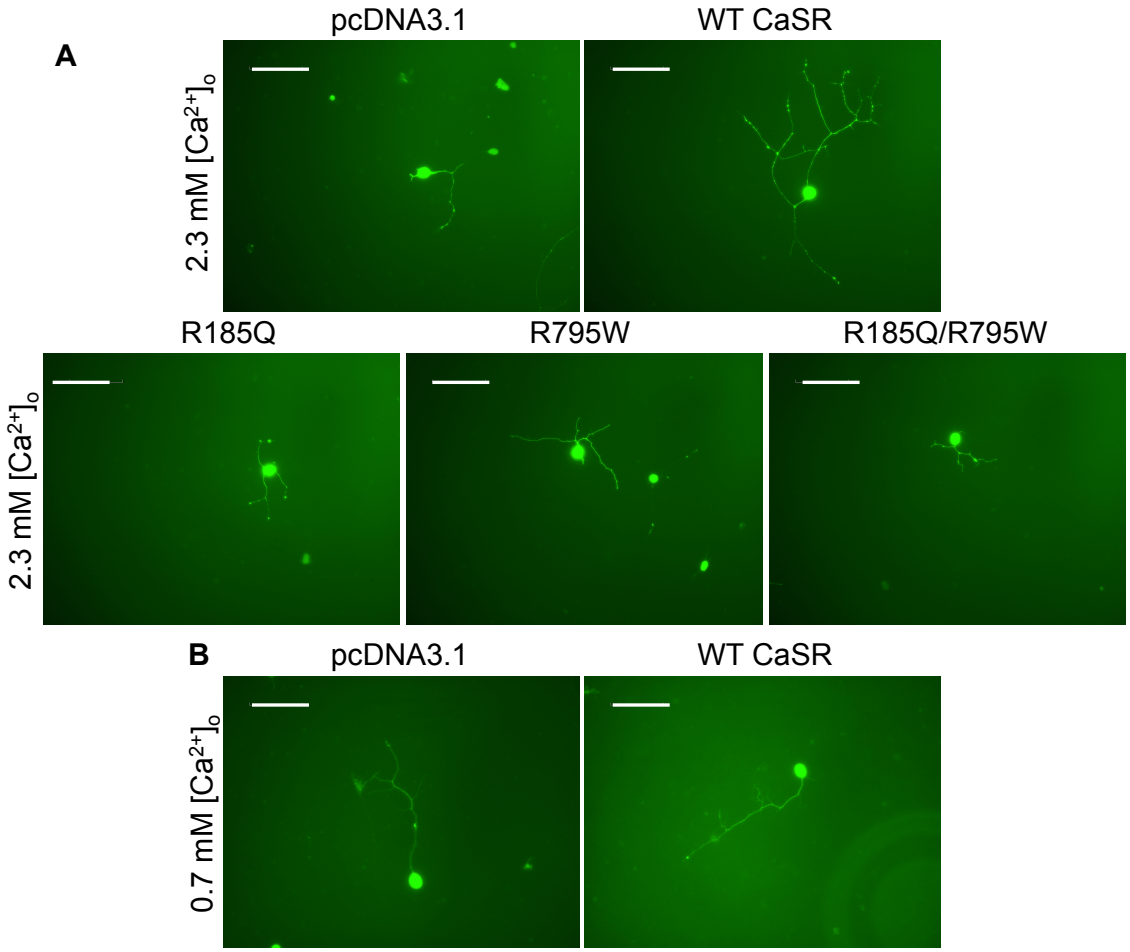

Figure 43: Representative images for Figure 42

A, Neurite outgrowth from transfected E18 SCG neurons, expressing control, WT and mutant CaSR constructs, grown in 2.3 mM $[Ca^{2+}]_o$ and in the absence of NGF.
B, Neurite outgrowth from transfected E18 SCG neurons, expressing control and WT CaSR constructs, grown in 0.7 mM $[Ca^{2+}]_o$ and in the absence of NGF. Scale bars 100 μm.

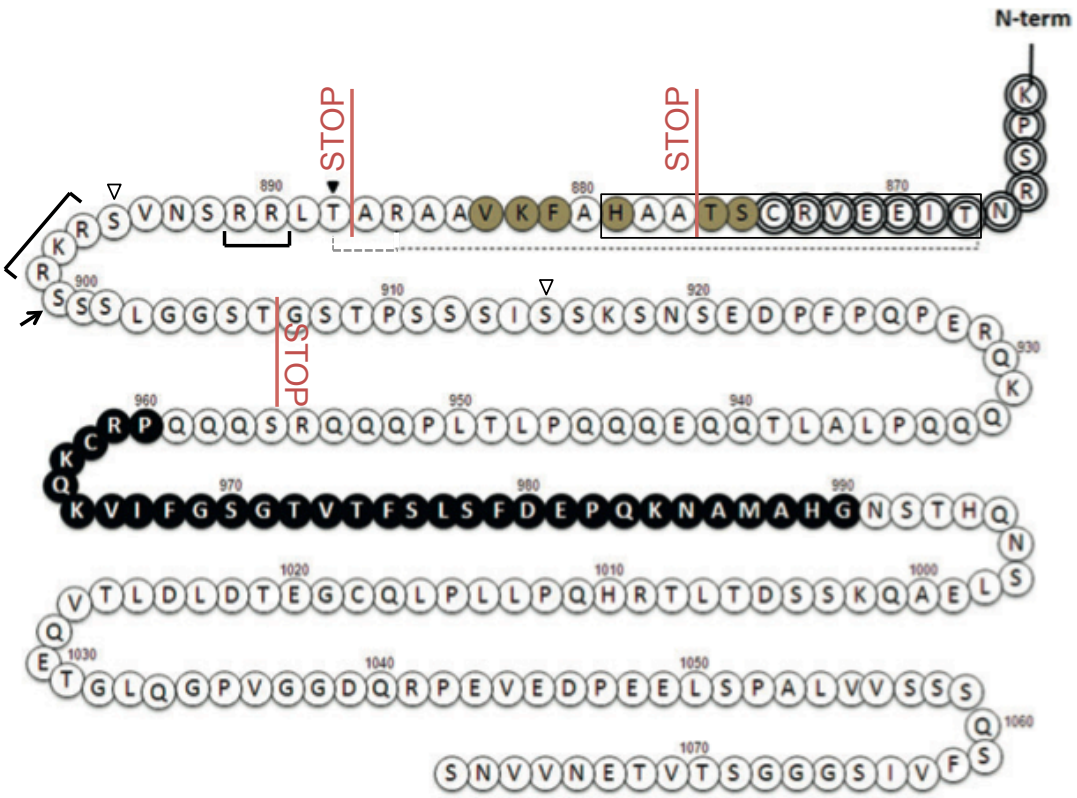

Figure 44: Truncation mutations of CaSR C-terminal domain

Three truncation mutants were employed in this study; A877X, T888X and G907X. G907X results in the loss a large proportion of the C-terminal domain, including a high affinity binding site for filamin-A (residues 960–990, labelled in black) and a minor PKC phosphorylation site (S915, white arrowhead). T888X also lacks arginine rich retention motifs (black brackets), a PKA phosphorylation site (S899, black arrow), a second minor PKC phosphorylation site (S895, white arrowhead) and acts as a phosphomimetic for the major PKC phosphorylation site at T888. A877X entirely lacks the T888 phosphorylation site, several residues important for PI-PLC activation (highlighted in grey), for cooperativity, resistance to desensitization and ER retention (residues 868–888 indicated by broken line) and disrupts a low-affinity binding site for filamin-A (residues 868-879, black box).
Figure and text adapted from Khan & Conigrave 2010.

8.2.3.3. Requirement for a region of the C-terminal domain for CaSR promoted growth

The finding that CaSR-promoted growth could be reconstituted in the absence of NGF by the overexpression of CaSR also provided a system in which to investigate the signalling pathways required for CaSR promoted growth, independently of those engaged by NGF. Since many of the signalling functions of CaSR are regulated by the C-terminal domain (Huang and Miller, 2007; Khan and Conigrave, 2010), the

first step in investigating the CaSR-dependent signalling pathways that promote axon growth and branching was to assess whether NGF-independent, CaSR-promoted axon growth occurred when C-terminal truncation mutants of the CaSR were over-expressed in E18 SCG neurons. Two truncation mutants were assessed; A877X and G907X, where X denotes the conversion of the amino acid defining codon into a stop codon (Figure 44). The truncation at residue 907 results in the loss a large proportion of the C-terminal domain, including a high affinity binding site for filamin-A (residues 960–990) and a minor PKC phosphorylation site (S915). Over-expression of the G907X mutant promotes significantly greater axon growth and branching compared to control (pcDNA3.1) transfected neurons, the magnitude of which is similar to that caused by over-expression of WT CaSR ($P < 0.001$ compared to CTR; $P > 0.05$ compared to WT for both axon length and branching in both cases; Dunn's multiple comparison post-hoc tests; Figure 45A). The over-expression of G907X does not alter the survival of E18 SCG neurons compared to control and WT CaSR transfected neurons ($P > 0.05$, one-way ANOVA; Figure 45)

In addition to the loss of a high affinity filamin-A binding site and minor PKC phosphorylation site that occurs in the G907X mutant, the A877X truncation mutant also lacks arginine rich retention motifs, a PKA phosphorylation site (S899), an additional minor PKC phosphorylation site (S895), and the major PKC phosphorylation site at T888. In contrast to the G907X mutant, over-expression of the A877X mutant does not increase the extent of axon growth compared to control transfected neurons when the culture medium contains 2.3 mM Ca^{2+} ($P > 0.05$ compared to CTR; $P < 0.001$ compared to WT for both axon length and branching; Dunn's multiple comparison post-hoc tests; Figure 45B). Moreover, over-expression of A877X significantly reduces the level of branching compared to control and WT CaSR transfected neurons ($P < 0.001$ compared to CTR; $P < 0.001$ compared to WT, Dunn's multiple comparison post-hoc tests; Figure 45B). The over-expression of A877X does not alter the survival of E18 SCG neurons compared to control and WT CaSR transfected neurons ($P > 0.05$, one-way ANOVA; Figure 45)

The ability of G907X to promote axon growth suggests that a surprisingly large portion of the C-terminal domain is dispensable for axon growth promotion.

Furthermore, taken together with the failure of the A877X mutant to promote growth, these data suggest that CaSR promoted axonal growth is dependent on a region of the C-terminal domain between residues 877 and 907.

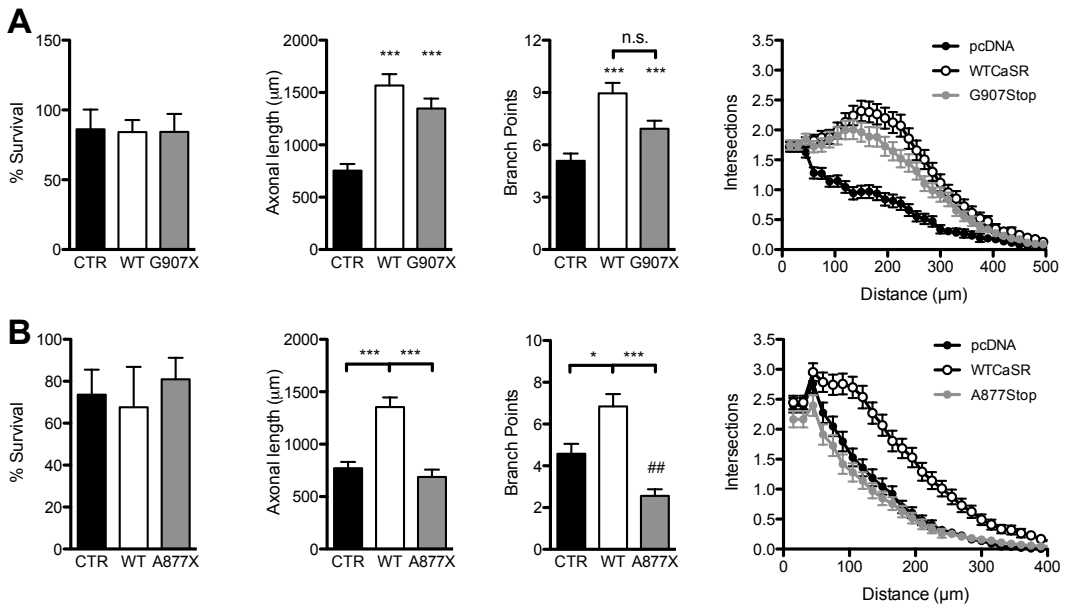

Figure 45: NGF-independent, CaSR-promoted axon growth and branching from E18 SCG neurons requires a region of the C-terminal domain between residues 877 and 907

A, CaSR promoted growth is maintained when CaSR is truncated at G907 in the C-terminal domain. No significant differences in survival are observed between control, WT CaSR and G907X transfected neurons ($P = 0.991$, ANOVA), However, significant differences are seen in the extent of axonal growth and branching between WT, CaSR and G907X transfected neurons ($P < 0.0001$, for both axon length and branching, Kruskal-Wallis test). The data in graphs represents means ± s.e.m. n = 223 – 259 cells per condition from three independent experiments.
B, CaSR-promoted growth is not maintained when CaSR is truncated at A877 in the C-terminal domain. No significant differences in survival are observed between control, WT CaSR and A877X transfected neurons ($P = 0.808$, ANOVA). Whilst wild type CaSR promotes a robust increase in axon length and branching compared to control transfected neurons ($P < 0.001$ and $P < 0.05$, respectively, Dunn's multiple comparison post-hoc tests) the over-expression of A877X is ineffective at enhancing axon elongation and reduces the level of branching compared to control transfected neurons. Data in graphs represents means ± s.e.m. n = 182 – 210 cells per condition from four independent experiments. Dunn's multiple comparison post-hoc tests: * = $P < 0.05$; *** = $P < 0.001$; ## = $P < 0.01$ compared to CTR.

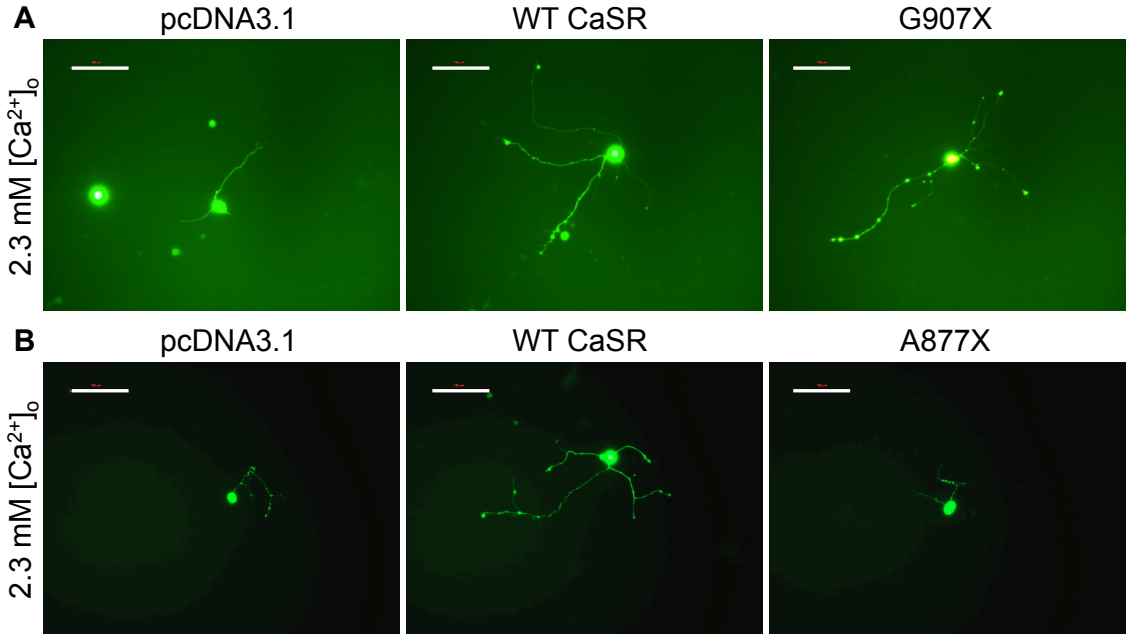

Figure 46: Representative images for Figure 45

A, Neurite outgrowth from transfected E18 SCG neurons, expressing control, WT and the G907X truncated CaSR constructs, grown in 2.3 mM $[Ca^{2+}]_o$ and in the absence of NGF.
B, Neurite outgrowth from transfected E18 SCG neurons, expressing control, WT and the A877X truncated CaSR constructs, grown in 2.3 mM $[Ca^{2+}]_o$ and in the absence of NGF. Scale bars 100 μm.

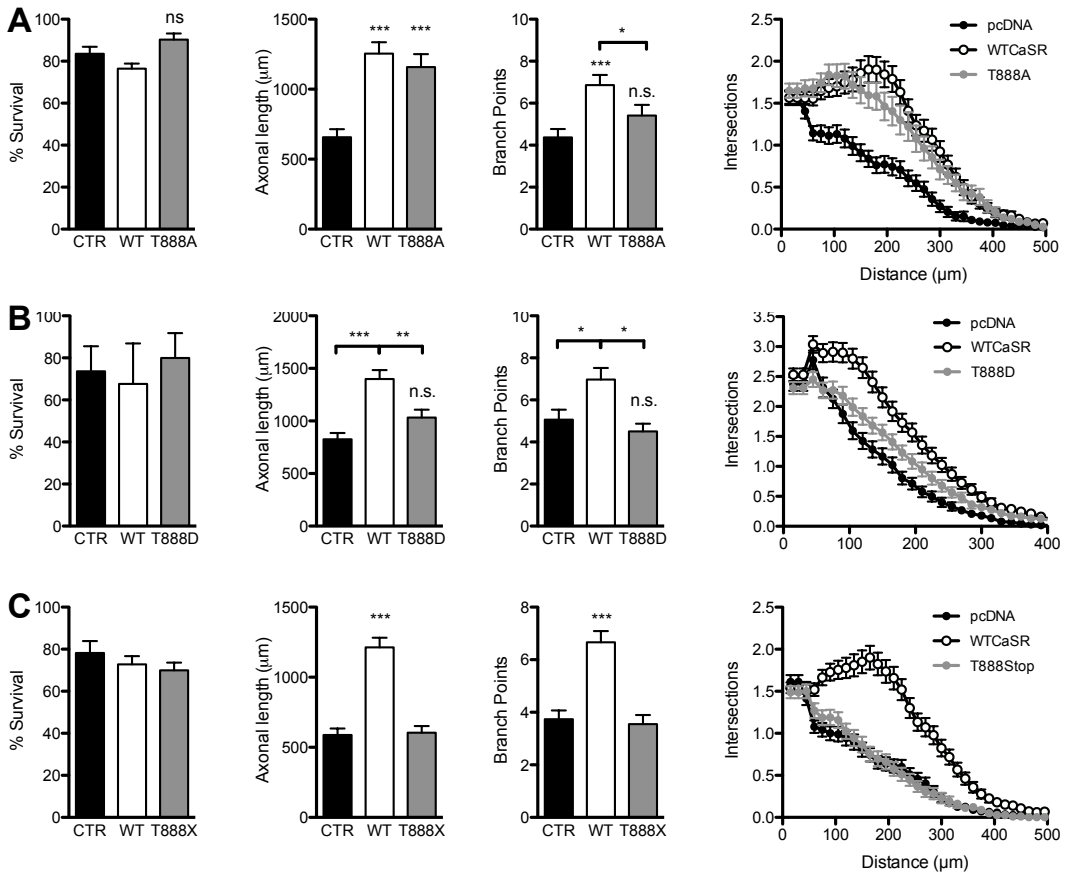

Figure 47: T888 is a regulatory site for CaSR-promoted growth, which is selectively required for branching.

***A*,** CaSR-promoted growth is maintained when the PKC phosphorylation site T888 is mutated to Alanine. No significant differences in survival are observed between control, WT CaSR and T888A transfected neurons ($P = 0.095$, ANOVA). However, significant differences are seen in the extent of axonal growth and branching between WT, CaSR and T888A transfected neurons ($P < 0.0001$, for both axon length and branching, Kruskal-Wallis test). The conversion of T888 to alanine significantly reduces the extent axon branching compared to WT CaSR transfected neurons. Data in graphs represents means ± s.e.m. n = 180 – 210 cells per condition from three independent experiments.
***B*,** CaSR-promoted growth and branching is abolished when T888 is mutated to Aspartic acid. No significant differences in survival are observed between control, WT CaSR and T888D transfected neurons ($P = 0.841$, ANOVA). However, significant differences are seen in the extent of axonal growth and branching comparing WT CaSR with both control, and T888D transfected neurons ($P < 0.0001$, for axon length, $P = 0.0083$ for branching, Kruskal-Wallis test). Data in graphs represents means ± s.e.m. n = 205 – 260 cells per condition from four independent experiments.
***C*,** Truncation of CaSR at T888 abolishes CaSR-promoted growth and branching. No significant differences in survival are observed between control, WT CaSR and T888X transfected neurons ($P = 0.470$, ANOVA) However, significant differences are seen in the extent of axonal growth and branching comparing WT CaSR with both control, and T888X transfected neurons ($P < 0.0001$, for axon length and branching, Kruskal-Wallis test)). Data in graphs represents means ± s.e.m. n = 248 – 278 cells per condition from three independent experiments. Dunn's multiple comparison post-hoc tests: * = $P < 0.05$; ** = $P < 0.01$; *** = $P < 0.001$.

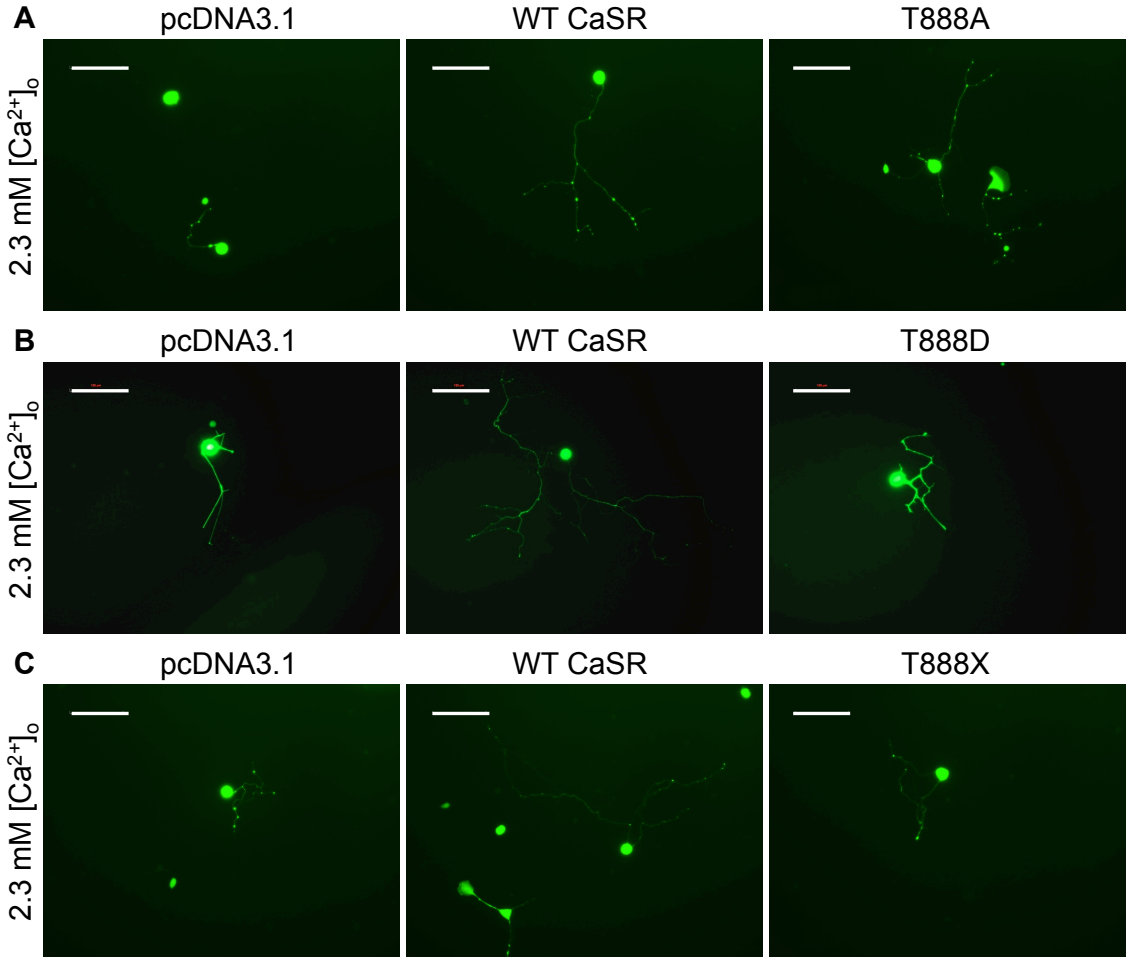

Figure 48: Representative images for Figure 47

A, Neurite outgrowth from transfected E18 SCG neurons, expressing control, WT and the T888A mutant CaSR constructs, grown in 2.3 mM $[Ca^{2+}]_o$ and in the absence of NGF.

B, Neurite outgrowth from transfected E18 SCG neurons, expressing control, WT and the T888D mutant CaSR constructs, grown in 2.3 mM $[Ca^{2+}]_o$ and in the absence of NGF.

C, Neurite outgrowth from transfected E18 SCG neurons, expressing control, WT and the T888X truncated CaSR constructs, grown in 2.3 mM $[Ca^{2+}]_o$ and in the absence of NGF. Scale bars 100 μm.

8.2.3.4. T888 is a regulatory site for CaSR promoted growth

The C-terminal region implicated as being necessary for CaSR-promoted growth houses the principle PKC phosphorylation site, T888, which is increasingly recognised as playing a key role in CaSR-mediated Ca^{2+}_i signalling, including the production of Ca^{2+}_i oscillations (Young et al., 2002; Davies et al., 2007; McCormick et al., 2010; Ward and Riccardi, 2012). Since NGF can also signal to modulate Ca^{2+}_i via TrkA/PLCγ (Reichardt, 2006), and the Ca^{2+}_i stimulated phosphatase calcineurin is required for NGF-promoted axon growth from sympathetic neurons *in vitro* and *in vivo* (Bodmer et al., 2011), the next step in investigating the CaSR-dependent signalling pathways that promote axon growth was to test whether T888 was involved. Firstly, a construct containing a mutation of T888 to alanine (T888A), which has been shown to potentiate Ca^{2+}_o stimulated Ca^{2+}_i responses, and appears to promote sustained Ca^{2+}_i elevations over Ca^{2+}_i oscillations in HEK-293 cells (Young et al., 2002; Davies et al., 2007), was transfected into E18 SCG neurons cultured in the absence of NGF in medium containing 2.3 mM Ca^{2+}. Over-expression of the T888A mutant does not affect neuronal survival ($P > 0.05$; one-way ANOVA; Figure 47A), and promotes as robust axon growth as over-expression of WT CaSR ($P < 0.001$ compared to CTR, $P > 0.05$ compared to WT, Dunn's multiple comparison post-hoc tests; Figure 47A). In contrast, T888A is not able to significantly enhance the degree of axon branching ($P > 0.05$ compared to CTR; $P < 0.05$ compared to WT, Dunn's multiple comparison post-hoc tests; Figure 47A). The differential requirement for T888 in the promotion of axon elongation and branching observed in these experiments raised the possibility that CaSR-promoted axon growth may not require T888 phosphorylation or Ca^{2+}_i oscillations, whereas CaSR-promoted branching could require one or both of these processes.

To further explore these possibilities, constructs containing mutations that have previously been shown to mimic phosphorylation at T888 (T888D and T888X), and thus reduce the sensitivity of CaSR in stimulating Ca^{2+}_i responses: (Jiang et al., 2002), were over-expressed in E18 SCG neurons cultured with high Ca^{2+}_o in the absence of NGF. While the over-expression of either mutant construct does not affect neuronal survival compared to control and WT CaSR transfected neurons ($P > 0.05$; one-way ANOVAs Figure 47B&C), both constructs are unable to promote axonal growth (T888D: $P > 0.05$ compared to CTR, $P < 0.01$ compared to WT, Figure 47B; T888X: $P > 0.05$ compared to CTR, $P < 0.001$ compared to WT Figure

47C; Dunn's multiple comparison post-hoc tests) and branching (T888D: $P > 0.05$ compared to CTR, $P < 0.05$ compared to WT Figure 47B; T888X: $P > 0.05$ compared to CTR, $P < 0.001$ compared to WT Figure 47C; Dunn's multiple comparison post-hoc tests). Although additional work could determine whether the additional loss of residues 888 – 906 contributes to the lack of growth promotion in the case of T888X, for instance by the use of a L889X CaSR mutant, the close mimicking of the effect of T888X by T888D, tends to argue against this hypothesis. Furthermore, the residual non-significant trend towards increased growth promotion in T888D (Figure 47B) may be explained by the previous observation that T888X has a stronger inhibitory effect on CaSR coupling to Ca^{2+}_i responses than T888D (Jiang et al., 2002). Therefore, when taken together these data imply that constitutive phosphorylation at T888 may exert a strong negative regulation on CaSR-promoted axon growth and branching.

One possible explanation of the above data is that sustained elevations in $[Ca^{2+}]_i$ are required for CaSR promoted growth, with oscillatory Ca^{2+}_i activity selectively contributing to branching. However, these data do not explicitly address whether endogenous levels of T888 phosphorylation play a role in CaSR promoted growth. In order to assess whether endogenous levels of T888 phosphorylation could be detected in E18 SCG cultures, neurons were cultured for 24 hours in medium containing either 0.7 mM or 2.3 mM Ca^{2+}_o, in the presence or absence of NGF, before being fixed and immunostained with an anti-β-III tubulin antibody and an antibody raised against the phosphorylated T888 site of CaSR (Figure 49). This pilot study indicates that the greatest levels of phospho-T888 immunoreactivity are observed in neurons cultured in medium containing 2.3 mM Ca^{2+}_o in the presence of NGF, with immunoreactivity being localized to protrusions around axonal growth cones, discreet regions of the axon and the boundaries of the cell soma. Whilst these findings are very preliminary, and should thus be interpreted with caution, they appear to indicate that T888 undergoes phosphorylation in discreet cellular domains in conditions where CaSR-promoted growth occurs. Since in heterologous and parathyroid cells T888 phosphorylation reflects PKC-mediated feedback inhibition of CaSR signalling following CaSR-mediated increases in $[Ca^{2+}]_i$ (Davies et al., 2007; Ward and Riccardi, 2012), this putative increase of T888 phosphorylation is consistent with CaSR coupling to Ca^{2+}_i signalling in SCG neurons.

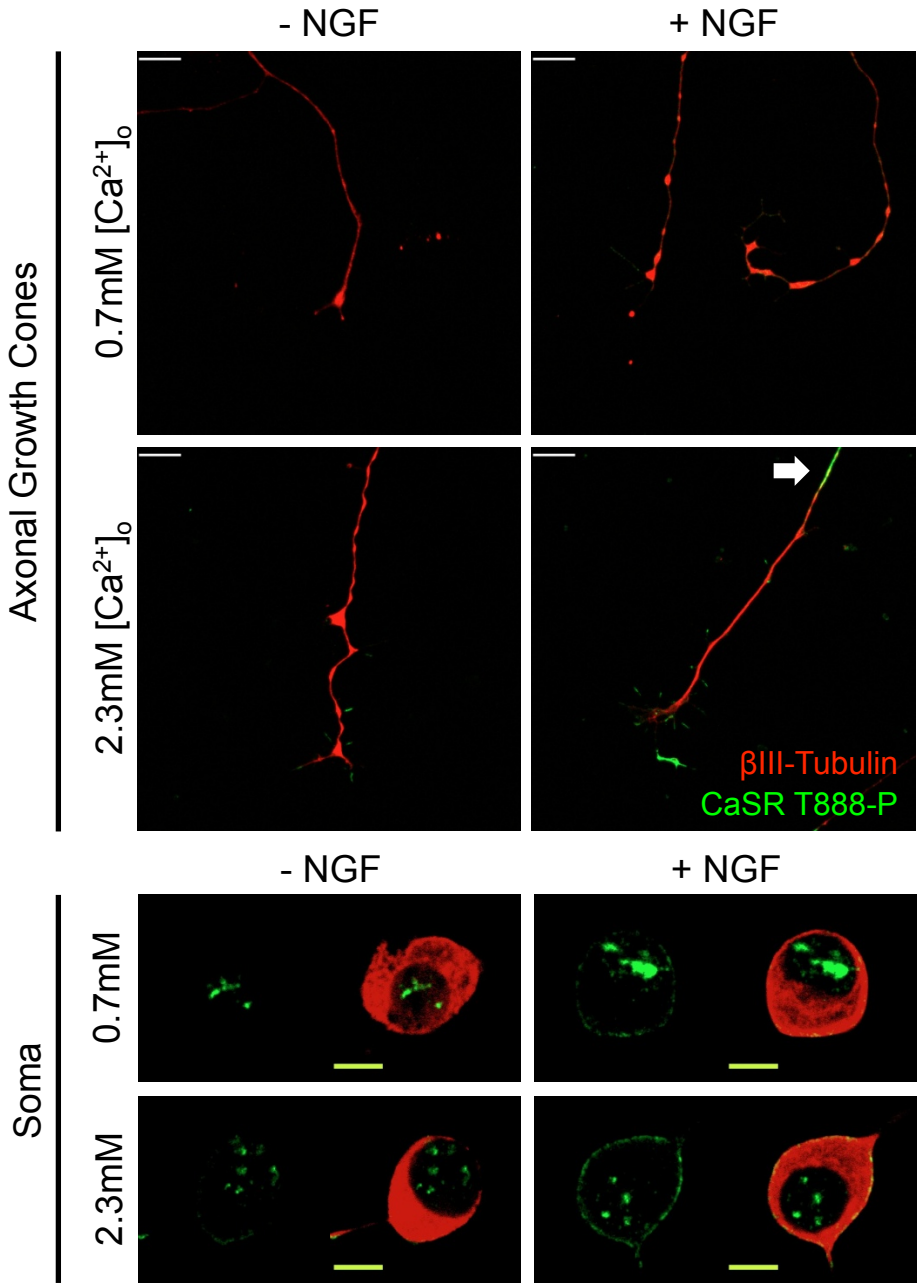

Figure 49: Preliminary indications are that T888 phosphorylation is increased in conditions where CaSR promoted growth occurs.

Apparent increases in the levels of phospho-T888 immunoreactivity are observed in 2.3 mM Ca^{2+}_o in the presence of 10 ng/ml NGF, with far less staining apparent in 0.7 mM Ca^{2+}_o in the presence of NGF and 2.3 mM Ca^{2+}_o in the absence of NGF. The least robust phospho-T888 staining is observed in 0.7 mM Ca^{2+}_o in the absence of NGF. The elevated phospho-T888 immunoreactivity in the 2.3 mM Ca^{2+}_o + NGF condition appears to localise to protrusions around axonal growth cones, discreet regions of the axon (white arrow) and the boundaries of the cell soma. 10 μm scale bars.

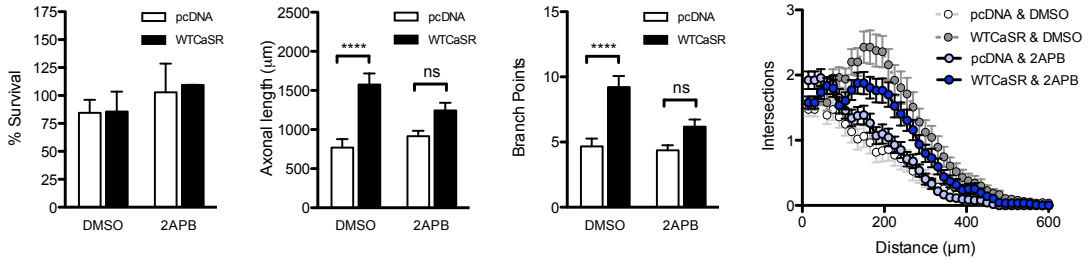

Figure 50: 50 µM 2-APB appears to inhibit CaSR-promoted growth

No significant differences are observed between the survival of control transfected and WT CaSR transfected neuron treated either with DMSO or 2-APB (CaSR genotype x 2-APB treatment interaction $P = 0.881$). However, 50 µM 2-APB inhibits CaSR-promoted axon growth (CaSR genotype x 2-APB treatment interaction $P = 0.0270$), with a non-significant main effect of pharmacology ($P = 0.380$) and a significant main effect of CaSR expression ($P < 0.0001$). 50 µM 2-APB also inhibits CaSR-promoted branching (CaSR genotype x 2-APB treatment interaction $P = 0.0275$), with significant main effects of pharmacology ($P = 0.0073$) and CaSR expression ($P < 0.0001$). Data in graphs represents means ± s.e.m. n = 114 cells per condition from two independent experiments. Bonferroni's multiple comparison post-hoc tests: **** = $P < 0.0001$.

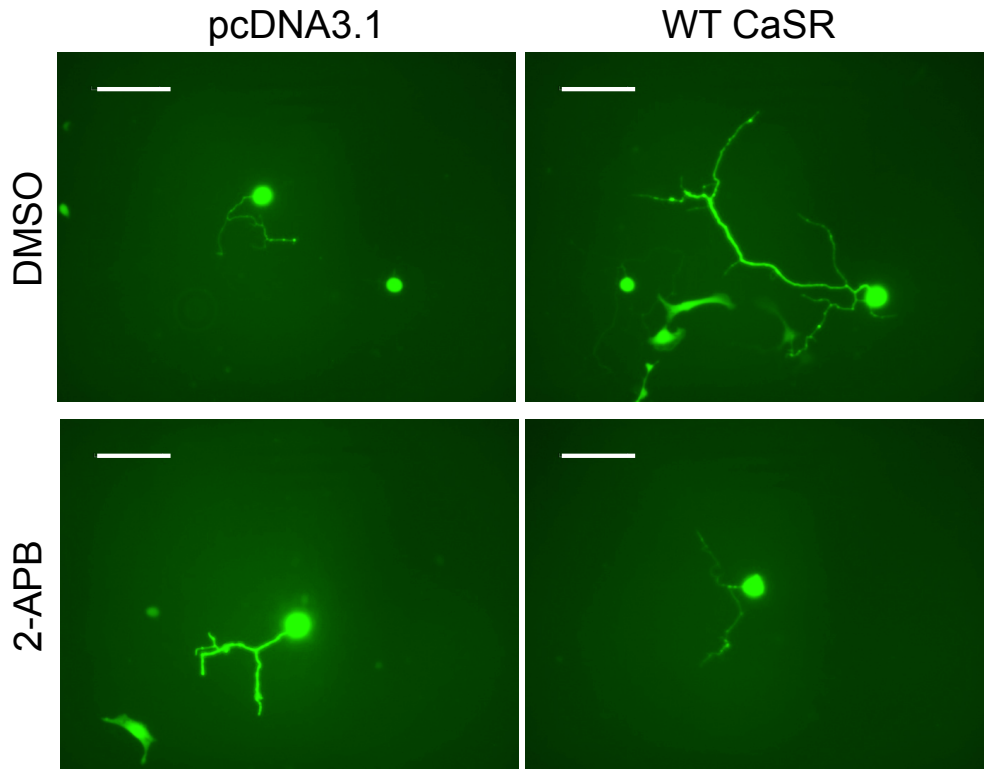

Figure 51: Representative images for Figure 50

Neurite outgrowth from transfected E18 SCG neurons, expressing control or WT CaSR constructs, grown either with or without 50 µM 2-APB in 2.3 mM $[Ca^{2+}]_o$ and in the absence of NGF. Scale bars 100 µm.

8.2.3.5. 2-APB may inhibit CaSR promoted growth

CaSR is well known to couple to IP_3 mediated Ca^{2+}_i release via PLCβ (Brown and Macleod, 2001; Hofer and Brown, 2003). Furthermore, CaSR-induced increases in $[Ca^{2+}]_i$ require Ca^{2+} release from thapsigargin sensitive intracellular stores (Breitwieser and Gama, 2001). This suggests that both sustained and oscillatory changes in Ca^{2+}_I, and hence CaSR-promoted axonal growth and branching, could rely on IP_3 receptor (IP_3R) activity to release Ca^{2+} from intracellular stores. Accordingly, experiments were performed to determine whether a pharmacological inhibitor of IP_3R, 2-APB could prevent CaSR-promoted axon outgrowth and branching from E18 SCG neurons transfected with WT CaSR and cultured in medium containing 2.3 mM Ca^{2+}. 2-APB was used at 50 μM, a concentration that has been shown to inhibit IP_3R signalling (Maruyama et al., 1997) and alter the proliferation of HEK-293 cells (Mignen et al., 2005). Preliminary data (n = 2 independent cultures) indicate that 50 μM 2-APB antagonises CaSR-promoted axon growth (CaSR x 2-APB treatment interaction P = 0.0270; two-way ANOVA), and branching (CaSR genotype x 2-APB treatment interaction P = 0.0275; two-way ANOVA), without affecting survival (CaSR x 2-APB treatment interaction P = 0.881; two-way ANOVA; Figure 50). If confirmed, these data would support the hypothesis that Ca^{2+}_i release is involved in CaSR-promoted axonal growth and branching. However, assessing whether Ca^{2+}_i activity is a mediator or a modulator of CaSR promoted growth will require further work, including Ca^{2+}_i imaging. It will be especially interesting to determine the degree to which CaSR generates sustained and oscillatory changes in Ca^{2+}_i, and how these are altered in the T888A and T888D mutants.

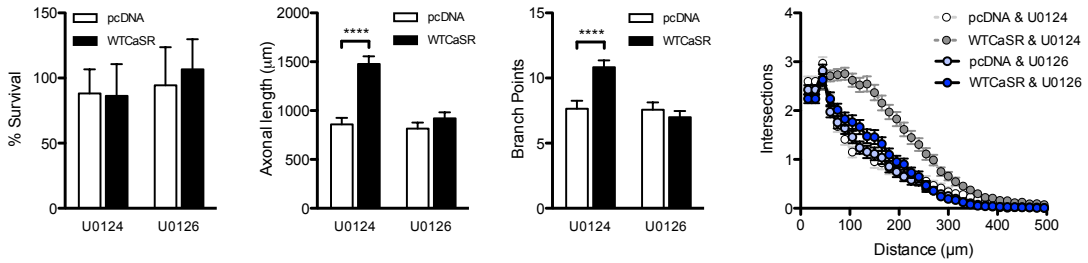

Figure 52: MEK1/2 inhibition abolishes CaSR-promoted axon growth.

No significant differences are observed in survival between control or WT CaSR transfected cultures treated with either 10 µM U0126 or 10 µM U0124 (CaSR genotype x pharmacological treatment interaction $P = 0.569$; main effect pharmacology $P = 0.292$; main effect CaSR $P = 0.672$). However, 10 µM U0126, but not 10 µM U0124 significantly inhibits CaSR-promoted axon growth ($P = 0.0002$) and branching (CaSR genotype x pharmacological treatment interactions $P = 0.0002$ and $P = 0.0007$, respectively) Data in graphs represents means ± s.e.m. n = 214 - 249 cells per condition from four independent experiments. Bonferroni's multiple comparison post-hoc tests are shown: **** = $P < 0.0001$.

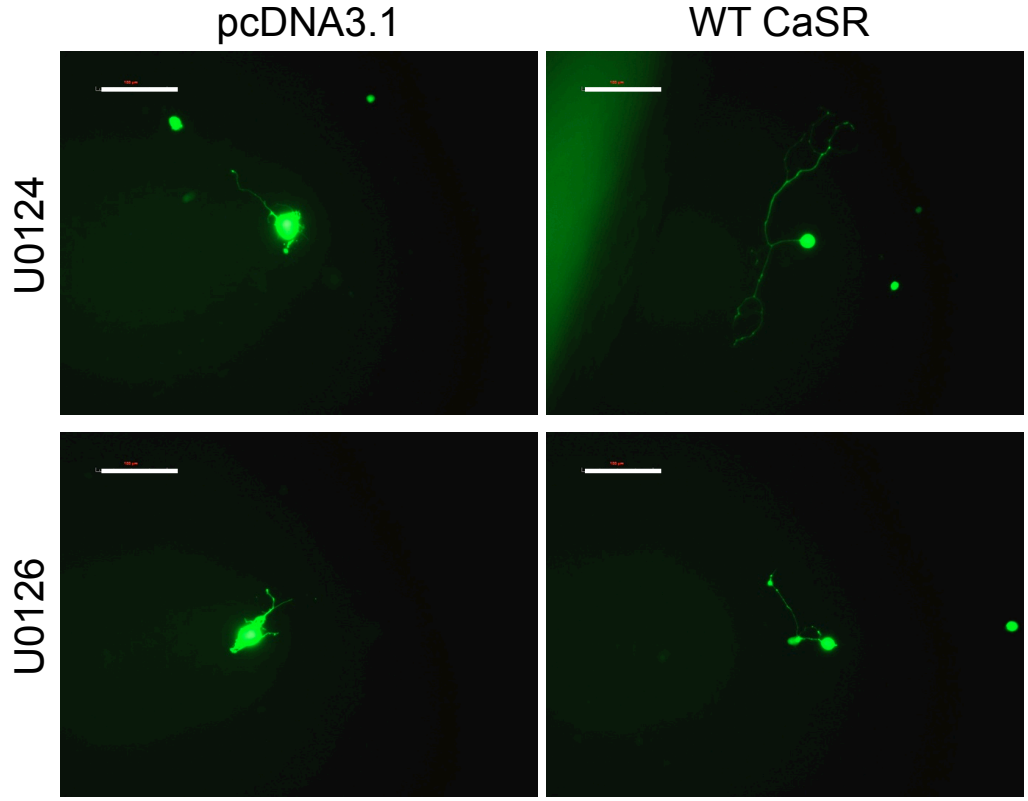

Figure 53: Representative images for Figure 52

Neurite outgrowth from transfected E18 SCG neurons, expressing control or WT CaSR constructs, treated with either 10 µM U0126 or 10 µM U0124 in 2.3 mM $[Ca^{2+}]_o$ and in the absence of NGF. Scale bars 100 µm.

8.2.3.6. ERK1/2 phosphorylation is required for CaSR-promoted growth

CaSR is known to signal via ERK1/2 (McNeil et al., 1998; Kifor et al., 2001; Corbetta et al., 2002; Hofer and Brown, 2003). Although there is some indication that PKC activity may be required for ERK1/2 coupling in parathyroid cells (Corbetta et al., 2002), and ERK1/2 activation is mediated by $G_{q/11}$/Pi-PLC/PKC in CaSR expressing HEK-293 cells (Kifor et al., 2001), whether CaSR mediated engagement of this pathway requires Ca^{2+}_i signalling in other cell types is not known. However, there are several lines of evidence suggesting these two pathways could interact in neurons. In striatal neurons, signalling to ERK1/2 by the homologous receptor mGluR5 is partially transmitted via IP_3 / Ca^{2+}_i (Mao et al., 2005), while Ca^{2+}_i and ERK1/2 cooperate in the induction of Arc transcription downstream of mGluR5 (Kumar et al., 2012b). Furthermore, Ca^{2+}_i stimulated ERK1/2 activation is thought to be a major mediator of synaptic plasticity events (Orban et al., 1999; Wiegert and Bading, 2011). Moreover, many factors that have been shown to modulate NGF-promoted growth, but not survival, do so though ERK1/2 signalling in sympathetic neurons (O'Keeffe et al., 2008; Moubarak et al., 2010; McKelvey et al., 2012), including TNFα, reverse signalling which requires modulation of $[Ca^{2+}]_i$ (Kisiswa et al., 2013). Together, these previous observations prompted an investigation into whether CaSR-promoted axon growth and branching requires ERK1/2 phosphorylation.

Initially, this investigation looked at whether the MEK1/2 inhibitor, U0126, which prevents activation of ERK1/2 by phosphorylation (Favata et al., 1998), could block CaSR-promoted axon outgrowth and branching from E18 SCG neurons over-expressing WT CaSR in the absence of NGF. The inactive analogue of U0126, U0124 was used as a control. Treatment of cultures with 10 μM U0126 totally prevents CaSR-promoted axon growth and branching, whilst 10 μM U0124 has no effect on these parameters (Figure 52). These data strongly suggest that ERK1/2 phosphorylation is required for CaSR-promoted growth.

In order to further probe the relationship between CaSR over-expression and ERK1/2 phosphorylation, immunocytochemistry using anti-ERK1/2 and anti-phospho-ERK1/2 antibodies, was used to assess the levels of total ERK1/2 and phospho-ERK1/2 in the soma of E18 SCG neurons transfected with either pcDNA3.1 (control) or WT CaSR and cultured for 24 hours without NGF.

Preliminary data show that over-expression of WT CaSR induces a significant increase in phospho-ERK1/2 compared to control transfected neurons ($P = 0.0019$, t-test with Welch's correction Figure 54A; $P < 0.0001$, ANOVA with Bonferroni's post-hoc test Figure 54B), without altering total-ERK1/2 levels ($P > 0.05$, t-test; Figure 54). Furthermore, preliminary data also indicates that this increase in phospho-ERK1/2 is not observed upon transfection with either the DDN or A877X mutant CaSR constructs ($P > 0.05$; ANOVA with Bonferroni's post-hoc tests; Figure 54B). Since these preliminary data raised the possibility that ERK1/2 phosphorylation lies downstream of CaSR activation in the signalling pathways that promotes axonal growth axon, the somal levels of total ERK1/2 and phospho-ERK1/2 were also determined in non-transfected E18 SCG neurons that had been cultured for 24 hours in medium containing either 0.7 mM or 2.3 mM Ca^{2+}, either with or without 10 ng/ml NGF. No significant differences are observed in total-ERK1/2 levels between neurons cultured in any of the four conditions Figure 56). In contrast, the level of phospo-ERK1/2 is significantly higher when neurons are cultured in medium containing 2.3 mM Ca^{2+} plus NGF compared to medium containing 0.7 mM Ca^{2+} plus NGF ($P < 0.0001$; ANOVA with Bonferroni's post-hoc test; Figure 56) No significant increase in phospho-ERK1/2 is observed between neurons cultured with 0.7 mM or 2.3 mM Ca^{2+} in the absence of NGF ($P > 0.05$; ANOVA with Bonferroni's post-hoc test; Figure 56). Taken together, these data raise the possibility that ERK1/2 phosphorylation could be a key event mediating CaSR-promoted axon growth. It will be interesting to determine by further experiments whether this CaSR promoted increase in ERK1/2 phosphorylation is dependent upon Ca^{2+}_i signalling.

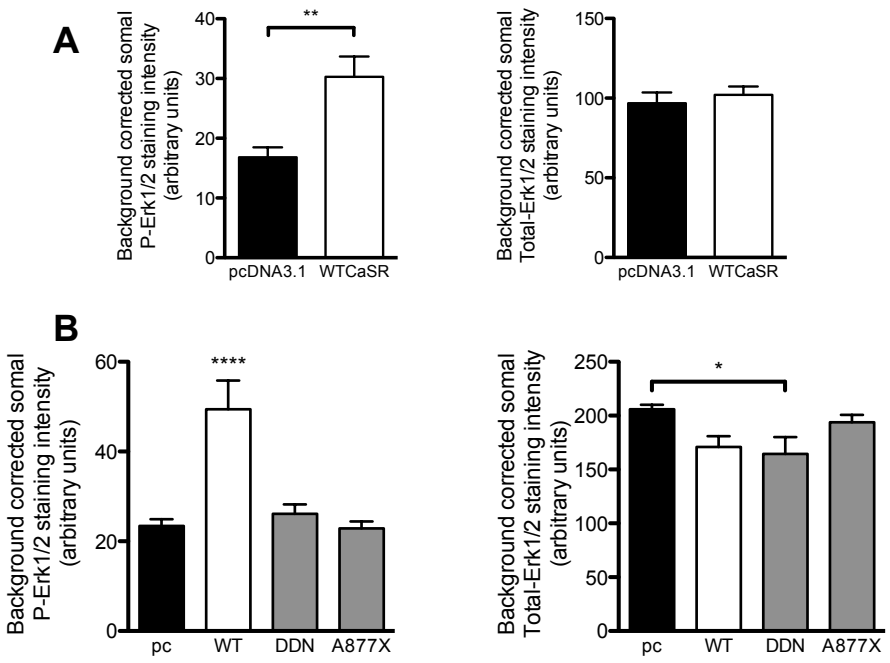

Figure 54: Preliminary data suggesting ERK1/2 phosphorylation may be increased when WT CaSR is over-expressed.

***A*,** A pilot experiment suggests over-expression of WT CaSR promotes ERK1/2 phosphorylation ($P = 0.0019$, Unpaired t-test with Welch's correction), without altering levels of total ERK1/2 ($P = 0.539$, Unpaired t-test). Data in graphs show means ± s.e.m. n = 15 cells per condition, from one experiment.
***B*,** Preliminary data also suggest over-expression of WT CaSR promotes ERK1/2 phosphorylation ($P < 0.0001$, ANOVA with Bonferroni's post-hoc test), whereas mutated (DDN = double dominant negative R185Q/R795W mutation) and truncated (A877X) CaSR constructs do not. A slight difference in total-ERK1/2 somal staining is also observed when DDN CaSR is over-expressed in this experiment ($P = 0.02$, ANOVA with Bonferroni's post-hoc test). Data in graphs represents means ± s.e.m. n = 25 cells per condition (phospho-ERK1/2) and 10 cells per condition (total-ERK1/2), from one experiment.
* = $P < 0.05$; ** = $P < 0.01$; **** = $P < 0.0001$ ANOVA with Bonferroni's multiple comparison post-hoc tests.

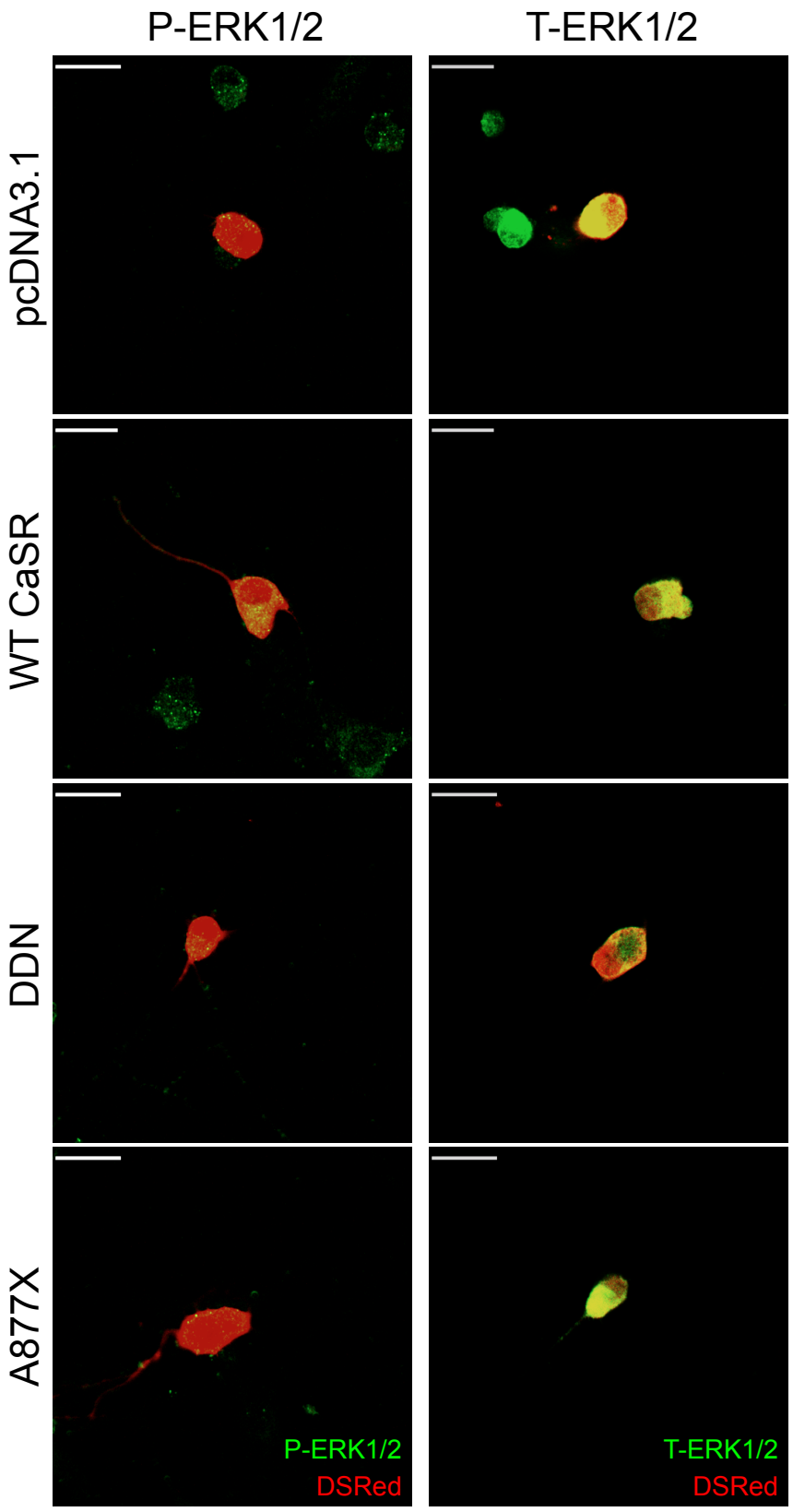

Figure 55: Representative images for Figure 54

Images taken from experiment shown in Figure 54B. Single image planes acquired through the cell soma, just above the plain of the neurites. Scale bars 20 µm.

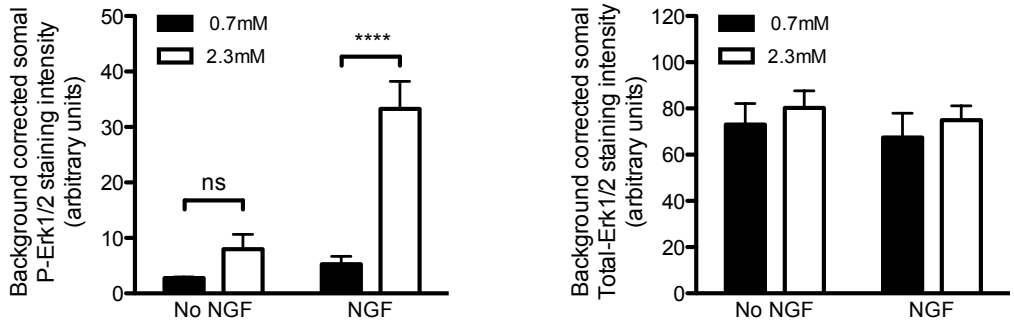

Figure 56: NGF-mediated ERK1/2 phosphorylation requires elevated $[Ca^{2+}]_o$

Quantification of phospho-ERK1/2 levels reveals a highly significant NGF x $[Ca^{2+}]_o$ interaction (P = 0.0001, two-way ANOVA), indicating that the increase in ERK1/2 phosphorylation in the presence of NGF varies significantly with $[Ca^{2+}]_o$. Accordingly, Bonferroni's post-hoc tests show a significant difference in ERK1/2 phosphorylation between 0.7 mM and 2.3 mM $[Ca^{2+}]_o$ in the presence of NGF ($P < 0.0001$), whereas no significant difference is observed in the absence of NGF. There are also significant main effects of $[Ca^{2+}]_o$ $P < 0.0001$ and NGF P = 0.0001, two-way ANOVA). No significant differences are observed in total-ERK1/2 levels (NGF x $[Ca^{2+}]_o$ interaction P = 0.990; main effect $[Ca^{2+}]_o$ P = 0.386; main effect NGF P = 0.522; two-way ANOVA). Data in graphs represents means + s.e.m. n = 37 cells per condition (phospho-ERK1/2) and 18 cells per condition (total ERK1/2) from three independent experiments. **** = $P < 0.0001$, Bonferroni's multiple comparison post-hoc tests.

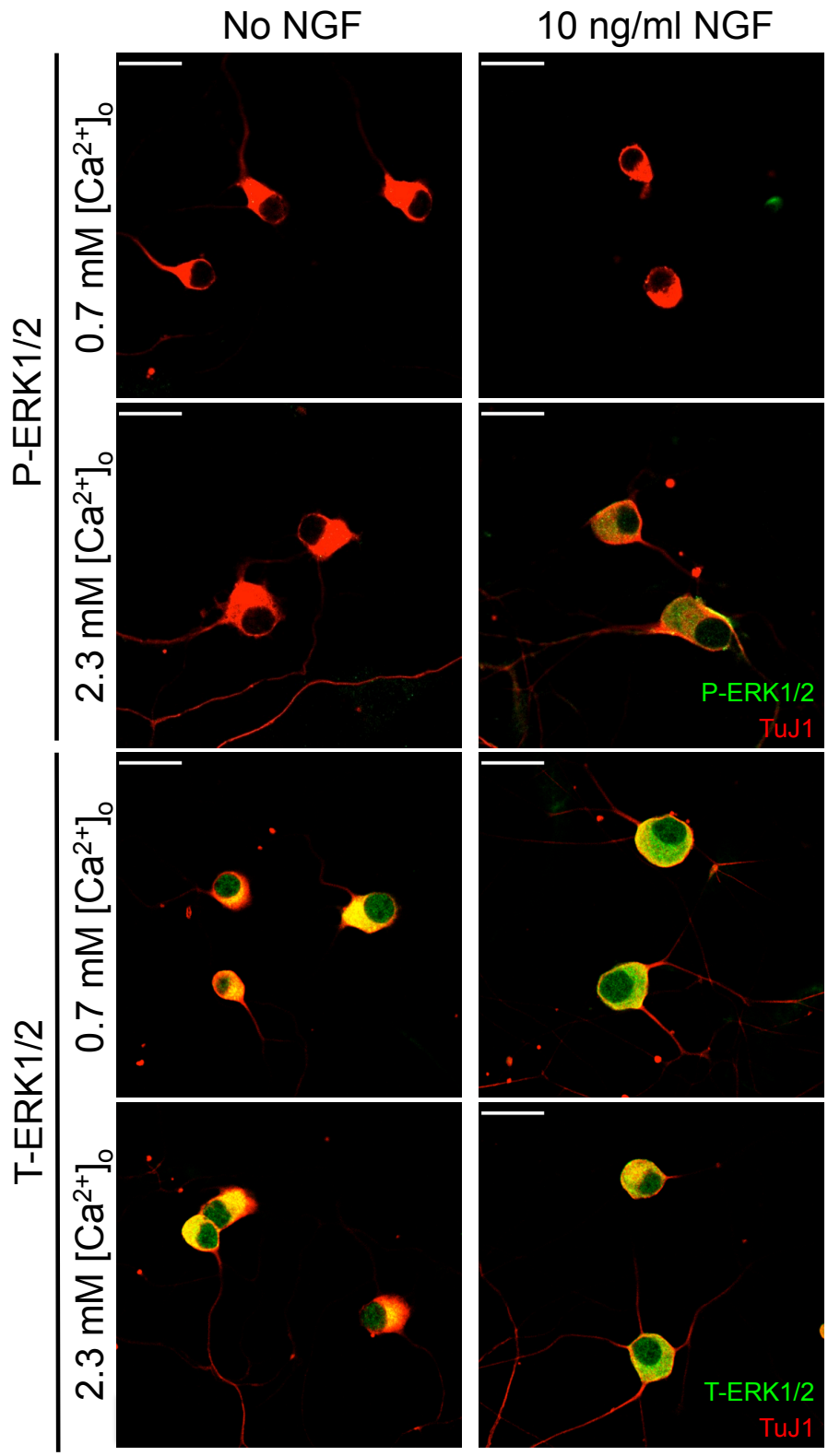

Figure 57: Representative images for Figure 56

Single image planes acquired through the cell soma, just above the plain of the neurites. Scale bars 20 μm.

8.2.4. Discussion

The data presented in this chapter have contributed to our understanding of how CaSR promotes axon outgrowth and branching from E18 SCG neurons. The data support the previously suggested conclusion that the effect of CaSR on axon growth is regulated at the level of CaSR expression (Vizard et al., 2008) and further suggest that in 2.3 mM Ca^{2+}_o, elevated CaSR expression is necessary and sufficient to promote axonal growth and branching. Previous data from NGF-supplemented cultures indicated that elevated $[Ca^{2+}]_o$ promotes axon outgrowth from SCG neurons when CaSR is highly expressed, at E18, but not from E18 *Casr* $^{-/-}$ SCG neurons or from developmental ages when *Casr* mRNA expression is low (Vizard et al., 2008). Furthermore, over-expression of WT CaSR in P1 SCG neurons that are normally not responsive to elevated $[Ca^{2+}]_o$ in the presence of NGF reconstitutes CaSR-promoted growth, but over-expression of WT CaSR in NGF-supplemented E18 SCG cultures does not further increase CaSR-promoted growth in response to elevated $[Ca^{2+}]_o$ (Vizard et al., 2008). In contrast, the data in this chapter reveals that CaSR-promoted growth in response to elevated $[Ca^{2+}]_o$ is absent in E18 SCG cultures lacking NGF, where neuronal survival is supported by caspase inhibitors. Over-expression of functional CaSR, but not the functionally impaired mutants R185Q or R795W, is sufficient to reconstitute CaSR-promoted growth in culture medium containing high levels of Ca^{2+}_o, in the absence of NGF. Additionally, CaSR appears to be up-regulated by high $[Ca^{2+}]_o$ in the presence, but not the absence of NGF. Since impaired CaSR expression is sufficient to abolish CaSR-promoted growth in the presence of NGF (Vizard et al., 2008), and CaSR over-expression is sufficient to reconstitute it in the absence of NGF, elevated CaSR expression in high $[Ca^{2+}]_o$ appears to be the key determinant of CaSR-promoted growth, with or without NGF. Therefore, CaSR expression appears to be both necessary and sufficient to promote axonal growth and branching from perinatal SCG neurons in high $[Ca^{2+}]_o$.

This effect could yet be further explored. For example, if the interpretation of the data in this chapter is correct, over-expression of CaSR in SCG neurons that express low levels of CaSR, such as those from E16, should be sufficient to reconstitute CaSR-promoted, growth not only in the presence of NGF as previously shown (Vizard et al., 2008), but also in its absence. Furthermore, the data in this chapter do not illuminate the mechanism by which high $[Ca^{2+}]_o$ and NGF cooperate to

elevate CaSR expression. For example, the possibility that increased somal CaSR immunoreactivity in culture medium containing 2.3 mM Ca^{2+} and NGF involves the redistribution of CaSR from neurites to the soma cannot be excluded, as the relationship between $[Ca^{2+}]_o$, NGF and CaSR distribution in axons has not yet been examined. Nonetheless, the presence of phospho-T888 immunoreactivity in axons and growth cones at 2.3 mM $Ca^{2+}{}_o$ in the presence of NGF argues against a complete redistribution of CaSR from axons to the soma in these culture conditions. Furthermore, it is not clear whether increased somal CaSR immunoreactivity when E18 SCG neurons are cultured in medium containing high $[Ca^{2+}]_o$ and NGF reflects increased expression of CaSR at the mRNA level, increased translation of *Casr* mRNA or decreased turnover of CaSR protein, or a mixture of all three. Thus, Western blot analysis should be performed on sympathetic cultures to confirm whether total CaSR protein levels are indeed increased in SCG neurons cultured in high $[Ca^{2+}]_o$ in the presence of NGF. Furthermore, it would be interesting to examine *Casr* mRNA and CaSR protein levels in the SCG of $NGF^{-/-}$; $Bax^{-/-}$ double knock-out embryos compared to $NGF^{+/+}$; $Bax^{-/-}$ controls, to assess whether NGF contributes to the perinatal up-regulation of CaSR expression that occurs *in vivo* (Vizard et al., 2008), while $[Ca^{2+}]_o$ is naturally high(Kovacs and Kronenberg, 1997).

Importantly, the ability to reconstitute CaSR-promoted axon growth and branching in the absence of NGF by over-expression of CaSR provided an experimental system in which the signalling mechanisms underlying CaSR-promoted growth could be explored. Over-expression of CaSR truncation mutants has shown that a large portion of the C-terminal domain is dispensable for CaSR-promoted growth, including a high affinity filamin-A binding site that has previously been shown to regulate CaSR coupling to ERK1/2 signalling (Awata et al., 2001; Hjälm et al., 2001; Zhang and Breitwieser, 2005). Furthermore, over-expression of truncated mutants of CaSR has defined a requirement for residues 877 – 906 of the C-terminal domain for CaSR-promoted growth. There are several reported interaction sites within this portion of the C-terminal domain whose disruption may contribute to the lack of effectiveness of the A877X mutant in stimulating axon growth. These interaction sites include arginine rich retention motifs between residues 890–899 (Stepanchick et al., 2010), the major PKC phosphorylation site at T888 (Bai et al., 1998b; Jiang et al., 2002; Young et al., 2002; Davies et al., 2007) and several

residues important for PI-PLC activation (Ray et al., 1997). In addition, the removal of residues between 877-906 disrupts a region that has been shown to be important for receptor cooperativity, resistance to desensitization and ER retention (residues 868 – 888) (Gama and Breitwieser, 1998), as well as a low affinity filamin-A binding site (residues 868 - 879) (Zhang and Breitwieser, 2005) (Figure 44).

Additional experiments have identified T888 as an important regulatory site for CaSR promoted growth. Mutations that have been shown to either constitutively mimic the effects of phosphorylation at this site (T888D and T888X), or prevent its phosphorylation (T888A), alter the coupling of CaSR to fluctuations in $[Ca^{2+}]_i$ (Jiang et al., 2002), and, in the case of T888A, promote sustained rises in $[Ca^{2+}]_i$ over oscillatory $Ca^{2+}{}_i$ activity (Davies et al., 2007). The abolition of CaSR-promoted axon growth by phosphomimetic mutations and the disruption of branching by both phosphomimetic and non-phosphorylatable mutations are consistent with the hypothesis that sustained elevations in $[Ca^{2+}]_i$ are required for CaSR-promoted axonal elongation, while $Ca^{2+}{}_i$ oscillatory activity also selectively contributes to branching. However, as the effects of T888 mutations on $Ca^{2+}{}_i$ dynamics in SCG neurons remain to be determined, it is possible that less well-characterized processes, similarly regulated by T888 phosphorylation, may underlie the effects of T888 mutations on axon growth and branching. For example, the binding of β-arrestins to CaSR is regulated by phosphorylation of CaSR and can modestly promote desensitization of CaSR (Pi et al., 2005). However, the binding of β-arrestin to CaSR can also regulate the generation of IP_3 (Lorenz et al., 2007). Moreover, preliminary data above indicate that inhibition of the IP_3R with 2-APB antagonizes CaSR promoted growth. Since the best characterized off-target effects of 2-APB also affect $Ca^{2+}{}_i$ homeostasis by other routes, such as TRP channel modulation (Xu et al., 2005; Togashi et al., 2008; Harteneck and Gollasch, 2011) and inhibition of Ca^{2+} ATPases (Peppiatt et al., 2003), the data presented in this chapter lend tentative support to the hypothesis that $Ca^{2+}{}_i$ dynamics are important for CaSR-promoted growth. Nonetheless, $Ca^{2+}{}_i$ imaging studies are required to provide a more unambiguous testing of this hypothesis. Furthermore, the sub-cellular localization and frequency of $Ca^{2+}{}_i$ signals need to be determined, since it is known that different $Ca^{2+}{}_i$ signals can underlie vastly different responses at neural growth cones, from attraction and repulsion to extension and growth arrest

(Henley and Poo, 2004), while nuclear Ca^{2+}_i signals can control gene transcription (Hardingham et al., 1997; Wiegert and Bading, 2011).

Other questions raised by the data related to the involvement of T888 in CaSR-promoted growth are yet to be resolved. Firstly, it is interesting to speculate why over-expression of A877X reduces the level of axon branching below that seen in control transfected neurons. It is theoretically possible that truncation at this residue promotes the sequestration and reduces the functions of other proteins normally involved in promoting axon branching. Alternatively, T876, which is effectively the C-terminal residue in the A877X mutant, has been shown to be important for receptor cooperativity and the generation of Ca^{2+}_i oscillations (Miedlich et al., 2002), raising the possibility that altered function of T876 in the A877X mutant could produce alterations in Ca^{2+}_i signalling that are unfavourable to branching. Ca^{2+}_i imaging studies of the A877X mutant may be informative in addressing this possibility. Secondly, the biological significance and reproducibility of the pilot phospho-T888 immunocytochemical study remains to be determined. Given that both phospho-T888 CaSR and total somal CaSR protein expression appear to be up-regulated in the presence of NGF when $[Ca^{2+}]_o$ is 2.3 mM, a careful analysis of both phospho-T888 and total CaSR immunoreactivity by Western blot will be required to ascertain whether a higher or lower proportion of the cellular CaSR pool is phosphorylated in the presence of NGF when $[Ca^{2+}]_o$ is 2.3 mM compared to other conditions. A reduction in T888 phosphorylation occurs at high $[Ca^{2+}]_o$ to allow a sustained elevation of $[Ca^{2+}]_i$ (McCormick et al., 2010). If sustained elevations in $[Ca^{2+}]_i$ are indeed required for CaSR-promoted axonal growth, it may be expected that the high Ca^{2+}_o/NGF-dependent increase in total CaSR expression would be greater than the increase in T888 phosphorylation, such that the proportion of CaSR phosphorylated at T888 is actually lower when axon growth is being promoted compared to culture conditions when CaSR-promoted growth does not occur. Alternatively, since the role of T888 phosphorylation in regulating CaSR-dependent signalling has not been previously explored in neurons, it is possible that the apparent selective localization of phospho-T888 CaSR to growth cones, discreet regions of axons and the outside of the soma could represent a biologically significant observation, if repeatable. Similar mechanisms appear to operate for mGluR5, the trafficking of which is regulated by cdk5-dependent phosphorylation of a binding site for the scaffolding protein, Homer

that disrupts Homer binding (Orlando et al., 2009), and PKC-dependent phosphorylation of a calmodulin binding site that inhibits the binding of calmodulin to mGluR5 and reduces cell surface expression of the receptor (Lee et al., 2008). Furthermore, there is evidence that mGluR5 activation results in distinct Ca^{2+}_i signals depending on its sub-cellular localization. Only intracellular mGluR5 stimulation couples to the ERK1/2 / Elk-1 pathway, while both cell surface and intracellular receptors stimulate JNK, CaMK and CREB pathways (Jong et al., 2009). Moreover, it has been suggested that stimulation of cell surface mGluR5 receptors preferentially generates transient Ca^{2+}_i responses, and that ERK1/2 activation results from the more sustained Ca^{2+}_i responses induced by intracellular mGluR5 receptors (Jong et al., 2009).

Importantly, the data in this chapter provides evidence that ERK1/2 activity is required for CaSR-promoted axon growth and branching. The MEK1/2 inhibitor U0126, but not the inactive analogue U0124, abolishes both axon growth and branching from cultured E18 SCG neurons, while preliminary data indicate that ERK1/2 phosphorylation may be increased in neurons over-expressing WT CaSR. Furthermore, preliminary data suggest that the increase in ERK1/2 phosphorylation does not occur when mutated receptors, that do not promote axon elongation and branching, are over-expressed in SCG neurons. In addition, ERK1/2 phosphorylation is increased by 2.3 mM Ca^{2+}_o in the presence, but not the absence, of NGF, paralleling the increase in CaSR expression observed under the same culture conditions. If the pattern of phospho-ERK1/2 changes observed thus far withstands further repetition, and are validated by Western blot analysis of non-transfection based experiments, they will represent a convincing case that CaSR-promoted axon growth acts through ERK1/2 signalling.

It will be interesting to further explore how CaSR activity initiates ERK1/2 signalling in sympathetic neurons. There are numerous recognised precedents for CaSR coupling to this pathway (McNeil et al., 1998; Kifor et al., 2001; Corbetta et al., 2002; Hofer and Brown, 2003), and the majority of studies implicate the interaction of filamin-A with the C-terminal domain of CaSR in coupling to ERK1/2 signalling (Hjälm et al., 2001; Zhang and Breitwieser, 2005; Huang et al., 2006a). Whilst the data presented in this chapter indicate that the high affinity filamin-A binding site that is lost in the G907X truncation mutant is not required for CaSR-

promoted axon growth and branching, the A877X mutation of CaSR that cannot promote axon outgrowth from cultured SCG neurons disrupts an alternative, lower affinity filamin-A binding site, which can also mediate coupling of CaSR to ERK1/2 (Zhang and Breitwieser, 2005). Accordingly, it would be interesting to determine whether CaSR-dependent phosphorylation of ERK1/2 and CaSR-promoted axon growth is impaired in filamin deficient sympathetic neurons, since siRNA mediated silencing of filamin impairs CaSR-mediated ERK1/2 signalling in HEK-293 cells (Huang et al., 2006a).

There is some evidence that PKC activity may be required for coupling CaSR activity to ERK1/2 signalling in parathyroid cells (Corbetta et al., 2002) and HEK-293 cells (Kifor et al., 2001). Moreover, Ca^{2+}_i is an established regulator of ERK1/2 activation in neurons (Orban et al., 1999; Luttrell, 2003; Wiegert and Bading, 2011). Indeed, this pathway operates downstream of the homologous receptor, mGluR5 in striatal neurons (Mao et al., 2005; Kumar et al., 2012b) and downstream of TNFα reverse signalling in sympathetic neurons (Kisiswa et al., 2013). Given that the above data suggest putative roles for both Ca^{2+}_i and ERK1/2 in transducing CaSR activity into enhanced axonal outgrowth and branching from SCG neurons, it is interesting to speculate whether there could be a functional connection between these two pathways. This question could be approached experimentally by assessing the effects of the cell permeant calcium chelator, BAPTA-AM on ERK1/2 phosphorylation in CaSR over-expressing cells.

Finally, it will be interesting to determine by Western blot, and perhaps knockout studies, whether one particular isoform of ERK is responsible for mediating CaSR-promoted axon growth. Despite sharing 90% amino acid sequence identity (Boulton et al., 1991), it is now known that ERK1 and ERK2 are not functionally equivalent (Vantaggiato et al., 2006). Transgenic mice containing a null mutation in a single ERK isoform have demonstrated the physiological significance of differences in ERK function. While loss of ERK 2 results in embryonic lethality (Adams and Sweatt, 2002), ERK1 deficiency produces a milder phenotype, affecting thymocyte maturation (Pagès et al., 1999) and synaptic plasticity (Mazzucchelli et al., 2002). One possible explanation of the differences in ERK functionality is the slower rate of nuclear-cytoplasmic shuttling of ERK1 compared to ERK2, a process that is regulated by the ERK N-terminal domain (Marchi et al.,

2008). Since the nuclear versus cytoplasmic localization of class C GPCRs (specifically mGluR5) can have consequences for their downstream signalling to ERKs (Jong et al., 2009), it would also be interesting to assess whether nuclear expression of CaSR can be unambiguously detected in sympathetic neurons, and whether activation of CaSR in different sub-cellular compartments is of functional importance.

8.2.5. Chapter specific acknowledgements

I would like to thank Dr. Tom Vizard (Oxford University) for his contributions to the design and implementation of several transfection experiments, and also for plasmid stocks.

8.3. Results Chapter 3: An Expression Screen of CaSR mRNA and functionally related transcripts in Postnatal CNS Development

8.3.1. Introduction

Since CaSR was first cloned from the bovine parathyroid gland, and a similar transcript was observed in the brain (Brown et al., 1993), the expression and function of CaSR in the CNS has been a topic of growing interest (Yano et al., 2004; Bouschet and Henley, 2005; Bandyopadhyay et al., 2010). For instance, CaSR expression has been shown in GnRH neurons of the murine basal forebrain, where it appears to regulate neuronal migration (Chattopadhyay et al., 2007). To date, all other subsequent CaSR expression studies in the CNS have been based on rat brain, and have reported expression of CaSR in a diverse selection of brain regions at some stage of development, or in the adult, including; the cortex (Rogers et al., 1997; Ferry et al., 2000), cerebellum (Ruat et al., 1995; Rogers et al., 1997; Ferry et al., 2000) and hippocampus (Ruat et al., 1995; Chattopadhyay et al., 1997a; Rogers et al., 1997; Ferry et al., 2000; Vizard et al., 2008; Mudò et al., 2009). Despite the widely reported hippocampal expression of CaSR, its role there is not well understood. The only functional study on the role of CaSR in the hippocampus has revealed that CaSR promotes dendritic outgrowth from murine pyramidal neurons in the first postnatal week (Vizard et al., 2008).

CaSR has recently been shown to regulate axonal growth in the PNS, within a narrow developmental window (Vizard et al., 2008). Importantly, the level of CaSR expression appears to be the key determinant that defines this developmental window (Vizard et al., 2008). Furthermore, up-regulation of CaSR expression appears to be necessary and sufficient for CaSR-promoted axon growth and branching in elevated $[Ca^{2+}]_o$ (see Results chapter 2). However, existing studies of CaSR expression in rat CNS, while interesting, either lack quantification of expression levels, or provide insufficient temporal resolution for optimal hypothesis driven research on the roles of CaSR in the developing CNS. This study aims to determine the developmental expression profile of *Casr* mRNA and protein in murine hippocampus, cortex and cerebellum, with a high temporal resolution, over the first three postnatal weeks. Furthermore, this study has also

characterised the temporal mRNA expression profiles of genes with known developmental importance, or functions related to CaSR, in order to derive a testable hypothesis to guide future explorations into CaSR function in the CNS, particularly in the hippocampus.

8.3.2. Methods

8.3.2.1. RT-QPCR

8.3.2.1.1. Tissue Collection

CD-1 mouse pups were killed either by decapitation or, from P25 onwards, a rising concentration of CO_2. Following decapitation, sub-regions of the brain were dissected rapidly in cold HBSS (Invitrogen) and minced in RNA Save (Geneflow), ensuring the environment and instruments used were sterile and RNase free. The regions dissected were: One hippocampus per animal; half of a cerebellum that had been divided by a sagittal cut along the midline; a strip of cortical rind from the same rostrocaudal level as the septal hippocampus, extending from retrosplenial cortex dorsomedially to the entorhinal cortex ventrolaterally. Samples were incubated at 4°C for 18 - 72 hours, after which RNA Save was removed and the samples were transferred to -80°C until RNA extraction.

8.3.2.1.2. RNA Extraction

RNA was extracted using the RNeasy Lipid Tissue Mini Kit (Qiagen), according to the manufacturer's instructions. Briefly, samples were homogenized in Qiazol lysis reagent (Qiagen) by passing through a P1000 several times, followed by multiple passages through a 26-gauge needle. Following phenol-chloroform based removal of DNA, lipids, carbohydrates and proteins, the aqueous fraction was mixed with an equal volume of 70% ethanol before being loaded onto spin filter columns. A 40-minute on column DNA digestion step, using RNase free DNase (Qiagen), was included in the RNA extraction protocol. Purified total RNA was eluted from spin columns in 70 µl RNase free H_2O, and stored at -80°C until use.

8.3.2.1.3. QPCR Parameters

RNA was reverse transcribed for one hour, at 45°C, using Affinity Script reverse transcriptase (Agilent) in 20-40 µl reactions containing 5 mM dNTPs (Roche) and 5 µM random hexamer primers (Fermentas). Transcript levels were quantified by the amplification of 2 µl cDNA in a 20 µl reaction using the Brilliant III Ultra-Fast QPCR Master Mix (Agilent). Forward and reverse primers were at a concentration

of 100 nM each and the dual-labelled probe concentration was 250 nM. PCR was performed on an Mx3000P (Stratagene) using cycling parameters consisting of an initial 3 minute, 95°C Taq polymerase activation step, followed by 45 cycles of 10 – 12 seconds at 95°C and 30 – 40 seconds at 60°C. A standard curve was generated for each primer-probe set for each QPCR run by amplifying a 3-fold serial dilution series of reverse transcribed adult mouse total Brain RNA (Clontech). Values for the levels of each cDNA were derived by reference to the standard curve generated for that cDNA. The levels of each target cDNA were expressed relative to the geometric mean of the reference cDNAs, gapdh and SDHA. Primer and probe sequences are detailed in Table 5.

Target	Type	Sequence
Casr (CaSR)	Forward	AAA GGA CCT TTA CCC GTG
	Reverse	TGG AGC TAT TGA GTA ACC T
	Probe	FAM-CGC CTT CCT CGT GAC TTC TC-BHQ1
Gabbr1 ($GABA_{B1}$)	Forward	GAA TCA TCG TGG GAC TTT
	Reverse	AGA AAC CAG ACA TAC TTC TT
	Probe	FAM-AAG AGC CGT TCC TTA TAG ACC T-BHQ1
Gabbr2 ($GABA_{B2}$)	Forward	AAT CAT CCT CAA CGC CAT
	Reverse	TTC ACC TCT CTG CTG TCT
	Probe	FAM-AAC CAA CTT CTT CGG AGT CAC GG-BHQ1
Gapdh (GAPDH)	Forward	GAG AAA CCT GCC AAG TAT G
	Reverse	GGA GTT GCT GTT GAA GTC
	Probe	FAM-AGA CAA CCT GGT CCT CAG TGT-BHQ1
Grm1 (mGluR1)	Forward	AGT TCT CAC TCA TTG GAA
	Reverse	TCA GAA AGT AGT CAT CAA AC
	Probe	FAM-ACC TGA CCT CTG GAG ACT G-BHQ1
Grm5 (mGluR5)	Forward	GGT AGA CAT AGT GAA GAG AT
	Reverse	TAT CTT TGA AAG CCT CCA T
	Probe	FAM-TTC TCC ATA GTT GCC TTC TGT GT-BHQ1

Target	Type	Sequence
Mtap2 (MAP2)	Forward	CTT GTG AAT ACT TCT CCT T
	Reverse	AAA TTA TTT CTC TAT GGT TTG T
	Probe	FAM-AGA ATG AAT ATG ACA CCT GCT C-BHQ1
Sdha (SDHA)	Forward	GGA ACA CTC CAA AAA CAG
	Reverse	CCA CAG CAT CAA ATT CAT
	Probe	FAM-CCT GCG GCT TTC ACT TCT CT-BHQ1
Syn2 (Synapsin II)	Forward	ATC ACC GAG AGA TGC TTA
	Reverse	CTG GAA GTC GTA GTG ATT
	Probe	FAM-CCA CTT TGA CCT TGC CCA-BHQ1
Wnt2 (Wnt2)	Forward	CTT TGT AGA TGC CAA GGA
	Reverse	CAG CAT GTC CTC AGA GTA
	Probe	FAM-AGG AGC CAC TCA CAC CAT-BHQ1
Wnt5a (Wnt5a)	Forward	GTC TTC CAA GTT CTT CCT
	Reverse	TGA TAT ATA CTT CTG ACA TCT GA
	Probe	FAM-TAT TCA TAC CTA GAG ACC ACC AAG A-BHQ1
Wnt7a (Wnt7a)	Forward	CGA GTG TCA GTT TCA GTT CC
	Reverse	CTT GCT TCT CCT TGT CGC
	Probe	FAM-CAC AGT CGC TCA GGT TGC C-BHQ1

Table 5 - Primer & Probe details

MGI gene symbols are provided in bold italics, above protein symbols in brackets.

8.3.2.2. Histology

8.3.2.2.1. Tissue Collection, Fixation and Sectioning

CD-1 mouse pups were killed under terminal anesthesia (Euthetal) by transcardial perfusion with PBS and 1.5% PFA. Brains were removed and post-fixed in either 1.5% or 4% PFA for 3 hours. Brains were cryoprotected in 30% Sucrose (w/v in PBS), embedded in OCT (Sakura) and frozen in isopentane cooled by dry ice.

14 μm tissue sections were cut on a Leica CM1850UV cryostat and collected onto Xtra-adhesive slides (Leica). Slide mounted sections were stored at -80°C until staining. When comparing protein expression between different ages through a developmental age series, all sectioning and staining were performed in parallel.

8.3.2.2.2. Immunohistochemistry

Sections were defrosted, for 30 minutes at room temperature, and washed three times with 0.1% Triton X-100 in PBS (0.1% PBS-T) for 5 minutes per wash. After washing, sections were blocked for 90 minutes in 0.1% PBS-T containing 5% goat serum and 1% BSA (blocking solution). Primary antibodies were diluted in blocking solution (see Table 6 for dilution factors of each antibody used), applied to the sections and incubated, at 4°C, for 48 – 72 hours. In cases where NeuN staining was performed, sections were blocked, after the initial 0.1% PBS-T washes, by using a Mouse-on-mouse kit (Vector Laboratories) according to the manufacturer's instructions (except that incubation times were lengthened to 90 minutes for primary and 30 minutes for secondary antibodies). After completion of NeuN staining, the standard protocol for CaSR staining was followed.

Following incubation with primary antibodies, sections were washed three times with 0.1% PBS-T for 5 minutes per wash. Secondary antibodies were diluted in blocking solution and sections were incubated with secondary antibodies, for 45 minutes at room temperature, in the dark. For CaSR staining biotinylated secondary antibodies were used. After three 5 minute washes in 0.1% PBS-T, slides were incubated, for one hour at room temperature, in biotinylated goat anti-rabbit secondary antibody. After a further three 5 minute washes with 0.1% PBS-T, sections were incubated for 30 minutes in Dylight-488 conjugated streptavidin (Vector Laboratories) that had been diluted 1/500 in 0.1% PBS-T.

Following secondary antibody incubation, sections were washed three times with 0.1% PBS-T, for 5 minutes per wash, before being counterstained with Propidium Iodide (Sigma) or TOTO-III (Invitrogen) (1/10,000 in 0.1% PBS-T) for 10 minutes at room temperature. After three 5 minute washes with 0.1% PBS-T, slides were coverslipped in Vectashield (Vector Laboratories), left to dry and stored in the dark, at 4°C, until imaging.

Target	Host	Dilution	Manufacturer
CaSR	Rabbit	1/200	MBL
NeuN	Mouse	1/500	Millipore
Biotin-anti Rabbit	Goat	1/500	Vector Laboratories
Dylight 549-anti Mouse	Goat	1/500	Stratech

Table 6 - Antibodies used for immunohistochemistry

8.3.2.2.3. Microscopy

Images were acquired using a Zeiss LSM510 confocal microscope through a 20x 0.5 NA Plan-Neofluar objective (Zeiss). Image montaging and contrast adjustments were performed in Photoshop.

8.3.3. Results

8.3.3.1. CaSR expression is developmentally regulated in multiple brain regions

Developmental regulation of *Casr* transcript expression has previously been investigated in two studies of the rat brain (Chattopadhyay et al., 1997b; Ferry et al., 2000). However neither of these studies used a truly quantitative method to determine transcript levels. In order to clarify the possible roles of CaSR in our model organism, a quantitative screen of *Casr* mRNA expression was carried out in mouse by RT-QPCR.

8.3.3.1.1. Two peaks of CaSR expression in the developing hippocampus

The developmental profile of *Casr* mRNA expression in the postnatal hippocampus shows two clear peaks of elevated expression, the first at P5 and the second at P14 (Figure 58A). The first peak in CaSR mRNA expression follows a period of marked induction from low levels of expression at E18, and CaSR mRNA levels drop after P5 to reach lower stable levels between P7 and P10. Interestingly, this pattern of induction, with a peak at P5 followed by lower stabilization, resembles the developmental expression profile of *Mtap2* transcripts that encode MAP2, a protein expressed at high levels in dendrites. In addition, this first peak in CaSR transcript expression corresponds to the developmental period during which CaSR has been previously shown to promote dendrite outgrowth from cultured

pyramidal cells (Vizard et al., 2008). Thus, it is possible that this first peak in *Casr* expression serves to promote growth and branching of dendrites.

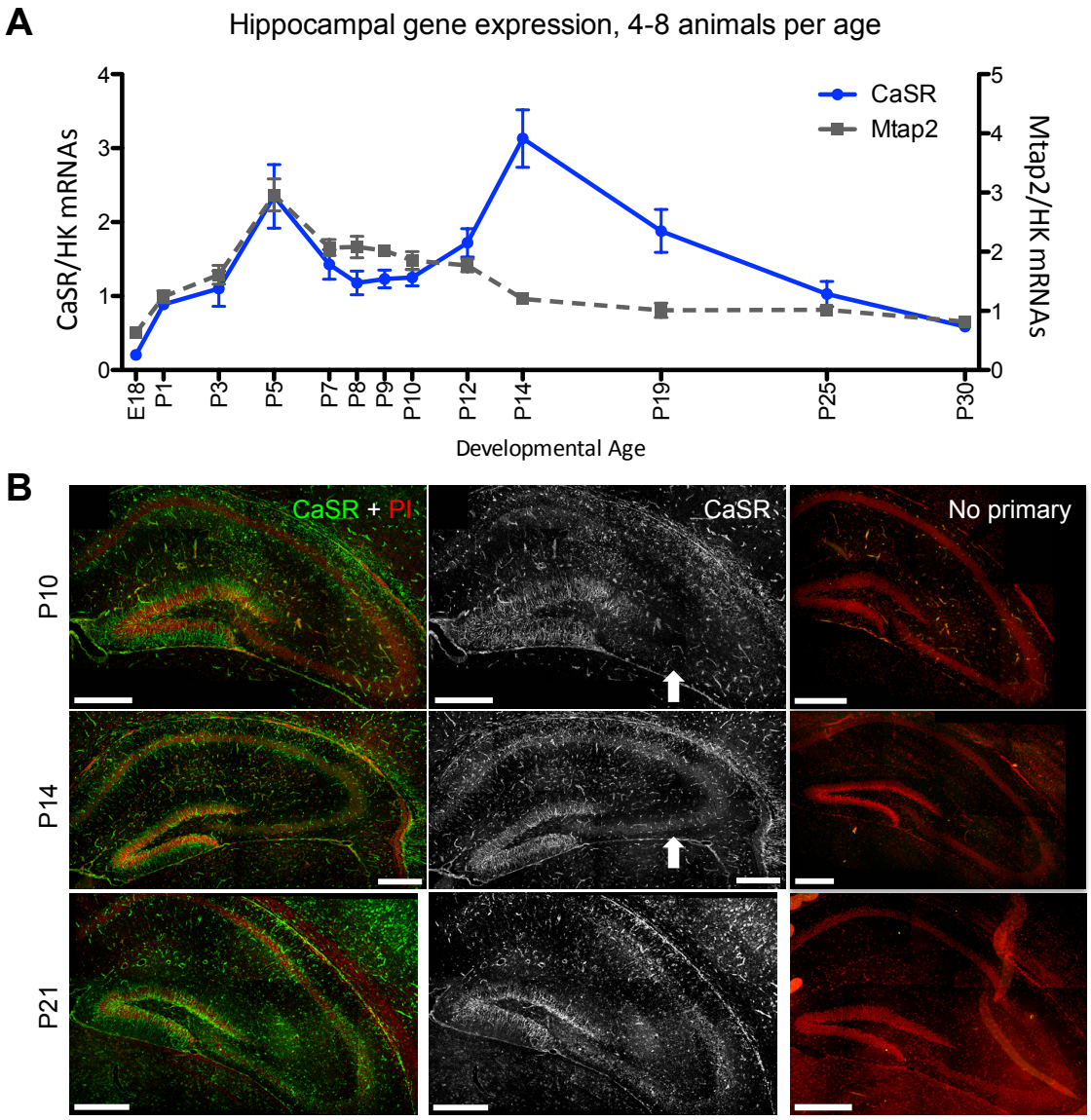

Figure 58: Two peaks of CaSR expression in the developing hippocampus

A, CaSR mRNA expression relative to GAPDH and SDHA mRNAs (data represents means ± s.e.m., n = 4 - 8 animals per age) in the developing hippocampus. Mtap2 mRNA expression relative to GAPDH and SDHA mRNAs in the same samples is shown for comparison (dashed grey line).
B, Immunohistochemical staining of the developing hippocampus, using a rabbit polyclonal antibody raised against the extracellular N-terminus of CaSR suggests an increase in CaSR expression in the pyramidal layer between P10 and P14 (white arrows). The pyramidal cell layer is distinguished by nuclear propidium iodide (PI) staining (red). In all cases CaSR immunostaining was undetectable in no primary controls. Scale bars 200 μm.

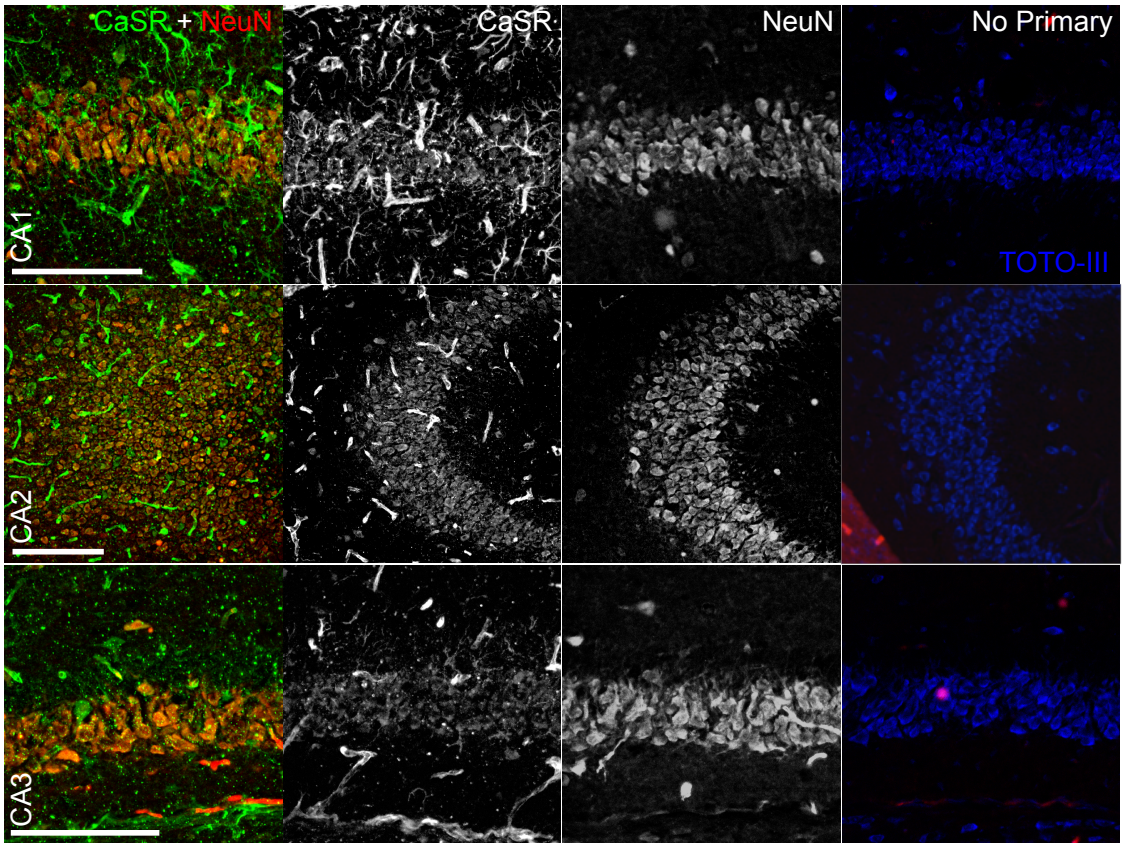

Figure 59: At P14 CaSR is expressed in the principal CA1-3 layers of the hippocampus

High power images of each CA subfield at P14 show that CaSR immunostaining colocalizes with NeuN staining, indicating that the induction of expression between P10 and P14 is, at least in part due to neuronal CaSR expression.
In all cases, no staining was observed in no primary antibody controls processed in parallel (right panels). Scale bars 100 μm.

The second peak in hippocampal *Casr* mRNA expression at P14 follows a marked increase in transcript levels from P10 (Figure 58A). *Casr* mRNA expression levels decline steadily from P14, reaching 4-fold lower levels by P30. To confirm the expression pattern of CaSR by a complimentary technique, an immunohistochemical analysis of the hippocampus was performed at P10, P14 and P21. For this purpose, a previously published antibody (Vizard et al., 2008) was used, raised against the N-terminal domain of CaSR, and further validated during this project (Results Chapter 2, Figure 41). Immunohistochemical analysis revealed a clear increase in CaSR immunoreactivity within the pyramidal cell layer between the ages of P10 and P14 (Figure 59B) that co localized with NeuN staining (Figure 59). CaSR staining of the pyramidal cell layer decreased in intensity from P14 to P21, although staining was still evident at this latter age. Taken together, these data suggest that, in addition to its role in promoting hippocampal neuron

dendrite growth during the first postnatal week (Vizard et al., 2008), CaSR may have a functional role in the developing hippocampus towards the end of the second postnatal week.

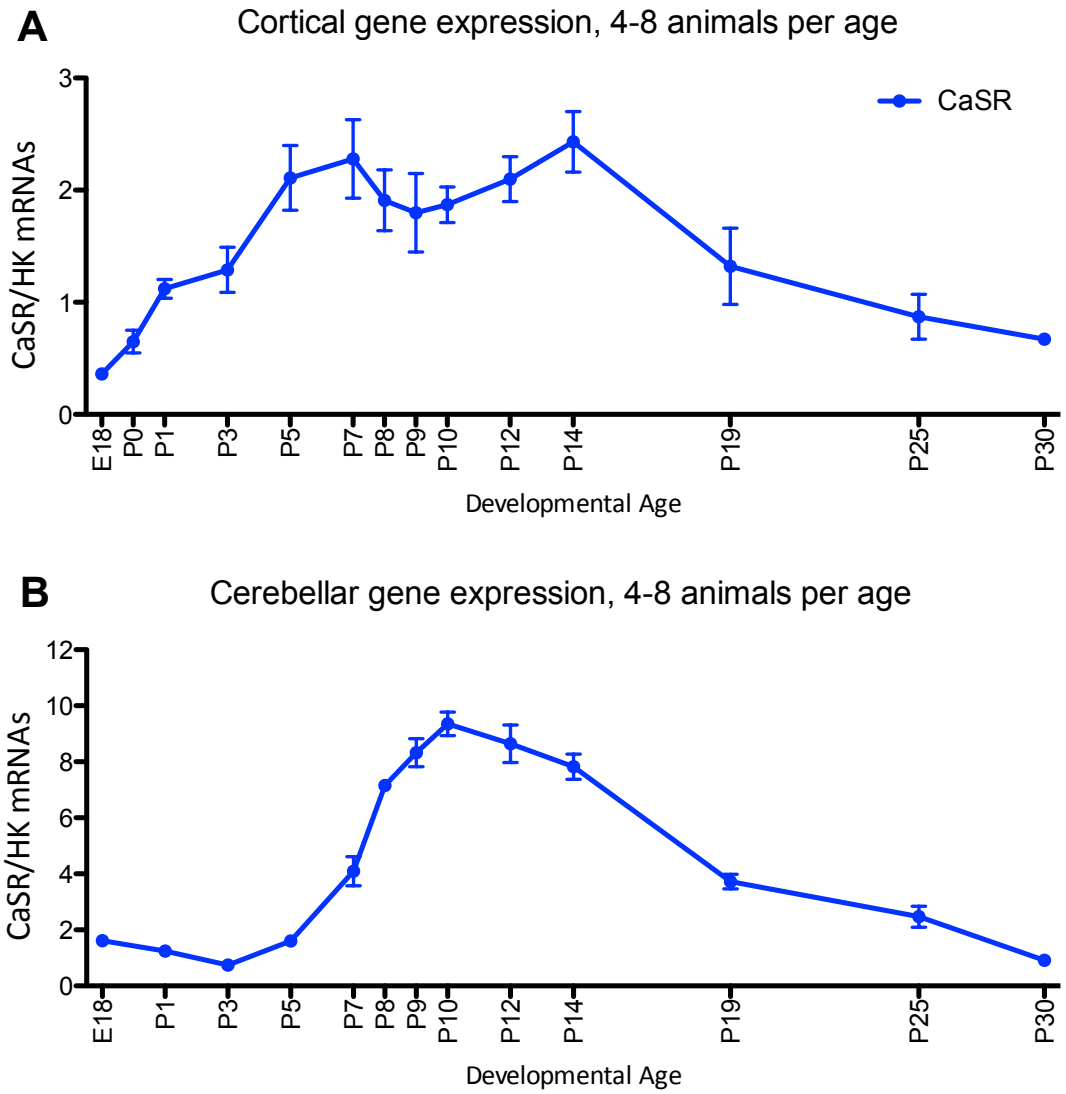

Figure 60: Broad peaks of elevated CaSR mRNA expression in postnatal cortex and cerebellum

A, Cortical CaSR mRNA expression relative to GAPDH and SDHA mRNAs (data represents means ± s.e.m., n = 4 - 8 animals per age).
B, Cerebellar CaSR mRNA expression relative to GAPDH and SDHA mRNAs (data represents means ± s.e.m., n = 4 - 8 animals per age).

8.3.3.1.2. Broad peaks of elevated *Casr* mRNA expression in postnatal cortex and cerebellum

Several studies have revealed roles for CaSR in modulating synaptic function between cortical neurons (Phillips et al., 2008; Chen et al., 2010; Vyleta and Smith, 2011). Studies of CaSR expression have reported developmental regulation in the orbital cortex (Ferry et al., 2000), expression in scattered cells of adult cortex (Rogers et al., 1997; Mudò et al., 2009), and localization of CaSR to nerve terminals (Ruat et al., 1995). In order to examine the temporal profile of *Casr* mRNA expression in the developing cortex, RT-QPCR was performed on RNA extracted from cortical samples at a range of ages between E18 and P30. A marked induction of *Casr* transcript expression is observed between E18 and P5, similar to that observed for *Casr* mRNA in the hippocampus over the same period (Figure 60A). Cortical *Casr* mRNA expression also declines gradually between P14 and P30. However, the cortex lacks the two clearly resolved peaks in *Casr* transcript expression seen in the hippocampus, and CaSR mRNA expression in the cortex is perhaps best described as exhibiting a broadly elevated peak between P5 and P14.

Developmental (Ferry et al., 2000) and adult expression data (Ruat et al., 1995; Rogers et al., 1997; Mudò et al., 2009) have also been reported for CaSR in the cerebellum. To clarify the quantitative progression of the developmental changes in CaSR mRNA expression, RT-QPCR was performed on RNA extracted from cerebellar samples. Following a slight decline from E18 to P3, a near sigmoidal, 10-fold increase in CaSR transcript expression levels is observed between P3 and P10 (Figure 60B). Thereafter, *Casr* mRNA expression declines gradually, with levels at P30 similar to those of P3.

8.3.3.2. Dynamic regulation of transcripts with known developmental importance

For comparative purposes, the expression of selected transcripts with known developmental importance were also quantified in the cDNA samples that were used to determine the expression profile of *Casr* mRNA. Each transcript was chosen on the basis of having either previously reported associations with CaSR or an established role in synapse formation and function.

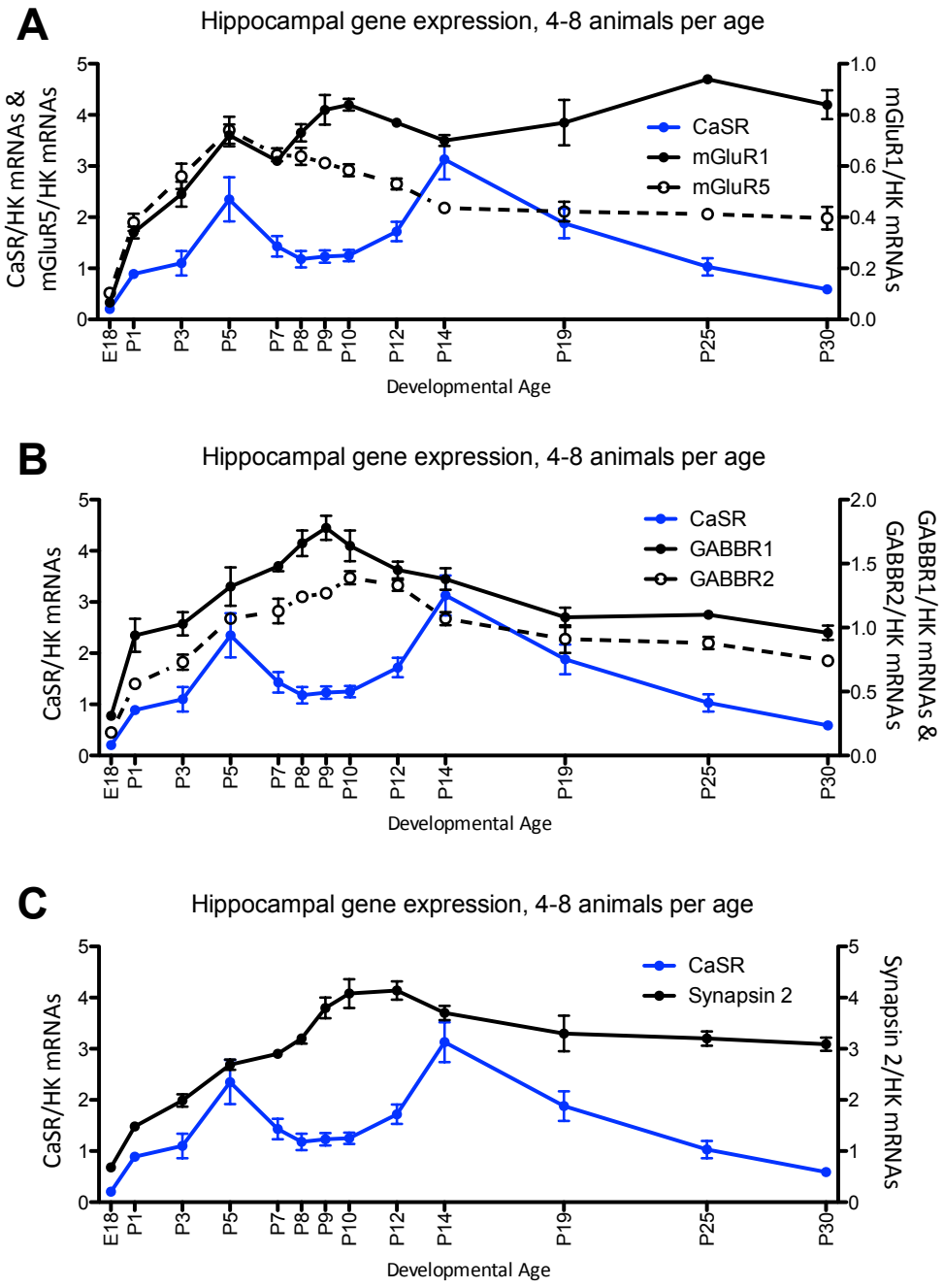

Figure 61: Expression patterns of selected synaptic protein mRNAs in developing hippocampus

A, Comparison of CaSR mRNA expression relative to GAPDH and SDHA mRNAs in the developing hippocampus with transcripts encoding mGluR1 and mGluR5 in the same samples (solid black and dashed black line, respectively). Data represents means ± s.e.m. shown, n = 4 - 8 animals per age.
B, Comparison of CaSR mRNA expression relative to GAPDH and SDHA mRNAs in the developing hippocampus with transcripts encoding GABBR1 and GABBR2 in the same samples (solid black and dashed black line, respectively). Mean ± s.e.m. shown, n = 4 - 8 animals per age.
C, Comparison of CaSR mRNA expression relative to GAPDH and SDHA mRNAs in the developing hippocampus with Synapsin 2 mRNA in the same samples (solid black line). Data represents means ± s.e.m. shown, n = 4 - 8 animals per age.

8.3.3.2.1. Expression of selected synaptic protein mRNAs in developing hippocampus

CaSR has been found to form heterodimers with other class C GPCRs, namely $GABA_BRs$ (Chang et al., 2007) and mGluRs (Gama et al., 2001). Both have established roles in synaptic function, and their heterodimers with CaSR can exhibit altered expression and function relative to CaSR homodimers (Gama et al., 2001; Chang et al., 2007). For these reasons the developmental expression of mRNAs encoding two isoforms of each receptor, all known to dimerize with CaSR, were determined.

The expression profiles of *Grm1* and *Grm5* mRNAs (encoding mGluR1 and mGluR5, respectively) exhibit near identical patterns of induction between E18 and P5, which in turn resemble the induction of CaSR mRNA over the same period (Figure 61A). In common with CaSR, the expression levels of both glutamate receptor mRNAs drop slightly between P5 and P7. However, the expression patterns of *Grm1* and *Grm5* transcripts diverge after P7. While *Grm5* transcript levels gradually decline between P7 and P14 to reach a level that remains stable from P14 to P30, *Grm1* mRNA levels increase slightly from P7 to P10 and remain broadly steady between P10 and P30.

Gabbr1 and *Gabbr2* mRNAs (encoding $GABA_BR1$ and $GABA_BR2$, respectively) exhibit very similar gene expression patterns throughout the developmental period studied. Both mRNAs are steadily up-regulated from E18 and reach peak levels of expression in the middle of the second postnatal week when *Casr* mRNA expression is comparatively low. After peaking, the levels of both transcripts gradually decline to reach approximately 40% lower levels by P30 (Figure 61B).

Syn2 mRNA (encoding synapsin 2) exhibits a comparatively simple pattern of gene expression, undergoing a 6-fold progressive increase in expression from E18 to P9, with little notable change in expression levels occuring between P9 and P30 (Figure 61C).

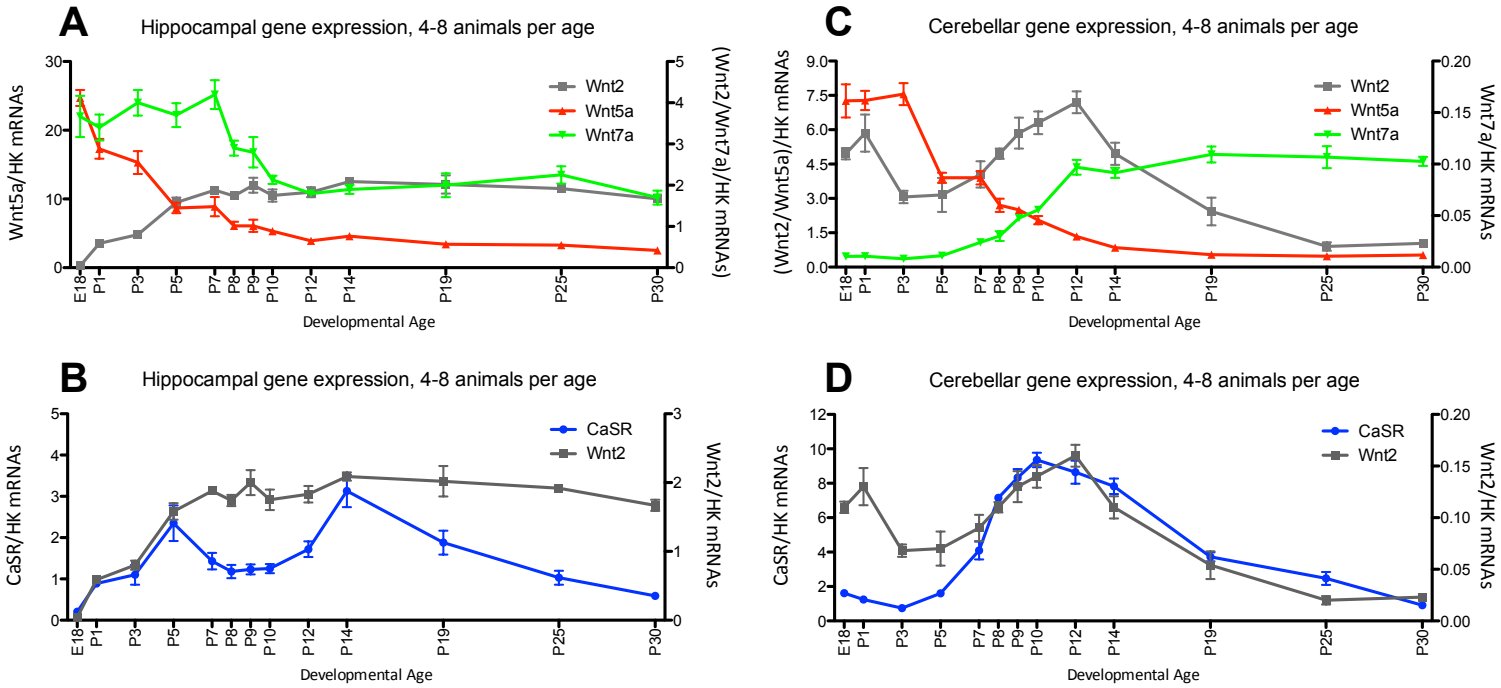

Figure 62: Expression patterns of Wnt2, Wnt5a & Wnt7a mRNAs in developing hippocampus & cerebellum

A, Patterns of mRNA expression for Wnt2, Wnt5a and Wnt7a, each relative to GAPDH and SDHA mRNAs in the developing hippocampus (grey, red and green lines, respectively). Data represents means ± s.e.m. shown, $n = 4$ - 8 animals per age.
B, Comparison of CaSR mRNA expression with that of Wnt2 mRNA expression in the developing hippocampus (blue and grey lines, respectively). Data represents means ± s.e.m. shown, $n = 4$ - 8 animals per age.
C, Patterns of mRNA expression for Wnt2, Wnt5a and Wnt7a, each relative to GAPDH and SDHA mRNAs, in the developing cerebellum (grey, red and green lines, respectively). Data represents means ± s.e.m. shown, $n = 4$ - 8 animals per age.
D, Comparison of CaSR mRNA expression with that of Wnt2 mRNA in the developing cerebellum (blue and grey lines, respectively). Data represents means ± s.e.m. shown, $n = 4$ - 8 animals per age.

8.3.3.2.2. Expression of Wnt2, Wnt5a & Wnt7a mRNAs in developing hippocampus & cerebellum

The expression profiles of three Wnt family member mRNAs were determined for comparison with CaSR mRNA expression. Wnt2 has both functional parallels with CaSR, in regulating hippocampal dendritic growth (Wayman et al., 2006), and similar expression patterns in the brains of rats (Wayman et al., 2006) and humans (Kang et al., 2011). Wnt5a regulates sympathetic axonal growth (Bodmer et al., 2009), has reported roles at inhibitory (Cuitino et al., 2010) and excitatory (Varela-Nallar et al., 2010) hippocampal synapses, and is secreted under the control of CaSR in colon cancer cells (MacLeod et al., 2007). In contrast, Wnt7a has no known association with CaSR, but has recently been established as a regulator of excitatory synaptogenesis and plasticity (Ciani et al., 2011) through the Frizzled-5 receptor (Sahores et al., 2010).

In the hippocampus, the most striking changes in the expression of these three Wnt family member mRNAs occur before the end of the second postnatal week. The expression levels of *Wnt7a* transcripts are highest in the first postnatal week, decline 2.5-fold between P7 and P12 and remain relatively stable between P12 and P30 (Figure 62A). *Wnt5a* mRNA expression levels are highest level at E18 and fall 6-fold between E18 and P8. Thereafter, *Wnt5a* transcript levels decline modestly between P8 and P30. Interestingly, the expression pattern for *Wnt2* mRNA resembles the inverse of the *Wnt5a* mRNA expression pattern. The induction of *Wnt2* mRNA expression follows a very similar pattern to that of *Casr* mRNA (Figure 62B), increasing between E18 and P5. However, the expression patterns of these two mRNAs diverge between P5 and P14. Whilst *Casr* transcript levels dip between P5 and P10, before rising to a second peak at P14, *Wnt2* mRNA expression levels remains high between P5 and P14, even appearing to increase slightly. Furthermore, the expression patterns of *Casr* and *Wnt2* mRNAs diverge again after P14, with *Casr* transcript expression declining but *Wnt2* transcript expression persisting at similar levels to those observed during the second postnatal week.

In the cerebellum, some marked differences in the expression patterns of the mRNAs encoding the three *Wnt* family members are observed. *Wnt7a* exhibits an mRNA expression pattern close to the mirror image of that seen in the

hippocampus; initially low levels of Wnt7a transcripts steadily rise from P5 until reaching a stable, almost 10-fold higher level at P12 (Figure 62C). The *Wnt5a* mRNA expression profiles in the developing hippocampus and cerebellum are similar. In both brain regions, the highest levels of *Wnt5a* transcripts are expressed during the perinatal period and *Wnt5a* mRNA expression decreases gradually from this period to stabilize at 5-10 fold lower levels towards the end of the second postnatal week. An early peak in *Wnt2* mRNA expression levels occurs at P1 in the developing cerebellum. Following an approximately 2-fold decrease in *Wnt2* mRNA levels between P1 and P3, *Wnt2* transcript levels remain stable between P3 and P5 and thereafter increase by approximately 2-fold between P5 and P12. *Wnt2* mRNA expression decreases by 8-fold between P12 and P25 and remains stable between P25 and P30. Interestingly, in the cerebellum there are similarities in the expression patterns of *Casr* and *Wnt2* mRNAs (Figure 62D).

8.3.4. Discussion

This study has confirmed the expression of CaSR mRNA and protein in the murine hippocampus, and demonstrated that it undergoes a similar developmental regulation to that previously reported in rat (Chattopadhyay et al., 1997a). Moreover, the highly quantitative nature of RT-QPCR and the large number of developmental ages analysed has uncovered two distinct developmental peaks of hippocampal *Casr* mRNA expression. The first peak of *Casr* mRNA expression correlates with a peak in the expression of *Mtap2* mRNA (encoding the dendritic marker, MAP2), and may correspond to the established role of CaSR in regulating dendritic growth during this developmental window (Vizard et al., 2008). In contrast, the second peak in CaSR transcript expression at P14 may indicate a novel function for CaSR. To confirm the increased expression of CaSR between P10 and P14, and the subsequent fall in CaSR expression levels thereafter, the developing hippocampus was analysed using immunohistochemistry. Images from CaSR stained sections of P10, P14 and P21 hippocampus have revealed that CaSR protein expression increases markedly in the vicinity of the pyramidal cell layer from P10 to P14, and appears to decrease between P14 and P21. Higher magnification images of P14 sections suggest that a large part of the increase in CaSR protein expression can be attributed to enhanced expression by pyramidal neurons within all CA regions. However, if CaSR were localised to basket cell terminals, as has been reported in the cerebellum (Ruat et al., 1995), it would be

hard to exclude the possibility that these may also contribute to the observed pyramidal layer staining. The second peak in CaSR expression at P14 occurs during a period when synaptogenesis is occurring extremely rapidly in the hippocampus (Steward and Falk, 1991), reflected by high levels of *Syn2* mRNA expression in the RNA samples analysed. Interestingly, the other class C GPCRs whose expression was characterised in this chapter all display large increases in transcript levels over the first postnatal week and, with the exception of *mGluR5* mRNA, all reach peak expression levels between P10 and P14. These data serve to highlight the possibility of related functions for CaSR, mGluRs and $GABA_BRs$ (Gama et al., 2001; Chang et al., 2007). Moreover, given the level of interest in the role of CaSR at mature synapses (Phillips et al., 2008; Chen et al., 2010; Vyleta and Smith, 2011), it will be interesting to explore whether neuronal expression of CaSR at P14 could underlie a novel role for CaSR at developing synapses.

Cortical *Casr* expression has been previously reported (Ruat et al., 1995; Rogers et al., 1997; Ferry et al., 2000; Mudò et al., 2009). Whilst the developmental profile of *Casr* mRNA expression in the developing cortex determined in the current study lacks the striking dual peak of expression observed in the hippocampus, *Casr* transcripts levels rise during the first postnatal week and fall during the third postnatal week in a similar manner to the hippocampus. This raises the possibility that there may be some similarities in CaSR function and the transcriptional regulation of CaSR expression in the two brain regions. Although CaSR expression has previously been detected in the cerebellum (Ruat et al., 1995; Rogers et al., 1997; Ferry et al., 2000; Mudò et al., 2009), the developmental profile of expression there has not been quantitatively determined. The cerebellum is derived from the first rhombomere of the developing hindbrain (Sillitoe and Joyner, 2007), in contrast to the telencephalic structures of the cortex and hippocampus. Given the greater divergence in developmental history, it is perhaps not surprising that the pattern of *Casr* mRNA expression in the developing cerebellum is fundamentally different to that in the developing hippocampus and cortex. In particular, in contrast to the hippocampus and cortex, *Casr* mRNA levels do not increase between E18 and P5 in the developing cerebellum. Instead, high level expression of *Casr* mRNA is induced between P5 and P10. However, it is interesting to note that the pattern of declining *Casr* mRNA expression from P14 to P30 is a feature of all three brain regions analysed, raising the possibility that CaSR

may play important developmental roles within the first two postnatal weeks across multiple brain regions.

There are a host of possible processes that CaSR could be hypothesized to play a role in modulating based on the temporal expression profiles of *Casr* mRNA in the developing cortex and cerebellum. For instance, most migratory and proliferative functions will be largely complete by the beginning of the second postnatal week in the developing cortex, with the exception of differentiated cortical astrocytes which continue to exhibit local proliferation (Ge et al., 2012). Therefore, given the relatively low level of *Casr* mRNA expression at the beginning of the first postnatal week in the developing cortex, it would seem unlikely that CaSR would play a major role in regulating the proliferation and migration of cortical neurons during this period. However, the high level expression of Casr mRNA between P5 and P14 raises the possibility that CaSR may potentially regulate the proliferation of differentiated cortical astrocytes, although there are mixed data relating to the role of CaSR in mediating the proliferation of astrocytes and astrocytoma cells (Chattopadhyay et al., 1999b; Chattopadhyay et al., 1999a; Chattopadhyay et al., 2000; Yano et al., 2004). Alternatively, the majority of dendritic growth and branching in the cortex occurs during the first three postnatal weeks (Wong and Ghosh, 2002; Barnes and Polleux, 2009) and CaSR has been linked to hippocampal dendritic arborization (Vizard et al., 2008). Therefore the high level expression of CaSR mRNA in the developing cortex between P5 and P14 may suggest that CaSR modulates the growth and elaboration of cortical neuron dendrites. Moreover, visual cortex dendritic spine density increases most rapidly at the start and end of the second postnatal week, as axons from the lateral geniculate nucleus arrive and eye opening occurs, respectively (Whitford et al., 2002), while synaptogenesis between fast spiking GABAergic interneurons in layer 5/6 and their targets occurs from P5 to P18 (Pangratz-Fuehrer and Hestrin, 2011).

Foliation of the cerebellum continues until approximately P14 in mice (Sillitoe and Joyner, 2007), raising the possibility that the high level expression of *Casr* mRNA in the developing cerebellum between P8 and P14 may reflect a role for CaSR in regulating the foliation process. There is some evidence that CaSR may contribute to the proliferation of oligodendrocyte precursor cells and decreased MBP levels are detected in P12 cerebellum from *Casr* $^{-/-}$ mice, compared to *Casr* $^{+/+}$ littermates

(Chattopadhyay et al., 2008). Furthermore, maturation of Purkinje cell output and dendritic branching mature especially rapidly between P12 and P18 (McKay and Turner, 2005). In addition, there is a progressive switch in the innervation of Purkinje cell soma between P7 and P20 with climbing fiber inputs to perisomatic spines decreasing as inputs from GABAergic basket cells, which have been reported to express CaSR (Ruat et al., 1995), increase and become ensheathed by Bergmann glial processes (Ichikawa et al., 2011). In conclusion, there are many processes occurring in the developing cortex and cerebellum that occur during the period when CaSR expression is high raising the possibility that CaSR may modulate these processes. However, more detailed studies of the cell types expressing CaSR and the sub-cellular localization of CaSR expression will be needed before any testing of these largely speculative possibilities can proceed further.

The data on Wnt family member mRNA expression provide some helpful perspectives on gene expression studies in the postnatal brain. Firstly, *Wnt2* mRNA expression is induced in a similar fashion to *Casr* mRNA expression in the hippocampus, and also follows a similar pattern of expression in the cerebellum, at least beyond P3. These similarities lend some support to the idea that the significant spatio-temporal correlation between these two transcripts recently reported in human post-mortem tissue (Kang et al., 2011) may also have some relevance in mice. Accordingly, the data in this chapter complement limited data obtained by RT-QPCR and *in situ* hybridization in rat hippocampus, which suggested an up-regulation of *Wnt2* transcripts during the first postnatal week (Wayman et al., 2006). Furthermore, Wnt2 and CaSR are reported to share a function in the regulation of hippocampal dendritic growth (Wayman et al., 2006; Vizard et al., 2008). In this instance, *Wnt2* expression was promoted by neural activity in a CREB dependent manner (Wayman et al., 2006). It would therefore be interesting to determine whether neuronal activity and CREB play any role in the induction of hippocampal *Casr* expression during the first postnatal week, and whether there is any functional connection between CaSR- and Wnt2-promoted dendrite growth.

Secondly, the data above reveals falling levels of *Wnt5a* mRNA expression during the first postnatal week in both hippocampus and cerebellum. These findings are

complimentary to previously published expression data for the embryonic mouse hippocampus, where *Wnt5a* mRNA was highly expressed in the cortical hem at E12.5, the structure that gives rise to the primordial hippocampus, with expression gradually receding to strong expression mainly limited to the dentate gyrus at E16.5 (Grove et al., 1998). Another study reports a reduction in Wnt5a protein expression in the rat hippocampus from E18 to P0, steady low levels of Wnt5a between P0 and P5 and a substantial increase in Wnt5a protein expression between P5 and P60 (Varela-Nallar et al., 2010). In the developing hippocampus, *Wnt5a* has been shown to play a role in excitatory synapse formation (Varela-Nallar et al., 2010), and the regulation of postsynaptic $GABA_A$ receptor trafficking (Cuitino et al., 2010). Taken together with the mRNA expression data above, it would appear that functional Wnt5a expression is either regulated at the level of translation rather than transcription in the postnatal rodent hippocampus or the patterns of Wnt5a expression in the developing mouse and rat hippocampus are different. Interestingly, Wnt5a regulates NGF-promoted growth and branching in perinatal SCG (Bodmer et al., 2009), much like CaSR (Vizard et al., 2008), and CaSR has been reported to promote the secretion of Wnt5a from colon cancer cells (MacLeod et al., 2007). Thus it would be interesting to assess whether any functional links exist between CaSR and Wnt5a in the nervous system.

Finally, the data in this chapter have revealed falling hippocampal, but rising cerebellar, *Wnt7a* mRNA expression during the second postnatal week. The cerebellar gene expression profile matches a previously reported up-regulation of *Wnt7a* mRNA within granule cells of the developing cerebellum (Lucas and Salinas, 1997), that has been associated with enhanced synapse formation between granule cells and incoming mossy fibers (Hall et al., 2000). Although Wnt7a has also been reported to promote synapse formation in the developing hippocampus (Gogolla et al., 2009; Ciani et al., 2011), *Wnt7a* transcript levels decline in the hippocampus as synapse formation accelerates. Nonetheless, Wnt7a protein remains at detectable levels at P15, especially in the dentate gyrus and CA3 (Ciani et al., 2011), where expression levels in slice cultures appear to be regulated by synaptic activity and environmental enrichment (Gogolla et al., 2009). As in the case of Wnt5a, there seems to be a disparity between the expression levels of Wnt7a mRNA and protein, suggesting that in some cell types functional Wnt expression may be regulated at the level of translation rather than the level of

transcription. These findings therefore underscore an important caveat of mRNA expression studies; mRNA expression represents only one of many possible regulatory steps to for the control of biological function. Thus, while such data can provide a useful guide to hypothesis driven research, they also have marked limitations.

In conclusion, the data presented in this chapter illuminate the expression patterns of CaSR in greater spatial and temporal resolution than has been achieved before, confirming the developmental regulation of its expression in the murine CNS and providing a guide for speculation on its role in diverse brain regions. In the following chapter, one hypothesis of great interest will be tested; does CaSR regulate hippocampal synaptogenesis?

8.3.5. Chapter specific acknowledgements

I would like to thank Dr. Sean Wyatt (Cardiff University) for assistance with primer design, optimization of RT-QPCR protocols and data collection, Dr. Eduardo Torres (Cardiff University) for help optimizing perfusion protocols and Dr. Helen Waller-Evans (Cardiff University) for help performing perfusions, sectioning and staining tissue.

8.4. Results Chapter 4: *In vitro* testing of a hypothesized role for CaSR in synaptogenesis

8.4.1. Introduction

Synapses represent critical sites of information transmission in the nervous system, where chemical messages may be passed between cells. Synaptic dysfunction and defective formation of synapses during development are thought to underlie numerous neuropsychiatric conditions (van Spronsen and Hoogenraad, 2010; Penzes et al., 2011; Waites and Garner, 2011). Accordingly, synaptic formation and plasticity are very well studied processes that are often investigated in the hippocampus, which represents a well-characterized model system (Bourne and Harris, 2008).

There is great interest in roles for CaSR at synapses, where it may sense fluctuations in $[Ca^{2+}]_o$ resulting from neural activity (Vassilev et al., 1997a; Yano et al., 2004; Bouschet and Henley, 2005; Bandyopadhyay et al., 2010). Moreover, pre-synaptic CaSR in cortical neurons is reported to regulate tonic glutamate release (Vyleta and Smith, 2011), and increase presynaptic release probability via a NSCC in compensation for activity evoked decreases in $[Ca^{2+}]_o$ (Phillips et al., 2008; Chen et al., 2010). Hippocampal CaSR expression has been reported on numerous occasions (Ruat et al., 1995; Chattopadhyay et al., 1997a; Rogers et al., 1997; Ferry et al., 2000; Vizard et al., 2008; Mudò et al., 2009). Despite this widely reported expression, the role of hippocampal CaSR is not well understood, although some functions have been reported, including the promotion of dendritic growth from pyramidal neurons in the first postnatal week (Vizard et al., 2008). The RT-QPCR and histological expression data in Results Chapter 3 of this thesis have revealed two distinct developmental peaks of hippocampal *Casr* expression (Results Chapter 3, Figure 58). While the first peak at P5 likely corresponds to the previously published role of CaSR in regulating dendritic growth (Vizard et al., 2008), the second peak at P14 may indicate a novel function. Interestingly, this second peak in CaSR expression occurs at a period during which synaptogenesis is occurring extremely rapidly in the developing hippocampus (Steward and Falk, 1991). Although individuals with CaSR mutations may present with seizures from childhood (Kapoor et al., 2008; Nakajima et al., 2009), the developmental

significance of synaptic CaSR has not been investigated. This chapter tests the hypothesis that CaSR may play a role in synapse formation.

8.4.2. Methods

8.4.2.1. Hippocampal Cultures

Hippocampi were either dissected from E18 mouse embryos of the CD1 strain for pharmacological experiments or from crosses of *Nestin*-Cre^{+ve} / *Casr*$^{loxP/+}$ double-transgenic mice for Nestin-CaSR-KO experiments (see Results Chapter 1, section 8.1.2.4 for more details of this mouse stain). Dissections were performed in PBS, after which hippocampi were transferred to 1x HBSS (without Ca^{2+} and Mg^{2+}) and Trypsin was added to a concentration of 1 mg/ml (Worthington). Following a 20 minute incubation, at 37°C, trypsin activity was quenched by the addition of soy-bean trypsin inhibitor (Sigma) to a final concentration of 1 mg/ml. A single cell suspension was produced by gently passing trypsinized hippocampi through a P1000 pipette tip. DNase I (Roche) was added to the single cell suspension to a final concentration of 0.05 mg/ml. Following mixing by passing the suspension through a P1000 pipette tip, cells were pelleted from the suspension by centrifugation, at 700 rpm, for 10 minutes. After removal of the supernatant, cells were resuspended in neurobasal medium supplemented with 2% B27 (Gibco), 2 mM Glutamax (Invitrogen), 100 units/ml Penicillin and 0.1 mg/ml Streptomycin (Sigma). The volume of media used for resuspension was 300 µl per pair of hippocampi. The number of viable cells in the suspension was then counted by haemocytometry.

Cells were plated to a density of 40,000 cells per cm^2, in tissue culture dishes that had been pre-coated with Poly-L-Lysine (0.5 mg/ml, Sigma), using the novel "Macro-Island" configuration (See 8.4.3.2), or, for comparison, on circular 12 mm diameter glass coverslips placed within the wells of four-well dishes. Glass coverslips on which cells were to be plated were pretreated with pure nitric acid overnight, washed in deionized water, then heated to 40 – 50°C in 1M HCl for four hours, washed again in deionized water, then in absolute ethanol for one hour, before air drying and autoclaving. Untreated glass coverslips were used for the Macro-Island protocol, which were removed 4-18 hours after plating, at which point the tissue culture dishes were flooded with 2 ml of culture medium. Cells

were incubated at 37°C, with 5% CO_2, for 12 days. 600 µl of culture medium was replaced with fresh culture medium after each 3-4 days of culture.

8.4.2.2. RNA Extraction & QPCR

RNA extractions were performed on four or five replicate sister cultures per time point using the RNeasy Mini kit (Qiagen) according to manufacturer's instructions. Briefly, samples were homogenised in RLT buffer supplemented with 143mM β-mercaptoethanol. Each sample was mixed with an equal volume of 70% ethanol before being loaded onto spin filter columns. A 40-minute on column DNA digestion step, using RNase free DNase (Qiagen), was included in the RNA extraction protocol. Purified total RNA was eluted from spin columns in 70 µl RNase free H_2O, and stored at -80°C until use.

RNA was reverse transcribed, for one hour at 45°C, using Affinity Script reverse transcriptase (Agilent) in 20 - 40 µl reactions containing 5 mM dNTPs (Roche) and 5 µM random hexamer primers (Fermentas). RNA levels were quantified by the amplification of 2 µl cDNA in a 20 µl reaction. For GAPDH quantification, FastStart Universal SYBR Green Master Mix with Rox reference dye (Roche) was used. For CaSR and SDHA quantification, FastStart Universal Probe Master with Rox reference (Roche) was used. PCR was performed on an Mx3000P QPCR machine (Stratagene) using cycling parameters consisting of 40 cycles of denaturing at 95°C for 30 seconds, annealing at either 58°C (CaSR), 57°C (SDHA) or 51°C (GAPDH) for 1 minute and extension at 72°C for 30 seconds. Standard curves were generated for each run by using serial four-fold dilutions of reverse-transcribed RNA from E18 SCG. Primers and probes used for CaSR and SDHA were identical to those detailed in Table 5 (Results Chapter 3, Methods section). CaSR dual-labelled probe concentration was 400 nM and SDHA dual labelled probe concentration was 200 nM. Primers used for GAPDH SYBR Green detection were: Forward, 5'- TCC CAC TCT TCC ACC TTC-3' and reverse, 5'-CTG TAG CCG TAT TCA TTG TC-3', as previously published (Vizard et al., 2008). The identity of correct PCR products was verified by melting curve analysis at the end of the GAPDH SYBR Green PCR run. All sample data was normalised to the mean of GAPDH and SDHA mRNA levels.

8.4.2.3. Immunocytochemistry

Cultures were fixed at the indicated times using either 4% PFA, for 20 minutes at room temperature, or 100% Methanol, for 5 minutes at -20°C. Cultures were permeabilised with either 0.02% or 0.5% TritonX-100 in PBS (following Methanol and PFA fixation, respectively) before being blocked, for one hour at room temperature, in PBS containing 5% BSA. Fixed cultures were incubated overnight, at 4°C, with primary antibodies and washed three times in PBS. Following washing, the cultures were incubated with secondary antibodies for one hour at room temperature. Primary antibodies were diluted in PBS containing 1% BSA. See Table 7 for primary antibodies used and their dilutions. Secondary antibodies were raised in goat, conjugated to either Alexa-488, -546, or -647 dyes (Invitrogen), and diluted 1/600 in PBS containing 1% BSA. Cultures were mounted in ProLong Gold antifade medium with DAPI (Invitrogen) under 9 mm circular coverslips, partially sealed with nail polish, and allowed to dry for at least 24 hours before imaging.

Target	Host	Dilution	Manufacturer
MAP2	Chicken	1/1000	Abcam
βIII Tubulin	Mouse	1/1000	R&D
CaSR	Rabbit	1/200	Imgenex
PSD-95	Mouse	1/300	Thermo Scientific
Gephyrin	Mouse	1/300	Synaptic Systems
GFP	Chicken	1/500	Abcam
vGlut1	Guinea Pig	1/1000	Synaptic Systems
vGAT	Guinea Pig	1/300	Synaptic Systems

Table 7 - Antibodies used for immunocytochemistry

8.4.2.4. Confocal Microscopy & Puncta Analysis

Fields containing dendrites from at least three different neurons were selected. Proximal dendritic regions were avoided by ensuring a distance of at least 20μm from the edge of the field to the nearest soma. The selection of fields for imaging was performed using only MAP2 staining, to avoid selection bias. Image stacks were acquired using a 63x, 1.4 Numerical Aperture, Plan-Apochromat objective

(Zeiss), at a z-interval of 0.2 μm. Synaptic puncta analysis was performed on image stacks using Volocity 6 software (Perkin Elmer) using standard thresholding protocols, detailed below.

Synaptic puncta were detected by a three-stage process. Firstly, presynaptic puncta were detected using the "Find Objects" tool, applied to the far-red channel (false coloured blue in Figures 65B, 68, 70). Secondly, postsynaptic puncta were similarly detected using the "Find Objects" tool, applied to the green channel. In each instance, the automatically detected puncta were refined by the application of size-based filters adapted from those used by the Salinas lab (UCL, shared by personal communication). These included the "Separate Touching Objects" tool and the "Exclude Objects by Size" tool, the latter of which was run twice, to exclude puncta both too small and too large to represent genuine synaptic staining. The details of the filters used for each marker are detailed in Table 8. Gephyrin puncta not overlapping with MAP2 staining were excluded using the "Exclude non-touching" tool. Finally, to produce data on colocalised pre and postsynaptic markers, areas where the two populations overlap were detected using the "Intersect" tool. MAP2 volume was detected by the application of the "Find objects" tool to the red channel, supplemented by the inclusion of the "Fill holes in objects" tool. Statistical analyses were performed using Graphpad Prism 5.

Marker	Object size guide (μm^3)	Exclude objects < (μm^3)	Exclude objects > (μm^3)
Gephyrin	0.3	0.02	5
PSD-95	0.1	0.02	5
vGAT	0.3	0.02	6
vGlut1	0.3	0.02	6

Table 8 - Size based filters applied to putative synaptic puncta detected in Volocity

8.4.3. Results

8.4.3.1. Postnatal lethality of Nestin-CaSR-KO mice

Casr knockout mice that survive until P14 would be a useful tool, both to further validate the QPCR data indicating a second peak in *Casr* mRNA expression at this age (Results Chapter 3, Figure 58), and to investigate the consequences of the loss of CaSR expression on the nervous system *in vivo*. This has not previously been possible, as globally deleted *Casr* knockout mice die perinatally (Ho et al., 1995; Kos et al., 2003). Furthermore, no nervous system specific conditional knockouts have yet been reported using the more recent floxed *Casr* model (Chang et al., 2008). Thus, to our knowledge, the Nestin-CaSR-KO mice bred for this study represent the first attempt to genetically probe the role of CaSR in the nervous system. To be maximally useful, these mice would have to survive into adolescence.

Figure 63 relates the cumulative results of all genotyping performed on the offspring of crosses between *Nestin*-Cre^{+ve} / *Casr*$^{fl/+}$ mice. χ^2 tests were performed to compare the observed frequency of viable Nestin-CaSR-KO mice (either *Nestin*-Cre$^{+ve/-}$ / *Casr*$^{fl/fl}$ or *Nestin*-Cre$^{+ve/+ve}$ / *Casr*$^{fl/fl}$) at each developmental age studied with the expected frequency if Mendelian inheritance were the sole determinant of viable offspring genotypes. No significant difference was found for any age studied between E13 and P2 (Figure 63A, B), even when compared to the maximum expected frequency (25% Nestin-CaSR-KO, which is expected when either parent carries two copies of the *Nestin*-Cre^{+ve} allele). While some ages suffer from small sample sizes, it is extremely unlikely that the close to expected (18.75%) frequency of viable Nestin-CaSR-KOs observed in the large sample of 57 embryos assessed at E18 (P = 0.864) cannot be completely accounted for by Mendelian inheritance alone. Therefore, Nestin-CaSR-KO mice do not exhibit any selective embryonic lethality

A

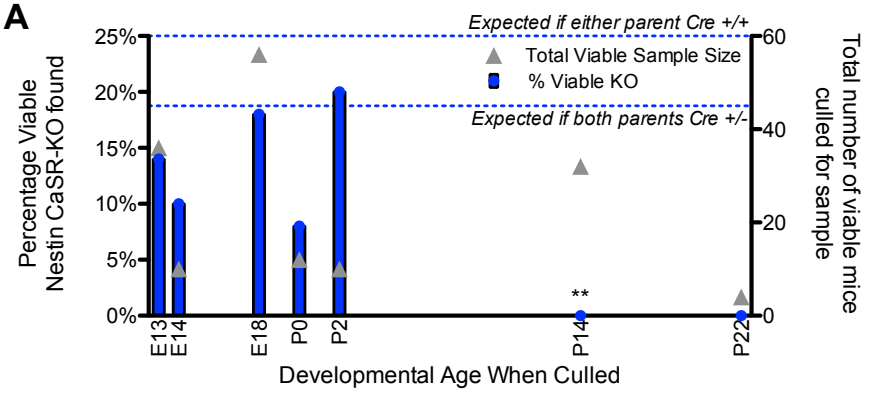

B

	18.75% KOs		25% KOs	
	χ^2	2-tailed *P*	χ^2	2-tailed *P*
E13	0.558	0.4549	2.37	0.1237
E14	0.503	0.4784	1.2	0.2733
E18	0.029	0.8641	1.524	0.217
P0	0.855	0.3552	1.778	0.1824
P2	0.01	0.9193	0.133	0.715
P14	7.385	*0.0066*	10.667	*0.0011*
P22	0.923	0.3367	1.333	0.2482

C

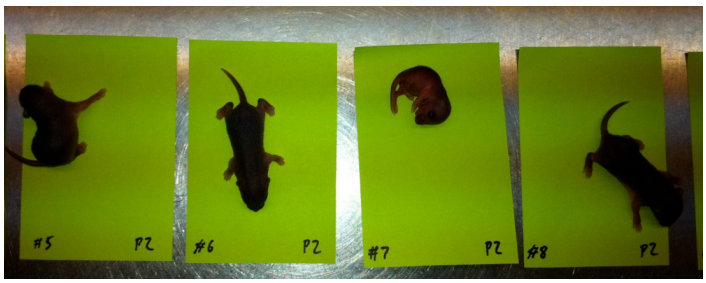

Figure 63: Postnatal lethality in Nestin-CaSR-KO mice (either Nestin-Cre$^{+/-}$/CaSR$^{fl/fl}$ or Nestin-Cre$^{+/+}$/CaSR$^{fl/fl}$)

A, Comparing the percentage of viable mice found to be Nestin-CaSR-KOs (left axis, blue bars) in litters culled at various ages through embryonic and postnatal development with the expected frequencies of Mendelian inheritance (blue dotted horizontal lines). Sample size at each age plotted as grey triangles (right axis) varies between 4 mice (P22) and 57 embryos (E18). Multiple litters were culled at all ages except E14, P2 and P22. No viable Nestin-CaSR-KOs were found at P14 or P22. Statistical comparisons of observed with expected frequencies by χ^2 tests; ** = $P < 0.01$.

B, Results of χ^2 tests for the data in panel A. Comparisons to the expected percentage of viable Nestin-CaSR-KOs are given for the case when both parents are *Nestin*-Cre $^{+/-}$ (18.75%) and when either parent is *Nestin*-Cre $^{+/+}$, a variable that cannot be determined by our current genotyping protocol. Results achieving statistical significance in red italics.

C, At P2, surviving Nestin-CaSR-KO mice are visibly small and unhealthy. Live mice pictured before culling. #7 = Nestin-CaSR-KO; the other three animals pictured all have at least one copy of full length *Casr* intact; #6 = full WT (i.e. *Nestin*-Cre $^{-ve}$ / *Casr* $^{+/+}$).

While no significant deviation from expected Mendelian frequencies is observed in viable mice amongst the small number analysed at P0 or P2, Nestin-CaSR-KO mice are visibly small and unhealthy by P2 (Figure 63C). This phenotype is visually indistinguishable from that of globally deleted P2 *Casr* $^{-/-}$ pups. Furthermore, no viable Nestin-CaSR-KO mice were found at any age examined beyond P2, including amongst the large sample of 34 mice at P14, which differs highly significantly from the expected frequency under the rules of Mendelian inheritance (P = 0.0066 against 18.75%; P = 0.0011 against 25%). It is therefore clear that Nestin-CaSR-KO mice suffer from highly penetrant postnatal lethality prior to P14, with sub-normal health visually apparent from P2. Thus, Nestin-CaSR-KO could not be used to determine the role of CaSR in modulating synaptogenesis *in vivo.*

8.4.3.2. Development of "Macro-Island" culture technique

Dissociated hippocampal cultures provide an advantageous platform for investigating cellular and molecular aspects of hippocampal neuronal development. While neurons from rat are most commonly used for this purpose, mouse neurons may also be used (Kaech and Banker, 2006). Although mouse hippocampal neurons are considered more difficult to culture, they provide the advantage of many more available knockout models than rats. Since long-term hippocampal cultures are typically established from late embryonic hippocampus, they are especially useful for the study of genetic models exhibiting perinatal lethality. Strains affected by this problem include globally deleted *Casr* knockout mice (Ho et al., 1995; Kos et al., 2003) and the recently bred Nestin-CaSR-KO mice, which exhibit similar growth defects to *Casr*$^{-/-}$ pups and die within a few days of birth (Figure 63).

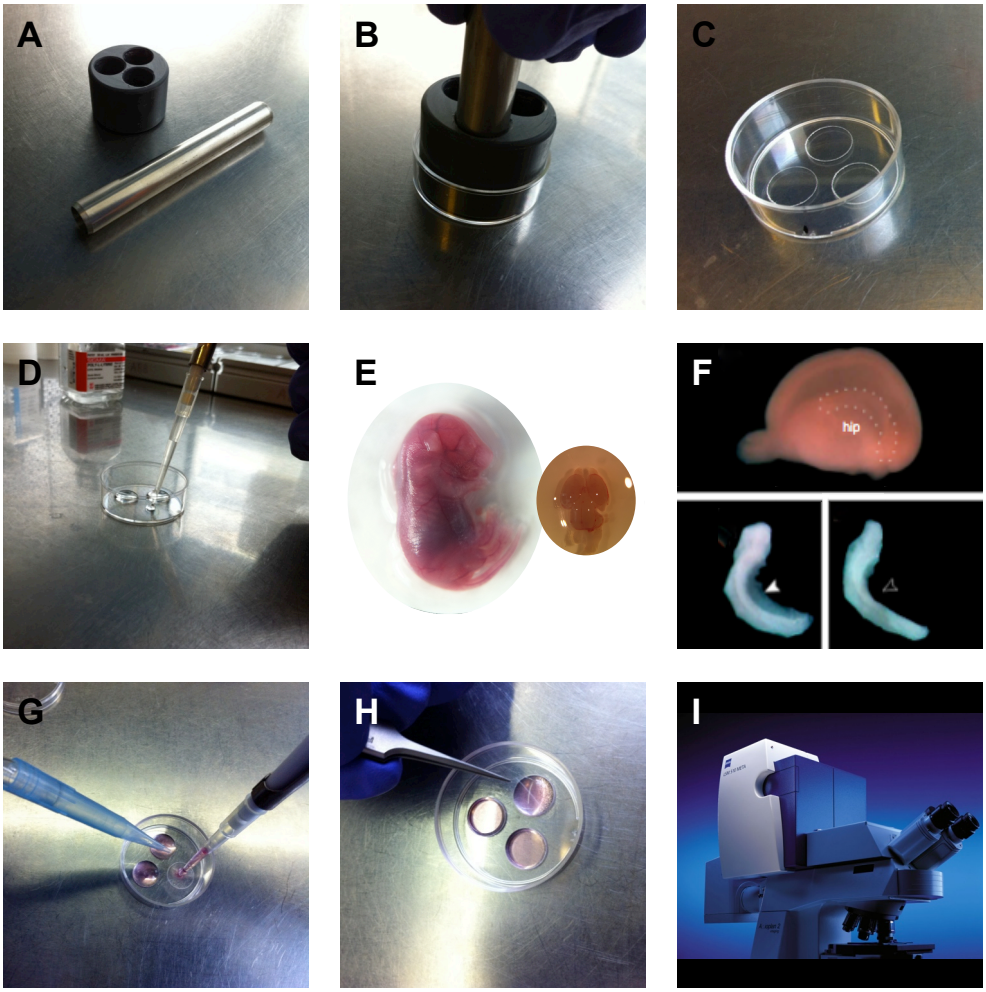

Figure 64: Development of "Macro-Island" culture technique

A, A specially prepared jig and drill are used for cutting Macro-Islands.
B, C, Rotation of the sharp ended drill within each channel through the jig cuts the edges of each Macro-Island in the base of a 35 mm tissue culture dish pre-coated with poly-L-lysine.
D, After washing dishes to remove any cutting debris, and allowing them to dry, sterile water is added to coat each Macro-Island. Dishes are kept in humidified chambers at 37°C while a cell suspension is prepared.
E, E18 mouse embryos are collected and their brains removed.
F, Each cortical hemisphere is isolated, the meninges are removed and the hippocampus is dissected from the medial surface. Any remaining cortical tissue or meninges (white arrowhead) are removed (panel F adapted from Fath *et al*, (2008)).
G, After trypsinisation of hippocampi, a dissociated cell suspension is prepared. Immediately after the water coating each macro-island is aspirated, the cell suspension is slowly expelled from a pipette tip in a straight, upright position.
H, Temporary flotation of 10 mm glass coverslips upon the drop of media in each Macro-Island ensures cells settle with an even distribution across the surface. Coverslips are carefully added and removed with sterile forceps. After removal of coverslips, the remaining plating medium is removed and the whole dish flooded with culture medium.
I, After fixation and staining, a 9 mm coverslip is mounted to each Macro-Island, the sides of the dish are cut away, and the resulting flat specimen can be imaged by confocal microscopy using a high-NA, low working distance objective.

For these reasons a novel approach to culturing mouse hippocampal neurons was developed: The "Macro-Island" technique, based on a previously reported "micro-island" technique for semi-automated analysis of dopaminergic neuronal survival (Planken et al., 2010). The protocol for establishing Macro-Island cultures is depicted in Figure 64. This novel method facilitates the maintenance of high quality, long-term murine hippocampal cultures, plated at a uniform density (Figure 65A) in a format that is amenable to imaging by confocal microscopy using a high numerical aperture, low working distance objective (Figure 65B).

Having confirmed the expression of CaSR in the developing hippocampus, at a stage at which synapses are rapidly forming *in vivo* (See Results Chapter 3, Figure 58), it was necessary to test whether CaSR is also expressed in dissociated hippocampal cultures, before using this experimental system to test the hypothesis that CaSR plays a role in synaptogenesis. A preliminary assessment was accomplished using two complimentary techniques. As dynamic regulation of *Casr* mRNA was observed *in vivo*, the expression pattern of *Casr* mRNA through the *in vitro* development of hippocampal cultures was assessed by RT-QPCR (Figure 66A). *Casr* mRNA expression within cultured hippocampal neurons is apparent at all time points assessed. Expression of *Casr* transcripts (relative to GAPDH and SDHA) is lowest in T0 samples, representing dissociated hippocampal tissue from E18, before plating. In the cultures assessed, higher levels of *Casr* mRNA expression are observed throughout the *in vitro* development of hippocampal neurons, with a peak in mRNA expression at 10 DIV. Expression appears to remain high at 12 DIV, returning to levels close to those observed at earlier stages of culture by 19 DIV (Figure 66A).

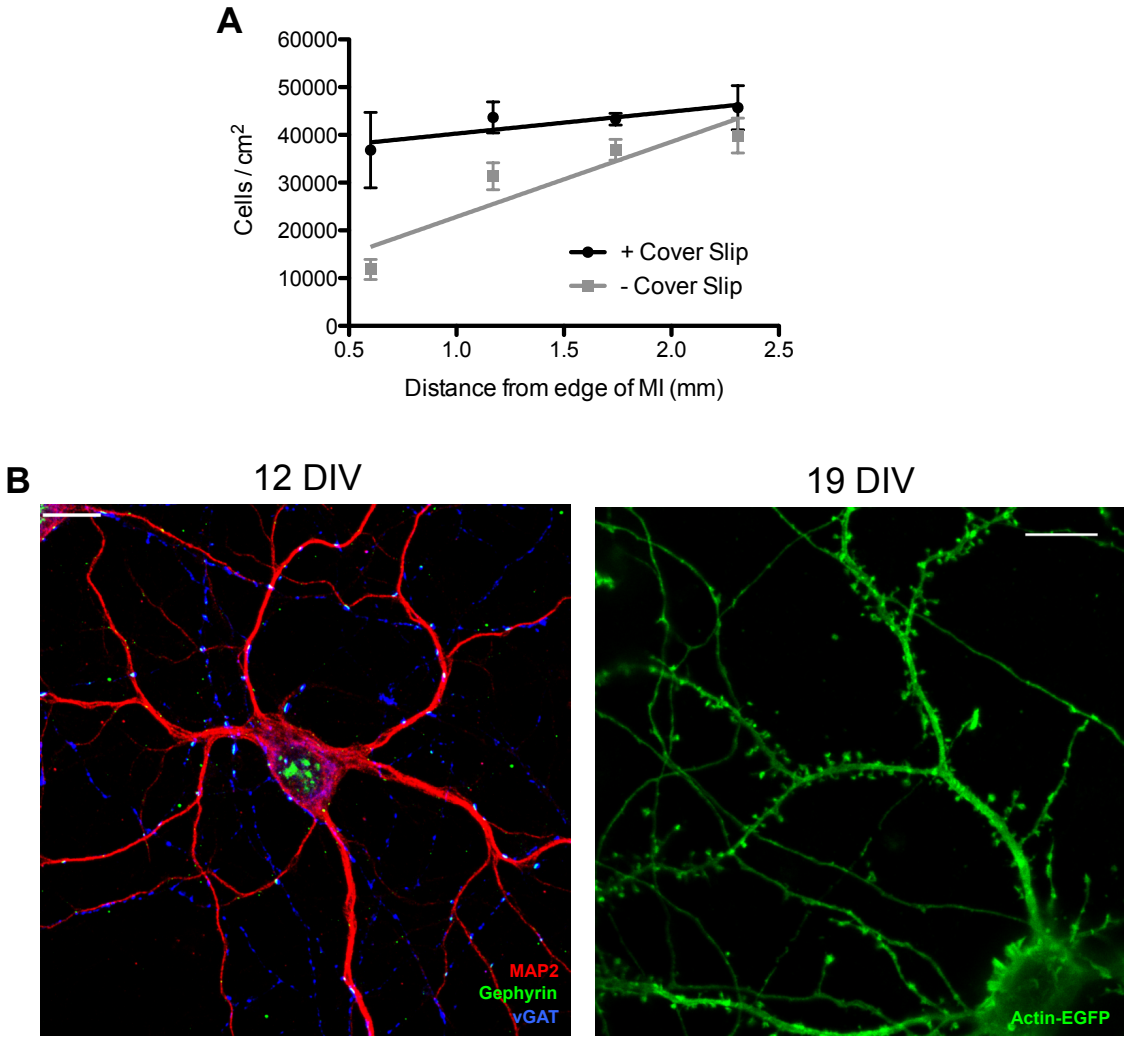

Figure 65: Benefits of the Macro-Island culture technique

A, Prevention of edge effects on cell density by the temporary flotation of cover slips on droplets of cell suspension plated in Macro-Islands. Linear regression analysis indicates a positive correlation between distance from the edge of the Macro-Island and cell density in the absence of a coverslip (r^2 = 0.639; $P < 0.0001$, F test). In contrast, correction by cover slip flotation results in a line of best fit that does not significantly differ from horizontal (r^2 = 0.0656; P = 0.227, runs test). Neither line of best fit significantly deviates from linearity (P = 1, + Cover Slip; P = 0.667, - Cover Slip, runs tests). Crucially, the slopes of each line differ significantly (P = 0.0169, linear regression). Density counted at 1 DIV, n = 5 Macro-Islands.
B, High-resolution images can be obtained by confocal microscopy of healthy hippocampal neurons after up to three weeks of *in vitro* development. Pictured are inhibitory synaptic puncta at 12 DIV and dendritic spines at 19 DIV. 10 µm scale bars. MAP2 staining identifies dendrites. Gephyrin is an inhibitory synapse postsynaptic marker; vGAT is a presynaptic marker for inhibitory synapses.

In order to confirm that the observed *Casr* mRNA expression results in detectable levels of protein expression, and assess the cellular type and sub-cellular localization of CaSR protein, a preliminary immunocytochemical analysis was performed. Negative controls (no anti-CaSR primary antibody) were set up in all cases, in which no CaSR immunoreactivity was detected (data not shown). In cultures fixed at 14 DIV, and thus shortly after the peak in CaSR mRNA expression *in vitro*, CaSR immunoreactivity is detected using two antibodies targeted to different regions of the protein. One antibody had been raised against an epitope in the N-terminal extracellular domain of CaSR (also used in Results Chapter 3) and is already published for use in immunocytochemistry (Vizard et al., 2008). The second antibody, used to validate the results of the first, had been raised against an epitope in the C-terminal intracellular domain of CaSR. Each antibody produces a distinctive pattern of staining, not replicated by the other. The extracellular epitope targeted antibody stains non-neuronal processes, while the intracellular epitope targeted antibody stains neuronal nuclei. As both antibodies do not replicate these staining features, it is doubtful whether they represent genuine CaSR expression. However, both antibodies do replicate a punctate pattern of staining along neuronal processes (Figure 66B).

Such punctate staining is often indicative of synaptic localization. Indeed, prior studies have reported a synaptic localization for CaSR in adult rat brain (Ruat et al., 1995) and cortical synaptosomal preparations (Chen et al., 2010). In order to better assess the likelihood that the punctate CaSR staining observed in these cultures represents a new instance of synaptic localization, neurons were cultured for 21 DIV, since by this stage hippocampal cultures have formed well-developed synaptic networks, including dendritic spines receiving synaptic input (Papa et al., 1995) and mature GABAergic synapses (Swanwick et al., 2006). Punctate staining of CaSR along neuronal processes is replicated at this later age, with particularly intense staining around the soma (Figure 66C). High-resolution images were taken to assess the degree of colocalisation with the excitatory synaptic markers vGlut1 and PSD-95 (pre- and post-synaptic, respectively) and the inhibitory synapse markers vGAT and Gephyrin (pre- and post-synaptic, respectively). While little or no colocalisation of CaSR-positive puncta with vGAT- or Gephyrin-positive puncta is observed, and many CaSR-positive puncta are likely to be extrasynaptic, a partial, but incomplete, colocalisation of CaSR-positive puncta with PSD-95-

positive puncta, and an occasional overlap of CaSR-positive puncta with vGlut1-positive puncta, is apparent (Figure 66C).

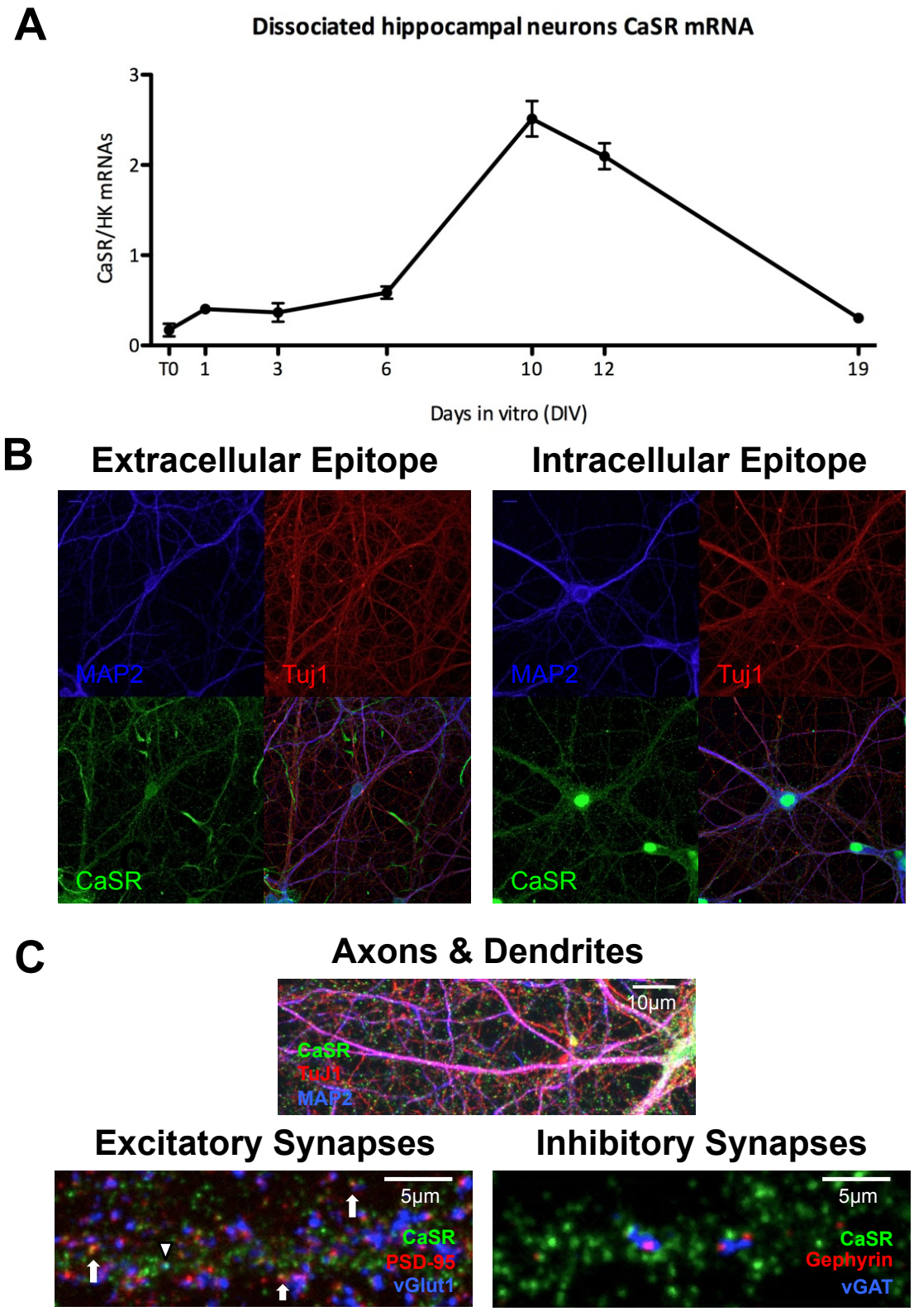

Figure 66: CaSR expression in dissociated hippocampal cultures

A, RNA extracted from sister cultures of hippocampal neurons indicates detectable levels of *Casr* mRNA expression at all stages of their *in vitro* development. Expression increases soon after plating, but reaches a peak at 10 DIV, declining thereafter. n = 5 cultures per age, except 3 DIV n = 4 & 12 DIV n = 3. Data represent means ± s.e.m.
B, CaSR expression can also be detected at the protein level by immunocytochemistry in 14 DIV cultures. Staining with two antibodies targeted to an extracellular and to an intracellular epitope of CaSR produce some common and some distinct features. Only the extracellularly targeted antibody shows staining of non-neuronal cells, while only the intracellularly targeted antibody stains neuronal nuclei. However, a punctate expression pattern along neural processes is a common feature of staining both antibodies. MAP2 staining identifies dendrites. Tuj1 is an antibody against neuron specific β-III tubulin.
C, In 21 DIV cultures CaSR immunostaining (by the antibody targeted to an extracellular epitope) continues to exhibit a punctate pattern clustered at the cell soma (right hand side of "Axons & Dendrites" panel) and apparent along neural processes. While many CaSR puncta are likely to be extrasynaptic, there is a partial, but incomplete, colocalisation of CaSR puncta with PSD-95 (post synaptic excitatory synapse marker - white arrows) and occasional overlap with vGlut1 puncta is observed (presynaptic excitatory synapse marker - arrowhead). In contrast, little or no colocalisation with Gephyrin or vGAT (post and presynaptic markers of inhibitory synapses, respectively) is observed.

8.4.3.3. Pharmacological manipulations of CaSR in vitro

With the Macro-Island culture technique in place and having confirmed the expression of CaSR in hippocampal cultures, it became possible to test the hypothesis that CaSR regulates synaptogenesis *in vitro*. The most appealing means of testing this hypothesis was to assess the density of synaptic structures following acute treatments with calcimimetic and calcilytic compounds. This experimental protocol would allow CaSR function to be selectively manipulated during the period at which it is expressed at the highest levels in culture and synaptogenesis is proceeding rapidly.

However, the data obtained for 3 hour incubations with calcimimetic or calcilytic compounds at 12 DIV (Figure 67) are not supportive of a role for CaSR in regulating synaptogenesis *in vitro*. No changes in the density of excitatory synapses (defined as colocalised vGlut1- and PSD-95-positive puncta; n=4) or inhibitory synapses (defined as colocalised vGAT- and Gephyrin-positive puncta; n=3) are observed between control cultures and cultures treated with calcimimetic or calcilytic compounds. Neither are there any significant differences in the overall density of any individually considered synaptic marker between control cultures and cultures treated with calcimimetic or calcilytic compounds (Figure 67).

Additionally, pilot experiments using 24 hour incubations with calcimimetic and calcilytic compounds at 12DIV also failed to provide any evidence that CaSR regulates synaptic development (data not shown).

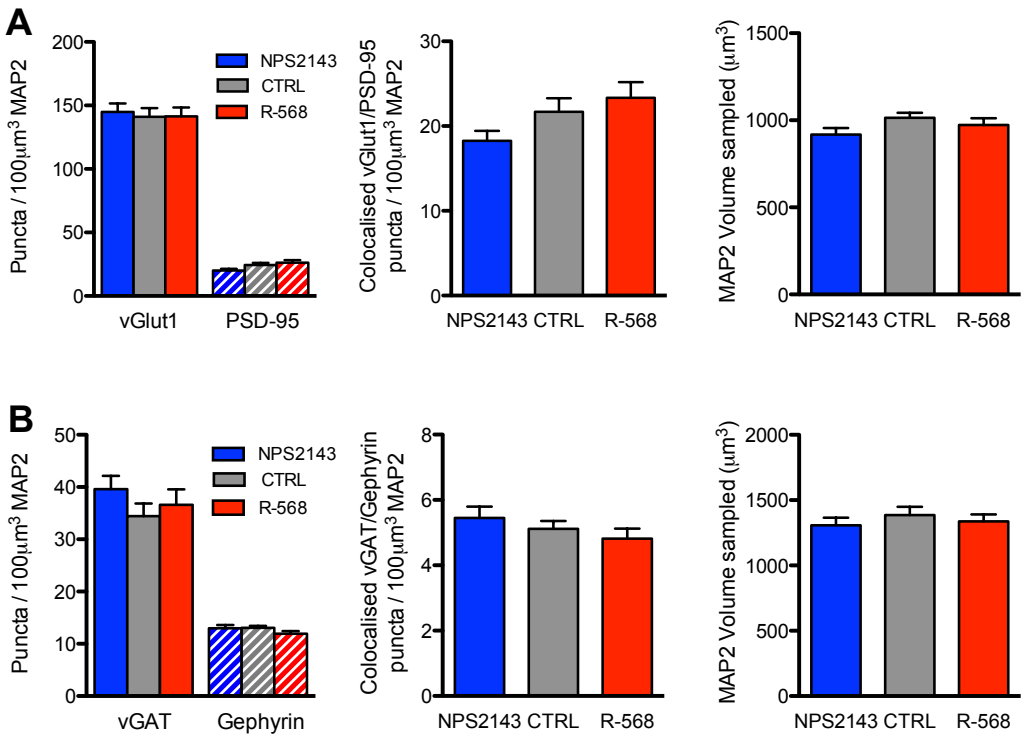

Figure 67: Effects of pharmacological manipulations of CaSR activity *in vitro* on inhibitory and excitatory synaptogenesis

A, Quantification of excitatory synaptic puncta staining in 12 DIV hippocampal neurons, relative to dendritic volume (measured by MAP2 staining), following 3 hour incubations with either 500 nM NPS2143 (a Calcilytic compound), 500 nM R-568 (a Calcimimetic compound) or an equivalent volume of DMSO (CTRL). No significant differences are observed in the density of vGlut1- or PSD-95-positive puncta when these markers are considered separately (vGlut1 $P = 0.8866$; PSD-95 $P = 0.0836$), or when they are colocalised ($P = 0.1528$). Equivalent volumes of MAP2 were sampled ($P = 0.1579$). 15 images per culture, n = 4 independent experiments.
B, Quantification of inhibitory synaptic puncta following the same treatments. No significant differences are observed in the density of vGAT- or Gephyrin-positive puncta when these markers are considered separately (vGAT $P = 0.3869$; Gephyrin $P = 0.1622$), or when they are colocalised ($P = 0.3390$). Equivalent volumes of MAP2 were sampled ($P = 0.5562$). 15 images per culture, n = 3 independent experiments.
All stats by one-way ANOVAs. All data represent means ± s.e.m.

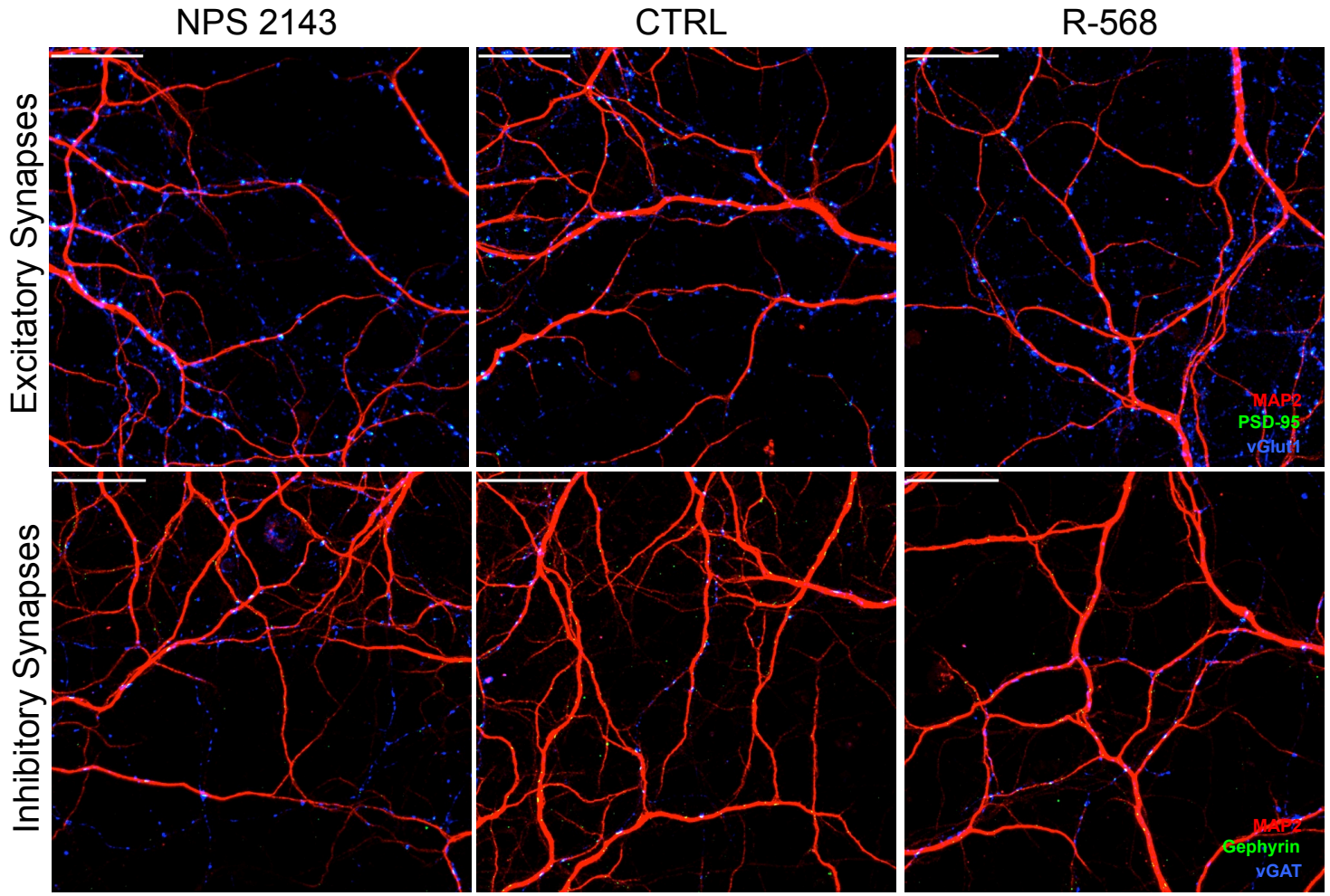

Figure 68: Representative Images for Figure 67

Excitatory and inhibitory synaptic puncta staining in pharmacologically treated cultures of hippocampal neurons at 12 DIV. Scale bars 20 µm.

8.4.3.4. Synapse formation is normal in cultures of Nestin-CaSR-KO mice

Given the limitations of these pharmacological experiments, including a lack of positive controls for compound efficacy, genetic experiments were also performed. Since the *Nestin-Cre* line expresses Cre throughout the CNS, including the hippocampus (Tronche et al., 1999), cultures can be set-up from Nestin-CaSR-KO embryos in which *Casr* deletion is verified in another region of the CNS by PCR (See Results Chapter 1, Figure 37, for example genotyping data derived from a separate experiment). An analysis of cultures derived from Nestin-CaSR-KO embryos and Nestin-Cre expressing littermate control embryos reveals no differences in the density of excitatory synapses or inhibitory synapses between the two genotypes (in both instances, 3 cultures of each genotype from n = 2 independent experiments). Whilst no significant differences in the overall density of vGlut1-, PSD-95- or vGAT-positive puncta are observed between genotypes when these markers are individually considered (Figure 69), a small, but significant, decrease in the density of Gephyrin-positive puncta is apparent in KO cultures compared to control cultures (P = 0.0084). Since this effect does not impinge on inhibitory synapse formation at this developmental stage (as measured by colocalisation of Gephyrin- and vGAT-positive puncta), its biological significance is unclear.

In summary, *in vivo* and *in vitro* expression data led to the hypothesis that CaSR plays a role in modulating synaptogenesis. Because of the postnatal lethality of Nestin-CaSR-KO mice, this hypothesis was tested *in vitro* using the novel Macro-Island technique for culturing hippocampal neurons. However, data from two complimentary experimental approaches (pharmacological and genetic) fails to support this hypothesis.

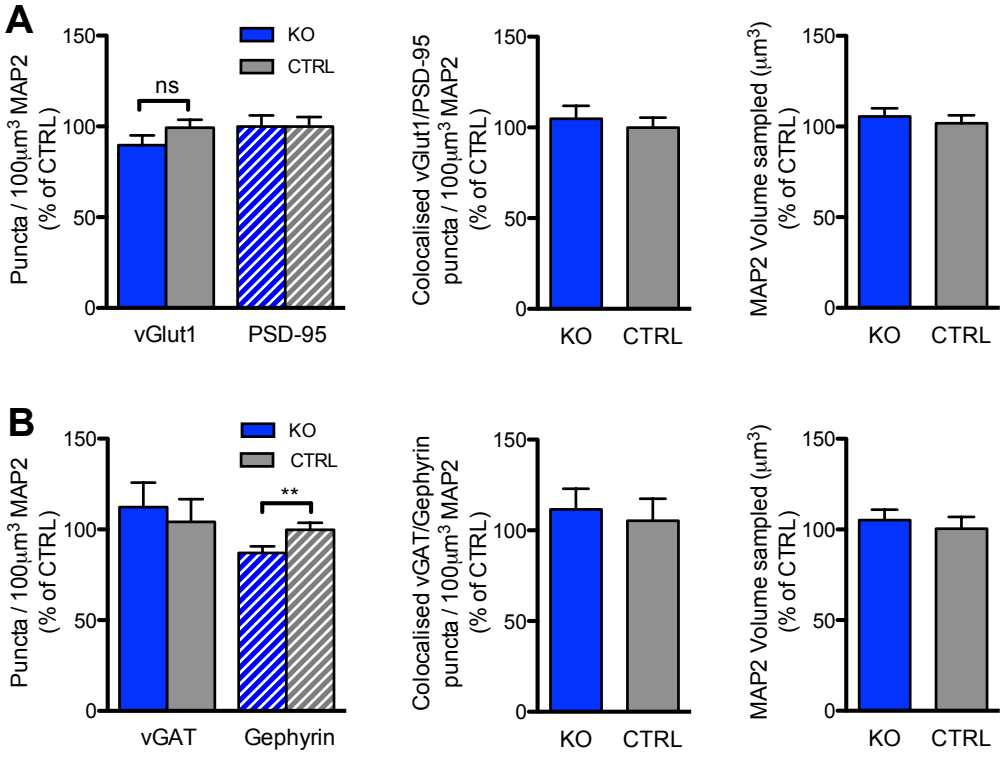

Figure 69: Synapse formation is normal in cultures of Nestin-CaSR-KO mice

A, Quantification of excitatory synaptic puncta staining in 12 DIV hippocampal neurons from embryos derived by crosses of *Nestin*-Cre $^{+ve}$ / *Casr* $^{fl/+}$ mice. KO = Nestin-CaSR-KO; CTRL = *Nestin*-Cre $^{+ve}$ / *Casr* $^{+/+}$. Data are expressed relative to dendritic volume (measured by MAP2 staining) and normalised to control means. No significant differences are observed in the density of vGlut1- or PSD-95-positive puncta between genotypes when these markers are considered separately (vGlut1 $P = 0.0543$; PSD-95 $P = 0.7118$), or when they are colocalised ($P = 0.9599$). Equivalent volumes of MAP2 were sampled ($P = 0.4550$). 15 images per culture; 6 KO and 6 CTRL cultures from n = 2 independent experiments.

B, Quantification of inhibitory synaptic puncta. No significant difference was observed in the density of inhibitory synapses where markers were colocalised ($P = 0.5615$) or in the density of vGAT-positive puncta when considered separately (vGAT $P = 0.4601$). However, Gephyrin-positive puncta density was significantly decreased in KO cultures compared to control cultures ($P = 0.0084$). Equivalent volumes of MAP2 were sampled ($P = 0.3381$). 14 - 15 images per culture; 6 KO and 6 CTRL cultures from n = 2 independent experiments.

All stats by unpaired t-tests, except vGAT alone and Colocalised vGAT/Gephyrin (where data are not normally distributed and can't be normalised by transformation), for which significance was assessed by Mann Whitney tests. ** = $P < 0.01$. All data represent means ± s.e.m.

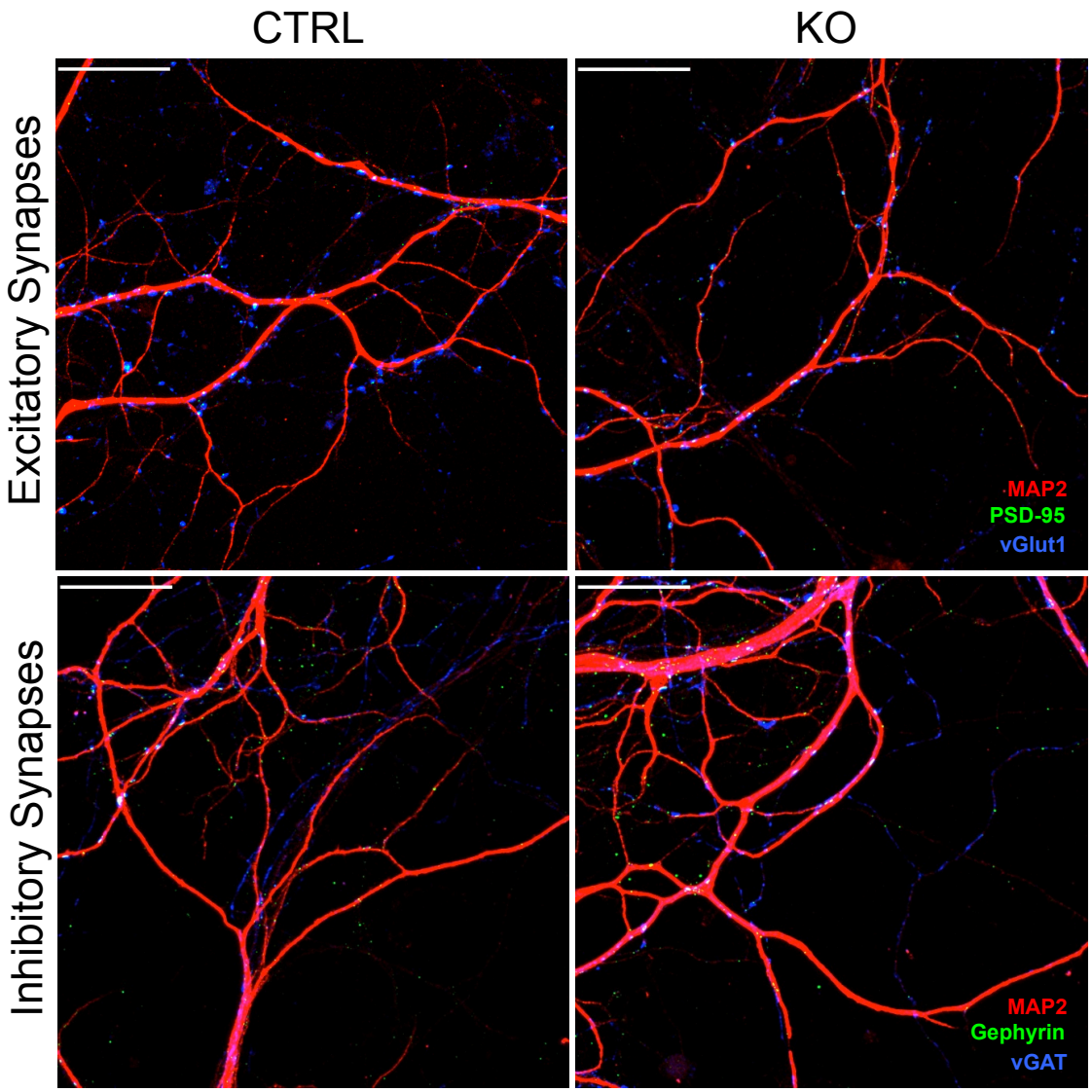

Figure 70: Representative Images for Figure 69

Excitatory and inhibitory synaptic puncta staining in CaSR-Nestin-KO and control cultures of hippocampal neurons at 12 DIV. Scale bars 20 μm.

8.4.4. Discussion

This study reports the generation of Nestin-CaSR-KO mice, in which exon 7 of *Casr* undergoes Cre-dependent deletion in the nervous system. Whilst these mice should have been useful for studying hippocampal development in the absence of CaSR *in vivo*, postnatal lethality, reminiscent of the phenotype of exon 5-deleted *Casr*$^{-/-}$ mice (Ho et al., 1995), makes them unsuitable for *in vivo* analysis. The data gathered to date are insufficient to determine whether the postnatal lethality of Nestin-CaSR-KO mice is a result of a loss of function of CaSR in the intended target, the nervous system, or of *Nestin-Cre* strain driven Cre expression and recombination in other organs. *Nestin* driven Cre expression has been previously reported in cells of other organs including the heart, kidney, intestine and lungs for this strain (http://cre.jax.org/Nes/Nes-CreNano.html). Furthermore, since *PTH* deletion is sufficient to rescue the postnatal lethal phenotype and growth defects of *Casr*$^{-/-}$ mice (Kos et al., 2003), and the phenotype is reproduced by parathyroid specific *Casr* exon 7 deletion (Chang et al., 2008), it would be informative to assess whether CaSR expression in the parathyroid is affected in the Nestin-CaSR-KO mice. If the postnatal lethality of Nestin-CaSR-KO mice is replicated by crosses of floxed *Casr* mice with other Cre-expressing lines exhibiting greater specificity for the nervous system, such observations may represent a novel physiological dependence for CaSR in the developing nervous system.

Preliminary data have shown that CaSR is expressed in long term dissociated hippocampal cultures. These data are in accordance with previous studies indicating the presence of CaSR in cultured hippocampal neurons (Ye et al., 1997; Chang et al., 2007; Vizard et al., 2008; Lu et al., 2010). Furthermore, an up-regulation of *Casr* mRNA has previously been reported in cultured rat osteoblasts, where low levels of *Casr* transcripts at 3 DIV increase to higher levels at 5 and 7 DIV (Chattopadhyay et al., 2004). Therefore, although the passing temporal up-regulation of *Casr* mRNA in dissociated hippocampal cultures represents a novel finding, it is not without precedent. If this finding can be replicated in repeat studies, it would be interesting to explore what regulates *Casr* mRNA expression in hippocampal cultures. CaSR immunostaining has revealed a punctate pattern of CaSR protein expression along neuronal processes at both 14 DIV and 21 DIV. Interestingly, a comparatively small proportion of CaSR puncta colocalize with presynaptic markers at 21 DIV, the location at which CaSR has so far been thought

to act in cortical neuron cultures (Phillips et al., 2008; Chen et al., 2010; Vyleta and Smith, 2011). A partial colocalisation of CaSR with PSD-95 in these preliminary expression studies raises the possibility that CaSR could indeed also function postsynaptically. However, it should be noted that many puncta did not colocalize with synaptic markers, suggesting either an entirely separate extrasynaptic role for CaSR, or that a large proportion of expressed CaSR is internalized. Further, more extensive colocalization studies will be required to fully understand the sub-cellular distribution of CaSR in hippocampal neurons, and whether it changes over time *in vitro*.

Despite a great deal of interest in the roles of CaSR at synapses (Vassilev et al., 1997a; Yano et al., 2004; Bouschet and Henley, 2005; Bandyopadhyay et al., 2010) and some reported roles in modulating pre-synaptic physiology (Phillips et al., 2008; Chen et al., 2010; Vyleta and Smith, 2011), this study, using both pharmacological and genetic methods, has been unable to find any evidence to suggest that CaSR regulates synaptogenesis *in vitro.* However, the possibility that CaSR could play a role later in the *in vitro* development of hippocampal neurons, for instance in the emergence or plasticity of dendritic spines, cannot be excluded. Indeed, several other proteins including BDNF (Ji et al., 2005; Ji et al., 2010), $p75^{NTR}$ (Zagrebelsky et al., 2005), Nogo-A (Zagrebelsky et al., 2010) and Cux1/2 transcription factors (Cubelos et al., 2010) regulate both the overall branching of dendrites and the morphology of dendritic spines. Furthermore, CaSR is able to signal to PI3K, which is emerging as an important regulator of filopodia and spine dynamics in synapse formation and function (Luikart et al., 2008; Yoshihara et al., 2009; Shen and Cowan, 2010; Cuesto et al., 2011). In addition, CaSR can signal to the Rho family of small GTPases in some instances (Ward, 2004), including stimulation of RhoA-mediated actin stress fiber assembly and process retraction in HEK-293 cells (Davies et al., 2006). Moreover, RhoA and other Rho family GTPases have come to be viewed as key signalling hubs in morphological plasticity of spines due to their regulation of actin cytoskeletal dynamics (Ethell and Pasquale, 2005; Tada and Sheng, 2006; Bourne and Harris, 2008; Cingolani and Goda, 2008; Von Bohlen Und Halbach, 2009; Lin and Koleske, 2010). Thus, CaSR could potentially play a role in spinogenesis or morphological plasticity later in development. This hypothesis could be tested *in vitro* using Macro-Island cultures, but should ideally be assessed *in vivo*. Importantly, since synaptic $[Ca^{2+}]_o$ fluctuations are thought to

be dependent on the frequency of neuronal stimulation (Vassilev et al., 1997a), synaptic activity under basal conditions *in vitro* could simply be insufficient for changes in $[Ca^{2+}]_o$ to occur that are detectible by CaSR, underscoring the need for alternative approaches in determining whether CaSR regulates any aspect of spinogenesis or morphological plasticity. One particularly attractive approach would involve the viral delivery of Cre directly into regions of interest in the CNS of floxed *Casr* mice (Papale et al., 2009).

However, even if endogenous CaSR plays no role in synapse formation or function, it may prove interesting to study the effects of over-expressing mutant variants of CaSR, such as the R898Q mutation, which has been linked to clinical epilepsy (Kapoor et al., 2008) and A844P, with which an individual presented with seizures from childhood (Nakajima et al., 2009). Moreover, the R898Q mutation has been found to alter CaSR expression levels by the disruption of an arginine-rich retention motif in the C-terminal domain (Stepanchick et al., 2010), raising the possibility that CaSR overexpression at the cell surface may alter E/I balance, a critical factor in the development of neural circuits (Kehrer et al., 2008; Lu et al., 2009; LeBlanc and Fagiolini, 2011). Furthermore, an additional role for CaSR in the regulation of neuronal excitability through the sodium leak channel, NALCN was recently uncovered using postnatal hippocampal cultures (Lu et al., 2010). While the *in vivo* significance of this function is unclear, it raises the possibility that disruptions of E/I balance due to CaSR dysfunction may be due to its functional interactions with ion channels (Riccardi and Kemp, 2012), rather than alterations at the level of structure (Vizard et al., 2008). Again, future experiments to assess whether CaSR regulates the E/I balance of neural networks should ideally be conducted using a variety of complementary approaches.

During the course of this study, a novel method for culturing murine hippocampal neurons has been developed. Four key features of the Macro-Island technique are worth highlighting. Firstly, these cultures are established on tissue culture plastic. The Davies lab has repeatedly observed that cultures of many neuronal populations are of higher quality on tissue culture plastic than on glass coverslips (unpublished observations, admittedly largely subjective). In this case, three separate circular grooves of 10 mm diameter are carved into the base of a 35 mm tissue culture dish (pre-coated with poly-L-lysine), using a custom cutter and jig

(See Figure 64A-C). After careful washing to remove cutting debris, and drying of the plate surface, the groove surrounding each Macro-Island enables plating of cell suspension in three discreet, stable 80 µl droplets on the surface of the dish (See Figure 64G).

Secondly, despite plating the cell suspension in droplets, a uniform plating density can be achieved by the temporary flotation of a 10 mm glass coverslip on top of each droplet (See Figure 64H). The weight of the coverslip is insufficient to disrupt the stability of the droplet, but, since it is the same size and shape as the Macro-Island, the suspension below forms a thin film of uniform height between the two surfaces. As a result, the edge effects that cause dramatic variations in density when plating cell suspension in droplets are ameliorated (Figure 65A). This is an important advance, since the survival of hippocampal neurons in culture is highly dependent upon density (Brewer et al., 1993). Thus Macro-Islands prevent the amplification of initial differences in plating density over time in culture due to regional variation in density-dependent survival.

Thirdly, the configuration of the three Macro-Islands in each dish facilitates the removal of any dead cells that may have become dislodged from the culture surface and tend to float towards the centre of the dish. Immediately before media changes, dishes can be gently swirled to encourage debris to move towards the centre. The lack of attached cells at the centre of the dish (Figure 64) then permits removal of medium from the centre, without fear of causing disruption to cells immediately underneath the flow of liquid.

Finally, the lack of any raised barrier for maintaining discreet pools of media (such as are found in four well dishes of the same size) facilitates analysis of immunocytochemically stained Macro-Island cultures by confocal microscopy, since a high N.A., low working distance objective can readily approach the coverslipped cells without impediment (Figure 64I, 65B).

In summary, the experiments described in this chapter aimed to test the hypothesis that CaSR has a role in regulating synaptogenesis. A novel *in vitro* culture method was developed to circumvent perinatal lethality in the available *in vivo* conditional CaSR knockout model. While CaSR is clearly expressed in hippocampal cultures, pharmacological and genetic manipulations of hippocampal

cultures failed to provide evidence that CaSR regulates hippocampal neuron synaptogenesis *in vitro*.

8.4.5. Chapter specific acknowledgements

I would like to thank Dr. Pedro Chacón (Cardiff University) for helpful advice and hippocampal culture protocols, Prof. Patricia Salinas (UCL) and her lab members including Dr. Lorenza Ciani and Dr. Sara Sibilla for helpful advice and synaptic puncta analysis protocols, Mr John Harris (Cardiff University) for practical work crafting Macro-Island tools in the workshop, Dr Sean Wyatt for assistance with primer design, optimization of RT-QPCR protocols and data collection and Dr. Yukiko Goda (UCL) for the generous gift of the Actin-GFP plasmid.

9. General discussion

Since the initial cloning of CaSR from bovine parathyroid, CaSR has been recognized as a key regulator of systemic Ca^{2+} homeostasis (Brown et al., 1993). When expressed by parathyroid chief cells, CaSR is able to sense changes in serum $[Ca^{2+}]_o$ of just 2-3% and couples reduced serum $[Ca^{2+}]_o$ to PTH release by CaSR signalling through $G\alpha_q$/PLC/$Ca^{2+}{}_i$ (Brown, 1991). In turn, PTH promotes the selective reuptake of Ca^{2+} from pro-urine in the kidney and the net release of Ca^{2+} by bone, thus constituting a negative feedback loop for the control of systemic Ca^{2+} homeostasis (Hofer and Brown, 2003). However, work over the last two decades has revealed the widespread expression of CaSR in other tissues and other roles of CaSR beyond systemic Ca^{2+} homeostasis (Riccardi and Kemp, 2012).

CaSR expression has been repeatedly reported in the CNS (Ruat et al., 1995; Chattopadhyay et al., 1997a; Rogers et al., 1997; Ferry et al., 2000; Vizard et al., 2008; Mudò et al., 2009), where great interest has been focused on potential roles for CaSR at synapses (Vassilev et al., 1997a; Yano et al., 2004; Bouschet and Henley, 2005; Bandyopadhyay et al., 2010). This interest largely relates to the potential for CaSR to sense fluctuations in $[Ca^{2+}]_o$ resulting from neural activity (Egelman and Montague, 1998, 1999; Rusakov and Fine, 2003), which are predicted to drop from 1.5 mM to just 0.8 mM under high frequency stimulation (Vassilev et al., 1997a) and as such would fall well within the sensitivity range of CaSR (Yano et al., 2004). Accordingly, some functions for CaSR in modulating presynaptic physiology have recently been reported (Phillips et al., 2008; Chen et al., 2010; Vyleta and Smith, 2011). Presynaptic CaSR in cortical neurons regulates tonic glutamate release (Vyleta and Smith, 2011), and increases presynaptic release probability via a NSCC in compensation for activity evoked decreases in $[Ca^{2+}]_o$ (Phillips et al., 2008; Chen et al., 2010). Furthermore, CaSR appears to mediate increases in neuronal excitability that occur upon reduction of $[Ca^{2+}]_o$ via coupling to NALCN (Lu et al., 2010). However, CaSR may also facilitate the structural development of neural networks in the CNS. CaSR has been shown to regulate the migration of hypothalamic GnRH neurons during embryonic development (Chattopadhyay et al., 2007) and data from organotypic slice cultures indicate that CaSR regulates the gross dendritic architecture of hippocampal

pyramidal neurons during the first week of postnatal development (Vizard et al., 2008).

The expression of CaSR has also been reported in several regions of the PNS, including the adult rat dorsal root ganglia (Ferry et al., 2000; Mudò et al., 2009) and trigeminal ganglion (Heyeraas et al., 2008). The observation that CaSR is expressed in the late embryonic and early postnatal mouse SCG, led to the discovery of an unexpected effect of Ca^{2+}_o in promoting axonal growth and branching from cultured sympathetic neurons, which is confined to a perinatal developmental window when CaSR expression is high (Vizard et al., 2008). However, Ca^{2+}_o does not regulate neuronal survival at this developmental age. Importantly, the *in vivo* relevance of this effect was established by the observation that *Casr*$^{-/-}$ mice exhibit impaired innervation of the iris, a target of the SCG (Vizard et al., 2008).

These recent glimpses into some of the roles for CaSR in the nervous system raise many unanswered questions. Furthermore, in comparison to the numerous established roles for Ca^{2+}_i in the development and plasticity of the nervous system (Henley and Poo, 2004; Spitzer, 2006; Cohen and Greenberg, 2008; Spitzer, 2008; Wiegert and Bading, 2011), our understanding of CaSR-mediated effects of changes in $[Ca^{2+}]_o$ remain poorly understood. In particular, there is a great need to understand and characterize the *in vivo* relevance of CaSR-mediated alterations in nervous system function (Bandyopadhyay et al., 2010). The data contained within this thesis have furthered our knowledge of the roles of CaSR in the developing nervous system in four key areas: The signalling underlying a previously reported role for CaSR in regulating axonal growth and branching from perinatal sympathetic neurons (Vizard et al., 2008); the expression and function of CaSR in the early stages of SCG development; the expression of CaSR in the murine CNS and the function of CaSR in hippocampal neuron development..

9.1. CaSR signalling in late embryonic SCG neurons

Understanding the signalling mechanisms underlying CaSR-promoted axonal growth and branching from perinatal sympathetic neurons has been identified as a major priority for future work (Spitzer, 2008). However, the requirement for NGF in CaSR-promoted axon outgrowth from E18 SCG neurons (Vizard et al., 2008) has

previously complicated the analysis of downstream signalling pathways that are engaged following CaSR activation. Data in results chapter 2 of this thesis have advanced our understanding of this critical question. A key initial advance was the observation that, in contrast to NGF supplemented cultures, high $[Ca^{2+}]_o$ fails to increase CaSR expression in the absence of NGF. Moreover, whilst the ability of Ca^{2+}_o to promote axon outgrowth is NGF-dependent, the over-expression of WT CaSR in E18 SCG neurons promotes axon growth in the absence of NGF. However, over-expression of the FHH-linked CaSR mutants R795W and R185Q does not promote axon growth, and over-expression of WT CaSR does not promote axon growth and branching in culture medium containing 0.7 mM Ca^{2+}_o, indicating that the promotion of SCG neuron axon outgrowth and branching requires functional CaSR and elevated $[Ca^{2+}]_o$. These findings also suggest, when taken together with those of Vizard *et al* (2008), that in 2.3 mM Ca^{2+}_o elevated CaSR expression is necessary and sufficient for CaSR-promoted axonal growth in late embryonic SCG cultures. This conclusion is highly complimentary to the previous suggestion that since $[Ca^{2+}]_o$ is tonically elevated *in utero,* reaching around 1.7 mM by late gestation (Kovacs and Kronenberg, 1997), the modulation of axonal growth and branching by CaSR is likely to be controlled primarily by the level of CaSR expression rather than by fluctuations in $[Ca^{2+}]_o$ (Vizard et al., 2008).

Over-expression of WT CaSR in E18 SCG neurons provided a platform for the investigation of CaSR signalling in the absence of NGF-dependent signalling. These investigations revealed a key role for a portion of the C-terminal domain of CaSR between residues 877 and 907 in promoting axon growth. Several other studies using truncation mutants of CaSR have indicated that a surprisingly large portion of the C-terminal domain is dispensable for various signalling functions (Ray et al., 1997; Gama and Breitwieser, 1998; Zhang and Breitwieser, 2005). However, data from these and other publications have also led to an appreciation that the C-terminal domain of CaSR houses numerous regulatory and protein binding sites important for CaSR cell surface expression, cooperativity, desensitization and downstream signalling (Huang and Miller, 2007; Khan and Conigrave, 2010). There are several reported interaction sites contained within the portion of the C-terminal domain found to be required for CaSR-promoted axon growth. These interaction sites include arginine rich ER retention motifs between residues 890–899 (Stepanchick et al., 2010); a major PKC phosphorylation site at T888 (Bai et al.,

1998b; Jiang et al., 2002; Young et al., 2002; Davies et al., 2007) and several residues important for PI-PLC activation (Ray et al., 1997). In addition, the removal of residues between 877-906 disrupts a region that has been shown to be important for receptor cooperativity, resistance to desensitization and ER retention (residues 868–888) (Gama and Breitwieser, 1998), as well as a low affinity filamin-A binding site (residues 868-879) (Zhang and Breitwieser, 2005).

T888 within this region of the CaSR C-terminal domain plays a key role in CaSR-mediated Ca^{2+}_i signalling, including the production of Ca^{2+}_i oscillations (Young et al., 2002; Davies et al., 2007; McCormick et al., 2010; Ward and Riccardi, 2012). Over-expression of constructs encoding phosphomimetic mutations of this residue (T888D and T888X) reduce the ability of CaSR to stimulate Ca^{2+}_i responses compared to over-expression of WT CaSR (Jiang et al., 2002). Conversely, constructs containing the non-phosphorylatable T888A mutation have been shown to potentiate Ca^{2+}_o stimulated Ca^{2+}_i responses, and appear to promote sustained Ca^{2+}_i elevations over Ca^{2+}_i oscillations in HEK-293 cells (Young et al., 2002; Davies et al., 2007). Further experimental work in chapter 2 of this thesis indicates that phosphomimetic and non-phosphorylatable T888 mutants are unable to promote axonal growth when they are over-expressed in SCG neurons, while the T888A mutation disrupts CaSR-promoted axon branching, but not axon elongation. These data raise the possibility that CaSR-promoted axon growth does not require T888 phosphorylation or Ca^{2+}_i oscillations, whereas CaSR-promoted branching requires one or both of these processes. This hypothesis finds further support from the preliminary findings that phospho-T888 immunoreactivity is observed in neurons cultured in medium containing 2.3 mM Ca^{2+}_o in the presence of NGF, since in heterologous and parathyroid cells T888 phosphorylation reflects PKC-mediated feedback inhibition of CaSR signalling following CaSR-mediated increases in $[Ca^{2+}]_i$ (Davies et al., 2007; Ward and Riccardi, 2012). Furthermore, preliminary data also indicate that a pharmacological inhibitor of the IP_3R, 2-APB antagonizes CaSR-promoted axon growth and branching, which is also supportive of an involvement of $[Ca^{2+}]_i$ in CaSR-promoted axon growth, since CaSR-induced increases in $[Ca^{2+}]_i$ require Ca^{2+} release from thapsigargin sensitive intracellular stores (Breitwieser and Gama, 2001). Taken together, the data in results chapter 2 suggest that Ca^{2+}_i may be involved in the downstream signalling from CaSR that results in enhanced axon outgrowth and branching from E18 SCG neurons. This possibility is well

supported by the literature, since for example, CaSR mediated regulation of PTH secretion in the parathyroid gland is controlled by signalling through Ca^{2+}_i (Brown and Macleod, 2001). Furthermore, the homologous mGluR5 receptor signals through Ca^{2+}_i responses in neuronal cells (Jong et al., 2009) and is regulated by phosphorylation of its C-terminal tail (Lee et al., 2008), which is mediated by PKC in CHO cells (Nash et al., 2002). Moreover, the R795W mutation of human CaSR, which is unable to promote axon growth from cultured SCG neurons, is impaired in signalling to Ca^{2+}_i (Bai et al., 1996) and several residues in the membrane proximal region of the C-terminal domain of CaSR, which are required for PI-PLC activation (Ray et al., 1997), are lost in the CaSR-A877X mutant that cannot promote axon growth.

Data presented in results chapter 2 also provides evidence that ERK1/2 activity is required for CaSR-promoted axon growth and branching. The MEK1/2 inhibitor U0126, but not the inactive analogue U0124, abolishes both axon growth and branching from cultured E18 SCG neurons, while preliminary data indicate that ERK1/2 phosphorylation may be increased under conditions where CaSR-promoted axon growth is observed in both transfected and non-transfected cells. This finding is plausible in light of the literature, since CaSR is known to signal via ERK1/2 in other cells (McNeil et al., 1998; Kifor et al., 2001; Corbetta et al., 2002; Hofer and Brown, 2003). Interestingly, Ca^{2+}_o induced ERK1/2 phosphorylation has been shown to be impaired by CaSR-R795W expression in HEK-293 cells (Hobson et al., 2003) and over-expression of CaSR-R795W does not promote axon outgrowth and branching from SCG neurons. Filamin binding sites have been reported to mediate CaSR coupling to ERK1/2 signalling (Awata et al., 2001; Hjälm et al., 2001; Zhang and Breitwieser, 2005; Huang et al., 2006a). CaSR-promoted ERK1/2 phosphorylation in E18 SCG neurons is not likely to be mediated by the high affinity filamin-A binding site that is lost in the G907X truncation mutant, since this mutant is capable of promoting axon growth and branching. However, a low affinity filamin-A binding site that is preserved by G907X but disrupted in the A877X truncation mutant can also mediate ERK1/2 activation by CaSR (Zhang and Breitwieser, 2005) and is thus a good candidate for involvement in CaSR-promoted axonal growth. Alternatively, there is some evidence that PKC activity may be required for coupling CaSR activity to ERK1/2 signalling in parathyroid cells (Corbetta et al., 2002) and HEK-293 cells overexpressing CaSR (Kifor et al., 2001).

Moreover, Ca^{2+}_i is an established regulator of ERK1/2 activation in neurons (Orban et al., 1999; Luttrell, 2003; Wiegert and Bading, 2011). Indeed, this pathway operates downstream of the homologous receptor, mGluR5 in striatal neurons (Mao et al., 2005; Kumar et al., 2012b) and downstream of TNFα reverse signalling in sympathetic neurons (Kisiswa et al., 2013). Given that the data presented in results chapter 2 suggest putative roles for both Ca^{2+}_i and ERK1/2 in transducing CaSR activity into enhanced axonal outgrowth and branching from SCG neurons, it is interesting to speculate whether there could be a functional connection between these two pathways.

9.2. CaSR in early embryonic SCG

The finding that in 2.3 mM Ca^{2+}_o, elevated CaSR expression is necessary and sufficient for CaSR promoted axonal growth in late embryonic SCG cultures raised the possibility that CaSR could have similar roles during other periods of elevated developmental CaSR expression. Accordingly, results chapter 1 of this thesis includes data showing that elevated $[Ca^{2+}]_o$ can promote neurite outgrowth from cultured E13 SCG neural cells, which also express high levels of CaSR. However, E13 Nestin-CaSR-KO embryos do not display a deficit in proximal axon outgrowth from the SCG compared to wild type embryos. While it is possible that the wholemount analysis method used to analyze proximal axon growth is not sufficiently sensitive to detect a deficit between wild type and Nestin-CaSR-KO embryos, the possibility that the effect of $[Ca^{2+}]_o$ on neurite outgrowth from E13 SCG neural cells represents either an *in vitro* artifact, or it is not mediated by CaSR, cannot be excluded. However, if CaSR does mediate enhanced neurite outgrowth from E13 SCG neural cells in response to elevated $[Ca^{2+}]_o$, it differs from CaSR-promoted axon elongation and branching from E18 SCG neurons, as it is not NGF-dependent. Accordingly, it would be interesting to determine whether elevated $[Ca^{2+}]_o$ also promotes CaSR expression in E13 SCG cultures in the absence of NGF. Both outcomes from this analysis would be interesting, since if no up-regulation of CaSR were observed, it would indicate a potential difference in the mechanism by which Ca^{2+}_o promotes neurite outgrowth *in vitro* at two stages of embryonic SCG development. However, if a promotion of CaSR expression in the absence of exogenous NGF was observed, further experiments could attempt to determine whether HGF, which is expressed by E13 SCG neural cells along with its receptor

Met (Maina et al., 1998), is required at this developmental stage instead of NGF for CaSR up-regulation. HGF may represent a more physiologically relevant trophic factor for sympathetic neuroblasts and neurons at E13, as sympathetic neural cells of this developmental age express the NGF receptors, TrkA and $p75^{NTR}$ at very low levels (Wyatt and Davies, 1995). Since signalling downstream of HGF/Met and NGF/TrkA converge on both the Ras and PI3K pathways (Yang et al., 1998), there is a possibility that autocrine HGF signalling through Met could engage the same signalling mechanism by which NGF promotes CaSR expression in the presence of 2.3 mM Ca^{2+}_o in E18 sympathetic neurons.

Although $[Ca^{2+}]_o$ does not appear to regulate the survival of neuroblasts/neurons over 24 hours of culture, the possibility that $[Ca^{2+}]_o$ may exert a subtle effect on the proliferation, differentiation or apoptosis of neural cells cannot be excluded. HGF, which also promotes process outgrowth from neural cells of the E13 SCG, has been shown to selectively modulate sympathetic neuroblast survival and differentiation (Maina et al., 1998). Accordingly, the literature contains a great deal of evidence that CaSR activation can regulate proliferation (Mailland et al., 1997; Chattopadhyay et al., 1998; Chattopadhyay et al., 1999b; Bilderback et al., 2002; Chattopadhyay et al., 2004; Dvorak et al., 2004; Tfelt-Hansen et al., 2004; Rey et al., 2010; Li et al., 2011), differentiation (Oda et al., 2000; Komuves et al., 2002; Mentaverri et al., 2006; Aguirre et al., 2010) and apoptosis (Lin et al., 1998; Lorget et al., 2000; Wu et al., 2005; Mentaverri et al., 2006) in other cell types. However, this question has not been further addressed in this thesis.

9.3. CaSR expression in the CNS

Developmental regulation of *Casr* transcript expression has previously been investigated in two studies of the rat brain (Chattopadhyay et al., 1997b; Ferry et al., 2000). As neither of these studies used a truly quantitative method to determine transcript levels, results chapter 3 provides data from a quantitative RT-QPCR screen of *Casr* mRNA expression in the developing mouse hippocampus, cortex and cerebellum. Developmental regulation of *Casr* transcript expression is observed in all three regions of the CNS examined, with elevated expression exhibited during the first three postnatal weeks in accordance with the previously reported data on rat brain (Chattopadhyay et al., 1997b; Ferry et al., 2000).

Two clear peaks of elevated *Casr* mRNA expression occur in the developing postnatal hippocampus, the first at P5 and the second at P14. The first peak of *Casr* mRNA expression correlates with a peak in the expression of *Mtap2* mRNA (encoding the dendritic marker, MAP2), and may correspond to the established role of CaSR in regulating dendritic growth during this developmental window (Vizard et al., 2008). In contrast, the second peak in *Casr* transcript expression at P14 may indicate a novel function for CaSR. The increased expression of CaSR between P10 and P14, and the subsequent fall in CaSR expression levels thereafter, was confirmed in the developing hippocampus using immunohistochemistry, which also indicates that a substantial induction of CaSR expression occurs between P10 and P14 in the pyramidal cell layer. A selective localization of CaSR to the CA2 subfield has been previously reported in some (Ferry et al., 2000; Mudò et al., 2009), but not all (Ruat et al., 1995; Chattopadhyay et al., 1997a; Rogers et al., 1997), studies. The reason for this discrepancy is not clear, but no evidence of selective CaSR localization within particular hippocampal subfields is apparent in this study.

Casr expression has been previously reported in both the cortex and cerebellum (Ruat et al., 1995; Rogers et al., 1997; Ferry et al., 2000; Mudò et al., 2009). The developmental time course of cortical *Casr* mRNA expression reported indicates transcript levels that rise during the first postnatal week and fall during the third postnatal week in a similar manner to the hippocampus. In contrast, in the developing cerebellum *Casr* mRNA levels do not increase between E18 and P5. Instead, high level expression of *Casr* mRNA is induced between P5 and P10. However, it is interesting to note that the pattern of declining *Casr* mRNA expression from P14 to P30 is a feature of all three brain regions analysed, raising the possibility that CaSR may play important developmental roles within the first two postnatal weeks across multiple brain regions. There are a large number of processes occurring in the developing cortex and cerebellum during the period when CaSR expression is high (discussed in Results Chapter 3, Discussion), raising the possibility that CaSR may modulate some of these processes. However, more detailed studies of the cortical and cerebellar cell types expressing CaSR and the sub-cellular localization of CaSR expression will be needed before any testing of these largely speculative possibilities can proceed further. However, the data on cerebellar *Casr* mRNA expression are consistent with a previous report of CaSR up-

regulation by cerebellar oligodendrocytes during the second postnatal week (Ferry et al., 2000). Interestingly, there is evidence that CaSR may contribute to the proliferation of oligodendrocyte precursor cells and decreased MBP levels are detected in P12 cerebellum from *Casr* $^{-/-}$ mice, compared to *Casr* $^{+/+}$ littermates (Chattopadhyay et al., 2008).

9.4. Testing the hypothesis that CaSR regulates synaptogenesis

CaSR has been previously localized to synapses (Ruat et al., 1995; Chen et al., 2010), where it has reported roles in the modulation of pre-synaptic physiology (Phillips et al., 2008; Chen et al., 2010; Vyleta and Smith, 2011). The second peak in *Casr* transcript expression at P14, reported in Results Chapter 3, which was also validated by immunohistochemistry, occurs at a period during which synaptogenesis is occurring extremely rapidly in the developing hippocampus (Steward and Falk, 1991). Although individuals with CaSR mutations may present with seizures from childhood (Kapoor et al., 2008; Nakajima et al., 2009), the developmental significance of synaptic CaSR has not been investigated. Accordingly, Results Chapter 4 of this thesis tested the hypothesis that CaSR may regulate synaptogenesis.

Perinatal lethality was observed with high penetrance in Nestin-CaSR-KO mice, the available *in vivo* conditional CaSR knockout model, bred to explore the roles of CaSR in the nervous system. This phenotype is reminiscent of that reported for exon 5-deleted *Casr*$^{-/-}$ mice (Ho et al., 1995) and makes Nestin-CaSR-KO mice unsuitable for *in vivo* analysis. Therefore, a novel *in vitro* method, known as "Macro-Islands", was developed for the long-term culture of hippocampal neurons. The "Macro-Islands" protocol is based on a previously reported "micro-island" technique for semi-automated analysis of dopaminergic neuronal survival (Planken et al., 2010). CaSR expression was detected in hippocampal cultures, as has previously been reported (Ye et al., 1997; Chang et al., 2007; Vizard et al., 2008; Lu et al., 2010). Furthermore, preliminary data indicate that *Casr* mRNA expression levels are highest at 12 DIV and that CaSR protein exhibits a punctate expression pattern at 14 and 21 DIV, with a partial colocalisation of CaSR with PSD-95 observed at 21 DIV. Taken together, these preliminary findings raised the possibility that CaSR may play a postsynaptic role in the regulation of synapse

formation. However, this study, using both pharmacological and genetic methods, has been unable to find any evidence to suggest that CaSR regulates synaptogenesis *in vitro.*

9.5. Future work

Key experiments to better characterize CaSR signalling in E18 SCG neurons will include Ca^{2+}_i imaging of non-transfected cells, and cells over-expressing WT CaSR and phosphomimetic and non-phosphorylatable T888 CaSR mutants. Additionally, it will be important to assess the effects of Ca^{2+}_i calcium chelation and reduced filamin expression on ERK1/2 phosphorylation to determine whether Ca^{2+}_i and/or filamin are required for ERK1/2 phosphorylation.

In order to determine whether CaSR mediates the effects of $[Ca^{2+}]_o$ on neurite outgrowth from E13 SCG neural cells *in vitro*, cultures from CaSR knockout embryos must be analyzed alongside cultures from wild type mice. Ca^{2+}_i signalling can also be engaged by direct entry of Ca^{2+} from the extracellular space via numerous ion channels (Berridge et al., 2003). These include TRPC channels, the expression of which can be regulated by NGF in PC12 cells, where they modulate neurite outgrowth (Kumar et al., 2012a). If CaSR does not mediate the effects of $[Ca^{2+}]_o$ on neurite outgrowth from E13 SCG neural cells, it would be interesting to explore whether TRPC channels are involved.

Similarities in the expression patterns of *Wnt2* and *Casr* in the hippocampus and cerebellum are reminiscent of a spatio-temporal correlation between these two transcripts recently reported in human post-mortem tissue (Kang et al., 2011) and a shared function between Wnt2 and CaSR in the regulation of hippocampal dendritic growth (Wayman et al., 2006; Vizard et al., 2008). Hippocampal *Wnt2* expression is promoted by neural activity in a CREB dependent manner (Wayman et al., 2006). It would therefore be interesting to determine whether neuronal activity and CREB play any role in the induction of hippocampal *Casr* expression during the first postnatal week, and whether there is any functional connection between CaSR- and Wnt2-promoted dendrite growth. Furthermore, functional similarities also exist between CaSR and Wnt5a, which both regulate NGF-promoted growth and branching in perinatal SCG (Vizard et al., 2008; Bodmer et al., 2009). Since CaSR has been reported to promote the secretion of Wnt5a from

colon cancer cells (MacLeod et al., 2007), it would be interesting to test whether Wnt5a is involved in CaSR-promoted axonal growth in the E18 SCG.

Further exploration of the local actions of CaSR on the CNS *in vivo* represents an important area for future work. The data gathered to date are insufficient to determine whether the postnatal lethality of Nestin-CaSR-KO mice is a result of a loss of function of CaSR in the intended target, the nervous system, or of *Nestin-Cre* strain driven Cre expression and recombination in other organs. It would be particularly interesting to assess whether CaSR expression in the parathyroid is affected in the Nestin-CaSR-KO mice, since *PTH* deletion is sufficient to rescue the postnatal lethal phenotype and growth defects of $Casr^{-/-}$ mice (Kos et al., 2003), and the phenotype is reproduced by parathyroid specific *Casr* exon 7 deletion (Chang et al., 2008). If the postnatal lethality of Nestin-CaSR-KO mice is replicated by crosses of floxed *Casr* mice with other Cre-expressing lines exhibiting greater specificity for the nervous system, such observations may represent a novel physiological dependence for CaSR in the developing nervous system. However, another particularly attractive future approach would involve the viral delivery of Cre directly into regions of interest in the CNS (Papale et al., 2009) of floxed *Casr* mice. In addition, it would be interesting to determine through further *in vitro* work, whether any alterations in synaptic development are observed following over-expression of mutant CaSR variants, such as the R898Q mutation, which has been linked to clinical epilepsy (Kapoor et al., 2008) and A844P, with which an individual presented with seizures from childhood (Nakajima et al., 2009).

Finally, the data contained within this thesis add to the existing foundation of knowledge, facilitating the testing of further hypotheses regarding potential roles for CaSR in the central nervous system. This should ideally be performed by methods including the targeted disruption of *Casr* expression in particular cell types or regions of the CNS *in vivo*.

10. Bibliography

Adams JP, Sweatt JD (2002) Molecular psychology: roles for the ERK MAP kinase cascade in memory. Annual review of pharmacology and toxicology 42:135-163.

Aggleton JP, Pearce JM (2001) Neural systems underlying episodic memory: insights from animal research. Philosophical transactions of the Royal Society of London Series B, Biological sciences 356:1467-1482.

Aggleton JP, Brown MW (2006) Interleaving brain systems for episodic and recognition memory. Trends in Cognitive Sciences 10:455-463.

Aguirre A, González A, Planell JA, Engel E (2010) Extracellular calcium modulates in vitro bone marrow-derived Flk-1+ CD34+ progenitor cell chemotaxis and differentiation through a calcium-sensing receptor. Biochemical and Biophysical Research Communications 393:156-161.

Airaksinen MS, Saarma M (2002) The GDNF family: signalling, biological functions and therapeutic value. Nature Reviews Neuroscience 3:383-394.

Altman J, Bayer SA (1990) Mosaic organization of the hippocampal neuroepithelium and the multiple germinal sources of dentate granule cells. The Journal of comparative neurology 301:325-342.

Andres R, Forgie A, Wyatt S, Chen Q, De Sauvage FJ, Davies AM (2001) Multiple effects of artemin on sympathetic neurone generation, survival and growth. Development 128:3685-3695.

Arevalo JC, Conde B, Hempstead BL, Chao MV, Martin-Zanca D, Perez P (2000) TrkA immunoglobulin-like ligand binding domains inhibit spontaneous activation of the receptor. Molecular and cellular biology 20:5908-5916.

Arévalo JC, Wu SH (2006) Neurotrophin signaling: many exciting surprises! Cellular and molecular life sciences : CMLS 63:1523-1537.

Arimura N, Kaibuchi K (2007) Neuronal polarity: from extracellular signals to intracellular mechanisms. Nature Reviews Neuroscience 8:194-205.

Arthur JM, Lawrence MS, Payne CR, Rane MJ, McLeish KR (2000) The calcium-sensing receptor stimulates JNK in MDCK cells. Biochemical and Biophysical Research Communications 275:538-541.

Arulpragasam A, Magno AL, Ingley E, Brown SJ, Conigrave AD, Ratajczak T, Ward BK (2012) The adaptor protein 14-3-3 binds to the calcium-sensing receptor and attenuates receptor-mediated Rho kinase signalling. The Biochemical journal 441:995-1006.

Awata H, Huang C, Handlogten ME, Miller RT (2001) Interaction of the calcium-sensing receptor and filamin, a potential scaffolding protein. The Journal of biological chemistry 276:34871-34879.

Bai M (2004) Structure-function relationship of the extracellular calcium-sensing receptor. Cell Calcium 35:197-207.

Bai M, Trivedi S, Brown EM (1998a) Dimerization of the extracellular calcium-sensing receptor (CaR) on the cell surface of CaR-transfected HEK293 cells. The Journal of biological chemistry 273:23605-23610.

Bai M, Trivedi S, Kifor O, Quinn SJ, Brown EM (1999) Intermolecular interactions between dimeric calcium-sensing receptor monomers are important for its normal function. Proceedings of the National Academy of Sciences of the United States of America 96:2834-2839.

Bai M, Trivedi S, Lane CR, Yang Y, Quinn SJ, Brown EM (1998b) Protein kinase C phosphorylation of threonine at position 888 in Ca2+o-sensing receptor (CaR)

inhibits coupling to Ca2+ store release. The Journal of biological chemistry 273:21267-21275.

Bai M, Quinn S, Trivedi S, Kifor O, Pearce SH, Pollak MR, Krapcho K, Hebert SC, Brown EM (1996) Expression and characterization of inactivating and activating mutations in the human Ca2+o-sensing receptor. The Journal of biological chemistry 271:19537-19545.

Bamji SX, Majdan M, Pozniak CD, Belliveau DJ, Aloyz R, Kohn J, Causing CG, Miller FD (1998) The p75 neurotrophin receptor mediates neuronal apoptosis and is essential for naturally occurring sympathetic neuron death. The Journal of cell biology 140:911-923.

Bandyopadhyay S, Tfelt-Hansen J, Chattopadhyay N (2010) Diverse roles of extracellular calcium-sensing receptor in the central nervous system. J Neurosci Res 88:2073-2082.

Barde YA (1994) Neurotrophic factors: an evolutionary perspective. Journal of Neurobiology 25:1329-1333.

Barkat TR, Polley DB, Hensch TK (2011) A critical period for auditory thalamocortical connectivity. Nature Neuroscience 14:1189-1194.

Barnes AP, Polleux F (2009) Establishment of axon-dendrite polarity in developing neurons. Annual review of neuroscience 32:347-381.

Bavelier D, Levi DM, Li RW, Dan Y, Hensch TK (2010) Removing brakes on adult brain plasticity: from molecular to behavioral interventions. J Neurosci 30:14964-14971.

Belgard TG, Marques AC, Oliver PL, Abaan HO, Sirey TM, Hoerder-Suabedissen A, García-Moreno F, Molnár Z, Margulies EH, Ponting CP (2011) A transcriptomic atlas of mouse neocortical layers. Neuron 71:605-616.

Belliveau DJ, Krivko I, Kohn J, Lachance C, Pozniak C, Rusakov D, Kaplan D, Miller FD (1997) NGF and neurotrophin-3 both activate TrkA on sympathetic neurons but differentially regulate survival and neuritogenesis. Journal of Cell Biology 136:375-388.

Benito-Gutiérrez E, Garcia-Fernàndez J, Comella JX (2006) Origin and evolution of the Trk family of neurotrophic receptors. Molecular and cellular neurosciences 31:179-192.

Benson DL, Cohen PA (1996) Activity-independent segregation of excitatory and inhibitory synaptic terminals in cultured hippocampal neurons. J Neurosci 16:6424-6432.

Benvenuti S, Comoglio PM (2007) The MET receptor tyrosine kinase in invasion and metastasis. Journal of Cellular Physiology 213:316-325.

Berridge MJ, Bootman MD, Roderick HL (2003) Calcium signalling: dynamics, homeostasis and remodelling. Nature Reviews Molecular Cell Biology 4:517-529.

Bespalov MM, Sidorova YA, Tumova S, Ahonen-Bishopp A, Magalhães AC, Kulesskiy E, Paveliev M, Rivera C, Rauvala H, Saarma M (2011) Heparan sulfate proteoglycan syndecan-3 is a novel receptor for GDNF, neurturin, and artemin. The Journal of cell biology.

Bielas S, Higginbotham H, Koizumi H, Tanaka T, Gleeson J (2004) Cortical neuronal migration mutants suggest separate but intersecting pathways. Annual Review of Cell and Developmental Biology 20:593-618.

Bilderback TR, Lee F, Auersperg N, Rodland KD (2002) Phosphatidylinositol 3-kinase-dependent, MEK- independent proliferation in response to CaR activation. American journal of physiology Cell physiology 283:C282-288.

Bodmer D, Ascaño M, Kuruvilla R (2011) Isoform-specific dephosphorylation of dynamin1 by calcineurin couples neurotrophin receptor endocytosis to axonal growth. Neuron 70:1085-1099.

Bodmer D, Levine-Wilkinson S, Richmond A, Hirsh S, Kuruvilla R (2009) Wnt5a mediates nerve growth factor-dependent axonal branching and growth in developing sympathetic neurons. J Neurosci 29:7569-7581.

Bortone D, Polleux F (2009) KCC2 expression promotes the termination of cortical interneuron migration in a voltage-sensitive calcium-dependent manner. Neuron 62:53-71.

Boudot C, Saidak Z, Boulanouar A, Petit L, Gouilleux F, Massy Z, Brazier M, Mentaverri R, Kamel S (2010) Implication of the calcium sensing receptor and the Phosphoinositide 3-kinase/Akt pathway in the extracellular calcium-mediated migration of RAW 264.7 osteoclast precursor cells. Bone 46:1416-1423.

Boulton TG, Nye SH, Robbins DJ, Ip NY, Radziejewska E, Morgenbesser SD, DePinho RA, Panayotatos N, Cobb MH, Yancopoulos GD (1991) ERKs: a family of protein-serine/threonine kinases that are activated and tyrosine phosphorylated in response to insulin and NGF. Cell 65:663-675.

Bourne JN, Harris KM (2008) Balancing structure and function at hippocampal dendritic spines. Annual review of neuroscience 31:47-67.

Bouschet T, Henley JM (2005) Calcium as an extracellular signalling molecule: perspectives on the Calcium Sensing Receptor in the brain. Comptes rendus biologies 328:691-700.

Bouschet T, Martin S, Henley JM (2005) Receptor-activity-modifying proteins are required for forward trafficking of the calcium-sensing receptor to the plasma membrane. Journal of cell science 118:4709-4720.

Bouschet T, Martin S, Henley JM (2008) Regulation of calcium-sensing-receptor trafficking and cell-surface expression by GPCRs and RAMPs. Trends in pharmacological sciences 29:633-639.

Breitwieser GE, Gama L (2001) Calcium-sensing receptor activation induces intracellular calcium oscillations. American journal of physiology Cell physiology 280:C1412-1421.

Brewer GJ, Torricelli JR, Evege EK, Price PJ (1993) Optimized survival of hippocampal neurons in B27-supplemented Neurobasal, a new serum-free medium combination. J Neurosci Res 35:567-576.

Brown EM (1991) Extracellular Ca^{2+} sensing, regulation of parathyroid cell function, and role of Ca^{2+} and other ions as extracellular (first) messengers. Physiological Reviews 71:371-411.

Brown EM, Macleod RJ (2001) Extracellular calcium sensing and extracellular calcium signaling. Physiological Reviews 81:239-297.

Brown EM, Katz C, Butters R, Kifor O (1991) Polyarginine, polylysine, and protamine mimic the effects of high extracellular calcium concentrations on dispersed bovine parathyroid cells. Journal of bone and mineral research : the official journal of the American Society for Bone and Mineral Research 6:1217-1225.

Brown EM, Gamba G, Riccardi D, Lombardi M, Butters R, Kifor O, Sun A, Hediger MA, Lytton J, Hebert SC (1993) Cloning and characterization of an extracellular Ca^{2+} sensing receptor from bovine parathyroid. Nature 366:575-580.

Brown MW, Aggleton JP (2001) Recognition memory: What are the roles of the perirhinal cortex and hippocampus? Nature Reviews Neuroscience 2:51-61.

Cajal, Ramon, S (1888) Estructura de los centros nerviosos de las aves. In, pp 1–10. Trim. Hist. Norm. Pat.

Cajal, Ramon, S (1889) La textura del sistema nervioso del hombre y de los vertebrados. In. Moya, Madrid.

Calabrese B, Wilson MS, Halpain S (2006) Development and regulation of dendritic spine synapses. Physiology (Bethesda, Md) 21:38-47.

Campenot RB (1977) Local control of neurite development by nerve growth factor. Proceedings of the National Academy of Sciences of the United States of America 74:4516-4519.

Campenot RB, Draker DD, Senger DL (1994) Evidence that protein kinase C activities involved in regulating neurite growth are localized to distal neurites. Journal of neurochemistry 63:868-878.

Cavanaugh A, Huang Y, Breitwieser GE (2012) Behind the curtain: cellular mechanisms for allosteric modulation of calcium-sensing receptors. British journal of pharmacology 165:1670-1677.

Cavanaugh A, McKenna J, Stepanchick A, Breitwieser GE (2010) Calcium-sensing receptor biosynthesis includes a cotranslational conformational checkpoint and endoplasmic reticulum retention. The Journal of biological chemistry 285:19854-19864.

Chacón PJ, Arévalo MA, Tébar AR (2010) NGF-activated protein tyrosine phosphatase 1B mediates the phosphorylation and degradation of I-kappa-Balpha coupled to NF-kappa-B activation, thereby controlling dendrite morphology. Molecular and cellular neurosciences 43:384-393.

Chang W, Chen TH, Pratt S, Shoback D (2000) Amino acids in the second and third intracellular loops of the parathyroid Ca2+-sensing receptor mediate efficient coupling to phospholipase C. The Journal of biological chemistry 275:19955-19963.

Chang W, Pratt S, Chen TH, Bourguignon L, Shoback D (2001) Amino acids in the cytoplasmic C terminus of the parathyroid Ca2+-sensing receptor mediate efficient cell-surface expression and phospholipase C activation. The Journal of biological chemistry 276:44129-44136.

Chang W, Tu C, Chen TH, Bikle D, Shoback D (2008) The extracellular calcium-sensing receptor (CaSR) is a critical modulator of skeletal development. Science Signaling 1:ra1.

Chang W, Tu C, Cheng Z, Rodriguez L, Chen TH, Gassmann M, Bettler B, Margeta M, Jan LY, Shoback D (2007) Complex formation with the Type B gamma-aminobutyric acid receptor affects the expression and signal transduction of the extracellular calcium-sensing receptor. Studies with HEK-293 cells and neurons. The Journal of biological chemistry 282:25030-25040.

Charalampopoulos I, Vicario A, Pediaditakis I, Gravanis A, Simi A, Ibáñez CF (2012) Genetic dissection of neurotrophin signaling through the p75 neurotrophin receptor. Cell reports 2:1563-1570.

Chattopadhyay N, Ye CP, Yamaguchi T, Vassilev PM, Brown EM (1999a) Evidence for extracellular calcium-sensing receptor mediated opening of an outward K+ channel in a human astrocytoma cell line (U87). Glia 26:64-72.

Chattopadhyay N, Ye CP, Yamaguchi T, Kerner R, Vassilev PM, Brown EM (1999b) Extracellular calcium-sensing receptor induces cellular proliferation and activation of a nonselective cation channel in U373 human astrocytoma cells. Brain Research 851:116-124.

Chattopadhyay N, Ye CP, Yamaguchi T, Kifor O, Vassilev PM, Nishimura R, Brown EM (1998) Extracellular calcium-sensing receptor in rat oligodendrocytes: expression and potential role in regulation of cellular proliferation and an outward K+ channel. Glia 24:449-458.

Chattopadhyay N, Evliyaoglu C, Heese O, Carroll R, Sanders J, Black P, Brown EM (2000) Regulation of secretion of PTHrP by Ca(2+)-sensing receptor in human astrocytes, astrocytomas, and meningiomas. American journal of physiology Cell physiology 279:C691-699.

Chattopadhyay N, Espinosa-Jeffrey A, Tfelt-Hansen J, Yano S, Bandyopadhyay S, Brown EM, de Vellis J (2008) Calcium receptor expression and function in oligodendrocyte commitment and lineage progression: potential impact on reduced myelin basic protein in CaR-null mice. J Neurosci Res 86:2159-2167.

Chattopadhyay N, Légrádi G, Bai M, Kifor O, Ye C, Vassilev PM, Brown EM, Lechan RM (1997a) Calcium-sensing receptor in the rat hippocampus: A developmental study. Developmental Brain Research 100:13-21.

Chattopadhyay N, Legradi G, Bai M, Kifor O, Ye C, Vassilev PM, Brown EM, Lechan RM (1997b) Calcium-sensing receptor in the rat hippocampus: a developmental study. Brain research Developmental brain research 100:13-21.

Chattopadhyay N, Ye C, Yamaguchi T, Nakai M, Kifor O, Vassilev PM, Nishimura RN, Brown EM (1999c) The extracellular calcium-sensing receptor is expressed in rat microglia and modulates an outward K+ channel. Journal of neurochemistry 72:1915-1922.

Chattopadhyay N, Yano S, Tfelt-Hansen J, Rooney P, Kanuparthi D, Bandyopadhyay S, Ren X, Terwilliger E, Brown EM (2004) Mitogenic action of calcium-sensing receptor on rat calvarial osteoblasts. Endocrinology 145:3451-3462.

Chattopadhyay N, Jeong KH, Yano S, Huang S, Pang JL, Ren X, Terwilliger E, Kaiser UB, Vassilev PM, Pollak MR, Brown EM (2007) Calcium receptor stimulates chemotaxis and secretion of MCP-1 in GnRH neurons in vitro: potential impact on reduced GnRH neuron population in CaR-null mice. American journal of physiology Endocrinology and metabolism 292:E523-532.

Chédotal A (2010) Should I stay or should I go? Becoming a granule cell. Trends Neurosci 33:163-172.

Chen CJ, Barnett JV, Congo DA, Brown EM (1989) Divalent cations suppress 3',5'-adenosine monophosphate accumulation by stimulating a pertussis toxin-sensitive guanine nucleotide-binding protein in cultured bovine parathyroid cells. Endocrinology 124:233-239.

Chen W, Bergsman JB, Wang X, Gilkey G, Pierpoint CR, Daniel EA, Awumey EM, Dauban P, Dodd RH, Ruat M, Smith SM (2010) Presynaptic external calcium signaling involves the calcium-sensing receptor in neocortical nerve terminals. PloS one 5:e8563.

Cheng Z, Tu C, Rodriguez L, Chen TH, Dvorak MM, Margeta M, Gassmann M, Bettler B, Shoback D, Chang W (2007) Type B gamma-aminobutyric acid receptors modulate the function of the extracellular Ca2+-sensing receptor and cell differentiation in murine growth plate chondrocytes. Endocrinology 148:4984-4992.

Chevaleyre V, Siegelbaum S (2010) Strong CA2 pyramidal neuron synapses define a powerful disynaptic cortico-hippocampal loop. Neuron 66:560-572.

Chiarini A, Dal Pra I, Marconi M, Chakravarthy B, Whitfield JF, Armato U (2009) Calcium-sensing receptor (CaSR) in human brain's pathophysiology: roles in late-onset Alzheimer's disease (LOAD). Current pharmaceutical biotechnology 10:317-326.

Chilton JK (2006) Molecular mechanisms of axon guidance. Developmental Biology 292:13-24.

Ciani L, Boyle KA, Dickins E, Sahores M, Anane D, Lopes DM, Gibb AJ, Salinas PC (2011) Wnt7a signaling promotes dendritic spine growth and synaptic strength through Ca2+/Calmodulin-dependent protein kinase II. Proceedings of the

National Academy of Sciences of the United States of America 108:10732-10737.

Cingolani LA, Goda Y (2008) Actin in action: the interplay between the actin cytoskeleton and synaptic efficacy. Nature reviews Neuroscience 9:344-356.

Cohen S (1960) PURIFICATION OF A NERVE-GROWTH PROMOTING PROTEIN FROM THE MOUSE SALIVARY GLAND AND ITS NEURO-CYTOTOXIC ANTISERUM. Proceedings of the National Academy of Sciences of the United States of America 46:302-311.

Cohen S, Greenberg M (2008) Communication between the synapse and the nucleus in neuronal development, plasticity, and disease. Annual Review of Cell and Developmental Biology 24:183-209.

Cole D, Forsythe CR, Dooley JM, Grantmyre EB, Salisbury SR (1990a) Primary neonatal hyperparathyroidism: a devastating neurodevelopmental disorder if left untreated. Journal of Craniofacial Genetics and Developmental Biology 10:205-214.

Cole DEC, Forsythe CR, Dooley JM, Grantmyre EB, Sali sbury SR (1990b) Primary neonatal hyperparathyroidism: A devastating neurodevelopmental disorder if left untreated. Journal of Craniofacial Genetics and Developmental Biology 10:205-214.

Conigrave AD, Hampson D (2006) Broad-spectrum L-amino acid sensing by class 3 G-protein-coupled receptors. Trends in endocrinology and metabolism: TEM 17:398-407.

Conigrave AD, Quinn SJ, Brown EM (2000) L-amino acid sensing by the extracellular Ca2+-sensing receptor. Proceedings of the National Academy of Sciences of the United States of America 97:4814-4819.

Conklin BR, Bourne HR (1994) Homeostatic signals. Marriage of the flytrap and the serpent. Nature 367:22.

Conley YP, Mukherjee A, Kammerer C, DeKosky ST, Kamboh MI, Finegold DN, Ferrell RE (2009) Evidence supporting a role for the calcium-sensing receptor in Alzheimer disease. American journal of medical genetics Part B, Neuropsychiatric genetics : the official publication of the International Society of Psychiatric Genetics 150B:703-709.

Corbetta S, Lania A, Filopanti M, Vicentini L, Ballaré E, Spada A (2002) Mitogen-activated protein kinase cascade in human normal and tumoral parathyroid cells. The Journal of clinical endocrinology and metabolism 87:2201-2205.

Corbit KC, Foster DA, Rosner MR (1999) Protein kinase Cdelta mediates neurogenic but not mitogenic activation of mitogen-activated protein kinase in neuronal cells. Molecular and cellular biology 19:4209-4218.

Craig AM, Kang Y (2007) Neurexin-neuroligin signaling in synapse development. Curr Opin Neurobiol 17:43-52.

Crowley C, Spencer SD, Nishimura MC, Chen KS, Pitts-Meek S, Armanini MP, Ling LH, McMahon SB, Shelton DL, Levinson AD (1994) Mice lacking nerve growth factor display perinatal loss of sensory and sympathetic neurons yet develop basal forebrain cholinergic neurons. Cell 76:1001-1011.

Cubelos B, Sebastián-Serrano A, Beccari L, Calcagnotto ME, Cisneros E, Kim S, Dopazo A, Alvarez-Dolado M, Redondo JM, Bovolenta P, Walsh CA, Nieto M (2010) Cux1 and Cux2 regulate dendritic branching, spine morphology, and synapses of the upper layer neurons of the cortex. Neuron 66:523-535.

Cuesto G, Enriquez-Barreto L, Carames C, Cantarero M, Gasull X, Sandi C, Ferrus A, Acebes A, Morales M (2011) Phosphoinositide-3-Kinase Activation Controls Synaptogenesis and Spinogenesis in Hippocampal Neurons. J Neurosci 31:2721-2733.

Cuitino L, Godoy JA, Farías GG, Couve A, Bonansco C, Fuenzalida M, Inestrosa NC (2010) Wnt-5a modulates recycling of functional GABAA receptors on hippocampal neurons. J Neurosci 30:8411-8420.

Da Silva JS, Hasegawa T, Miyagi T, Dotti CG, Abad-Rodriguez J (2005) Asymmetric membrane ganglioside sialidase activity specifies axonal fate. Nature Neuroscience 8:606-615.

Danglot L, Triller A, Marty S (2006) The development of hippocampal interneurons in rodents. Hippocampus 16:1032-1060.

Davies AM (1988) The emerging generality of the neurotrophic hypothesis. Trends Neurosci 11:243-244.

Davies AM (1996) The neurotrophic hypothesis: where does it stand? Philosophical transactions of the Royal Society of London Series B, Biological sciences 351:389-394.

Davies AM (2003) Regulation of neuronal survival and death by extracellular signals during development. EMBO Journal 22:2537-2545.

Davies AM (2008) Neurotrophins giveth and they taketh away. Nature Neuroscience 11:627-628.

Davies AM (2009) Extracellular signals regulating sympathetic neuron survival and target innervation during development. Auton Neurosci 151:39-45.

Davies AM, Lee KF, Jaenisch R (1993) p75-Deficient trigeminal sensory neurons have an altered response to NGF but not to other neurotrophins. Neuron 11:565-574.

Davies SL, Gibbons CE, Vizard T, Ward DT (2006) Ca2+-sensing receptor induces Rho kinase-mediated actin stress fiber assembly and altered cell morphology, but not in response to aromatic amino acids. American journal of physiology Cell physiology 290:C1543-1551.

Davies SL, Ozawa A, McCormick WD, Dvorak MM, Ward DT (2007) Protein kinase C-mediated phosphorylation of the calcium-sensing receptor is stimulated by receptor activation and attenuated by calyculin-sensitive phosphatase activity. The Journal of biological chemistry 282:15048-15056.

de la Torre-Ubieta L, Bonni A (2011) Transcriptional regulation of neuronal polarity and morphogenesis in the Mammalian brain. Neuron 72:22-40.

Deckwerth TL, Elliott JL, Knudson CM, Johnson Jr EM, Snider WD, Korsmeyer SJ (1996) BAX is required for neuronal death after trophic factor deprivation and during development. Neuron 17:401-411.

Dent JA, Polson AG, Klymkowsky MW (1989) A whole-mount immunocytochemical analysis of the expression of the intermediate filament protein vimentin in Xenopus. Development 105:61-74.

Deppmann CD, Mihalas S, Sharma N, Lonze BE, Niebur E, Ginty DD (2008) A model for neuronal competition during development. Science 320:369-373.

Dijkhuizen PA, Ghosh A (2005) BDNF regulates primary dendrite formation in cortical neurons via the PI3-kinase and MAP kinase signaling pathways. Journal of neurobiology 62:278-288.

Dotti CG, Sullivan CA, Banker GA (1988) The establishment of polarity by hippocampal neurons in culture. J Neurosci 8:1454-1468.

Dvorak MM, Siddiqua A, Ward DT, Carter DH, Dallas SL, Nemeth EF, Riccardi D (2004) Physiological changes in extracellular calcium concentration directly control osteoblast function in the absence of calciotropic hormones. Proceedings of the National Academy of Sciences of the United States of America 101:5140-5145.

Dvorak MM, Chen TH, Orwoll B, Garvey C, Chang W, Bikle DD, Shoback DM (2007) Constitutive activity of the osteoblast Ca2+-sensing receptor promotes loss of cancellous bone. Endocrinology 148:3156-3163.

Egelman DM, Montague PR (1998) Computational properties of peri-dendritic calcium fluctuations. J Neurosci 18:8580-8589.

Egelman DM, Montague PR (1999) Calcium dynamics in the extracellular space of mammalian neural tissue. Biophys J 76:1856-1867.

Ehninger D, Li W, Fox K, Stryker MP, Silva AJ (2008) Reversing neurodevelopmental disorders in adults. Neuron 60:950-960.

Eichenbaum H, Yonelinas AP, Ranganath C (2007) The medial temporal lobe and recognition memory. Annual Review of Neuroscience 30:123-152.

English J, Pearson G, Wilsbacher J, Swantek J, Karandikar M, Xu S, Cobb MH (1999) New insights into the control of MAP kinase pathways. Experimental Cell Research 253:255-270.

Enomoto H, Crawford PA, Gorodinsky A, Heuckeroth RO, Johnson EM, Milbrandt J (2001) RET signaling is essential for migration, axonal growth and axon guidance of developing sympathetic neurons. Development 128:3963-3974.

Ernsberger U, Edgar D, Rohrer H (1989) The survival of early chick sympathetic neurons in vitro is dependent on a suitable substrate but independent of NGF. Developmental biology 135:250-262.

Ethell IM, Pasquale EB (2005) Molecular mechanisms of dendritic spine development and remodeling. Progress in Neurobiology 75:161-205.

Fagan AM, Zhang H, Landis S, Smeyne RJ, Silos-Santiago I, Barbacid M (1996) TrkA, but not TrkC, receptors are essential for survival of sympathetic neurons in vivo. J Neurosci 16:6208-6218.

Fame R, Macdonald J, Macklis J (2011) Development, specification, and diversity of callosal projection neurons. Trends Neurosci 34:41-50.

Fan GF, Ray K, Zhao XM, Goldsmith PK, Spiegel AM (1998) Mutational analysis of the cysteines in the extracellular domain of the human Ca2+ receptor: effects on cell surface expression, dimerization and signal transduction. FEBS letters 436:353-356.

Favata MF, Horiuchi KY, Manos EJ, Daulerio AJ, Stradley DA, Feeser WS, Van Dyk DE, Pitts WJ, Earl RA, Hobbs F, Copeland RA, Magolda RL, Scherle PA, Trzaskos JM (1998) Identification of a novel inhibitor of mitogen-activated protein kinase kinase. The Journal of biological chemistry 273:18623-18632.

Ferry S, Traiffort E, Stinnakre J, Ruat M (2000) Developmental and adult expression of rat calcium-sensing receptor transcripts in neurons and oligodendrocytes. European Journal of Neuroscience 12:872-884.

Fivaz M, Bandara S, Inoue T, Meyer T (2008) Robust neuronal symmetry breaking by Ras-triggered local positive feedback. Current biology : CB 18:44-50.

Forgie A, Wyatt S, Correll PH, Davies AM (2003) Macrophage stimulating protein is a target-derived neurotrophic factor for developing sensory and sympathetic neurons. Development 130:995-1002.

Francis N, Farinas I, Brennan C, Rivas-Plata K, Backus C, Reichardt L, Landis S (1999) NT-3, like NGF, is required for survival of sympathetic neurons, but not their precursors. Developmental biology 210:411-427.

Franklin SL, Davies AM, Wyatt S (2009) Macrophage stimulating protein is a neurotrophic factor for a sub-population of adult nociceptive sensory neurons. Molecular and cellular neurosciences 41:175-185.

Fritschy JM, Harvey RJ, Schwarz G (2008) Gephyrin: where do we stand, where do we go? Trends Neurosci 31:257-264.

Gama L, Breitwieser GE (1998) A carboxyl-terminal domain controls the cooperativity for extracellular Ca2+ activation of the human calcium sensing receptor. A study with receptor-green fluorescent protein fusions. The Journal of biological chemistry 273:29712-29718.

Gama L, Wilt SG, Breitwieser GE (2001) Heterodimerization of calcium sensing receptors with metabotropic glutamate receptors in neurons. The Journal of biological chemistry 276:39053-39059.

Gavalda N, Gutierrez H, Davies AM (2009) Developmental switch in NF- B signalling required for neurite growth. Development 136:3405-3412.

Ge W, Miyawaki A, Gage FH, Jan YN, Jan LY (2012) Local generation of glia is a major astrocyte source in postnatal cortex. Nature.

Gerdes J, Li L, Schlueter C, Duchrow M, Wohlenberg C, Gerlach C, Stahmer I, Kloth S, Brandt E, Flad HD (1991) Immunobiochemical and molecular biologic characterization of the cell proliferation-associated nuclear antigen that is defined by monoclonal antibody Ki-67. The American journal of pathology 138:867-873.

Gkogkas CG, Khoutorsky A, Ran I, Rampakakis E, Nevarko T, Weatherill DB, Vasuta C, Yee S, Truitt M, Dallaire P, Major F, Lasko P, Ruggero D, Nader K, Lacaille J, Sonenberg N (2012) Autism-related deficits via dysregulated eIF4E-dependent translational control. Nature:1-9.

Glebova NO, Ginty DD (2004) Heterogeneous Requirement of NGF for Sympathetic Target Innervation In Vivo. Journal of Neuroscience 24:743-751.

Glebova NO, Ginty DD (2005) Growth and survival signals controlling sympathetic nervous system development. Annual Review of Neuroscience 28:191-222.

Gogolla N, Galimberti I, Deguchi Y, Caroni P (2009) Wnt signaling mediates experience-related regulation of synapse numbers and mossy fiber connectivities in the adult hippocampus. Neuron 62:510-525.

Goold RG, Gordon-Weeks PR (2005) The MAP kinase pathway is upstream of the activation of GSK3beta that enables it to phosphorylate MAP1B and contributes to the stimulation of axon growth. Molecular and cellular neurosciences 28:524-534.

Graef IA, Wang F, Charron F, Chen L, Neilson J, Tessier-Lavigne M, Crabtree GR (2003) Neurotrophins and netrins require calcineurin/NFAT signaling to stimulate outgrowth of embryonic axons. Cell 113:657-670.

Grant MP, Stepanchick A, Cavanaugh A, Breitwieser GE (2011) Agonist-driven maturation and plasma membrane insertion of calcium-sensing receptors dynamically control signal amplitude. Science Signaling 4:ra78.

Grove EA, Tole S (1999) Patterning events and specification signals in the developing hippocampus. Cerebral cortex (New York, NY : 1991) 9:551-561.

Grove EA, Tole S, Limon J, Yip L, Ragsdale CW (1998) The hem of the embryonic cerebral cortex is defined by the expression of multiple Wnt genes and is compromised in Gli3-deficient mice. Development 125:2315-2325.

Gutierrez H, Davies AM (2007) A fast and accurate procedure for deriving the Sholl profile in quantitative studies of neuronal morphology. Journal of Neuroscience Methods 163:24-30.

Gutierrez H, Davies AM (2011) Regulation of neural process growth, elaboration and structural plasticity by NF-κB. Trends Neurosci 34:316-325.

Gutierrez H, Hale VA, Dolcet X, Davies AM (2005) NF-kappaB signalling regulates the growth of neural processes in the developing PNS and CNS. Development 132:1713-1726.

Gutierrez H, O'Keeffe GW, Gavaldà N, Gallagher D, Davies AM (2008) Nuclear factor kappa B signaling either stimulates or inhibits neurite growth depending on the phosphorylation status of p65/RelA. J Neurosci 28:8246-8256.

Hall AC, Lucas FR, Salinas PC (2000) Axonal remodeling and synaptic differentiation in the cerebellum is regulated by WNT-7a signaling. Cell 100:525-535.

Hanada R et al. (2009) Central control of fever and female body temperature by RANKL/RANK. Nature 462:505-509.

Handlogten ME, Huang C, Shiraishi N, Awata H, Miller RT (2001) The Ca2+-sensing receptor activates cytosolic phospholipase A2 via a Gqalpha -dependent ERK-independent pathway. The Journal of biological chemistry 276:13941-13948.

Hannan FM et al. (2012) Identification of 70 calcium-sensing receptor mutations in hyper- and hypo-calcaemic patients: evidence for clustering of extracellular domain mutations at calcium-binding sites. Human Molecular Genetics 21:2768-2778.

Hardingham GE, Chawla S, Johnson CM, Bading H (1997) Distinct functions of nuclear and cytoplasmic calcium in the control of gene expression. Nature 385:260-265.

Hardingham NR, Bannister NJ, Read JC, Fox KD, Hardingham GE, Jack JJ (2006) Extracellular calcium regulates postsynaptic efficacy through group 1 metabotropic glutamate receptors. J Neurosci 26:6337-6345.

Harrington A, Ginty DD (2013) Long-distance retrograde neurotrophic factor signalling in neurons. Nature Reviews Neuroscience 14:177-187.

Harrington AW, St Hillaire C, Zweifel LS, Glebova NO, Philippidou P, Halegoua S, Ginty DD (2011) Recruitment of Actin Modifiers to TrkA Endosomes Governs Retrograde NGF Signaling and Survival. Cell 146:421-434.

Harteneck C, Gollasch M (2011) Pharmacological modulation of diacylglycerol-sensitive TRPC3/6/7 channels. Current pharmaceutical biotechnology 12:35-41.

Hashimoto K, Tsujita M, Miyazaki T, Kitamura K, Yamazaki M, Shin HS, Watanabe M, Sakimura K, Kano M (2011) Postsynaptic P/Q-type Ca2+ channel in Purkinje cell mediates synaptic competition and elimination in developing cerebellum. Proceedings of the National Academy of Sciences of the United States of America 108:9987-9992.

Häusser M, Spruston N, Stuart GJ (2000) Diversity and dynamics of dendritic signaling. Science 290:739-744.

Hempstead BL, Martin-Zanca D, Kaplan DR, Parada LF, Chao MV (1991) High-affinity NGF binding requires coexpression of the trk proto-oncogene and the low-affinity NGF receptor. Nature 350:678-683.

Henley J, Poo MM (2004) Guiding neuronal growth cones using Ca2+ signals. Trends in Cell Biology 14:320-330.

Hensch TK (2005) Critical period plasticity in local cortical circuits. Nature reviews Neuroscience 6:877-888.

Herberger AL, Loretz CA (2013a) Morpholino oligonucleotide knockdown of the extracellular calcium-sensing receptor impairs early skeletal development in zebrafish. Comparative biochemistry and physiology Part A, Molecular & integrative physiology.

Herberger AL, Loretz CA (2013b) Vertebrate extracellular calcium-sensing receptor evolution: selection in relation to life history and habitat. Comparative biochemistry and physiology Part D, Genomics & proteomics 8:86-94.

Herrera-Vigenor F, Hernández-García R, Valadez-Sánchez M, Vázquez-Prado J, Reyes-Cruz G (2006) AMSH regulates calcium-sensing receptor signaling through direct interactions. Biochemical and Biophysical Research Communications 347:924-930.

Heyeraas KJ, Haug SR, Bukoski RD, Awumey EM (2008) Identification of a Ca2+-sensing receptor in rat trigeminal ganglia, sensory axons, and tooth dental pulp. Calcified tissue international 82:57-65.

Hindmarch C, Fry M, Yao ST, Smith PM, Murphy D, Ferguson AV (2008) Microarray analysis of the transcriptome of the subfornical organ in the rat: regulation by

fluid and food deprivation. American journal of physiology Regulatory, integrative and comparative physiology 295:R1914-1920.

Hirai S, Banba Y, Satake T, Ohno S (2011) Axon Formation in Neocortical Neurons Depends on Stage-Specific Regulation of Microtubule Stability by the Dual Leucine Zipper Kinase-c-Jun N-Terminal Kinase Pathway. J Neurosci 31:6468-6480.

Hjälm G, MacLeod RJ, Kifor O, Chattopadhyay N, Brown EM (2001) Filamin-A binds to the carboxyl-terminal tail of the calcium-sensing receptor, an interaction that participates in CaR-mediated activation of mitogen-activated protein kinase. The Journal of biological chemistry 276:34880-34887.

Ho C, Conner DA, Pollak MR, Ladd DJ, Kifor O, Warren HB, Brown EM, Seidman JG, Seidman CE (1995) A mouse model of human familial hypocalciuric hypercalcemia and neonatal severe hyperparathyroidism. Nature genetics 11:389-394.

Hobson SA, Wright J, Lee F, McNeil SE, Bilderback T, Rodland KD (2003) Activation of the MAP kinase cascade by exogenous calcium-sensing receptor. Molecular and cellular endocrinology 200:189-198.

Hoenderop JG, Nilius B, Bindels RJ (2005) Calcium absorption across epithelia. Physiological Reviews 85:373-422.

Hofer AM, Brown EM (2003) Extracellular calcium sensing and signalling. Nature Reviews Molecular Cell Biology 4:530-538.

Honma Y, Araki T, Gianino S, Bruce A, Heuckeroth R, Johnson E, Milbrandt J (2002) Artemin is a vascular-derived neurotropic factor for developing sympathetic neurons. Neuron 35:267-282.

Howard L, Wyatt S, Nagappan G, Davies AM (2013) ProNGF promotes neurite growth from a subset of NGF-dependent neurons by a p75NTR-dependent mechanism. Development 140:2108-2117.

Howe CL, Valletta JS, Rusnak AS, Mobley WC (2001) NGF signaling from clathrin-coated vesicles: evidence that signaling endosomes serve as a platform for the Ras-MAPK pathway. Neuron 32:801-814.

Hsu CI, Ho TS, Liou YR, Chang YC (2011) Morphological changes and synaptogenesis of corticothalamic neurons in the somatosensory cortex of rat during perinatal development. Cerebral cortex (New York, NY : 1991) 21:884-895.

Hu J, Spiegel AM (2007) Structure and function of the human calcium-sensing receptor: insights from natural and engineered mutations and allosteric modulators. Journal of cellular and molecular medicine 11:908-922.

Hu J, Hauache O, Spiegel AM (2000) Human Ca2+ receptor cysteine-rich domain. Analysis of function of mutant and chimeric receptors. The Journal of biological chemistry 275:16382-16389.

Huang C, Miller RT (2007) The calcium-sensing receptor and its interacting proteins. Journal of cellular and molecular medicine 11:923-934.

Huang C, Handlogten ME, Miller RT (2002) Parallel activation of phosphatidylinositol 4-kinase and phospholipase C by the extracellular calcium-sensing receptor. The Journal of biological chemistry 277:20293-20300.

Huang C, Hujer KM, Wu Z, Miller RT (2004) The Ca2+-sensing receptor couples to Galpha12/13 to activate phospholipase D in Madin-Darby canine kidney cells. American journal of physiology Cell physiology 286:C22-30.

Huang C, Wu Z, Hujer KM, Miller RT (2006a) Silencing of filamin A gene expression inhibits Ca2+ -sensing receptor signaling. FEBS letters 580:1795-1800.

Huang C, Sindic A, Hill CE, Hujer KM, Chan KW, Sassen M, Wu Z, Kurachi Y, Nielsen S, Romero MF, Miller RT (2007a) Interaction of the Ca2+-sensing receptor with the inwardly rectifying potassium channels Kir4.1 and Kir4.2

results in inhibition of channel function. American journal of physiology Renal physiology 292:F1073-1081.
Huang EJ, Reichardt LF (2001) Neurotrophins: roles in neuronal development and function. Annual review of neuroscience 24:677-736.
Huang EJ, Reichardt LF (2003) Trk receptors: roles in neuronal signal transduction. Annual review of biochemistry 72:609-642.
Huang Y, Breitwieser GE (2007) Rescue of calcium-sensing receptor mutants by allosteric modulators reveals a conformational checkpoint in receptor biogenesis. The Journal of biological chemistry 282:9517-9525.
Huang Y, Niwa J, Sobue G, Breitwieser GE (2006b) Calcium-sensing receptor ubiquitination and degradation mediated by the E3 ubiquitin ligase dorfin. The Journal of biological chemistry 281:11610-11617.
Huang Y, Zhou Y, Castiblanco A, Yang W, Brown EM, Yang JJ (2009) Multiple Ca(2+)-binding sites in the extracellular domain of the Ca(2+)-sensing receptor corresponding to cooperative Ca(2+) response. Biochemistry 48:388-398.
Huang Y, Zhou Y, Yang W, Butters R, Lee HW, Li S, Castiblanco A, Brown EM, Yang JJ (2007b) Identification and dissection of Ca(2+)-binding sites in the extracellular domain of Ca(2+)-sensing receptor. The Journal of biological chemistry 282:19000-19010.
Huang ZJ (2009) Activity-dependent development of inhibitory synapses and innervation pattern: role of GABA signalling and beyond. The Journal of physiology 587:1881-1888.
Huang ZJ, Scheiffele P (2008) GABA and neuroligin signaling: linking synaptic activity and adhesion in inhibitory synapse development. Curr Opin Neurobiol 18:77-83.
Huang ZJ, Di Cristo G, Ango F (2007c) Development of GABA innervation in the cerebral and cerebellar cortices. Nature Reviews Neuroscience 8:673-686.
Ichikawa R, Yamasaki M, Miyazaki T, Konno K, Hashimoto K, Tatsumi H, Inoue Y, Kano M, Watanabe M (2011) Developmental Switching of Perisomatic Innervation from Climbing Fibers to Basket Cell Fibers in Cerebellar Purkinje Cells. J Neurosci 31:16916-16927.
Ji Y, Pang PT, Feng L, Lu B (2005) Cyclic AMP controls BDNF-induced TrkB phosphorylation and dendritic spine formation in mature hippocampal neurons. Nature Neuroscience 8:164-172.
Ji Y, Lu Y, Yang F, Shen W, Tang T, Feng L, Duan S, Lu B (2010) Acute and gradual increases in BDNF concentration elicit distinct signaling and functions in neurons. Nature Neuroscience 13:302-309.
Jiang H, Guo W, Liang X, Rao Y (2005) Both the establishment and the maintenance of neuronal polarity require active mechanisms: critical roles of GSK-3beta and its upstream regulators. Cell 120:123-135.
Jiang M, Oliva AA, Lam T, Swann JW (2001) GABAergic neurons that pioneer hippocampal area CA1 of the mouse: morphologic features and multiple fates. The Journal of comparative neurology 439:176-192.
Jiang YF, Zhang Z, Kifor O, Lane CR, Quinn SJ, Bai M (2002) Protein kinase C (PKC) phosphorylation of the Ca2+ o-sensing receptor (CaR) modulates functional interaction of G proteins with the CaR cytoplasmic tail. The Journal of biological chemistry 277:50543-50549.
Jong YJ, Kumar V, O'Malley KL (2009) Intracellular metabotropic glutamate receptor 5 (mGluR5) activates signaling cascades distinct from cell surface counterparts. The Journal of biological chemistry 284:35827-35838.
Kaas JH (2008) The evolution of the complex sensory and motor systems of the human brain. Brain Research Bulletin 75:384-390.

Kaech S, Banker G (2006) Culturing hippocampal neurons. Nature Protocols 1:2406-2415.

Kang HJ et al. (2011) Spatio-temporal transcriptome of the human brain. Nature 478:483-489.

Kapoor A, Satishchandra P, Ratnapriya R, Reddy R, Kadandale J, Shankar SK, Anand A (2008) An idiopathic epilepsy syndrome linked to 3q13.3-q21 and missense mutations in the extracellular calcium sensing receptor gene. Annals of neurology 64:158-167.

Katoh H, Yasui H, Yamaguchi Y, Aoki J, Fujita H, Mori K, Negishi M (2000) Small GTPase RhoG is a key regulator for neurite outgrowth in PC12 cells. Molecular and cellular biology 20:7378-7387.

Kayser MS, Nolt MJ, Dalva MB (2008) EphB receptors couple dendritic filopodia motility to synapse formation. Neuron 59:56-69.

Kehrer C, Maziashvili N, Dugladze T, Gloveli T (2008) Altered Excitatory-Inhibitory Balance in the NMDA-Hypofunction Model of Schizophrenia. Frontiers in Molecular Neuroscience 1:6.

Khan MA, Conigrave AD (2010) Mechanisms of multimodal sensing by extracellular Ca(2+)-sensing receptors: a domain-based survey of requirements for binding and signalling. British journal of pharmacology 159:1039-1050.

Kifor O, Diaz R, Butters R, Brown EM (1997) The Ca2+-sensing receptor (CaR) activates phospholipases C, A2, and D in bovine parathyroid and CaR-transfected, human embryonic kidney (HEK293) cells. Journal of Bone and Mineral Research 12:715-725.

Kifor O, Diaz R, Butters R, Kifor I, Brown EM (1998) The calcium-sensing receptor is localized in caveolin-rich plasma membrane domains of bovine parathyroid cells. The Journal of biological chemistry 273:21708-21713.

Kifor O, Kifor I, Moore FD, Butters RR, Cantor T, Gao P, Brown EM (2003) Decreased expression of caveolin-1 and altered regulation of mitogen-activated protein kinase in cultured bovine parathyroid cells and human parathyroid adenomas. The Journal of clinical endocrinology and metabolism 88:4455-4464.

Kifor O, MacLeod RJ, Diaz R, Bai M, Yamaguchi T, Yao T, Kifor I, Brown EM (2001) Regulation of MAP kinase by calcium-sensing receptor in bovine parathyroid and CaR-transfected HEK293 cells. American journal of physiology Renal physiology 280:F291-302.

Kim CH, Braud S, Isaac JT, Roche KW (2005) Protein kinase C phosphorylation of the metabotropic glutamate receptor mGluR5 on Serine 839 regulates Ca2+ oscillations. The Journal of biological chemistry 280:25409-25415.

Kim JA, Cho K, Shin MS, Lee WG, Jung N, Chung C, Chang JK (2008) A novel electroporation method using a capillary and wire-type electrode. Biosensors & bioelectronics 23:1353-1360.

Kisiswa L, Osório C, Erice C, Vizard T, Wyatt S, Davies AM (2013) TNFα reverse signaling promotes sympathetic axon growth and target innervation. Nature Neuroscience 16:865-873.

Komuves L, Oda Y, Tu CL, Chang WH, Ho-Pao CL, Mauro T, Bikle DD (2002) Epidermal expression of the full-length extracellular calcium-sensing receptor is required for normal keratinocyte differentiation. Journal of Cellular Physiology 192:45-54.

Kos CH, Karaplis AC, Peng JB, Hediger MA, Goltzman D, Mohammad KS, Guise TA, Pollak MR (2003) The calcium-sensing receptor is required for normal calcium homeostasis independent of parathyroid hormone. Journal of Clinical Investigation 111:1021-1028.

Kovacs CS, Kronenberg HM (1997) Maternal-fetal calcium and bone metabolism during pregnancy, puerperium, and lactation. Endocrine Reviews 18:832-872.

Kriegstein A, Alvarez-Buylla A (2009) The glial nature of embryonic and adult neural stem cells. Annual Review of Neuroscience 32:149-184.

Kumar S, Chakraborty S, Barbosa C, Brustovetsky T, Brustovetsky N, Obukhov AG (2012a) Mechanisms controlling neurite outgrowth in a pheochromocytoma cell line: the role of TRPC channels. Journal of Cellular Physiology 227:1408-1419.

Kumar V, Fahey PG, Jong YJ, Ramanan N, O'Malley KL (2012b) Activation of intracellular metabotropic glutamate receptor 5 in striatal neurons leads to up-regulation of genes associated with sustained synaptic transmission including Arc/Arg3.1 protein. The Journal of biological chemistry 287:5412-5425.

Kunishima N, Shimada Y, Tsuji Y, Sato T, Yamamoto M, Kumasaka T, Nakanishi S, Jingami H, Morikawa K (2000) Structural basis of glutamate recognition by a dimeric metabotropic glutamate receptor. Nature 407:971-977.

Kurki P, Vanderlaan M, Dolbeare F (1986) Expression of proliferating cell nuclear antigen (PCNA)/cyclin during the cell cycle. Experimental Cell Research 166:209-219.

Kurki P, Ogata K, Tan EM (1988) Monoclonal antibodies to proliferating cell nuclear antigen (PCNA)/cyclin as probes for proliferating cells by immunofluorescence microscopy and flow cytometry. Journal of Immunological Methods 109:49-59.

Kuruvilla R, Zweifel LS, Glebova NO, Lonze BE, Valdez G, Ye H, Ginty DD (2004) A neurotrophin signaling cascade coordinates sympathetic neuron development through differential control of TrkA trafficking and retrograde signaling. Cell 118:243-255.

Kwon HB, Sabatini BL (2011) Glutamate induces de novo growth of functional spines in developing cortex. Nature 474:100-104.

Lazarus S, Pretorius CJ, Khafagi F, Campion KL, Brennan SC, Conigrave AD, Brown EM, Ward DT (2011) A novel mutation of the primary protein kinase C phosphorylation site in the calcium-sensing receptor causes autosomal dominant hypocalcemia. European journal of endocrinology / European Federation of Endocrine Societies 164:429-435.

Lazzaro D, Price M, de Felice M, Di Lauro R (1991) The transcription factor TTF-1 is expressed at the onset of thyroid and lung morphogenesis and in restricted regions of the foetal brain. Development 113:1093-1104.

LeBlanc JJ, Fagiolini M (2011) Autism: a "critical period" disorder? Neural Plasticity 2011:921680.

Ledda F, Paratcha G, Ibáñez CF (2002) Target-derived GFRalpha1 as an attractive guidance signal for developing sensory and sympathetic axons via activation of Cdk5. Neuron 36:387-401.

Lee H, Chen CX, Liu YJ, Aizenman E, Kandler K (2005) KCC2 expression in immature rat cortical neurons is sufficient to switch the polarity of GABA responses. Eur J Neurosci 21:2593-2599.

Lee HJ, Mun HC, Lewis NC, Crouch MF, Culverston EL, Mason RS, Conigrave AD (2007) Allosteric activation of the extracellular Ca2+-sensing receptor by L-amino acids enhances ERK1/2 phosphorylation. The Biochemical journal 404:141-149.

Lee JH, Lee J, Choi KY, Hepp R, Lee JY, Lim MK, Chatani-Hinze M, Roche PA, Kim DG, Ahn YS, Kim CH, Roche KW (2008) Calmodulin dynamically regulates the trafficking of the metabotropic glutamate receptor mGluR5. Proceedings of the National Academy of Sciences of the United States of America 105:12575-12580.

Lee KF, Bachman K, Landis S, Jaenisch R (1994) Dependence on p75 for innervation of some sympathetic targets. Science 263:1447-1449.

Lee R, Kermani P, Teng KK, Hempstead BL (2001) Regulation of cell survival by secreted proneurotrophins. Science 294:1945-1948.

Levi-Montalcini R (1987) The nerve growth factor 35 years later. Science 237:1154-1162.

Levi-Montalcini R, Booker B (1960) DESTRUCTION OF THE SYMPATHETIC GANGLIA IN MAMMALS BY AN ANTISERUM TO A NERVE-GROWTH PROTEIN. Proceedings of the National Academy of Sciences of the United States of America 46:384-391.

Lewin GR, Barde YA (1996) Physiology of the neurotrophins. Annual Review of Neuroscience 19:289-317.

Li G, Xing W, Bai S, Hao J, Guo J, Li H, Li H, Zhang W, Yang B, Wu L (2011) The Calcium‐Sensing Receptor Mediates Hypoxia‐Induced Proliferation of Rat Pulmonary Artery Smooth Muscle Cells Through MEK1/ERK1, 2 and PI3K Pathways. Basic & Clinical Pharmacology & Toxicology 108:185-193.

Lin KI, Chattopadhyay N, Bai M, Alvarez R, Dang CV, Baraban JM, Brown EM, Ratan RR (1998) Elevated extracellular calcium can prevent apoptosis via the calcium-sensing receptor. Biochemical and Biophysical Research Communications 249:325-331.

Lin Y, Koleske AJ (2010) Mechanisms of synapse and dendrite maintenance and their disruption in psychiatric and neurodegenerative disorders. Annual review of neuroscience 33:349-378.

Lippman Bell JJ, Lordkipanidze T, Cobb N, Dunaevsky A (2010) Bergmann glial ensheathment of dendritic spines regulates synapse number without affecting spine motility. Neuron glia biology:1-8.

Liu K, Russo AF, Hsiung S, Adlersberg M, Franke TF, Gershon MD, Tamir H (2003) Calcium receptor-induced serotonin secretion by parafollicular cells: role of phosphatidylinositol 3-kinase-dependent signal transduction pathways. The Journal of neuroscience 23:2049-2057.

Lodato S, Rouaux C, Quast KB, Jantrachotechatchawan C, Studer M, Hensch TK, Arlotta P (2011) Excitatory projection neuron subtypes control the distribution of local inhibitory interneurons in the cerebral cortex. Neuron 69:763-779.

Lonze BE, Riccio A, Cohen S, Ginty DD (2002) Apoptosis, axonal growth defects, and degeneration of peripheral neurons in mice lacking CREB. Neuron 34:371-385.

López-Bendito G, Molnár Z (2003) Thalamocortical development: how are we going to get there? Nature Reviews Neuroscience 4:276-289.

Lorenz S, Frenzel R, Paschke R, Breitwieser GE, Miedlich SU (2007) Functional desensitization of the extracellular calcium-sensing receptor is regulated via distinct mechanisms: role of G protein-coupled receptor kinases, protein kinase C and beta-arrestins. Endocrinology 148:2398-2404.

Loretz CA (2008) Extracellular calcium-sensing receptors in fishes. Comparative biochemistry and physiology Part A, Molecular & integrative physiology 149:225-245.

Lorget F, Kamel S, Mentaverri R, Wattel A, Naassila M, Maamer M, Brazier M (2000) High extracellular calcium concentrations directly stimulate osteoclast apoptosis. Biochemical and Biophysical Research Communications 268:899-903.

Lu B, Wang KH, Nose A (2009) Molecular mechanisms underlying neural circuit formation. Curr Opin Neurobiol 19:162-167.

Lu B, Zhang Q, Wang H, Wang Y, Nakayama M, Ren D (2010) Extracellular calcium controls background current and neuronal excitability via an UNC79-UNC80-NALCN cation channel complex. Neuron 68:488-499.

Lu J, Karadsheh M, Delpire E (1999) Developmental regulation of the neuronal-specific isoform of K-Cl cotransporter KCC2 in postnatal rat brains. Journal of neurobiology 39:558-568.

Lucas FR, Salinas PC (1997) WNT-7a induces axonal remodeling and increases synapsin I levels in cerebellar neurons. Developmental Biology 192:31-44.

Luikart BW, Zhang W, Wayman GA, Kwon CH, Westbrook GL, Parada LF (2008) Neurotrophin-dependent dendritic filopodial motility: a convergence on PI3K signaling. J Neurosci 28:7006-7012.

Luo L (2000) Rho GTPases in neuronal morphogenesis. Nature Reviews Neuroscience 1:173-180.

Luttrell LM (2003) 'Location, location, location': activation and targeting of MAP kinases by G protein-coupled receptors. Journal of molecular endocrinology 30:117-126.

MacLeod RJ, Hayes M, Pacheco I (2007) Wnt5a secretion stimulated by the extracellular calcium-sensing receptor inhibits defective Wnt signaling in colon cancer cells. American journal of physiology Gastrointestinal and liver physiology 293:G403-411.

Maguire EA, Mullally SL (2013) The Hippocampus: A Manifesto for Change. Journal of experimental psychology General.

Mailland M, Waelchli R, Ruat M, Boddeke HG, Seuwen K (1997) Stimulation of cell proliferation by calcium and a calcimimetic compound. Endocrinology 138:3601-3605.

Maina F, Hilton MC, Andres R, Wyatt S, Klein R, Davies AM (1998) Multiple roles for hepatocyte growth factor in sympathetic neuron development. Neuron 20:835-846.

Makita T, Sucov HM, Gariepy CE, Yanagisawa M, Ginty DD (2008) Endothelins are vascular-derived axonal guidance cues for developing sympathetic neurons. Nature 452:759-763.

Mamillapalli R, VanHouten J, Zawalich W, Wysolmerski J (2008) Switching of G-protein usage by the calcium-sensing receptor reverses its effect on parathyroid hormone-related protein secretion in normal versus malignant breast cells. The Journal of biological chemistry 283:24435-24447.

Mao L, Yang L, Tang Q, Samdani S, Zhang G, Wang JQ (2005) The scaffold protein Homer1b/c links metabotropic glutamate receptor 5 to extracellular signal-regulated protein kinase cascades in neurons. J Neurosci 25:2741-2752.

Marchi M, D'Antoni A, Formentini I, Parra R, Brambilla R, Ratto GM, Costa M (2008) The N-terminal domain of ERK1 accounts for the functional differences with ERK2. PLoS ONE 3:e3873.

Marty S (2000) Differences in the regulation of neuropeptide Y, somatostatin and parvalbumin levels in hippocampal interneurons by neuronal activity and BDNF. Progress in brain research 128:193-202.

Marty S, Wehrlé R, Alvarez-Leefmans FJ, Gasnier B, Sotelo C (2002) Postnatal maturation of Na+, K+, 2Cl- cotransporter expression and inhibitory synaptogenesis in the rat hippocampus: an immunocytochemical analysis. Eur J Neurosci 15:233-245.

Maruyama T, Kanaji T, Nakade S, Kanno T, Mikoshiba K (1997) 2APB, 2-aminoethoxydiphenyl borate, a membrane-penetrable modulator of Ins(1,4,5)P3-induced Ca2+ release. Journal of biochemistry 122:498-505.

Mazzucchelli C, Vantaggiato C, Ciamei A, Fasano S, Pakhotin P, Krezel W, Welzl H, Wolfer DP, Pagès G, Valverde O, Marowsky A, Porrazzo A, Orban PC, Maldonado R, Ehrengruber MU, Cestari V, Lipp HP, Chapman PF, Pouysségur J, Brambilla R (2002) Knockout of ERK1 MAP kinase enhances synaptic plasticity in the striatum and facilitates striatal-mediated learning and memory. Neuron 34:807-820.

McCormick WD, Atkinson-Dell R, Campion KL, Mun HC, Conigrave AD, Ward DT (2010) Increased receptor stimulation elicits differential calcium-sensing receptor(T888) dephosphorylation. The Journal of biological chemistry 285:14170-14177.

McCullough J, Clague MJ, Urbé S (2004) AMSH is an endosome-associated ubiquitin isopeptidase. The Journal of cell biology 166:487-492.

McDonald NQ, Lapatto R, Murray-Rust J, Gunning J, Wlodawer A, Blundell TL (1991) New protein fold revealed by a 2.3-A resolution crystal structure of nerve growth factor. Nature 354:411-414.

McKay BE, Turner RW (2005) Physiological and morphological development of the rat cerebellar Purkinje cell. The Journal of physiology 567:829-850.

McKelvey L, Gutierrez H, Nocentini G, Crampton SJ, Davies AM, Riccardi CR, O'Keeffe GW (2012) The intracellular portion of GITR enhances NGF-promoted neurite growth through an inverse modulation of Erk and NF-κB signalling. Biology open 1:1016-1023.

McNeil SE, Hobson SA, Nipper V, Rodland KD (1998) Functional calcium-sensing receptors in rat fibroblasts are required for activation of SRC kinase and mitogen-activated protein kinase in response to extracellular calcium. The Journal of biological chemistry 273:1114-1120.

Mentaverri R, Yano S, Chattopadhyay N, Petit L, Kifor O, Kamel S, Terwilliger EF, Brazier M, Brown EM (2006) The calcium sensing receptor is directly involved in both osteoclast differentiation and apoptosis. FASEB journal : official publication of the Federation of American Societies for Experimental Biology 20:2562-2564.

Miedlich S, Gama L, Breitwieser GE (2002) Calcium sensing receptor activation by a calcimimetic suggests a link between cooperativity and intracellular calcium oscillations. The Journal of biological chemistry 277:49691-49699.

Miedlich SU, Gama L, Seuwen K, Wolf RM, Breitwieser GE (2004) Homology modeling of the transmembrane domain of the human calcium sensing receptor and localization of an allosteric binding site. The Journal of biological chemistry 279:7254-7263.

Mignen O, Brink C, Enfissi A, Nadkarni A, Shuttleworth TJ, Giovannucci DR, Capiod T (2005) Carboxyamidotriazole-induced inhibition of mitochondrial calcium import blocks capacitative calcium entry and cell proliferation in HEK-293 cells. Journal of cell science 118:5615-5623.

Mission JP, Takahashi T, Caviness VS (1991) Ontogeny of radial and other astroglial cells in murine cerebral cortex. Glia 4:138-148.

Mitchell DJ, Blasier KR, Jeffery ED, Ross MW, Pullikuth AK, Suo D, Park J, Smiley WR, Lo KW, Shabanowitz J, Deppmann CD, Trinidad JC, Hunt DF, Catling AD, Pfister KK (2012) Trk activation of the ERK1/2 kinase pathway stimulates intermediate chain phosphorylation and recruits cytoplasmic dynein to signaling endosomes for retrograde axonal transport. J Neurosci 32:15495-15510.

Miyoshi G, Fishell G (2011) GABAergic interneuron lineages selectively sort into specific cortical layers during early postnatal development. Cerebral cortex (New York, NY : 1991) 21:845-852.

Moubarak RS, Solé C, Pascual M, Gutierrez H, Llovera M, Pérez-García MJ, Gozzelino R, Segura MF, Iglesias-Guimarais V, Reix S, Soler RM, Davies AM, Soriano E, Yuste VJ, Comella JX (2010) The death receptor antagonist FLIP-L interacts with Trk and is necessary for neurite outgrowth induced by neurotrophins. J Neurosci 30:6094-6105.

Mudò G, Trovato-Salinaro A, Barresi V, Belluardo N, Condorelli D (2009) Identification of calcium sensing receptor (CaSR) mRNA-expressing cells in normal and injured rat brain. Brain research 1298:24-36.

Mun HC, Franks AH, Culverston EL, Krapcho K, Nemeth EF, Conigrave AD (2004) The Venus Fly Trap domain of the extracellular Ca2+ -sensing receptor is required for L-amino acid sensing. The Journal of biological chemistry 279:51739-51744.

Mun HC, Culverston EL, Franks AH, Collyer CA, Clifton-Bligh RJ, Conigrave AD (2005) A double mutation in the extracellular Ca2+-sensing receptor's venus flytrap domain that selectively disables L-amino acid sensing. The Journal of biological chemistry 280:29067-29072.

Murakoshi H, Yasuda R (2012) Postsynaptic signaling during plasticity of dendritic spines. Trends Neurosci 35:135-143.

Murakoshi H, Wang H, Yasuda R (2011) Local, persistent activation of Rho GTPases during plasticity of single dendritic spines. Nature 472:100-104.

Muto T, Tsuchiya D, Morikawa K, Jingami H (2007) Structures of the extracellular regions of the group II/III metabotropic glutamate receptors. Proceedings of the National Academy of Sciences of the United States of America 104:3759-3764.

Nakajima K, Yamazaki K, Kimura H, Takano K, Miyoshi H, Sato K (2009) Novel gain of function mutations of the calcium-sensing receptor in two patients with PTH-deficient hypocalcemia. Internal medicine (Tokyo, Japan) 48:1951-1956.

Nakayama AY, Harms MB, Luo L (2000) Small GTPases Rac and Rho in the maintenance of dendritic spines and branches in hippocampal pyramidal neurons. J Neurosci 20:5329-5338.

Nash MS, Young KW, Challiss RA, Nahorski SR (2001) Intracellular signalling. Receptor-specific messenger oscillations. Nature 413:381-382.

Nash MS, Schell MJ, Atkinson PJ, Johnston NR, Nahorski SR, Challiss RA (2002) Determinants of metabotropic glutamate receptor-5-mediated Ca2+ and inositol 1,4,5-trisphosphate oscillation frequency. Receptor density versus agonist concentration. The Journal of biological chemistry 277:35947-35960.

Newbern JM, Li X, Shoemaker SE, Zhou J, Zhong J, Wu Y, Bonder D, Hollenback S, Coppola G, Geschwind DH, Landreth GE, Snider WD (2011) Specific functions for ERK/MAPK signaling during PNS development. Neuron 69:91-105.

Nikoletopoulou V, Lickert H, Frade J, Rencurel C, Giallonardo P, Zhang L, Bibel M, Barde YA (2010) Neurotrophin receptors TrkA and TrkC cause neuronal death whereas TrkB does not. Nature 467:59-63.

Nishino J, Mochida K, Ohfuji Y, Shimazaki T, Meno C, Ohishi S, Matsuda Y, Fujii H, Saijoh Y, Hamada H (1999) GFR alpha3, a component of the artemin receptor, is required for migration and survival of the superior cervical ganglion. Neuron 23:725-736.

Nobes CD, Hall A (1995) Rho, rac, and cdc42 GTPases regulate the assembly of multimolecular focal complexes associated with actin stress fibers, lamellipodia, and filopodia. Cell 81:53-62.

Noctor SC, Flint AC, Weissman TA, Dammerman RS, Kriegstein AR (2001) Neurons derived from radial glial cells establish radial units in neocortex. Nature 409:714-720.

Nykjaer A, Willnow TE, Petersen CM (2005) p75NTR--live or let die. Curr Opin Neurobiol 15:49-57.

Nykjaer A, Lee R, Teng KK, Jansen P, Madsen P, Nielsen MS, Jacobsen C, Kliemannel M, Schwarz E, Willnow TE, Hempstead BL, Petersen CM (2004) Sortilin is essential for proNGF-induced neuronal cell death. Nature 427:843-848.

O'Donnell M, Chance RK, Bashaw GJ (2009) Axon growth and guidance: receptor regulation and signal transduction. Annual review of neuroscience 32:383-412.

O'Hara PJ, Sheppard PO, Thøgersen H, Venezia D, Haldeman BA, McGrane V, Houamed KM, Thomsen C, Gilbert TL, Mulvihill ER (1993) The ligand-binding domain in metabotropic glutamate receptors is related to bacterial periplasmic binding proteins. Neuron 11:41-52.

O'Keeffe GW, Gutierrez H, Pandolfi PP, Riccardi C, Davies AM (2008) NGF-promoted axon growth and target innervation requires GITRL-GITR signaling. Nature Neuroscience 11:135-142.

Oda Y, Tu CL, Pillai S, Bikle DD (1998) The calcium sensing receptor and its alternatively spliced form in keratinocyte differentiation. The Journal of biological chemistry 273:23344-23352.

Oda Y, Tu CL, Chang W, Crumrine D, Kömüves L, Mauro T, Elias PM, Bikle DD (2000) The calcium sensing receptor and its alternatively spliced form in murine epidermal differentiation. Journal of Biological Chemistry 275:1183-1190.

Oppenheim RW (1991) Cell death during development of the nervous system. Annual review of neuroscience 14:453-501.

Orban PC, Chapman PF, Brambilla R (1999) Is the Ras-MAPK signalling pathway necessary for long-term memory formation? Trends Neurosci 22:38-44.

Orlando LR, Ayala R, Kett LR, Curley AA, Duffner J, Bragg DC, Tsai LH, Dunah AW, Young AB (2009) Phosphorylation of the homer-binding domain of group I metabotropic glutamate receptors by cyclin-dependent kinase 5. Journal of neurochemistry 110:557-569.

Owen MJ, O'Donovan MC, Thapar A, Craddock N (2011) Neurodevelopmental hypothesis of schizophrenia. The British journal of psychiatry : the journal of mental science 198:173-175.

Pachnis V, Mankoo B, Costantini F (1993) Expression of the c-ret proto-oncogene during mouse embryogenesis. Development 119:1005-1017.

Pagano A, Rovelli G, Mosbacher J, Lohmann T, Duthey B, Stauffer D, Ristig D, Schuler V, Meigel I, Lampert C, Stein T, Prezeau L, Blahos J, Pin J, Froestl W, Kuhn R, Heid J, Kaupmann K, Bettler B (2001) C-terminal interaction is essential for surface trafficking but not for heteromeric assembly of GABA(b) receptors. J Neurosci 21:1189-1202.

Pagès G, Guérin S, Grall D, Bonino F, Smith A, Anjuere F, Auberger P, Pouysségur J (1999) Defective thymocyte maturation in p44 MAP kinase (Erk 1) knockout mice. Science 286:1374-1377.

Pangratz-Fuehrer S, Hestrin S (2011) Synaptogenesis of electrical and GABAergic synapses of fast-spiking inhibitory neurons in the neocortex. J Neurosci 31:10767-10775.

Papa M, Bundman MC, Greenberger V, Segal M (1995) Morphological analysis of dendritic spine development in primary cultures of hippocampal neurons. J Neurosci 15:1-11.

Papale A, Cerovic M, Brambilla R (2009) Viral vector approaches to modify gene expression in the brain. Journal of Neuroscience Methods 185:1-14.

Payne JA, Rivera C, Voipio J, Kaila K (2003) Cation-chloride co-transporters in neuronal communication, development and trauma. Trends Neurosci 26:199-206.

Pazyra-Murphy MF, Hans A, Courchesne SL, Karch C, Cosker KE, Heerssen HM, Watson FL, Kim T, Greenberg ME, Segal RA (2009) A retrograde neuronal survival response: target-derived neurotrophins regulate MEF2D and bcl-w. J Neurosci 29:6700-6709.

Penzes P, Cahill M, Jones K, Vanleeuwen J, Woolfrey K (2011) Dendritic spine pathology in neuropsychiatric disorders. Nature Neuroscience 14:285-293.

Peppiatt CM, Collins TJ, Mackenzie L, Conway SJ, Holmes AB, Bootman MD, Berridge MJ, Seo JT, Roderick HL (2003) 2-Aminoethoxydiphenyl borate (2-APB) antagonises inositol 1,4,5-trisphosphate-induced calcium release, inhibits calcium pumps and has a use-dependent and slowly reversible action on store-operated calcium entry channels. Cell Calcium 34:97-108.

Petersen OH, Michalak M, Verkhratsky A (2005) Calcium signalling: past, present and future. Cell Calcium 38:161-169.

Petrel C, Kessler A, Dauban P, Dodd RH, Rognan D, Ruat M (2004) Positive and negative allosteric modulators of the Ca2+-sensing receptor interact within overlapping but not identical binding sites in the transmembrane domain. The Journal of biological chemistry 279:18990-18997.

Phillips CG, Harnett MT, Chen W, Smith SM (2008) Calcium-sensing receptor activation depresses synaptic transmission. J Neurosci 28:12062-12070.

Pi M, Spurney RF, Tu Q, Hinson T, Quarles LD (2002) Calcium-sensing receptor activation of rho involves filamin and rho-guanine nucleotide exchange factor. Endocrinology 143:3830-3838.

Pi M, Oakley RH, Gesty-Palmer D, Cruickshank RD, Spurney RF, Luttrell LM, Quarles LD (2005) Beta-arrestin- and G protein receptor kinase-mediated calcium-sensing receptor desensitization. Molecular endocrinology (Baltimore, Md) 19:1078-1087.

Planas E, Poveda R, Sánchez S, Romero A, Puig MM (2003) Non-steroidal anti-inflammatory drugs antagonise the constipating effects of tramadol. European journal of pharmacology 482:223-226.

Planken A, Porokuokka LL, Hänninen AL, Tuominen RK, Andressoo JO (2010) Medium-throughput computer aided micro-island method to assay embryonic dopaminergic neuron cultures in vitro. Journal of neuroscience methods 194:122-131.

Pollak MR, Brown EM, Estep HL, McLaine PN, Kifor O, Park J, Hebert SC, Seidman CE, Seidman JG (1994) Autosomal dominant hypocalcaemia caused by a Ca(2+)-sensing receptor gene mutation. Nature genetics 8:303-307.

Puehringer D, Orel N, Lüningschrör P, Subramanian N, Herrmann T, Chao MV, Sendtner M (2013) EGF transactivation of Trk receptors regulates the migration of newborn cortical neurons. Nature Neuroscience.

Putcha GV, Deshmukh M, Johnson EM (1999) BAX translocation is a critical event in neuronal apoptosis: regulation by neuroprotectants, BCL-2, and caspases. J Neurosci 19:7476-7485.

Quinn SJ, Ye CP, Diaz R, Kifor O, Bai M, Vassilev P, Brown E (1997) The Ca2+-sensing receptor: a target for polyamines. The American journal of physiology 273:C1315-1323.

Rakic P (1988) Specification of cerebral cortical areas. Science 241:170-176.

Rakic P (2009) Evolution of the neocortex: a perspective from developmental biology. Nature Reviews Neuroscience 10:724-735.

Ray K, Northup J (2002) Evidence for distinct cation and calcimimetic compound (NPS 568) recognition domains in the transmembrane regions of the human Ca2+ receptor. The Journal of biological chemistry 277:18908-18913.

Ray K, Fan GF, Goldsmith PK, Spiegel A (1997) The carboxyl terminus of the human calcium receptor. Requirements for cell-surface expression and signal transduction. The Journal of biological chemistry 272:31355-31361.

Ray K, Clapp P, Goldsmith PK, Spiegel AM (1998) Identification of the sites of N-linked glycosylation on the human calcium receptor and assessment of their role in cell surface expression and signal transduction. The Journal of biological chemistry 273:34558-34567.

Ray K, Hauschild BC, Steinbach PJ, Goldsmith PK, Hauache O, Spiegel AM (1999) Identification of the cysteine residues in the amino-terminal extracellular domain of the human Ca(2+) receptor critical for dimerization. Implications for function of monomeric Ca(2+) receptor. The Journal of biological chemistry 274:27642-27650.

Redmond L, Kashani AH, Ghosh A (2002) Calcium regulation of dendritic growth via CaM kinase IV and CREB-mediated transcription. Neuron 34:999-1010.

Reichardt LF (2006) Neurotrophin-regulated signalling pathways. Philosophical transactions of the Royal Society of London Series B, Biological sciences 361:1545-1564.

Rey O, Young S, Yuan J, Slice L, Rozengurt E (2005) Amino acid-stimulated Ca2+ oscillations produced by the Ca2+-sensing receptor are mediated by a phospholipase C/inositol 1,4,5-trisphosphate-independent pathway that requires G12, Rho, filamin-A, and the actin cytoskeleton. The Journal of biological chemistry 280:22875-22882.

Rey O, Young S, Jacamo R, Moyer M, Rozengurt E (2010) Extracellular calcium sensing receptor stimulation in human colonic epithelial cells induces intracellular calcium oscillations and proliferation inhibition. Journal of Cellular Physiology 225:73-83.

Reyes-Ibarra AP, García-Regalado A, Ramírez-Rangel I, Esparza-Silva AL, Valadez-Sánchez M, Vázquez-Prado J, Reyes-Cruz G (2007) Calcium-sensing receptor endocytosis links extracellular calcium signaling to parathyroid hormone-related peptide secretion via a Rab11a-dependent and AMSH-sensitive mechanism. Molecular endocrinology (Baltimore, Md) 21:1394-1407.

Riccardi D, Brown EM (2010) Physiology and pathophysiology of the calcium-sensing receptor in the kidney. American journal of physiology Renal physiology 298:F485-499.

Riccardi D, Kemp PJ (2012) The calcium-sensing receptor beyond extracellular calcium homeostasis: conception, development, adult physiology, and disease. Annu Rev Physiol 74:271-297.

Riccio A, Pierchala BA, Ciarallo CL, Ginty DD (1997) An NGF-TrkA-mediated retrograde signal to transcription factor CREB in sympathetic neurons. Science 277:1097-1100.

Ridefelt P, Björklund E, Akerström G, Olsson MJ, Rastad J, Gylfe E (1995) Ca(2+)-induced Ca2+ oscillations in parathyroid cells. Biochemical and Biophysical Research Communications 215:903-909.

Ridley AJ, Hall A (1992) The small GTP-binding protein rho regulates the assembly of focal adhesions and actin stress fibers in response to growth factors. Cell 70:389-399.

Ridley AJ, Paterson HF, Johnston CL, Diekmann D, Hall A (1992) The small GTP-binding protein rac regulates growth factor-induced membrane ruffling. Cell 70:401-410.

Rivera C, Voipio J, Payne JA, Ruusuvuori E, Lahtinen H, Lamsa K, Pirvola U, Saarma M, Kaila K (1999) The K+/Cl- co-transporter KCC2 renders GABA hyperpolarizing during neuronal maturation. Nature 397:251-255.

Robertson AG, Banfield MJ, Allen SJ, Dando JA, Mason GG, Tyler SJ, Bennett GS, Brain SD, Clarke AR, Naylor RL, Wilcock GK, Brady RL, Dawbarn D (2001) Identification and structure of the nerve growth factor binding site on TrkA. Biochemical and Biophysical Research Communications 282:131-141.

Rogers KV, Dunn CK, Hebert SC, Brown EM (1997) Localization of calcium receptor mRNA in the adult rat central nervous system by in situ hybridization. Brain research 744:47-56.

Rosenbaum DM, Rasmussen SG, Kobilka B (2009) The structure and function of G-protein-coupled receptors. Nature 459:356-363.

Roskoski R (2012) ERK1/2 MAP kinases: structure, function, and regulation. Pharmacological research : the official journal of the Italian Pharmacological Society 66:105-143.

Ruat M, Molliver ME, Snowman AM, Snyder SH (1995) Calcium sensing receptor: molecular cloning in rat and localization to nerve terminals. Proceedings of the National Academy of Sciences of the United States of America 92:3161-3165.

Rubin E (1985) Development of the rat superior cervical ganglion: ganglion cell maturation. J Neurosci 5:673-684.

Rusakov DA, Fine A (2003) Extracellular Ca2+ depletion contributes to fast activity-dependent modulation of synaptic transmission in the brain. Neuron 37:287-297.

Ryba NJ, Tirindelli R (1997) A new multigene family of putative pheromone receptors. Neuron 19:371-379.

Sahores M, Gibb A, Salinas PC (2010) Frizzled-5, a receptor for the synaptic organizer Wnt7a, regulates activity-mediated synaptogenesis. Development 137:2215-2225.

Sala C, Cambianica I, Rossi F (2008) Molecular mechanisms of dendritic spine development and maintenance. Acta Neurobiol Exp (Wars) 68:289-304.

Scarisbrick IA, Jones EG, Isackson PJ (1993) Coexpression of mRNAs for NGF, BDNF, and NT-3 in the cardiovascular system of the pre- and postnatal rat. J Neurosci 13:875-893.

Sdrulla AD, Linden DJ (2007) Double dissociation between long-term depression and dendritic spine morphology in cerebellar Purkinje cells. Nature Neuroscience 10:546-548.

Seidah NG, Benjannet S, Pareek S, Chrétien M, Murphy RA (1996a) Cellular processing of the neurotrophin precursors of NT3 and BDNF by the mammalian proprotein convertases. FEBS letters 379:247-250.

Seidah NG, Benjannet S, Pareek S, Savaria D, Hamelin J, Goulet B, Laliberte J, Lazure C, Chrétien M, Murphy RA (1996b) Cellular processing of the nerve growth factor precursor by the mammalian pro-protein convertases. The Biochemical journal 314 (Pt 3):951-960.

Sentürk A, Pfennig S, Weiss A, Burk K, Acker-Palmer A (2011) Ephrin Bs are essential components of the Reelin pathway to regulate neuronal migration. Nature.

Shagin DA, Barsova EV, Yanushevich YG, Fradkov AF, Lukyanov KA, Labas YA, Semenova TN, Ugalde JA, Meyers A, Nunez JM, Widder EA, Lukyanov SA, Matz MV (2004) GFP-like proteins as ubiquitous metazoan superfamily: evolution of functional features and structural complexity. Molecular Biology and Evolution 21:841-850.

Shelly M, Lim BK, Cancedda L, Heilshorn SC, Gao H, Poo MM (2010) Local and long-range reciprocal regulation of cAMP and cGMP in axon/dendrite formation. Science 327:547-552.

Shen K, Cowan CW (2010) Guidance molecules in synapse formation and plasticity. Cold Spring Harb Perspect Biol 2:a001842.

Sherrard RM, Dixon KJ, Bakouche J, Rodger J, Lemaigre-Dubreuil Y, Mariani J (2009) Differential expression of TrkB isoforms switches climbing fiber-Purkinje cell synaptogenesis to selective synapse elimination. Developmental neurobiology 69:647-662.

Shi SH, Jan LY, Jan YN (2003) Hippocampal neuronal polarity specified by spatially localized mPar3/mPar6 and PI 3-kinase activity. Cell 112:63-75.

Sillitoe R, Joyner A (2007) Morphology, molecular codes, and circuitry produce the three-dimensional complexity of the cerebellum. Annual Review of Cell and Developmental Biology 23:549-577.

Silve C, Petrel C, Leroy C, Bruel H, Mallet E, Rognan D, Ruat M (2005) Delineating a Ca2+ binding pocket within the venus flytrap module of the human calcium-sensing receptor. The Journal of biological chemistry 280:37917-37923.

Slinker BK (1998) The statistics of synergism. Journal of molecular and cellular cardiology 30:723-731.

Smeyne RJ, Klein R, Schnapp A, Long LK, Bryant S, Lewin A, Lira SA, Barbacid M (1994) Severe sensory and sympathetic neuropathies in mice carrying a disrupted Trk/NGF receptor gene. Nature 368:246-249.

Sofroniew MV, Howe CL, Mobley WC (2001) Nerve growth factor signaling, neuroprotection, and neural repair. Annual Review of Neuroscience 24:1217-1281.

Spitzer NC (2006) Electrical activity in early neuronal development. Nature 444:707-712.

Spitzer NC (2008) Calcium: first messenger. Nature Neuroscience 11:243-244.

Stein V, Hermans-Borgmeyer I, Jentsch TJ, Hübner CA (2004) Expression of the KCl cotransporter KCC2 parallels neuronal maturation and the emergence of low intracellular chloride. The Journal of comparative neurology 468:57-64.

Stepanchick A, Breitwieser GE (2010) The cargo receptor p24A facilitates calcium sensing receptor maturation and stabilization in the early secretory pathway. Biochemical and Biophysical Research Communications 395:136-140.

Stepanchick A, McKenna J, McGovern O, Huang Y, Breitwieser GE (2010) Calcium sensing receptor mutations implicated in pancreatitis and idiopathic epilepsy syndrome disrupt an arginine-rich retention motif. Cellular physiology and biochemistry : international journal of experimental cellular physiology, biochemistry, and pharmacology 26:363-374.

Steward O, Falk PM (1991) Selective localization of polyribosomes beneath developing synapses: a quantitative analysis of the relationships between polyribosomes and developing synapses in the hippocampus and dentate gyrus. The Journal of comparative neurology 314:545-557.

Stöckel K, Paravicini U, Thoenen H (1974) Specificity of the retrograde axonal transport of nerve growth factor. Brain Research 76:413-421.

Sugden PH, Clerk A (1997) Regulation of the ERK subgroup of MAP kinase cascades through G protein-coupled receptors. Cellular signalling 9:337-351.

Sugihara I (2005) Microzonal projection and climbing fiber remodeling in single olivocerebellar axons of newborn rats at postnatal days 4-7. The Journal of comparative neurology 487:93-106.

Supèr H, Martínez A, Del Río JA, Soriano E (1998) Involvement of distinct pioneer neurons in the formation of layer-specific connections in the hippocampus. J Neurosci 18:4616-4626.

Suzuki K, Lavaroni S, Mori A, Okajima F, Kimura S, Katoh R, Kawaoi A, Kohn LD (1998) Thyroid transcription factor 1 is calcium modulated and coordinately regulates genes involved in calcium homeostasis in C cells. Molecular and cellular biology 18:7410-7422.

Swanwick CC, Murthy NR, Mtchedlishvili Z, Sieghart W, Kapur J (2006) Development of gamma-aminobutyric acidergic synapses in cultured hippocampal neurons. The Journal of comparative neurology 495:497-510.

Tada T, Sheng M (2006) Molecular mechanisms of dendritic spine morphogenesis. Curr Opin Neurobiol 16:95-101.

Tashiro A, Minden A, Yuste R (2000) Regulation of dendritic spine morphology by the rho family of small GTPases: antagonistic roles of Rac and Rho. Cerebral cortex (New York, NY : 1991) 10:927-938.

Tfelt-Hansen J, Chattopadhyay N, Yano S, Kanuparthi D, Rooney P, Schwarz P, Brown E (2004) Calcium-sensing receptor induces proliferation through p38 mitogen-activated protein kinase and phosphatidylinositol 3-kinase but not extracellularly regulated kinase in a model of humoral hypercalcemia of malignancy. Endocrinology 145:1211.

Tfelt-Hansen J, MacLeod RJ, Chattopadhyay N, Yano S, Quinn S, Ren X, Terwilliger EF, Schwarz P, Brown EM (2003) Calcium-sensing receptor stimulates PTHrP release by pathways dependent on PKC, p38 MAPK, JNK, and ERK1/2 in H-500 cells. American journal of physiology Endocrinology and metabolism 285:E329-337.

Thoenen H, Barde YA (1980) Physiology of nerve growth factor. Physiological Reviews 60:1284-1335.

Thompson J, Dolcet X, Hilton M, Tolcos M, Davies AM (2004) HGF promotes survival and growth of maturing sympathetic neurons by PI-3 kinase-and MAP kinase-dependent mechanisms. Molecular and Cellular Neuroscience 27:441-452.

Thomson AM, Jovanovic JN (2010) Mechanisms underlying synapse-specific clustering of GABA(A) receptors. Eur J Neurosci 31:2193-2203.

Tissir F, Goffinet AM (2003) Reelin and brain development. Nature Reviews Neuroscience 4:496-505.

Toba Y, Pakiam JG, Wray S (2005) Voltage-gated calcium channels in developing GnRH-1 neuronal system in the mouse. Eur J Neurosci 22:79-92.

Togashi K, Inada H, Tominaga M (2008) Inhibition of the transient receptor potential cation channel TRPM2 by 2-aminoethoxydiphenyl borate (2-APB). British journal of pharmacology 153:1324-1330.

Tole S, Grove EA (2001) Detailed field pattern is intrinsic to the embryonic mouse hippocampus early in neurogenesis. J Neurosci 21:1580-1589.

Tran T, Rubio M, Clem R, Johnson D, Case L, Tessier-Lavigne M, Huganir R, Ginty DD, Kolodkin A (2009) Secreted semaphorins control spine distribution and morphogenesis in the postnatal CNS. Nature 462:1065-1069.

Tronche F, Kellendonk C, Kretz O, Gass P, Anlag K, Orban PC, Bock R, Klein R, Schütz G (1999) Disruption of the glucocorticoid receptor gene in the nervous system results in reduced anxiety. Nature genetics 23:99-103.

Turner D, Buhl E, Hailer N, Nitsch R (1998) Morphological features of the entorhinal-hippocampal connection. Progress in Neurobiology 55:537-562.

Ultsch MH, Wiesmann C, Simmons LC, Henrich J, Yang M, Reilly D, Bass SH, de Vos AM (1999) Crystal structures of the neurotrophin-binding domain of TrkA, TrkB and TrkC. Journal of molecular biology 290:149-159.

Urfer R, Tsoulfas P, Soppet D, Escandón E, Parada LF, Presta LG (1994) The binding epitopes of neurotrophin-3 to its receptors trkC and gp75 and the design of a multifunctional human neurotrophin. The EMBO journal 13:5896-5909.

Urfer R, Tsoulfas P, O'Connell L, Hongo JA, Zhao W, Presta LG (1998) High resolution mapping of the binding site of TrkA for nerve growth factor and TrkC for neurotrophin-3 on the second immunoglobulin-like domain of the Trk receptors. The Journal of biological chemistry 273:5829-5840.

Valcanis H, Tan SS (2003) Layer specification of transplanted interneurons in developing mouse neocortex. J Neurosci 23:5113-5122.

van Spronsen M, Hoogenraad CC (2010) Synapse pathology in psychiatric and neurologic disease. Current neurology and neuroscience reports 10:207-214.

Vanhaesebroeck B, Guillermet-Guibert J, Graupera M, Bilanges B (2010) The emerging mechanisms of isoform-specific PI3K signalling. Nature reviews Molecular cell biology 11:329-341.

Vanhaesebroeck B, Leevers SJ, Ahmadi K, Timms J, Katso R, Driscoll PC, Woscholski R, Parker PJ, Waterfield MD (2001) Synthesis and function of 3-phosphorylated inositol lipids. Annual review of biochemistry 70:535-602.

Vantaggiato C, Formentini I, Bondanza A, Bonini C, Naldini L, Brambilla R (2006) ERK1 and ERK2 mitogen-activated protein kinases affect Ras-dependent cell signaling differentially. Journal of biology 5:14.

Varela-Nallar L, Alfaro IE, Serrano FG, Parodi J, Inestrosa NC (2010) Wingless-type family member 5A (Wnt-5a) stimulates synaptic differentiation and function of glutamatergic synapses. Proceedings of the National Academy of Sciences of the United States of America 107:21164-21169.

Vassilev PM, Mitchel J, Vassilev M, Kanazirska M, Brown EM (1997a) Assessment of frequency-dependent alterations in the level of extracellular Ca2+ in the synaptic cleft. Biophys J 72:2103-2116.

Vassilev PM, Ho-Pao CL, Kanazirska MP, Ye C, Hong K, Seidman CE, Seidman JG, Brown EM (1997b) Cao-sensing receptor (CaR)-mediated activation of K+ channels is blunted in CaR gene-deficient mouse neurons. NeuroReport 8:1411-1416.

Vetere G, Restivo L, Cole CJ, Ross PJ, Ammassari-Teule M, Josselyn SA, Frankland PW (2011) Spine growth in the anterior cingulate cortex is necessary for the consolidation of contextual fear memory. Proceedings of the National Academy of Sciences of the United States of America 108:8456-8460.

Vizard TN, O'Keeffe GW, Gutierrez H, Kos CH, Riccardi D, Davies AM (2008) Regulation of axonal and dendritic growth by the extracellular calcium-sensing receptor. Nature Neuroscience 11:285-291.

Von Bohlen Und Halbach O (2009) Structure and function of dendritic spines within the hippocampus. Ann Anat 191:518-531.

Vyleta NP, Smith SM (2011) Spontaneous glutamate release is independent of calcium influx and tonically activated by the calcium-sensing receptor. J Neurosci 31:4593-4606.

Waites CL, Garner CC (2011) Presynaptic function in health and disease. Trends Neurosci 34:326-337.

Ward D, Riccardi D (2012) New concepts in calcium-sensing receptor pharmacology and signalling. British journal of pharmacology 165:35-48.

Ward DT (2004) Calcium receptor-mediated intracellular signalling. Cell calcium 35:217-228.

Watson FL, Heerssen HM, Bhattacharyya A, Klesse L, Lin MZ, Segal RA (2001) Neurotrophins use the Erk5 pathway to mediate a retrograde survival response. Nature Neuroscience 4:981-988.

Wayman GA, Impey S, Marks D, Saneyoshi T, Grant WF, Derkach V, Soderling T (2006) Activity-dependent dendritic arborization mediated by CaM-kinase I activation and enhanced CREB-dependent transcription of Wnt-2. Neuron 50:897-909.

Wettschureck N, Lee E, Libutti SK, Offermanns S, Robey PG, Spiegel AM (2007) Parathyroid-specific double knockout of Gq and G11 alpha-subunits leads to a

phenotype resembling germline knockout of the extracellular Ca2+ -sensing receptor. Molecular endocrinology (Baltimore, Md) 21:274-280.

Whitford KL, Dijkhuizen P, Polleux F, Ghosh A (2002) Molecular control of cortical dendrite development. Annual review of neuroscience 25:127-149.

Wickramasinghe SR, Alvania RS, Ramanan N, Wood JN, Mandai K, Ginty DD (2008) Serum Response Factor Mediates NGF-Dependent Target Innervation by Embryonic DRG Sensory Neurons. Neuron 58:532-545.

Wiegert JS, Bading H (2011) Activity-dependent calcium signaling and ERK-MAP kinases in neurons: a link to structural plasticity of the nucleus and gene transcription regulation. Cell Calcium 49:296-305.

Wierman ME, Pawlowski JE, Allen MP, Xu M, Linseman DA, Nielsen-Preiss S (2004) Molecular mechanisms of gonadotropin-releasing hormone neuronal migration. Trends in endocrinology and metabolism: TEM 15:96-102.

Wiesel TN, Hubel DH (1963) SINGLE-CELL RESPONSES IN STRIATE CORTEX OF KITTENS DEPRIVED OF VISION IN ONE EYE. Journal of Neurophysiology 26:1003-1017.

Wiesmann C, Ultsch MH, Bass SH, de Vos AM (1999) Crystal structure of nerve growth factor in complex with the ligand-binding domain of the TrkA receptor. Nature 401:184-188.

Wong RO, Ghosh A (2002) Activity-dependent regulation of dendritic growth and patterning. Nature Reviews Neuroscience 3:803-812.

Wu Z, Tandon R, Ziembicki J, Nagano J, Hujer KM, Miller RT, Huang C (2005) Role of ceramide in Ca2+-sensing receptor-induced apoptosis. Journal of lipid research 46:1396-1404.

Wyatt S, Davies AM (1995) Regulation of nerve growth factor receptor gene expression in sympathetic neurons during development. Journal of Cell Biology 130:1435-1446.

Wyszynski M, Kharazia V, Shanghvi R, Rao A, Beggs AH, Craig AM, Weinberg R, Sheng M (1998) Differential regional expression and ultrastructural localization of alpha-actinin-2, a putative NMDA receptor-anchoring protein, in rat brain. J Neurosci 18:1383-1392.

Xing J, Kornhauser JM, Xia Z, Thiele EA, Greenberg ME (1998) Nerve growth factor activates extracellular signal-regulated kinase and p38 mitogen-activated protein kinase pathways to stimulate CREB serine 133 phosphorylation. Molecular and cellular biology 18:1946-1955.

Xu SZ, Zeng F, Boulay G, Grimm C, Harteneck C, Beech DJ (2005) Block of TRPC5 channels by 2-aminoethoxydiphenyl borate: a differential, extracellular and voltage-dependent effect. British journal of pharmacology 145:405-414.

Xu T, Yu X, Perlik A, Tobin W, Zweig J, Tennant K, Jones T, Zuo Y (2009) Rapid formation and selective stabilization of synapses for enduring motor memories. Nature 462:915-919.

Yamaguchi T, Chattopadhyay N, Kifor O, Sanders JL, Brown EM (2000) Activation of p42/44 and p38 mitogen-activated protein kinases by extracellular calcium-sensing receptor agonists induces mitogenic responses in the mouse osteoblastic MC3T3-E1 cell line. Biochemical and Biophysical Research Communications 279:363-368.

Yamashita T, Tucker KL, Barde YA (1999) Neurotrophin binding to the p75 receptor modulates Rho activity and axonal outgrowth. Neuron 24:585-593.

Yan H, Newgreen DF, Young HM (2003) Developmental changes in neurite outgrowth responses of dorsal root and sympathetic ganglia to GDNF, neurturin, and artemin. Developmental dynamics : an official publication of the American Association of Anatomists 227:395-401.

Yang G, Pan F, Gan W (2009) Stably maintained dendritic spines are associated with lifelong memories. Nature 462:920-924.
Yang XM, Toma JG, Bamji SX, Belliveau DJ, Kohn J, Park M, Miller FD (1998) Autocrine hepatocyte growth factor provides a local mechanism for promoting axonal growth. J Neurosci 18:8369-8381.
Yano S, Brown EM, Chattopadhyay N (2004) Calcium-sensing receptor in the brain. Cell Calcium 35:257-264.
Ye C, Ho-Pao CL, Kanazirska M, Quinn S, Rogers K, Seidman CE, Seidman JG, Brown EM, Vassilev PM (1997) Amyloid-beta proteins activate Ca(2+)-permeable channels through calcium-sensing receptors. J Neurosci Res 47:547-554.
Ye CP, Yano S, Tfelt-Hansen J, MacLeod RJ, Ren X, Terwilliger E, Brown EM, Chattopadhyay N (2004) Regulation of a Ca2+-activated K+ channel by calcium-sensing receptor involves p38 MAP kinase. J Neurosci Res 75:491-498.
Yoshihara Y, De Roo M, Muller D (2009) Dendritic spine formation and stabilization. Curr Opin Neurobiol 19:146-153.
Yoshii A, Constantine-Paton M (2010) Postsynaptic BDNF-TrkB signaling in synapse maturation, plasticity, and disease. Developmental neurobiology 70:304-322.
Yoshii A, Murata Y, Kim J, Zhang C, Shokat K, Constantine-Paton M (2011) TrkB and Protein Kinase M Regulate Synaptic Localization of PSD-95 in Developing Cortex. J Neurosci 31:11894-11904.
Young S, Wu SV, Rozengurt E (2002) Ca2+-stimulated Ca2+ oscillations produced by the Ca2+-sensing receptor require negative feedback by protein kinase C. The Journal of biological chemistry 277:46871-46876.
Yu Y, Bultje RS, Wang X, Shi SH (2009) Specific synapses develop preferentially among sister excitatory neurons in the neocortex. Nature 458:501-504.
Yu Y, He S, Chen S, Fu Y, Brown K, Yao X, Ma J, Gao K, Sosinsky G, Huang K, Shi S (2012) Preferential electrical coupling regulates neocortical lineage-dependent microcircuit assembly. Nature:1-6.
Yuan X, Jin M, Xu X, Song Y, Wu C, Poo MM, Duan S (2003) Signalling and crosstalk of Rho GTPases in mediating axon guidance. Nature Cell Biology 5:38-45.
Zagrebelsky M, Schweigreiter R, Bandtlow CE, Schwab ME, Korte M (2010) Nogo-a stabilizes the architecture of hippocampal neurons. J Neurosci 30:13220-13234.
Zagrebelsky M, Holz A, Dechant G, Barde YA, Bonhoeffer T, Korte M (2005) The p75 neurotrophin receptor negatively modulates dendrite complexity and spine density in hippocampal neurons. J Neurosci 25:9989-9999.
Zhang M, Breitwieser GE (2005) High affinity interaction with filamin A protects against calcium-sensing receptor degradation. The Journal of biological chemistry 280:11140-11146.
Zhang Z, Sun S, Quinn SJ, Brown EM, Bai M (2001) The extracellular calcium-sensing receptor dimerizes through multiple types of intermolecular interactions. The Journal of biological chemistry 276:5316-5322.
Zhang Z, Qiu W, Quinn SJ, Conigrave AD, Brown EM, Bai M (2002) Three adjacent serines in the extracellular domains of the CaR are required for L-amino acid-mediated potentiation of receptor function. The Journal of biological chemistry 277:33727-33735.
Zilles K, Amunts K (2010) Centenary of Brodmann's map--conception and fate. Nature Reviews Neuroscience 11:139-145.
Ziv NE, Smith SJ (1996) Evidence for a role of dendritic filopodia in synaptogenesis and spine formation. Neuron 17:91-102.
Zuo Y, Lin A, Chang P, Gan W (2005) Development of long-term dendritic spine stability in diverse regions of cerebral cortex. Neuron 46:181-189.